Clinical applications of optical coherence tomography in corneal surgery

Intraoperative optical coherence tomography imaging and exploration of predictors for graft detachment in Descemet Membrane endothelial keratoplasty

Marc Bastiaan Muijzer

Clinical applications of optical coherence tomography in corneal surgery

Intraoperative optical coherence tomography
imaging and exploration of predictors for
graft detachment in Descemet membrane endothelial keratoplasty

Marc Bastiaan Muijzer

Colofon

ISBN:	978-94-6458-378-6
Cover art:	Kim Baxter
Cover design:	Bas Muijzer
Lay-out:	Publiss | www.publiss.nl
Print:	Ridderprint | www.ridderprint.nl

The research described in this thesis was financially supported by the Dr. F.P. Fischerstichting, UitZicht, Stichting Vrienden van het UMC, COVID impulsfinanciering, NPO onderzoek, Carl Zeiss Meditec, and Carl Zeiss B.V.

Printing of this thesis was kindly financially supported by Visser Contactlenzen, Théa Pharma, Oculenti, Chipsoft, Tramedico, Stichting Blindenhulp, Rotterdamse stichting voor blindenbelangen, Synga Medical, Landelijke Stichting voor Blinden en Slechtzienden.

Clinical applications of optical coherence tomography in corneal surgery

Intraoperative optical coherence tomography imaging and exploration of predictors for graft detachment in Descemet membrane endothelial keratoplasty

Toepassingen van optische coherentietomografie in cornea chirurgie

Intra-operatieve optische coherentietomografie en identificatie van prognostische factoren voor het loslaten van het transplantaat na Descemet membraan endotheliale keratoplastiek
(met een samenvatting in het Nederlands)

Proefschrift

ter verkrijging van de graad van doctor aan de
Universiteit Utrecht
op gezag van de
rector magnificus, prof.dr. H.R.B.M. Kummeling,
ingevolge het besluit van het college voor promoties
in het openbaar te verdedigen op
donderdag 1 september 2022 des ochtends te 10.15 uur

door

Marc Bastiaan Muijzer
geboren op 25 november 1992
te Schiedam

Promotor:
Prof. dr. S.M. Imhof

Copromotoren:
dr. R.P.L. Wisse
dr.ir. H.J. Noordmans

Beoordelingscommissie:
Prof. dr. M.M. van Genderen
Prof. dr. P.G.M. van der Heijden
Prof. dr. M.J. Jager
Prof. dr. J.P. Ruurda
Prof. dr. S. Ni Dhubhghaill

Paranimfen:

Robbert Jongeneel
Tim Kies

TABLE OF CONTENTS

Chapter 1	General introduction	9
Part I	**Intraoperative optical coherence tomography**	**25**
Chapter 2	Clinical applications for intraoperative optical coherence tomography: a systematic review	27
Part II	**Applications of intraoperative optical coherence tomography in endothelial keratoplasty**	**61**
Chapter 3	Intraoperative optical coherence tomography-assisted Descemet membrane endothelial keratoplasty: towards more efficient, safer surgery	63
Chapter 4	Outcomes of the Advanced Visualization In Corneal Surgery Evaluation (ADVISE) trial; a non-inferiority randomized control trial to evaluate the use of intraoperative OCT during Descemet membrane endothelial keratoplasty	79
Chapter 5	Bilateral posterior lamellar corneal transplant surgery in an infant of 17 weeks old: surgical challenges and the added value of intraoperative optical coherence tomography.	101
Chapter 6	Automatic evaluation of graft orientation during Descemet Membrane Endothelial Keratoplasty using intraoperative OCT	113
Part III	**Data-driven approaches to identify risk factors for graft detachment in Descemet membrane endothelial keratoplasty**	**133**
Chapter 7	A machine learning approach to explore predictors of graft detachment following posterior lamellar keratoplasty: a nationwide registry study	135
Chapter 8	Video-grading of Descemet Membrane Endothelial Keratoplasty surgery to identify risk factors for graft detachment and rebubbling: a post-hoc analysis of the Advanced Visualization In Corneal Surgery Evaluation (ADVISE) trial	165

Chapter 9	Establishing a biomarker for the prediction of short-term graft detachment after Descemet membrane endothelial keratoplasty	187
Chapter 10	General discussion and summary	207
Appendices	Nederlandse samenvatting	224
	Dankwoord	228
	About the author	232
	List of publications	234

CHAPTER 1

GENERAL INTRODUCTION

Marc B Muijzer

INTRODUCTION TO THIS THESIS

Corneal diseases are among the leading causes for reversible blindness worldwide.[1] In cases where conservative measures fail the condition can be managed with a corneal transplantation, also known as keratoplasty. In particular, the treatment of corneal endothelial dysfunction underwent major changes in the past decades with the introduction of new (lamellar) surgical techniques, technological innovations, and advancing insights of the influence of practice patterns on postoperative outcomes. This thesis focuses on the use of optical coherence tomography and influence of practice patterns on postoperative outcomes in endothelial keratoplasty.

Anatomy of the cornea: a brief overview

The human eye consists of the following major structures: the cornea, iris, lens, retina, choroid, and optic nerve (**Figure 1**). The cornea constitutes the anterior transparent part of the human eye and has a crucial function in vision. The cornea transmits and refracts light entering the eye onto the retina and acts as a barrier to the external environment.[2] The absence of vascularization contributes to the corneal clarity, optical performance and relative immune privilege.[3,4] Moreover, as a result of this immune privilege the cornea is – presently – the only ocular tissue amendable to transplantation. The cornea is composed of five anatomical layers (from anterior to posterior): the epithelium, Bowman's layer, stroma, Descemet's membrane, and endothelium (**Figure 1**).

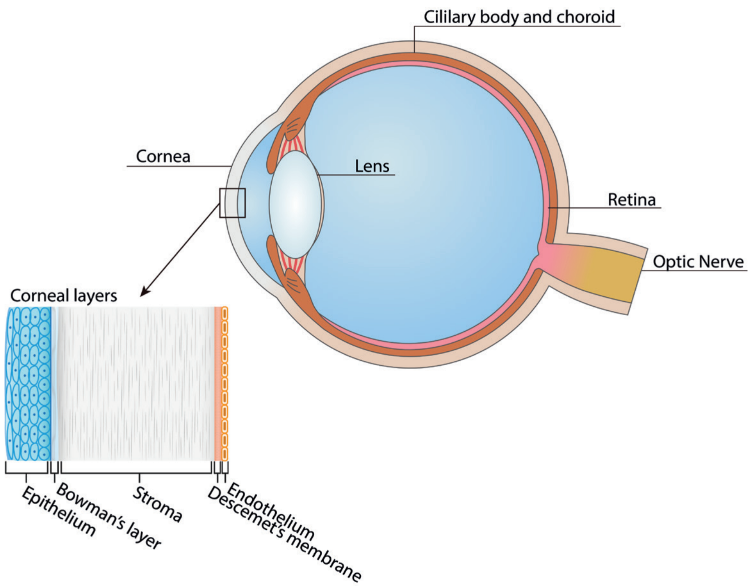

Figure 1. Schematic representation of the major eye structures and the corneal layers. (Images licensed and adapted ©Metamorworks (#207265241) and ©Alila Medical Media (#172206705) / Adobe Stock)

The epithelium is the outermost layer of the cornea. It is composed of 5-7 layers of non-keratinized, stratified, squamous epithelial cells.[2] The thickness of the epithelium across the cornea is highly uniform to maintain a smooth refractive surface.[2] Epithelial cells originate from stem cells located at the corneal limbus from which the epithelial cells migrate towards the corneal center, first horizontally and then vertically up towards the corneal surface.[3] Corneal epithelial cells have a short lifespan with a complete turnover every 5-7 days.[2,3] Numerous and tight intercellular bonds between epithelial cells provide a dense barrier to the external environment.[2,3]

Bowman's layer is a thin acellular collagenous layer directly underneath the corneal epithelium. The layer is composed of smaller, randomly arranged collagen fibrils (primarily type I and V).[2] Bowman's layer does not regenerate and injuries can result in scar tissue, compromising corneal transparency.[3,5] The function of bowman's layer is unclear, though it has been speculated that the layer functions as a barrier to certain pathogens and/or aids in maintaining the shape of the cornea.[2,3,5,6]

The stroma is the thickest corneal layer and is composed of 200-250 parallel arranged lamellae of collagen fibrils (primarily type I and V).[2,3] The corneal lamellae extend across the entire width of the cornea and are arranged at right angles relative to the fibers of the adjacent lamellae, with collagen fibrils approaching the limbus changing direction to run circumferentially.[2,3,7] The function of the stroma is to provide mechanical strength and tectonic stability to the cornea.[2,3] Keratocytes are the primary cell type of the stroma and have a role in maintaining stromal homeostasis by regulating the extracellular matrix environment and synthesizing collagen.[3] A thin layer of pre-Descemet stroma (just located before the Descemet membrane) is by some scientist seen as a distinct different layer of the cornea.[8] This has been an ongoing source of discussion, while it is recognized that the layer has a unique configuration of collagen fibrils and high tensile strength, it is argued that the layer is not anatomically different from the above stroma.[9–11] As a result, the layer has not been widely recognized as a separate layer of the cornea.

The next major layer is the Descemet Membrane, which lies between the stroma and endothelium. The layer is continuously secreted by the endothelial cells and gradually becomes thicker with age.[3] It functions as the basement membrane of the corneal endothelium and is composed largely of type IV collagen.[2]

The endothelium covers the entire posterior surface of the cornea and is composed of a single layer of hexagonal cells. The endothelium is crucial to the transparency of the cornea and its primary function is regulating corneal hydration.[2] The endothelium is a semi-permeable barrier between the anterior chamber and the stroma allowing for passive diffusion (leakage) of fluids and nutrients into the stroma.[3] Concomitantly, endothelial cells actively pump fluid from the stroma to the anterior chamber to maintain a relative state of dehydration to retain transparency.[2,3] Dysfunction of either the barrier or pump function can result in fluid accumulation in the stroma and reducing the corneal transparency.[12] Endothelial cells do not regenerate and the concentration of endothelial cells naturally decreases with age.[3] When endothelial cells are lost, the defects are restored by expansion and active migration of adjacent cells, resulting in loss of the hexagonal shape of the cells.[2,3] When the endothelial cell density decreases to the extent that endothelial pumping capacity fails to maintain the balance between inflow and outflow of fluid this may lead to corneal decompensation, named endothelial dysfunction.[2,12] Currently, the primary and definitive treatment for irreversible endothelial dysfunction is a corneal transplant. However, the worldwide shortage of human donor corneas has resulted in investigating alternative treatment.[12–14]

Fuchs endothelial corneal dystrophy (FECD) is the most common cause for irreversible endothelial dysfunction, affecting approximal 4% of the population over the age of 40, and currently one of the leading indications for corneal transplantation.[15–17] FECD is a bilateral progressive disease of the endothelium, characterized by an accelerated and irreversible loss of endothelial cells.[12,15,18] Primarily affecting patients in the later decades of life, though cases with early onset have been described.[12,15,19] The pathophysiology is not exactly clear and the disease is believed to be caused by a combination of environmental and genetic factors.[12,15,20] Clinical findings include the formation of excrescences of the Descemet membrane, known as "guttae", thickening of the DM, accelerated endothelial cell loss and morphological changes of the endothelial cells, such as pleomorphism and polymegathism.[15,18–20] These changes result in visual disturbances, including straylight complaints, loss of visual acuity and reduced contrast sensitivity. In more advanced stages stromal edema forms as a result of the decreased endothelial pump function further compromising visual function, particularly in the morning with improvement during the day. In severe cases epithelial bullae may develop, which, when ruptured, may lead to subepithelial fibrosis and vascularization.[18,20]

Another important cause for irreversible endothelial dysfunction is bullous keratopathy. Bullous keratopathy is caused by trauma resulting in acute loss of endothelial cells, ultrastructural alterations of the stroma, and eventually corneal decompensation.[12,21,22] The most notable cause of trauma is intraocular surgery and bullous keratopathy after cataract surgery accounts for 9% of the annual corneal transplantations performed in the United States of America.[12,23] Clinical presentation is characterized by severe corneal edema and formation of bullae.[12] Symptoms may present in the immediate post-traumatic period or years after the trauma. Lastly, despite advancing treatment options a considerable portion of corneal transplants require re-transplantation as a result of immunologic rejection or corneal decompensation caused by a dysfunctional donor cornea, such as gradual loss of endothelial cells or tissue trauma.[12,16,23,24] These indications are collectively called graft failure.

Corneal transplantation

Corneal transplantation, also known as keratoplasty, is a surgical procedure in which damaged or diseased cornea tissue is replaced by healthy corneal donor tissue (i.e., the graft). The first successful corneal transplantation was performed by dr. Eduard Zirm in 1905. [25] Since then surgical techniques, postoperative care, and donor tissue preparation have advanced considerably.[24–29] As a result of this continuous improvements corneal transplantation is one of the most successful forms of tissue transplantation effectively restoring vision in eyes with irreversible clouding of the cornea. Currently, corneal transplantation is the most performed tissue transplantation procedure worldwide.[13,14,24] Primary indications for keratoplasty are endothelial disorders (e.g., Fuchs, previous graft failure) and corneal ectatic disorders (e.g. keratoconus). Other indications include infections or trauma to preserve the eye, pain reduction, and for cosmetic reasons.[16]

For the majority of the 20th century, penetrating keratoplasty was the dominant corneal transplantation method available.[14,25,30] Penetrating keratoplasty involved transplanting all corneal layers (**Figure 2A**).[14] Notwithstanding, during penetrating keratoplasty often non-affected corneal tissue was sacrificed to restore vision and was the method prone to problems, such as poor wound healing, suture related complications, an unstable cornea surface, immunological rejection, long visual rehabilitation, and most importantly suboptimal visual outcomes.[14,31–33] This led to development of selective corneal transplantation techniques, only transplanting the diseased corneal tissue, known as lamellar keratoplasty. Two types of lamellar keratoplasty can be distinguished: anterior lamellar keratoplasty (ALK, **Figure 2B**) and posterior lamellar keratoplasty (PLK, **Figure 2C & 2D**), also known as endothelial keratoplasty (EK).[26,34]

Anterior lamellar keratoplasty is the selective transplantation of the corneal stroma, leaving the recipients Descemet membrane and endothelium in place.[14] This method was first described in the 1950's and found a renewed interest in the 1980's with the introduction of deep anterior lamellar keratoplasty (DALK).[26,28,35–37] DALK is arguably the most performed anterior lamellar procedure and increasingly replacing penetrating keratoplasty as the treatment of choice for anterior corneal opacities or advanced keratoconus.[16] During DALK, the Descemet's membrane and stroma must be completely separated by either manual or big bubble dissection.[26,35–37]

Nonetheless, both methods for separating the corneal layers are technically demanding and at high risk of Descemet rupture requiring conversion to penetrating keratoplasty, which prevented widespread adoption of this technique.[26,38,39] In addition, similar to penetrating keratoplasty DALK is prone to suture related complications, poor wound healing, long visual rehabilitation, suboptimal visual outcomes.[14,26,38]

Endothelial keratoplasty has become the most common performed corneal transplantation method worldwide.[16,17,23] In 1998 Gerrit Melles described the first feasible method for endothelial keratoplasty, which was later renamed deep lamellar endothelial keratoplasty (DLEK).[40,41] Since its introduction DLEK evolved into the two most common endothelial keratoplasty methods: Descemet stripping (automated) endothelial keratoplasty (DSEK/DSAEK) and Descemet membrane endothelial keratoplasty (DMEK), and modifications of these methods (e.g., thinner and partial donor grafts).[12,34,42] The DSEK/DSAEK method consists of the donor's endothelium, Descemet membrane, and a strip of posterior stroma similarly to DLEK, though does not require excision of the recipients posterior stroma.[43,44] Subsequently, DSEK evolved into DMEK consisting of only the donor's endothelium and Descemet membrane.[43] The surgical technique for both methods is largely similar. First the endothelium and Descemet membrane of the recipient are removed (i.e., descemetorhexis). Then the graft is inserted in the anterior chamber and positioned within the area of the descemetorhexis. Finally the graft is fixated by injecting gas into the anterior chamber under the graft to promote adherence to the recipient stroma. Key differences between a DSEK and DMEK surgery are the incision width, unfolding, and positioning of the graft as result of the donor tissue thickness. The DSEK graft is more rigid and as a result a larger incision (i.e., 3.5 – 4.5 mm) is required to insert graft with the endothelium facing inward in a taco configuration after which the graft is unfolded and positioned.[34] In comparison, in a DMEK a smaller incision (i.e., 2.2 – 2.8 mm) is used and the graft is inserted as a roll or scroll. After insertion the graft is carefully unfolded and positioned, avoiding to directly manipulate the vulnerable graft.[34,45] A critical step during surgery is identification of the endothelial side of the graft (i.e., graft orientation), which is inserted as a roll, and correctly positioning of the graft with the endothelial side facing away from the cornea.[34] Invertedly upside-down positioning of the graft impedes function, adherence, and may damage endothelial cells threatening long-term viability.[46–48] Several techniques have been described to identify the graft's orientation.[45,47,49] Only relatively recently surgeons obtained a tool to objective and safely assess graft orientation: intraoperative optical coherence tomography.[50,51] Even though DMEK is considered technical more challenging, it has increased in popularity due to its potential for faster visual recovery and improved visual outcome compared to DSEK.[52–59]

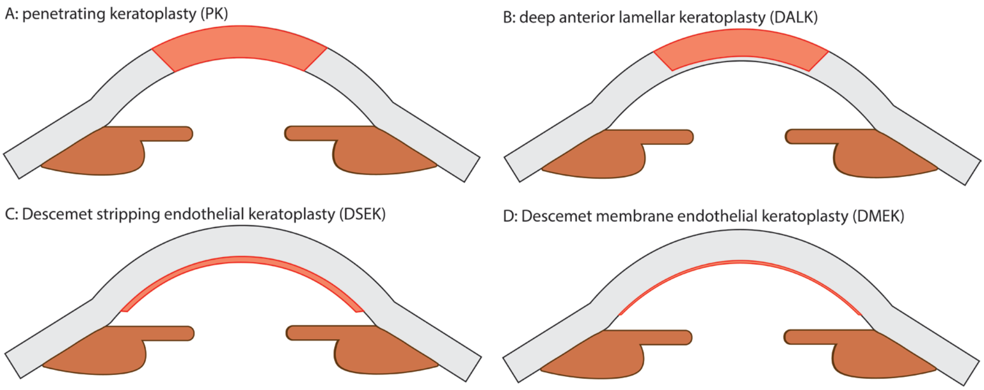

Figure 2. Schematic representation of the main corneal transplantation techniques. A: penetrating keratoplasty; B: deep anterior lamellar keratoplasty (DALK); C: Descemet stripping endothelial keratatoplasty (DSEK); D: Descemet membrane endothelial keratoplasty (DMEK).

The introduction of minimally invasive endothelial keratoplasty improved quality of life and quality of vision for many patients worldwide.[60–62] Notwithstanding, these techniques are troubled by a relative frequent complication: detachment of graft from the recipient cornea shortly after surgery.[34,63] Graft detachment frequently requires surgical re-intervention consisting of repeated injection of gas underneath the detached graft to re-adhere the graft. This procedure is commonly known as a rebubbling and it is estimated one in five patients require a rebubbling.[56–59,64] This is burdensome for patients, may result in a less viable graft, and is a strain on available healthcare resources.[63,65,66] The underlying cause of graft detachment is considered multifactorial[67–69], and a wide range of risk factors have been proposed and/or investigated relating to the donor, patient, and surgery (a detailed overview is provided in **Chapter 7**). In particular, practice patterns modifications – changing the surgical techniques and treatment protocols used – and technological innovation are promising directions for reducing graft detachments, because patient characteristics cannot be changed and we are restricted in donor tissue selection due to worldwide shortages.[17,34,50,70–74]

Optical coherence tomography

One of those technological innovations is optical coherence tomography (OCT) in the care for endothelial keratoplasty. OCT is a non-invasive in vivo imaging technique used to visualize structural and reflective properties of human tissue.[75,76] Using OCT, it is possible to obtain micron-resolution 2D and 3D images, that approach histology images. In the last decades, this technology revolutionized the field of ophthalmology significantly impacting research, diagnosis, and treatment for a wide range of ocular conditions.[77–83]

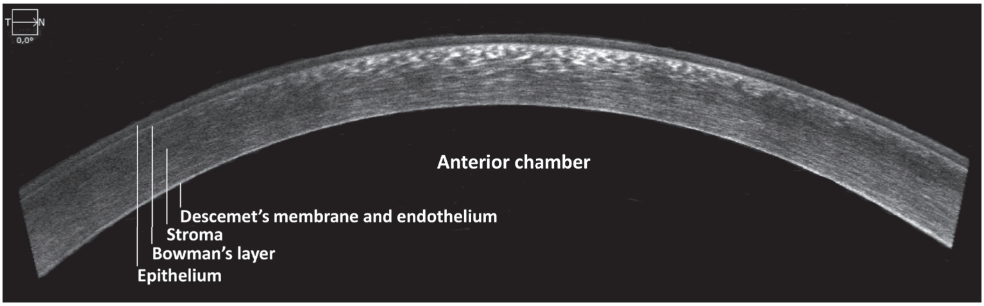

Figure 3. A example of a cross-sectional OCT scan (B-scan) of a healthy human cornea. The different corneal and retinal layers can be distinguished using the reflective properties of the layers and tissues. These reflective properties result in hyperfluorescent and hypofluorescent tissues, and the image is typically converted to a grayscale (shown) or pseudocolor image (not shown).

From the Michelson interferometer the OCT has evolved into the time domain (TD)-OCT and subsequently in the current standard: spectral domain (SD)-OCT.[75,76] The most recent advancement include the use of a scanning laser to achieve higher resolution and faster acquisition rates. This swept-source (SS) OCT is gradually introduced in clinical practice and is expected to eventually replace the SD-OCT.[84] The principle of OCT is based on the interference of near-infrared light between the tissue under investigation and a reference signal.[76] The OCT image is formed by the magnitude, phase, frequency shift, and polarization of this partially time-coherent light (i.e., low-coherence light) backscattered or back reflected from the sample tissue.[75] A single interferogram, known as an A-scan short for amplitude-scan, measures the depth reflectivity profile.[76] The A-scans can be laterally combined to produce a cross-sectional plane called a B-scan (**Figure 3**). Multiple B-scans can be combined to create a three-dimensional image of the scan area.[85] Modern OCT devices have an axial resolution of up to 5 μm and combined with a high acquisition time enable easy differentiation of tissues and layers of the eye.[76,82,85] Thanks to the clear optical structures in the eye, the signal is not perturbed and the infrared light can penetrate down to the deepest layers of the eye.[75,85] The OCT technology further developed in new imaging modalities including functional imaging (e.g., OCT angiography) and towards compact, mobile, and integrated devices (e.g., handheld devices and intraoperative systems.[81,85,86] In particular, the implementation of OCT in the surgical theatre (i.e., intraoperative OCT) has shown promising potential as outlined in **Chapter 2**.

Aim and outline of this thesis

The aims of this thesis were to investigate the role of intraoperative OCT; an emergent technology in ophthalmic surgery, study the applications of intraoperative OCT for endothelial keratoplasty, and investigate causes of graft detachment to advance practice patterns. The thesis has three main sections, subdivided in chapters based on the underlying publications.

The first section of this thesis focuses on the role of intraoperative OCT and how this influences the clinical/surgical practice. In **Chapter 2** we describe the clinical applications of intraoperative OCT across the different ophthalmic surgeries, limitations, and future directions.

The second section of this thesis focusses on the applications of intraoperative OCT on endothelial keratoplasty, specifically, DMEK. In **Chapter 3** we describe how intraoperative OCT impacted our clinical practice and led to the conceptualization of an intraoperative OCT-optimized surgical protocol for DMEK surgery. In **Chapter 4** we investigate the outcomes of our intraoperative OCT-optimized surgical protocol and utility of intraoperative OCT during DMEK in a randomized clinical trial. In challenging patients, the value and advantages of intraoperative OCT are most apparent. The intraoperative OCT proved indispensable in the treatment of an infant with a rare blinding corneal disease as illustrated in **Chapter 5**. In **Chapter 6** we present an automatic image analysis method to assess graft orientation in DMEK using intraoperative OCT.

In the third section of this thesis the focus moves to identification of predictive factors for graft detachment following endothelial keratoplasty. In **Chapter 7** we use modern analytic methods to explore the causes of graft detachment and influence of practice pattern variations in the Netherlands. In **Chapter 8** we zoom in on the micro level to evaluate the associations between manipulations and clinical practice variation during surgery and outcomes. Lastly, in **Chapter 9** we present a novel biomarker to predict graft detachment following DMEK surgery.

REFERENCES

1. World Health Organization. *World report on vision*. 2019.
2. Sabet S, Adampoulou A. Basic structure and function of the human cornea and adnexal structures. In: *Copeland RA and Afshari NA (Ed.). Copeland and Afshari's Principles and Practice of Cornea*. Jaypee Brothers Medical Publishers, 2003.
3. DelMonte DW, Kim T. Anatomy and physiology of the cornea. *Journal of Cataract and Refractive Surgery* 2011; 37: 588–598.
4. Streilein JW. New thoughts on the immunology of corneal transplantation. *Eye* 2003; 17: 943–948.
5. Sridhar MS. Anatomy of cornea and ocular surface. *Indian Journal of Ophthalmology* 2018; 66: 190–194.
6. Wilson SE, Hong JW. Bowman's layer structure and function: Critical or dispensable to corneal function? A Hypothesis. *Cornea* 2000; 19: 417–420.
7. Meek KM, Boote C. The organization of collagen in the corneal stroma. *Experimental Eye Research* 2004; 78: 503–512.
8. Dua HS, Faraj LA, Said DG, et al. Human corneal anatomy redefined: A novel pre-descemet's layer (Dua's Layer). *Ophthalmology* 2013; 120: 1778–1785.
9. Schwab IR. Who's on first? *Ophthalmology* 2013; 120: 1718–1719.
10. Jester J V., Murphy CJ, Winkler M, et al. Lessons in corneal structure and mechanics to guide the corneal surgeon. *Ophthalmology* 2013; 120: 1715–1717.
11. Schlötzer-Schrehardt U, Bachmann BO, Tourtas T, et al. Ultrastructure of the posterior corneal stroma. *Ophthalmology* 2015; 122: 693–699.
12. Price MO, Mehta JS, Jurkunas U V., et al. Corneal endothelial dysfunction: Evolving understanding and treatment options. *Progress in Retinal and Eye Research* 2020; 82: 100904.
13. Català P, Thuret G, Skottman H, et al. Approaches for corneal endothelium regenerative medicine. *Progress in Retinal and Eye Research* 2021; 100987.
14. Tan DTH, Dart JKG, Holland EJ, et al. Corneal transplantation. *The Lancet* 2012; 379: 1749–1761.
15. Klintworth GK. Corneal dystrophies. *Orphanet Journal of Rare Diseases* 2009; 4: 1–38.
16. Dunker SL, Armitage WJ, Armitage M, et al. Practice patterns of corneal transplantation in Europe: first report by the European Cornea and Cell Transplantation Registry. *Journal of cataract and refractive surgery* 2021; 47: 865–869.
17. Gain P, Jullienne R, He Z, et al. Global survey of corneal transplantation and eye banking. *JAMA Ophthalmology* 2016; 134: 167–173.
18. Matthaei M, Hribek A, Clahsen T, et al. Fuchs Endothelial Corneal Dystrophy: Clinical, Genetic, Pathophysiologic, and Therapeutic Aspects. *Annual Review of Vision Science* 2019; 5: 151–175.
19. Vedana G, Villarreal G, Jun AS. Fuchs endothelial corneal dystrophy: Current perspectives. *Clinical Ophthalmology* 2016; 10: 321–330.
20. Elhalis H, Azizi B, Jurkunas U. Fuchs Endothelial Corneal Dystrophy. *Ocular Surface* 2010; 8: 173–184.
21. Morishige N, Sonoda K-H. Bullous Keratopathy as a Progressive Disease. *Cornea* 2013; 32: S77–S83.
22. Yuen HKL, Rassier CE, Jardeleza MSR, et al. A morphologic study of Fuchs dystrophy and bullous keratopathy. *Cornea* 2005; 24: 319–327.

23. Eye Bank Association of America. 2019 Eye Banking Statistical Report. *Eye Bank Association of America* 2020; p11.
24. Alio JL, Montesel A, El Sayyad F, et al. Corneal graft failure: An update. *British Journal of Ophthalmology* 2021; 105: 1049–1058.
25. Moffatt SL, Cartwright VA, Stumpf TH. Centennial review of corneal transplantation. *Clinical and Experimental Ophthalmology* 2005; 33: 642–657.
26. Luengo-Gimeno F, Tan DT, Mehta JS. Evolution of deep anterior lamellar keratoplasty (DALK). *Ocular Surface* 2011; 9: 98–110.
27. Melles GRJ. Posterior lamellar keratoplasty: DLEK to DSEK to DMEK. *Cornea* 2006; 25: 879–881.
28. Singh R, Gupta N, Vanathi M, et al. Corneal transplantation in the modern era. *Indian Journal of Medical Research* 2019; 150: 7–72.
29. Ehlers N, Hjortdal J, Nielsen K. Corneal Grafting and Banking. *Dev Ophthalmol* 2009; 43: 1–14.
30. Teryy MA. Endothelial Keratoplasty: Why Aren't We All Doing Descemet Membrane Endothelial Keratoplasty? *Cornea* 2011; 31: 469–471.
31. Price MO, Gorovoy M, Price FW, et al. Descemet stripping automated endothelial keratoplasty 3-year graft and endothelial cell survival compared with penetrating keratoplasty. *Ophthalmology* 2013; 120: 246–251.
32. Price MO, Gorovoy M, Benetz BA, et al. Descemet's Stripping Automated Endothelial Keratoplasty Outcomes Compared with Penetrating Keratoplasty from the Cornea Donor Study. *Ophthalmology* 2010; 117: 438–444.
33. Hos D, Matthaei M, Bock F, et al. Immune reactions after modern lamellar (DALK, DSAEK, DMEK) versus conventional penetrating corneal transplantation. *Progress in Retinal and Eye Research* 2019; 73: 100768.
34. Price MO, Gupta P, Lass J, et al. EK (DLEK, DSEK, DMEK): New Frontier in Cornea Surgery. *Annual Review of Vision Science* 2017; 3: 69–90.
35. Anwar M. Technique in lamellar keratoplasty. *Trans Ophthalmol Soc UK* 1974; 94: 163–71.
36. Anwar M, Teichmann KD. Big-bubble technique to bare Descemet's membrane in anterior lamellar keratoplasty. *Journal of Cataract and Refractive Surgery* 2002; 28: 398–403.
37. Anwar M, Teichmann KD. Deep lamellar keratoplasty: Surgical techniques for anterior lamellar keratoplasty with and without baring of Descemet's membrane. *Cornea* 2002; 21: 374–383.
38. Cheng YYY, Visser N, Schouten JS, et al. Endothelial Cell loss and visual outcome of deep anterior lamellar keratoplasty versus penetrating keratoplasty: A randomized multicenter clinical trial. *Ophthalmology* 2011; 118: 302–309.
39. Wisse RPL, van den Hoven CML, van der Lelij A. Does lamellar surgery for keratoconus experience the popularity it deserves? *Acta Ophthalmologica* 2014; 92: 473–477.
40. Melles GR, Eggink FA, Lander F, et al. A surgical technique for posterior lamellar keratoplasty. *Cornea* 1998; 17: 618–626.
41. Terry MA, Ousley PJ. Deep lamellar endothelial keratoplasty in the first United States patients. *Cornea* 2001; 20: 239–243.
42. Lam FC, Baydoun L, Dirisamer M, et al. Hemi-descemet membrane endothelial keratoplasty transplantation: A potential method for increasing the pool of endothelial graft tissue. *JAMA Ophthalmology* 2014; 132: 1469–1473.
43. Price FW, Price MO. Descemet's stripping with endothelial keratoplasty in 200 eyes. Early challenges and techniques to enhance donor adherence. *Journal of Cataract and Refractive Surgery* 2006; 32: 411–418.

44. Melles GRJ, Wijdh RHJ, Nieuwendaal CP. A Technique to Excise the Descemet Membrane From a Recipient Cornea (Descemetorhexis). *Cornea* 2004; 23: 286–288.

45. Dapena I, Moutsouris K, Droutsas K, et al. Standardized “no-touch” technique for descemet membrane endothelial keratoplasty. *Archives of Ophthalmology* 2011; 129: 88–94.

46. Dragnea DC, Nobacht S, Gericke A, et al. Postoperative Repositioning of Inverted Descemet Membrane Endothelial Keratoplasty Grafts. *Cornea* 2019; 38: 162–165.

47. Bardan AS, Goweida MB, Goweini HF El, et al. Management of upside-down descemet membrane endothelial keratoplasty: A case series. *Journal of Current Ophthalmology* 2020; 32: 428.

48. Patel S V., Lass JH, Benetz BA, et al. Postoperative Endothelial Cell Density Is Associated with Late Endothelial Graft Failure after Descemet Stripping Automated Endothelial Keratoplasty. *Ophthalmology* 2019; 126: 1076–1083.

49. Veldman PB, Dye PK, Holiman JD, et al. The S-stamp in Descemet Membrane Endothelial Keratoplasty Safely Eliminates Upside-down Graft Implantation. *Ophthalmology* 2016; 123: 161–164.

50. Muijzer MB, Soeters N, Godefrooij DA, et al. Intraoperative Optical Coherence Tomography-Assisted Descemet Membrane Endothelial Keratoplasty: Toward More Efficient, Safer Surgery. *Cornea* 2020; 39: 674–679.

51. Patel AS, Goshe JM, Srivastava SK, et al. Intraoperative Optical Coherence Tomography-Assisted Descemet Membrane Endothelial Keratoplasty in the DISCOVER Study: First 100 Cases. *Am J Ophthalmol* 2020; 210: 167–173.

52. Dunker SL, Dickman MM, Wisse RPL, et al. Descemet Membrane Endothelial Keratoplasty versus Ultrathin Descemet Stripping Automated Endothelial Keratoplasty: A Multicenter Randomized Controlled Clinical Trial. *Ophthalmology* 2020; 127: 1152–1159.

53. Dunker SL, Veldman MHJ, Winkens B, et al. Real-World Outcomes of DMEK: A Prospective Dutch registry study. *American Journal of Ophthalmology* 2021; 222: 218–225.

54. Chamberlain W, Lin CC, Austin A, et al. Descemet Endothelial Thickness Comparison Trial: A Randomized Trial Comparing Ultrathin Descemet Stripping Automated Endothelial Keratoplasty with Descemet Membrane Endothelial Keratoplasty. *Ophthalmology* 2019; 126: 19–26.

55. Stuart A, Romano V, Virgili G, et al. Descemet’s membrane endothelial keratoplasty (DMEK) versus Descemet’s stripping automated endothelial keratoplasty (DSAEK) for corneal endothelial failure. *Cochrane Database of Systematic Reviews*. Epub ahead of print 2018. DOI: 10.1002/14651858.CD012097.

56. Pavlovic I, Shajari M, Herrmann E, et al. Meta- Analysis of postoperative outcome parameters comparing descemet membrane endothelial keratoplasty versus descemet stripping automated endothelial keratoplasty. *Cornea* 2017; 36: 1445–1451.

57. Singh A, Zarei-Ghanavati M, Avadhanam V, et al. Systematic Review and Meta-Analysis of Clinical Outcomes of Descemet Membrane Endothelial Keratoplasty Versus Descemet Stripping Endothelial Keratoplasty/Descemet Stripping Automated Endothelial Keratoplasty. *Cornea* 2017; 36: 1437–1443.

58. Zhu L, Zha Y, Cai J, et al. Descemet stripping automated endothelial keratoplasty versus descemet membrane endothelial keratoplasty: a meta-analysis. *International Ophthalmology* 2018; 38: 897–905.

59. Li S, Liu L, Wang W, et al. Efficacy and safety of Descemet’s membrane endothelial keratoplasty versus Descemet’s stripping endothelial keratoplasty: A systematic review and meta-analysis. *PLoS ONE* 2017; 12: 1–21.

60. Ang MJ, Chamberlain W, Lin CC, et al. Effect of Unilateral Endothelial Keratoplasty on Vision-Related Quality-of-Life Outcomes in the Descemet Endothelial Thickness Comparison Trial (DETECT): A Secondary Analysis of a Randomized Clinical Trial. *JAMA Ophthalmology* 2019; 137: 747–754.
61. Puri S, Robinson SB, Wang J, et al. Vision-related impact on quality of life in an elderly patient population after corneal transplantation. *Cornea* 2014; 33: 119–124.
62. Dunker SL, Dickman MM, Wisse RPL, et al. Quality of vision and vision-related quality of life after Descemet membrane endothelial keratoplasty: a randomized clinical trial. *Acta Ophthalmologica* 2021; 99: e1127–e1134.
63. Siebelmann S, Kolb K, Scholz P, et al. The Cologne rebubbling study: A reappraisal of 624 rebubblings after Descemet membrane endothelial keratoplasty. *British Journal of Ophthalmology* 2021; 105: 1082–1086.
64. Muijzer MB, van Luijk CM, van den Bogaerdt AJ, et al. Prospective evaluation of clinical outcomes between pre-cut corneal grafts prepared using a manual or automated technique: with one-year follow-up. *Acta Ophthalmologica* 2019; 97: 714–720.
65. Gerber-Hollbach N, Baydoun L, López EF, et al. Clinical outcome of rebubbling for graft detachment after descemet membrane endothelial keratoplasty. *Cornea* 2017; 36: 771–776.
66. Hayashi T, Schrittenlocher S, Siebelmann S, et al. Risk factors for endothelial cell loss after Descemet membrane endothelial keratoplasty (DMEK). *Scientific Reports* 2020; 10: 1–9.
67. Dunker S, Winkens B, Van Den Biggelaar F, et al. Rebubbling and graft failure in Descemet membrane endothelial keratoplasty: a prospective Dutch registry study. *British Journal of Ophthalmology* 2021; 1–7.
68. Nahum Y, Leon P, Mimouni M, et al. Factors Associated With Graft Detachment After Primary Descemet Stripping Automated Endothelial Keratoplasty. *Cornea* 2017; 36: 265–268.
69. Leon P, Parekh M, Nahum Y, et al. Factors Associated With Early Graft Detachment in Primary Descemet Membrane Endothelial Keratoplasty. *American Journal of Ophthalmology* 2018; 187: 117–124.
70. Terry MA, Shamie N, Chen ES, et al. Endothelial Keratoplasty. A Simplified Technique to Minimize Graft Dislocation, Iatrogenic Graft Failure, and Pupillary Block. *Ophthalmology* 2008; 115: 1179–1186.
71. Price FW, Price MO. Descemet's stripping with endothelial keratoplasty in 200 eyes. Early challenges and techniques to enhance donor adherence. *Journal of Cataract and Refractive Surgery* 2006; 32: 411–418.
72. Dirisamer M, Van Dijk K, Dapena I, et al. Prevention and management of graft detachment in descemet membrane endothelial keratoplasty. *Archives of Ophthalmology* 2012; 130: 280–291.
73. Kymionis GD, Mikropoulos DG, Portaliou DM, et al. New perspectives on lamellar keratoplasty. *Advances in Therapy* 2014; 31: 494–511.
74. Steverink JG, Wisse RPL. Intraoperative optical coherence tomography in descemet stripping automated endothelial keratoplasty: pilot experiences. *International Ophthalmology* 2017; 37: 939–944.
75. Fercher AF. Optical coherence tomography – development, principles, applications. *Zeitschrift fur Medizinische Physik* 2010; 20: 251–276.
76. Podoleanu AG. Optical coherence tomography. *Journal of Microscopy* 2012; 247: 209–219.
77. Schmidt-Erfurth U, Klimscha S, Waldstein SM, et al. A view of the current and future role of optical coherence tomography in the management of age-related macular degeneration. *Eye (Basingstoke)* 2017; 31: 26–44.

78. Dong ZM, Wollstein G, Schuman JS. Clinical utility of optical coherence tomography in glaucoma. *Investigative Ophthalmology and Visual Science* 2016; 57: OCT556–OCT567.

79. Adhi M, Duker JS. Optical coherence tomography-current and future applications. *Current Opinion in Ophthalmology* 2013; 24: 213–221.

80. Maccora KA, Sheth S, Ruddle JB. Optical coherence tomography in paediatric clinical practice. *Clinical and Experimental Optometry* 2019; 102: 300–308.

81. Kashani AH, Chen C, Gahm JK, et al. Optical Coherence Tomography Angiography: A Comprehensive Review of Current Methods and Clinical Applications. *Prog Retin Eye Res* 2018; 60: 66–100.

82. Fujimoto J, Swanson E. The development, commercialization, and impact of optical coherence tomography. *Investigative Ophthalmology and Visual Science* 2016; 57: OCT1–OCT13.

83. Ang M, Baskaran M, Werkmeister RM, et al. Anterior segment optical coherence tomography. *Progress in Retinal and Eye Research* 2018; 66: 132–156.

84. Kishi S. Impact of swept source optical coherence tomography on ophthalmology. *Taiwan journal of ophthalmology* 2016; 6: 58–68.

85. Muijzer MB, Schellekens PAWJ, Beckers HJM, et al. Clinical applications for intraoperative optical coherence tomography: a systematic review. *Eye (London, England)*. Epub ahead of print July 2021. DOI: 10.1038/s41433-021-01686-9.

86. Kim J, Maher JR, Levinson H, et al. Functional Optical Coherence Tomography: Principles and Progress. *Phys Med Biol* 2015; 60: 211–237.

PART 1

INTRAOPERATIVE OPTICAL COHERENCE TOMOGRAPHY

CHAPTER 2

CLINICAL APPLICATIONS FOR INTRAOPERATIVE OPTICAL COHERENCE TOMOGRAPHY: A SYSTEMATIC REVIEW

Marc B Muijzer; Peter AWJ Schellekens; Henny JM Beckers; Joke H de Boer; Saskia M. Imhof; Robert PL Wisse

Eye (Lond). 2022;36(2)

ABSTRACT

Aim: To provide an overview of the current state of intraoperative optical coherence tomography (iOCT).

Methods: A structured literature search was performed in Pubmed and Embase according to the preferred reporting items for systematic reviews and meta-analyses (PRISMA) guidelines. The included studies were independently evaluated by the same two reviewers to assess; the strength of evidence according to the Oxford Centre for Evidence-Based Medicine 2011 guidelines, the quality of evidence according to the Grading of Recommendations Assessment, Development and Evaluation (GRADE) guidelines, and were critically appraised using the Joanna Briggs institute critical appraisal tool for case series. Studies were included for qualitative analysis if they reported on clinical applications and outcomes of iOCT. Studies were excluded if they reported non-original research, reported on cadaver/non-human/mock eyes, or were either a non-peer-reviewed article, review, comment, case report, case series with less than 5 eyes, and/or were not published in English. We categorize the findings of various studies by their respective fields, including the use of iOCT in vitreoretinal surgery, corneal surgery, glaucoma surgery, cataract surgery , and paediatric ophthalmology.

Results: The iOCT technology is increasingly utilized in all forms of ophthalmic surgery. The superior visualization provided by iOCT aids in our clinical understanding of pathophysiology otherwise obscured due to poor visualization, and enabled surgeons to in-vivo study their practice patterns, achieving a greater understanding of the surgical interventions and their respective tissue alterations. Landmark prospective studies found that iOCT can significantly affect surgical decision making and can cause a subsequent change in surgical strategy, and the use of iOCT has potential to improve surgical outcome. Nevertheless the current body of research consists of low level evidence studies as the majority of studies consist of case reports/ series and pilot studies. In addition, technical limitations and the lack of iOCT compatible surgical instruments and automatic information processing tools can hamper integration in clinical practice.

Conclusion: iOCT is a promising new advancement in ophthalmic surgery with the ability to revolutionize ophthalmic surgery and improve treatment outcomes. Though adaption barriers and technical limitations need to be addressed.

2

INTRODUCTION

Optical coherence tomography (OCT) is a non-invasive *in vivo* imaging technique used to obtain micron-resolution 2D and 3D images of ocular tissues. The first OCT images were published back in 1993,[1] and in the following three decades OCT went from an object of research to an indispensable tool for studying, diagnosing, and treating ocular diseases.[2] Relatively recent the OCT was first introduced in the surgical theatre for intraoperative imaging and it has promising potential for a new paradigm shift in ophthalmic surgery.

OCT is a non-contact tomographic imaging modality that uses infrared light interferometry. The single interferograms (i.e. A-scan) are laterally combined to create a cross-sectional plane called a B-scan (**Figure 1**).[3] The high spatial resolution of modern OCT devices enables the clinician to easily differentiate tissues and layers and thank to the clear optical structures in the eye the signal is not perturbed. Furthermore, the use of OCT in practice is safe for both the patient and the clinician, as OCT does not emit harmful radiation. The development of OCT technology made systems increasingly compact and mobile, expanding its application from table-top devices, to slit-lamp mounted, handheld devices and integration into microscopes or probes.[4–7]

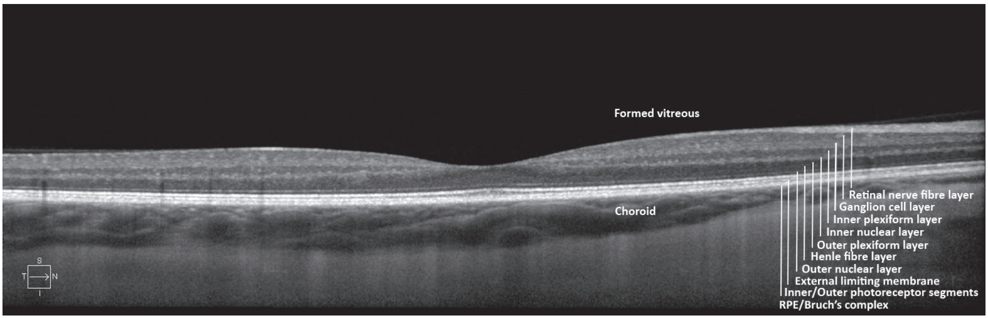

Figure 1. An OCT cross-sectional image (B-scan) of a healthy human retina. The different retinal layers can be distinguished using the reflective properties of the layers and tissues. These reflective properties result in hyperfluorescent and hypofluorescent tissues, and the image is typically converted to a grayscale (shown) or pseudocolor image (not shown) in order to highlight the retinal layers.

The first experiences with intraoperative OCT (iOCT), acquired with a handheld OCT device, were reported in 2005.[5] The first iOCT systems were either a handheld OCT device mounted to the surgical microscope or table-top devices were integrated into a microscope through its eyepiece.[7,8] Similar integrated custom-designed OCT systems were also developed at Duke University and by Ehlers and colleagues at Cleveland Clinic.[9–12] This led to the development and commercialization of fully integrated systems into surgical microscopes with direct assessment capabilities, for example the inclusion of a heads-up display in the eyepieces.[10,12–14]

The technical possibilities of iOCT evidently underwent significant improvement. More recently, also the clinical possibilities for using OCT during surgical procedures are taking shape, and there is a growing body of research in all ophthalmic surgical domains that can be used to evaluate the utility and added value of iOCT in ophthalmic surgery. Here, we provide a comprehensive systematic review of the current knowledge regarding iOCT and its applications.

METHODS

A structured literature search of titles and/or abstracts in Pubmed and Embase was performed on September 29th 2020. The literature search was performed according to the preferred reporting items for systematic reviews and meta-analyses (PRISMA) guidelines.[15] The search terms included: "optical coherence tomography ocular surgery", "intraoperative optical coherence tomography", "microscope integrated optical coherence tomography" "intraoperative optical coherence tomography eye", and all relevant synonyms and abbreviations. No date restrictions were set. The titles and abstracts of all retrieved articles were screened using pre-specified criteria for inclusion by two reviewers (M.M. and N.W.). The references of identified articles were manually checked to find potential relevant studies. Studies were included for full-text review and qualitative analysis if they reported on clinical applications and outcomes of iOCT. Studies were excluded if they reported non-original research, reported on cadaver/non-human/mock eyes, or were either a non-peer-reviewed article, review, comment, case report, case series with less than 5 eyes, and/or were not published in English.

The included studies were independently evaluated by the same two reviewers (M.M. and N.W.) to assess; the strength of evidence according to the Oxford Centre for Evidence-Based Medicine (OCEM) 2011 guidelines, the quality of evidence according to the Grading of Recommendations Assessment, Development and Evaluation (GRADE) guidelines, and were critically appraised using the Joanna Briggs institute critical appraisal tool for case series, as the majority of identified studies were classified as case series.[16–19] Disagreement between the reviewers was resolved by discussion and a third reviewer (R.W.) was consulted if necessary. The included studies were qualitatively analysed and grouped in the following domains; clinical decision making, vitreoretinal surgery, corneal and refractive surgery, cataract surgery, glaucoma surgery, paediatric ophthalmic surgery. The study design, number of subjects, level of evidence, critical appraisal, intervention and main findings related to iOCT were summarized in a table for each of the domains (**Supplementary tables 1-8**). The studies reporting on retinal membrane peeling and macular hole surgery, and refractive surgery were summarized in separate table.

RESULTS

A total of 1283 studies were identified after the initial literature search. A detailed overview of the selection process and reasons for exclusion after full-text screening is shown in **Figure 2**. After title and abstract screening 231 full-text articles were assessed for eligibility. For 16 articles the full-text was not available and attempts were made to retrieve these articles using other databases without success. Finally, after full-text review 102 articles were included for qualitative analysis. A detailed overview of the included studies, design, level of evidence, critical appraisal, and main findings can be found in the supplementary data. In the following subsections the outcomes of included studies are presented within their respective domain.

Feasibility of intraoperative OCT and impact on clinical decision making

The technological advancements of OCT made the systems increasingly mobile and compact, however, implementation of iOCT faced operational hurdles which prevented widespread adoption. First, the conditions for image acquisition are challenging, such as a sterile environment and supine patient. Second, image acquisition delays surgical workflow. Third, the OCT device is a significant investment with limited understanding of the benefits.[20] In this section we assess and the impact of iOCT on clinical decision making and review the different iOCT devices in use.

Impact of intraoperative OCT on clinical decision making

The introduction of iOCT in the surgical theatre has offered surgeons a previously unreachable source of information (**Figure 3**). A majority of early research focused on how this information was used by surgeons to aid clinical decision making (**Supplementary table 1**). The landmark prospective intraoperative and perioperative ophthalmic imaging with optical coherence tomography (PIONEER) and Determination of Feasibility of Intraoperative Spectral Domain Microscope Combined/ Integrated OCT Visualization During En Face Retinal and Ophthalmic Surgery (DISCOVER) studies by Ehlers et al. thoroughly investigated the impact of iOCT on clinical decision making.[20,21] In the PIONEER study the iOCT image altered surgical decision making in 68% of posterior lamellar keratoplasty and 46% of retinal membrane peeling procedures.[20] Similarly, in the DISCOVER study the OCT image provided valuable feedback in approximately 60% of surgeries, thereby altering surgical decision making in 46% of anterior segment surgeries and 29% of posterior segment surgeries.[21] The benefit of OCT-probes has not been demonstrated in large cohorts, but Mura et al. reported that using a OCT probe it was possible to image the retinal periphery, vitreous base and ciliary body, which would be challenging or even impossible using a conventional surgical microscope or other iOCT systems.[4]

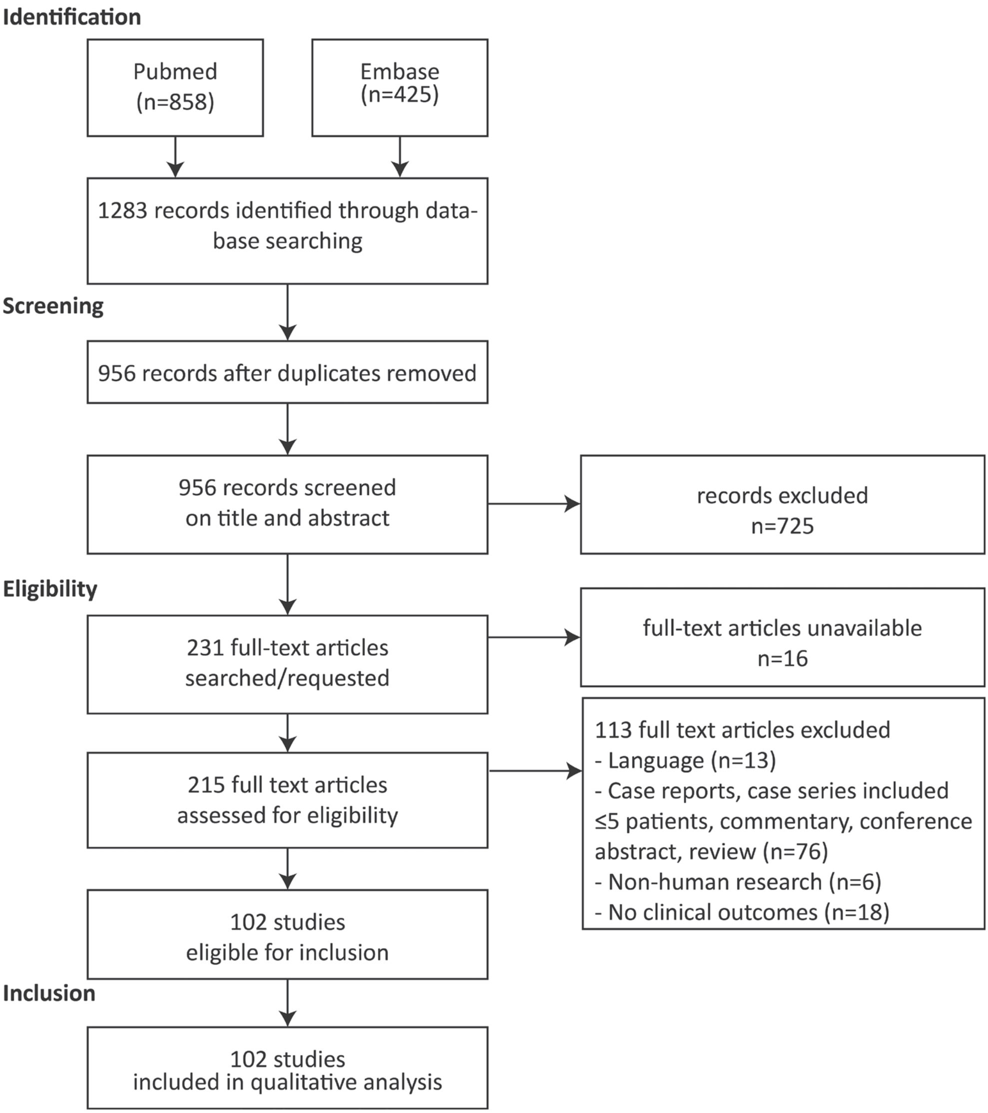

Figure 2. PRISM flowchart of the literature search, including an detailed overview of the identified studies, excluded articles and included articles.

Other studies reporting on the impact of iOCT on clinical decision making report similar results as the PIONEER and DISCOVER study.[8,14,22–25] The results of these studies suggest that the iOCT fills the gaps in surgical information and these insights may improve quality of care and surgical efficiency. Examples of surgical information provided by the iOCT included assessment of the completeness of retinal membrane peeling and adherence of posterior lamellar keratoplasty grafts. A detailed review of the impact and benefit of iOCT is provided in the following subsection for each surgical domain. Notwithstanding, the bias in the design of these studies deserves attention. In all studies the iOCT system was available to use at the surgeon's discretion and in none of the studies the researchers randomized for iOCT use. The evidence of the benefits of iOCT therefor remain indirect. In addition, the availability of iOCT may also lead to potential problems, such as data overload and fixation on irregularities of which the clinical relevance is unclear.

Intraoperative OCT devices

Three types of iOCT devices are currently used in practice (i.e. (mounted) handheld, microscope-integrated, and instrument/probe integrated) and these device types have their respective benefits and limitations. Handheld devices can be used in concordance to a surgical microscope, but also as a stand-alone device.[20] This flexibility is also their most notable advantage compared to dedicated iOCT platforms. However, the handling of a handheld device can be challenging because the system, if not mounted, is unstable which makes image acquisition difficult and has a steep learning curve.[5,20,26] To this end handheld devices are mounted (i.e. attached to the surgical microscope) and can be moved in place for image acquisition. The mounted systems use the stability and precise manoeuvrability in the x, y, and z plane offered by the surgical microscope, thereby significantly improving the speed, accuracy and reproducibility of iOCT imaging.[20] In the PIONEER study Ehlers et al. successfully obtained intraoperative images using a mounted handheld device in 98% of the eyes with a minimal impact on surgical workflow.[20] The median time to set up the iOCT was 1.7 minutes and the median time the surgery was paused measured 4.9 minutes per scan session.[20] Notwithstanding, pausing the surgery for image acquisition remains a major disadvantage of handheld systems. Moreover, during the PIONEER study a technician was present to support imaging and image acquisition may be more complicated without support.[20]

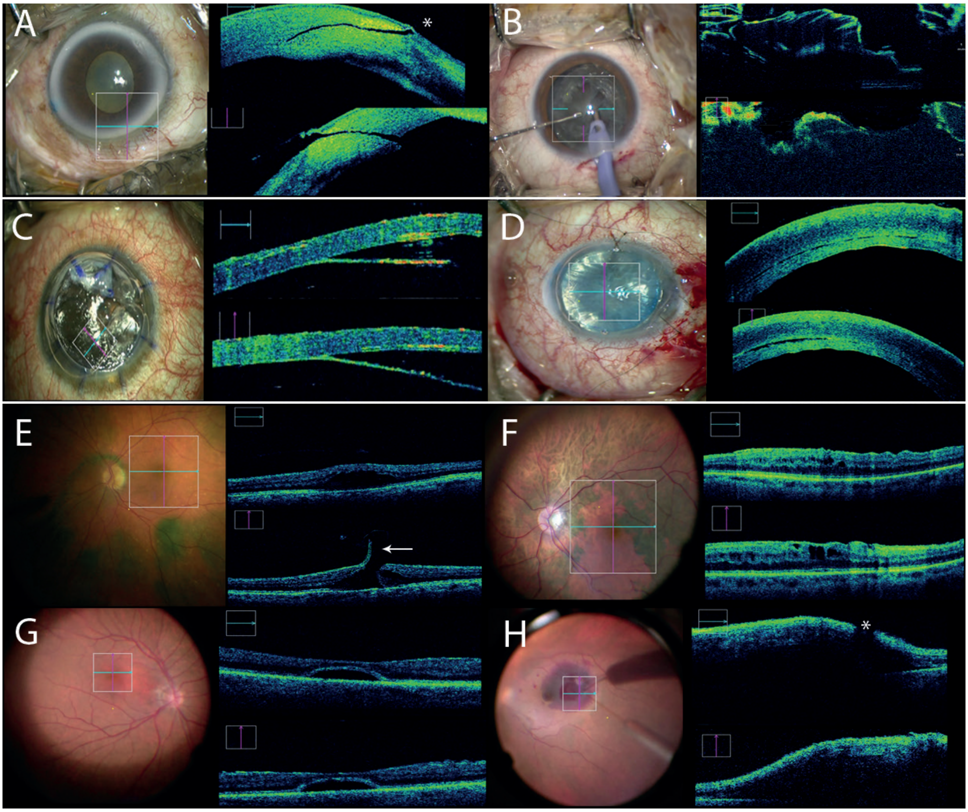

Figure 3. Examples of iOCT use. In each panel, the picture on the left shows an en face microscope image, and the corresponding live OCT images are shown on the right in two perpendicular planes (indicated by purple and turquoise crosshairs). A and B: an example of a self-sealing incision (indicated by the asterisk in A) and assessment of the groove depth (indicated by hashtags, #) during phacoemulsification (B). C and D: separation of the stroma and Descemet's layer during deep anterior lamellar keratoplasty (C), and assessment of the interface fluid in Descemet stripping automated endothelial keratoplasty (D). The thin layer of hyporeflectivity between the graft and stroma indicates the presence of fluid. E and F: intraoperative macular hole formation (E) with a membrane strand still attached to the retina (indicated by the arrow)and intraretinal cystic changes (F). The green indocyanine staining shows an incomplete staining of the inner limiting membrane, indicating the presence of an epiretinal membrane. Which can be confirmed in the OCT image. G and H: retained subretinal fluid (G) and tPA injected for submacular hemorrhage (H); the asterisk in H indicates the needle injection site, and the absolute shadowing in the microscope image in H indicates the presence of high-density material.

A microscope-integrated iOCT has several advantages compared to handheld devices. First, the integrated system can be used can be used without pausing the surgery and during surgical manoeuvres, thereby disrupting the surgical workflow less and lowering the threshold for its use. Second, integrating into the surgical microscope facilitates independent use by the surgeon without support of a technician. Third, the design creates more possibilities to integrate tools and algorithms to enhance surgery, such as decision aids and surgical guidance tools.[12]

Lastly, OCT technology has advanced to the point it can be integrated into probes and instrument for intraocular use. In contrast to handheld and integrated systems OCT probes and OCT-integrated instruments were developed to provide maximal flexibility during vitreoretinal surgery.[4] Using an OCT probe or instrument, the ciliary body and peripheral retina can be imaged easily, and image acquisition is not affected by the presence of cloudy media.[4] Despite these advantages, however, these probes and instruments have several disadvantages as well, including a limited field of view, a vulnerable design, costly non-reusable probe tips, relatively high risk of contamination, difficult image acquisition, and a steep learning curve for the surgeon.[4,27,28]

Vitreoretinal surgery

The use of OCT revolutionized the diagnosis and treatment of vitreoretinal diseases, and has become an indispensable tool in this field.[2] As result, iOCT was initially targeted primarily to vitreoretinal surgeons. Despite early research interest, iOCT has not yet enjoyed the same popularity as their table-top counterparts. Nevertheless, the body of research regarding iOCT during vitreoretinal surgery is extensive. Several studies have shown that the findings on the iOCT image can aid and alter surgical decision making in about 30-40% of vitreoretinal surgeries.[20,21] The iOCT images provide valuable insights in tissue dynamics and alterations following surgical interventions. As a diagnostic device the iOCT can be used to evaluate the retina for underlying conditions.[29] For example, in cases with a vitreous haemorrhage, pathology can be excluded or—if possible—treated.[30,31] Moreover, the direct imagery of iOCT allows for early detection of adverse events and management of these events.[32–34]

The use of iOCT has been reported for a variety of routine vitreoretinal procedures such as macular surgery and retinal detachment surgery (see sections 2.1 and 2.2), but also for challenging surgeries which entail a considerable risk of misplacement, incorrect removal of tissue, scar tissue formation, and/or poor surgical outcomes. Examples of challenging interventions were the in-depth visualization and assistance of iOCT is reported are; the placement of retinal implants and medical devices in the vitreous cavity,[35,36] retinal biopsies,[37] cystotomy for deroofing macular cysts,[38] and subretinal and submacular injections.[39] In particular, the use of subretinal and submacular injections is expected to increase and are crucial for novel gene therapies. The iOCT image allows for the genetic material to be delivered with improved accuracy.[39] The complete overview of included studies and outcomes can be found in **Supplementary table 2** (macular surgery) and **Supplementary table 3** (vitreoretinal surgery).

Retinal membrane peeling and macular hole surgery

The peeling of membranes of the retina (e.g. internal limiting membrane (ILM), epiretinal membrane (ERM), and pucker peelings) is a frequent performed procedures and among procedures in which the iOCT is most utilized.[20,21] The iOCT can be used to determine the starting point for the peel, to check for retina/macular hole formation after peeling, and/or to confirm that the peel is completed (**Supplementary table 2).**[20,21,33,40–44] Several studies revealed a considerable disagreement between the surgeon's observation and the OCT image in regard to peel completeness.[20,21,41,43,44] For example, in the DISCOVER study the iOCT showed residual membranes when the surgeon believed that the membrane was fully peeled in 20% of the cases. Conversely, in 40% of cases in which the surgeon suspected a residual membrane, iOCT revealed that the peel was complete, preventing the need for unnecessary surgical action.[21] Membrane peeling without the use of chromovitrectomy dyes has also been performed, albeit with limited success.[41,43] Leisser et al. reported successful peeling of the ERM without the use of dyes.[43] Although no significant differences in outcomes were found between the use of dyes and dye-free peeling. Moreover, chromovitrectomy dyes were still necessary for staining the ILM and posterior hyaloid. Another factor that may limit the success of performing dye-free iOCT-assisted membrane peeling is the shadow that metallic instruments cast over the peeling area, as well as suboptimal visualization of thin membranes.[21,41] The use of intravitreal dyes to enhance OCT contrast (i.e. dyeing the membranes to improving visualization on the iOCT image) has shown potential for iOCT-assisted membrane peeling and may improve surgeon feedback on the completeness of the peel. Indocyanine green, which is a widely used dye, enhances the reflectivity of the ILM and ERM (contrast ratio increased from 0.907 to 1.42, $p<0.001$).[45] Similarly, tissue reflectivity improved using triamcinolone and prednisolone acetate, though all contrast agents resulted in shadowing of the underlying tissue.[45]

Furthermore, iOCT has also been used to increase our understanding of tissue-instrument interactions and gain insight in retinal alterations after membrane peeling. The retina is a delicate tissue that can be damaged easily by surgical instruments. This has led to the introduction and preferences for using minimally traumatic instruments in recent years. On the other hand, no association has been found between increased retinal damage and subsequent alterations when using a specific type of instrument (e.g. pick, loop or duster) during membrane peeling.[11,46–48] During and immediately after peeling the ILM or ERM significant iatrogenic retinal alterations could be detected on the iOCT scans (**Supplementary table 2**), though the detected alterations resolved rapidly after releasing traction or after surgery. [44,46,47,49–56] The impact of these transient alterations is not yet fully understood, but studies have found no association with long-term worsening of functional or anatomical outcomes.[47,49,52–54,57]

The utility of iOCT during surgical treatment of macular holes has also received extensive attention and the shows promising results (**Supplementary table 2**). During macular hole repair surgery the release of traction, efficacy of the tamponade, and closure of the hole can be directly assessed on the iOCT image.[25,40,58] In addition during inverted flap procedures the positioning of the flap in the macular hole can be observed, even after fluid-air exchange.[25,33,59] Assessing efficacy of tamponade and hole closure may be useful to tailor face-down positioning after surgery.[60] Furthermore, using the iOCT Kumar and Yadav were able to identify a novel intraoperative sign predictive of macular hole closure. Kumar and Yadav named this sign the 'hole-door-sign': residual vertical tissue pillars at the macular hole edge after ILM peeling.[61] Eyes with the hole-door-sign had a 100% rate of closure without an neurosensory defect compared to 60% of the eyes without the hole-door-sign.[61] The studies of Inoue et al. and Tao et al. confirmed the predictive value of the hole-door-sign for macula hole closure, however, the authors reported contradicting results regarding the postoperative visual acuity in eyes with the hole-door-sign.[62,63]

The use of iOCT also provided valuable insights in macular hole dynamics. After ILM peeling the macular hole height and central hole diameter were reported to remain stable, whereas hole volume, base diameter, base area, top/apex diameter, and top/apex area increased compared to before ILM peeling.[46,51,64] Based on these insights in macular hole dynamics Ehlers et al. investigated the predictive value of retinal tissue dynamics for early macular hole closure. Their predictive model had an area under the curve of 0.974 and the most robust predictors for early macular hole closure were intraoperative change in macular hole volume, intraoperative change in minimal width, and pre-incision minimal width.[65] Both the hole-door-sign as well as the predictive model of Ehlers et al. may be a first step towards customized surgery.[61,65] In this regard, the use of volumetric iOCT may facilitate implementation for these and similar tools analysing tissue dynamics.[66,67]

Retinal detachment surgery

During surgical repair of retinal detachment (RD), the iOCT images can provide valuable information and aid clinical decision making, particularly in complex cases, as was shown by Abraham et al. [23] They reported that in 50% of complex RD cases the iOCT provided valuable feedback - which altered surgical management in 12% of cases - compared to 21% in non-complex cases ($p=0.01$).[23] In cases of RD with macular involvement, significant amounts of occult non-resolving sub-macular fluid have been observed after perfluoro-n-octane instillation, direct drainage, or a drainage retinotomy.[68] The presence sub-macular fluid could delay visual recovery, but does not appear to impact postoperative functional or anatomical outcomes, specifically the ellipsoid integrity.[69,70] The significant changes of the retinal tissue have been found resembling alterations observed after macular surgery, ranging from hyper-reflectance to disruption of the retinal layers.[71] However, the majority of detected alterations did not impact the clinical decision making in both RD and macular surgery, because it is not possible or unclear how to prevent or resolve these alterations.

Corneal and refractive surgery

The use of iOCT in corneal surgery is rapidly growing in popularity. Specifically, easy imaging of the cornea contributes to the low threshold for adopting the use of iOCT in corneal surgery. The corneal surgeon experiences only minimal loss of focus when using iOCT, and the optical properties of the cornea minimize shadowing of the image. The principal application of iOCT is in selective keratoplasty, which is considered to be technically demanding, particularly in cases with a cloudy or oedematous cornea. The PIONEER and DISCOVER study showed the advantages associated with access to iOCT technology during selective keratoplasty; specifically, the new information provided by iOCT led a critical change in surgical decision making in, respectively, 48% and 43% of lamellar corneal surgeries.[20,21] In this section the applications and benefits of iOCT in corneal and refractive surgery are reviewed. The detailed overview of the included studies and outcomes can be found in **Supplementary table 4** (cornea surgery) and **Supplementary table 5** (refractive surgery and corneal crosslinking).

Anterior corneal surgery

Deep lamellar anterior keratoplasty (DALK) is the selective transplantation of the corneal stroma, leaving the recipients Descemet membrane and endothelium in place. During DALK, the Descemet's membrane and anterior stroma must be completely separated by either manual or big bubble dissection. However, both methods for separating the layers are at risk of complications and separation of the layers is difficult to visualize using the en-face microscope view. In particular, successful big bubble formation in particular is dependent on the depth of the dissection plane for cannula placement.[72] The iOCT enables the surgeon to directly assess the depth of the dissection plane and if necessary place additional cuts or reposition the cannula.[73] Additionally, after injecting air between the corneal layers the surgeon can confirm separation of the layers and Descemet's membrane integrity.[74,75] Initials reports using iOCT during DALK showed that a deeper trephination depth can be achieved and the cannula can be placed closer to the Descemet's membrane (successful big bubble: 90.4±27.7 µm, failed big bubble: 136.7±24.2 µm, $p<0.01$), leading to a high rate of successful big-bubbles (≥70%).[72,74] Moreover, the use of iOCT enables the surgeon to attempt manual dissection in the case of an emphysematous opaque cornea after a failed attempt using the big bubble method.[74,75] Lastly, Guindolet et al. reported that femtosecond laser DALK with iOCT assistance resulted in a 100% success rate with respect to big bubble formation, with no perforations, in eighteen

DALK procedures.[76] They attributed this success to the accuracy of femtosecond laser cuts combined with direct assessment of corneal thickness using iOCT.

Similarly to assessing the dissection plane in DALK surgery Zakaria et al. used iOCT to guide dissection depth during pannus removal in limbal stem cell transplantation.[77] During surgery OCT pachymetry maps were made to assess how much tissue was removed and prevent accidental corneal perforation. In all 8 cases the pannus was completely removed and no corneal perforations were recorded.[77]

Posterior lamellar corneal surgery

Notable advantages of iOCT in corneal surgery are observed during posterior lamellar keratoplasty, such as Descemet stripping endothelial keratoplasty (DSEK) and Descemet membrane endothelial keratoplasty (DMEK), in which the posterior corneal layers are selectively replaced by a partial corneal graft.[78] A relative frequent and burdensome adverse event is postoperative detachment of the graft, which often necessitates additional surgical procedures. Although the underlying cause of graft detachment is considered multifactorial, though interface irregularities and/or the presence of fluid in the interface are believed to impede proper attachment of the graft.[79] In addition, interface fluid could lead to textural interface opacities and could negatively impact visual acuity.[80] The presence of interface fluid is not always evident in the en-face microscope view and the use of iOCT allows the surgeon to assess the interface in high detail, detect areas of non-adherence, or folds during surgery, which may require additional interventions (**Figure 4**).[26,81–84] For example, in 46 of 84 DSAEK procedures of the DISCOVER study persistent interface fluid was visualized, in which the surgeon deemed the graft well-attachment.[21] In addition, the iOCT image provides insight in the efficacy of surgical manoeuvres to reduce interface fluid and promote graft adherence, including: corneal swiping, venting incisions, and over-pressurizing the ocular globe.[82,85,86] All these manoeuvres were reported to significantly reduce interface fluid in DSAEK. However, the independent use of prolonged overpressure of the globe may only marginally reduce interface fluid. Titiyal et al. reported that interface fluid persisted after 8 minutes of overpressure, whereas by combined overpressure and corneal swiping interface fluid disappeared within 3 minutes.[87] Recently, we performed a similar study in which the use of overpressure in DMEK surgery was evaluated compared to using a minimal pressurization time. Similarly, our results indicated that refraining from prolonged overpressure during DMEK increases surgical efficacy without increasing the risk of postoperative adverse events.[79] Refraining from prolonged overpressure does not appear to increase risk of graft detachment, reduces surgical time and may prevent damage to the optic nerve head, especially relevant for patient with pre-existing glaucoma.

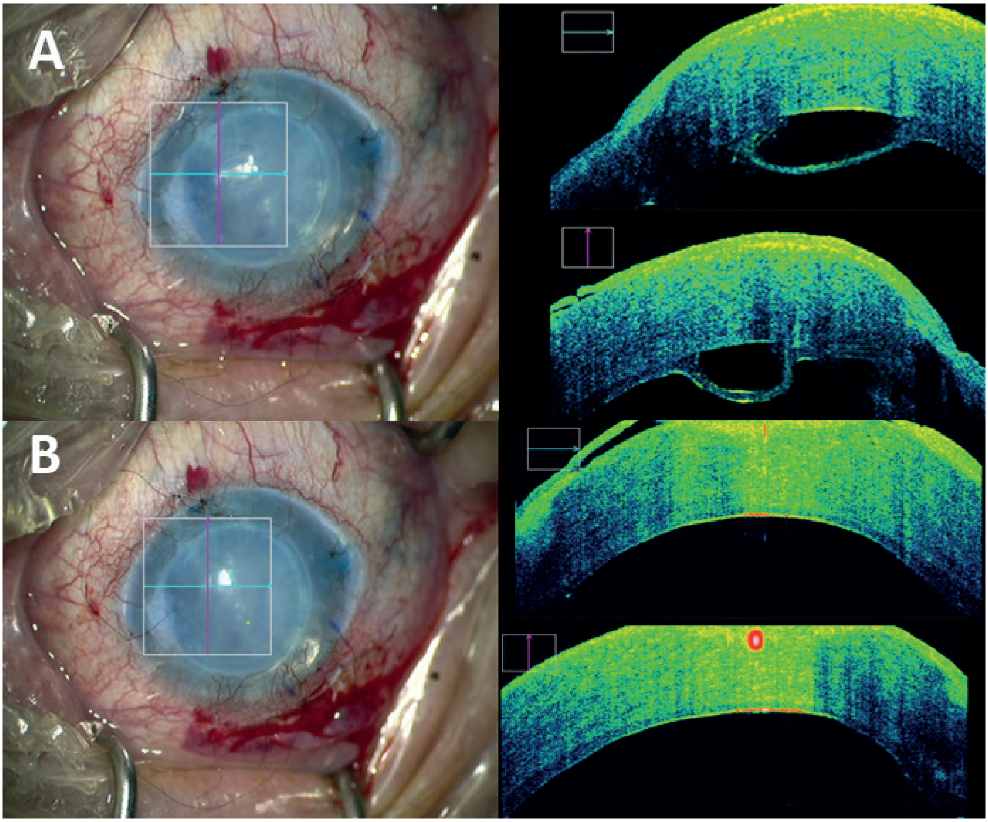

Figure 4. iOCT reveals an interface fluid. In each panel, the picture on the left shows an en face microscope image, and the corresponding live OCT images are shown on the right in two perpendicular planes (indicated by purple and turquoise crosshairs). A: an example of fluid/gas in the interface of a Descemet stripping automated endothelial keratoplasty (DSAEK). B: the same cornea shown in A, with a completely attached DSAEK graft.

Furthermore, iOCT can be useful while determining orientation, unfolding, and positioning the graft during DMEK.[84,88,89] Proper orientation of the graft must be determined in order to ensure functional graft adhesion (**Figure 5**). Currently used signs/methods (e.g. the Moutsouris-sign, stamps or circular cuts) are not always self-evident and poor visualization hinder proper assessment.[88,89] Not to mention, both stamps and cuts damage the graft resulting in endothelial cell loss.[79] More recently, iOCT has been used to determine graft orientation as the iOCT signal is not perturbed by cloudy media.[79,90,91] The natural rolling behavior of DMEK grafts can be well appreciated on the iOCT image, thereby preventing the need to manipulate, cut, or mark the graft to determine the orientation, subsequently preventing endothelial cell loss. In addition, both Saad et al. and Patel et al. reported that iOCT resulted in a shorter duration for unscrolling and positioning the DMEK graft, thereby reducing graft manipulation and improving surgical efficiency.[88,91]

Incorporating iOCT-guidance in posterior lamellar keratoplasty can optimize both the surgical techniques and surgical outcome. Nevertheless, care should be taken with iOCT-guided surgery, as it can lead to more (rigorous) manipulation and a more aggressive surgical approach, potentially leading to graft damage.[86] For example, the high-resolution images provided by iOCT can reveal small folds, non-adherence, and interface irregularities for which the clinical significance is yet unclear.

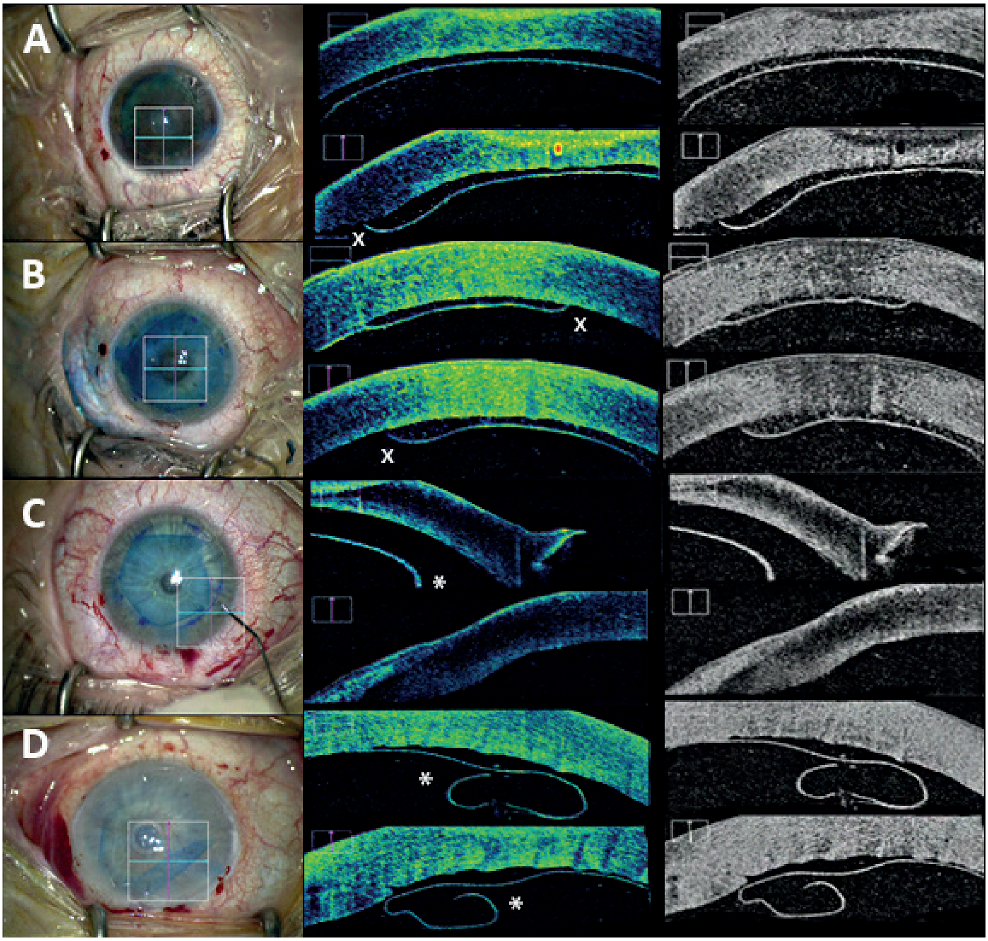

Figure 5. Use of iOCT to observe intraocular graft geometry in two perpendicular planes (purple and turquoise crosshairs) in high detail. Shown are four examples of an en face microscope view (left column) and the unaltered OCT image (right column). The naturally curling motion of the graft in Descemet membrane endothelial keratoplasty can be used to determine the graft's orientation. In panels A and B, the "x" indicates were the graft curls towards the recipient's cornea, indicating proper orientation of the graft. In panels C and D, the asterisks indicate were the graft curls away from the recipient's cornea, indicating incorrect (i.e., upside-down) graft orientation.

Corneal crosslinking and refractive surgery

Corneal crosslinking (CXL) is now the first-line treatment for progressive corneal ectasia, particularly keratoconus.[92] During CXL the penetration of riboflavin in the corneal stroma a key factor that determines treatment efficacy and iOCT has been successfully used to visualize the penetration depth of riboflavin by the noticeable hyper-reflectance of riboflavin.[93] Importantly, the depth of riboflavin penetration was lower in epithelium-on CXL (149.39±15.63 µm) compared to epithelium-off procedures (191.04±32.18 µm), suggesting that penetration depth could be used to determine treatment efficacy.[93]

Several studies reported successful use of OCT to measure corneal thickness and/or corneal dissection depth during CXL and refractive surgery.[94,95] Compared to the current gold standard for measuring corneal thickness, ultrasound pachymetry, OCT pachymetry has several advantages. OCT pachymetry is a non-contact technique that uses the corneal apex reflection for alignment and a larger area of the cornea can be measured. This is relevant for CXL as it allows the thinnest part of the cornea—which is often paracentrally located—to be detected more easily and obtaining a thickness map of the entire cornea reduces the risk of inadvertently damaging the corneal endothelium due to UV radiation in CXL.[94,96] The agreement of measurements between OCT pachymetry and ultrasound pachymetry is high (intraclass correlation coefficient 0.80), and OCT measurements are highly repeatable. Therefore, iOCT pachymetry provides a more standardized measurement, with higher accuracy and negligible risks compared to ultrasound pachymetry.[97] Furthermore, Siebelmann et al. demonstrated the use of iOCT for determining the depth during corneal laser dissection and may be particularly beneficial for therapeutical corneal ablation, because preoperative OCT scans can become inaccurate during the docking process.[98]

Titiyal et al. and Torbey et al. described the use of iOCT to assess the position and vaulting of implantable collamer lens.[99,100] In both studies a high significant correlation was found between intraoperative and postoperative vaulting (Titiyal et al. $r=0.954$; $p<0.001$; Torbey et al. $r=0.81$, $p<0.001$).[99,100] This is clinically relevant, given that extreme vaulting is associated with a postoperative residual refractive error or postoperative complications such as cataract or iatrogenic acute glaucoma, which may necessitate removal of the lens.[99]

Cataract surgery

Although the use of iOCT during cataract surgery is still its infancy, it has high potential. Worldwide, cataract surgery is the most commonly performed form of ophthalmic surgery and is arguably one of the safest.[101] In this section we review the current applications and potential of iOCT during cataract surgery. A detailed overview of included studies and outcomes can be found in **Supplementary table 6**. The learning curve associated with performing microsurgery—including cataract surgery—is considered both steep and demanding.[102] In this respect, the use of iOCT could improve this procedure and serve as an aid during cataract surgery training. Compared to conventional surgery, iOCT provides superior tissue visualization of the groove depth and construction of self-sealing corneal incisions, thereby enabling the supervisors to directly guide the trainee and provide feedback in real time.[103,104] Notwithstanding, no study to date has been performed investigating the use of iOCT during cataract surgery training.

The use of iOCT may also benefit experienced cataract surgeons for timely detection and management of surgical complications. For example, Titiyal et al. reported that Descemet membrane detachment after stromal hydration could only be observed using iOCT.[104] This is particularly relevant in the case of extensive Descemet membrane detachment, which is usually not self-resolving. Likewise, Cendelin et al. reported that stromal hydration negatively impacted incision architecture in 14 of 69 eyes and resulted in wound gaping in two cases, which subsequently required intervention.[105] Additionally, the OCT image could aid surgeons in confirming placement of the intra-ocular lens (IOL) in the capsule bag,[103,106] detecting capsular defects,[107] identifying true posterior polar cataract, and confirming separation of the posterior polar plaque and capsule.[103]

Importantly, studies have shown the potential of iOCT in optimizing the refractive outcome following cataract surgery. The iOCT images and the associated data provide information regarding the lens' intraocular position and can be used to optimize IOL calculations and future IOL designs. Hadded et al. reported a strong correlation between the meridian lens position and anterior chamber depth (ACD).[108] Similarly, Hirschall et al. found that intraoperative ACD measured using OCT was more representative for postoperative ACD and the intraoperative ACD was a significantly better predictor for postoperative manifest refractive outcome.[109–111] Integrating iOCT data into current IOL power calculation formulas can improve refractive outcome.[111] Hirschall et al. showed that combining preoperative and intraoperative ACD measurements refractive surprises can be reduced with 2.8 percent-point and would have resulted in a different IOL power in 7.1% of cases.[111]

Furthermore, the iOCT has led to new insights regarding morphology of cataracts and effects of lens fragments. In 2016, Amir-Asgari et al. assessed the effect of swirling/pinballing lens fragments in the anterior chamber and the endothelial damage that these fragments can cause, finding that smaller particles with higher velocity tend to inflict more damage than larger, slower moving particles.[112] Titiyal et al. used the iOCT to investigate morphological characteristics and dynamics of white cataracts and posterior polar cataracts.[113,114] Distinct characteristics of white cataract that were observed on OCT in different degrees included; the convexity of the anterior capsule, arrangement and reflectance of cortical fibres, presence of clefts, and homogenous ground glass appearance.[114] In posterior polar cataract they identified differences in delineating of the posterior capsule, reflectivity of the posterior polar opacity and underlying capsule, and adherence of the opacity to the posterior capsule.[113] Based on these features the authors propose new classification systems for these types of cataract, thereby aiding patient care and future research.

Glaucoma surgery

The goal of glaucoma surgery is to either increase the outflow of aqueous humour by drainage into the subconjunctival space or improve trabecular outflow.[115] Unfortunately, however, scleral tissue is poorly transparent to light in the visible and infrared spectrum; thus, initial experiences using iOCT in glaucoma surgery were rather unsuccessful in terms of providing the surgeon with improved visualization. Nevertheless, several studies have reported on the added value of iOCT in glaucoma surgery.

Most of the studies investigating the use of iOCT during glaucoma surgery consist of case reports or small case series, reporting on bleb needling[116], trabeculectomy,[117] canaloplasty,[118] long-tube glaucoma drainage devices,[119] and angle surgery.[117] Only three studies describing iOCT use during ab-interno trabeculotomy met the inclusion criteria for this review (**Supplementary table 7**). In all three studies the authors reported that cleft and incision patterns could be observed on the OCT image after trabecular meshwork tissue removal, thereby providing an indication of the surgery's success.[120–122] Notwithstanding, all three studies noted that image acquisition was challenging and they needed a gonioprism lens for visualizing the anterior chamber angle. Only Junker et al. reported successful visualization of the trabecular meshwork without a gonioprism lens in 2 of 5 surgeries, although acquiring images took 15 minutes compared to 2-4 minutes for surgeries with a gonioprism lens.[120] Visualizing deeper angle structures or structures embedded in dense scleral tissue is both demanding and time-consuming—or simply not possible—using currently available OCT devices, as dense scleral tissue is impenetrable to the wavelength used in iOCT devices, thereby completely shadowing the OCT image.[123] Possible solutions to overcome the visualization challenges and improve utility of the iOCT include using a longer wavelength for better tissue penetration and adjustable scanning directions.

Furthermore, new forms of microscopic and minimally invasive surgical glaucoma procedures are coming on the market which could benefit from iOCT; small devices (e.g. stents an microshunts) often must be placed correctly in either the trabecular meshwork or the subconjunctival space/anterior chamber.[124] Placing these devices in the suprachoroidal space is another option, but is currently hampered by poor clinical success. It has not been investigated if iOCT could improve the results of suprachoroidal placements of glaucoma devices.

Pediatric ophthalmic surgery

In infants, young children, and mentally impaired patients, performing an OCT examination is often difficult—or even impossible—using a table-top OCT device. Thus, the introduction of mobile OCT devices, including handheld and microscope-integrated devices, made it possible to exam these patients.[125] This is particularly valuable for examining new-borns and infants with a congenital eye disease, in which early structural changes were previously difficult to examine and study. Using iOCT makes it possible to examine ocular structures and the extent of the underlying pathology (**Supplementary table 8**). Furthermore, if surgical intervention is indicated, iOCT can be used to determine the degree of intervention required and assist clinical decision making (**Figure 6**). For example, Hong et al. used iOCT during surgical reconstruction of the anterior segment in infants with Peter's anomaly, finding that iOCT image led to a change in the surgical approach in 7 out of 33 cases (21%), as well as providing new information compared to both the preoperative examination and the en face ophthalmic microscope view.[126] Importantly, the use of iOCT prevented removal of the crystalline lens in 5 patients.[126] The authors concluded that disease severity in Peter's anomaly is often overestimated without the benefit of OCT examination, including overestimating the angle closure, ACD, and iridocorneal adhesion, leading the authors to conclude that OCT should be incorporated into the standard care of infants with Peter's anomaly.[126] Similarly, Bradfield et al. used iOCT to determine obstruction of the anterior chamber angle or Schlemm's canal during paediatric glaucoma surgery.[127] In 8 of 13 glaucomatous eyes an obstruction could be observed on the OCT image and in cases with an absent Schlemm's canal the procedure could be directly altered or reverted to a tube-shunt procedure.[127]

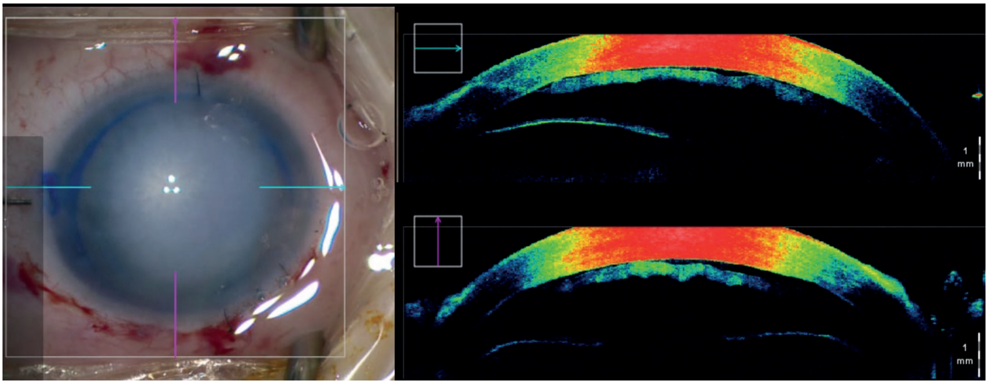

Figure 6. A 3-month-old infant with severe posterior polymorphous dystrophy. Note that the opaque cornea precludes visualization of the anterior chamber. Shown at the right are two perpendicular planes of the cornea (the purple and turquoise crosshairs). In both planes, the DSEK graft is visible as a tissue mass directly under the hyper-reflective cornea. The graft is stretched, but not yet completely attached, prior to the injection of gas. Note that iOCT was invaluable for performing endothelial keratoplasty in this infant.

Furthermore, Sharma et al. compared a cohort of iOCT-assisted paediatric keratoplasty's to a historical cohort.[128] The use of iOCT affected surgical decision making in 45% and 33% of anterior and posterior lamellar keratoplasty.[128] During penetrating keratoplasty significant more concomitant procedures were performed in the iOCT-assisted cohort (29/40) compared to the historical cohort (4/15).[128] Moreover, the incidence of secondary or repeated interventions was significantly lower in the iOCT-assisted group compared to the historical cohort (p=0.04).[128] Similar, Siebelmann et al. found that iOCT proved very useful for diagnosis in paediatric patients and in 5 cases the decision to treat was directly the result of the OCT image.[129]

Lastly, Pihlblad et al. investigated the potential of iOCT during paediatric strabismus surgery.[130] The extraocular muscle insertion distance was measured with different OCT devices and compared to measurements using a calliper in 19 paediatric patients. In 71% and 89% of cases the muscle insertion point was accurately visualized with, respectively, a handheld and microscope integrated OCT device. [130]

DISCUSSION

In this review, we summarized the current knowledge and opportunities provided by OCT during surgery. New research shows that iOCT can actively support the surgeon by providing direct, real-time feedback during surgery. This enables the surgeon – with unprecedented in-depth resolution – to review events, interactions and tissue changes intraoperatively. OCT imaging can improve the safety of surgical procedures, promote the development of novel surgical procedures, and stimulate evidence-based medicine. The use of intrasurgical biomedical imaging has drastically changed other fields of surgery and is increasingly a cornerstone of new procedures.[131,132] In our opinion iOCT has a similar potential to advance ophthalmic surgery.

iOCT is a tool that aids in our clinical understanding of pathophysiology otherwise obscured due to poor visualization, and enabled surgeons to in-vivo study their practice patterns, achieving a greater understanding of the surgical interventions and their respective tissue alterations.[20,21] Nevertheless the current body of research consists of low level evidence studies as the majority of studies consist of case reports/series and pilot studies. Moreover, a lot of studies lack objective measurable outcomes and are therefore poorly comparable. This is a major limitation of this review, as it is difficult to objectively quantify the putative benefits of iOCT. In addition, large studies to date focus mainly on the perceived benefits of the surgeon. Perceived benefits from a patient's perspective should arguably be addressed more in future iOCT research.

Admittedly, iOCT itself has inherent limitations that limit its effectiveness and utility. First, acquisition of an iOCT platform represents a significant investment for most practices. Second, iOCT is a supplementary tool and the presence of the iOCT is not essential to safely performing the surgery itself. Current use of iOCT provides surgeons with new insights and evidence shows this improves surgical management and safety; in particular the detection of complications and if possible treatment. However, it remains debatable if the use of iOCT directly leads to significantly better postoperative outcomes in routine procedures, because most studies lacked a control group or did not find significant differences in postoperative outcomes. This does not mean that altered surgical decision making using iOCT has not improved outcomes for individual patients, but it is unclear to which extend iOCT improves surgical outcomes for the general patient. Third, current methods for manually reviewing the OCT image are inefficient; thus, information that could improve surgical outcome cannot be processed easily by the surgeon.[12] Integrating of tools for automatic information processing and clinical decision aids will increase the efficacy of iOCT, possibly rendering manual reviewing obsolete. Several groups have investigated and/or developed promising algorithms for; macular hole closure[65] or analyses of donor-recipient interface in posterior lamellar keratoplasty.[85,86,133] The use of augmented reality and the application of an stereoscopic OCT interface should be explored.[9] Augmented reality environments may improve the transmission of information, providing the surgeon with – at that moment the most – essential information.[134] The implementation of stereoscopic OCT opens up a new dimension and the volumetric data may be invaluable for future clinical tools.[9,133]

Two major technical limitations of iOCT should be addressed. All OCT technology is limited in the scanning speed and spatial resolution. Most iOCT platforms in use are spectral-domain OCT's with an acquisition speed of ~30.000 A-scan per second, limiting the amount and quality of B-scans that can be made within a reasonable timeframe.[3] Real time visualization of tissue manipulation requires higher a-scan rates and/or more compact scan area's.[135] The use of swept-source OCT intraoperatively could mitigate this limitation. The unprecedented high rate of A-scans per second of swept-source OCT can significantly improve image quality, acquisition speed, and therefore the effectiveness in live imaging of tissue manipulation or interventions.[136] Moreover, swept-source OCT technology uses an 1050 nm wavelength, which has an improved penetrating depth, aiding the use of iOCT in glaucoma surgery. The other technical limitations is most difficult to mitigate; the inability – or with considerable loss of resolution – of OCT to scan through non-transparent, opaque, or cloudy tissue, as shown by the inability to visualize thin and small structures through clouded media.[103]

Frequently encountered limitations and operational hurdles in iOCT is the learning curve and ease of use. The iOCT systems can be difficult to operate and are therefore time-consuming, particularly in the case of certain types of glaucoma and vitreoretinal surgery. Targeting and focusing the iOCT image may be aided by implementation of image tracking and autofocus options. In addition, the use of metallic instruments or other non-transparent tools can obscure the surgeon's actions and cast a shadow on the tissue. However, suitable IR-transparent and iOCT-compatible instruments have been tested and will likely be available in the near future, although these instruments result in significant investments next to the iOCT-platform.[12]

Lastly, advances in iOCT may also facilitated the development of robotic surgical systems, and we expect iOCT to reach its full potential in this field. For example, iOCT can aid navigation and provide direct feedback to the surgical robot as is already shown in the *in vivo* distance measurements of the Preceyes' ophthalmic surgical robot platform.[137,138]

In summary, iOCT is a promising new advancement in ophthalmic surgery with the ability to revolutionize ophthalmic surgery and improve treatment outcomes. Though adaption barriers and technical limitations need to be addressed. Ideally, future iOCT platforms should have a modular design, have image tracking and autofocus or able to handle voice-activated controls, and offer extensive review capabilities, with the ability to integrate automated image-analysis tools and compatibility with robotic surgical systems.

ACKNOWLEDGEMENTS

The authors are grateful to Nikita Witzenburg, for her assistance in the literature search, assessing the level and quality of evidence, and the critical appraisal of the studies, and to Curtis Barrett PhD for his English editing services.

REFERENCES

1. Fercher AF, Hitzenberger CK, Drexler W, Kamp G SH. In vivo optical coherence tomography. *American Journal of Ophthalmology* 1993; 116: 113–4.
2. Schmidt-Erfurth U, Klimscha S, Waldstein SM, et al. A view of the current and future role of optical coherence tomography in the management of age-related macular degeneration. *Eye (Basingstoke)* 2017; 31: 26–44.
3. Fercher AF. Optical coherence tomography – development, principles, applications. *Zeitschrift für Medizinische Physik* 2010; 20: 251–276.
4. Mura M, Iannetta D, Nasini F, et al. Use of a new intra-ocular spectral domain optical coherence tomography in vitreoretinal surgery. *Acta Ophthalmologica* 2016; 94: 246–252.
5. Geerling G. Intraoperative 2-Dimensional Optical Coherence Tomography as a New Tool for Anterior Segment Surgery. *Archives of Ophthalmology* 2005; 123: 253.
6. Stehouwer M, Verbraak FD, De Vries HR, et al. Scanning beyond the limits of standard OCT with a Fourier domain optical coherence tomography integrated into a slit lamp: The SL SCAN-1. *Eye* 2011; 25: 97–104.
7. Ehlers JP, Tao YK, Farsiu S, et al. Integration of a spectral domain optical coherence tomography system into a surgical microscope for intraoperative imaging. *Investigative Ophthalmology and Visual Science* 2011; 52: 3153–3159.
8. Binder S, Falkner-Radler CI, Hauger C, et al. Feasibility of intrasurgical spectral-domain optical coherence tomography. *Retina* 2011; 31: 1332–1336.
9. Shen L, Carrasco-Zevallos O, Keller B, et al. Novel microscope-integrated stereoscopic heads-up display for intrasurgical optical coherence tomography. *Biomedical optics express* 2016; 7: 1711–1726.
10. Tao YK, Srivastava SK, Ehlers JP. Microscope-integrated intraoperative OCT with electrically tunable focus and heads-up display for imaging of ophthalmic surgical maneuvers. *Biomedical*
11. Seider MI, Carrasco-Zevallos OM, Gunther R, et al. Real-Time Volumetric Imaging of Vitreoretinal Surgery with a Prototype Microscope-Integrated Swept-Source OCT Device. *Ophthalmology Retina* 2018; 2: 401–410.
12. Ehlers JP, Srivastava SK, Feiler D, et al. Integrative advances for OCT-guided ophthalmic surgery and intraoperative OCT: microscope integration, surgical instrumentation, and heads-up display surgeon feedback. *PloS one* 2014; 9: e105224.
13. Ehlers JP, Kaiser PK, Srivastava SK. Intraoperative Optical Coherence Tomography Utilizing the RESCAN 700: Preliminary Results from the DISCOVER study. *British Journal of Ophthalmology* 2014; 98: 1329–1332.
14. Runkle A, Srivastava SK, Ehlers JP. Microscope-integrated OCT Feasibility and Utility with the EnFocus System in the DISCOVER Study. *Ophthalmic Surgery Lasers and Imaging Retina* 2017; 48: 216–222.
15. Moher D, Liberati A, Tetzlaff J, et al. Preferred reporting items for systematic reviews and meta-analyses: the PRISMA statement. *Journal of clinical epidemiology* 2009; 62: 1006–1012.
16. Howick J, Chalmers I, Glasziou P, et al. *Explanation of the 2011 Oxford Centre for Evidence-Based Medicine (OCEBM) Levels of Evidence*. 2011.
17. Group OL of EW. *The Oxford Levels of Evidence 2*. 2011.
18. Munn Z, Barker TH, Moola S, et al. Methodological quality of case series studies: an introduction to the JBI critical appraisal tool. *JBI database of systematic reviews and implementation reports*. Epub ahead of print September 2019. DOI: 10.11124/JBISRIR-D-19-00099.

19. Guyatt G, Oxman AD, Akl EA, et al. GRADE guidelines: 1. Introduction - GRADE evidence profiles and summary of findings tables. *Journal of Clinical Epidemiology* 2011; 64: 383–394.
20. Ehlers JP, Dupps WJ, Kaiser PK, et al. The Prospective Intraoperative and Perioperative Ophthalmic ImagiNg with Optical CoherEncE TomogRaphy (PIONEER) Study: 2-year results. *American journal of ophthalmology* 2014; 158: 999–1007.
21. Ehlers JP, Modi YS, Pecen PE, et al. The DISCOVER Study 3-Year Results: Feasibility and Usefulness of Microscope-Integrated Intraoperative OCT during Ophthalmic Surgery. *Ophthalmology* 2018; 125: 1014–1027.
22. Khan M, Srivastava SK, Reese JL, et al. Intraoperative OCT-assisted Surgery for Proliferative Diabetic Retinopathy in the DISCOVER Study. *Ophthalmology Retina* 2017; 176: 139–148.
23. Abraham JR, Srivastava SK, K Le T, et al. Intraoperative OCT-Assisted Retinal Detachment Repair in the DISCOVER Study: Impact and Outcomes. *Ophthalmology Retina* 2020; 4: 378–383.
24. Ehlers JP, Goshe J, Dupps WJ, et al. Determination of feasibility and utility of microscope-integrated optical coherence tomography during ophthalmic surgery: The DISCOVER study RESCAN results. *JAMA Ophthalmology* 2015; 133: 1124–1132.
25. Yee P, Sevgi DD, Abraham J, et al. iOCT-assisted macular hole surgery: outcomes and utility from the DISCOVER study. *The British journal of ophthalmology*. Epub ahead of print May 2020. DOI: 10.1136/bjophthalmol-2020-316045.
26. Knecht PB, Kaufmann C, Menke MN, et al. Use of intraoperative fourier-domain anterior segment optical coherence tomography during descemet stripping endothelial keratoplasty. *American journal of ophthalmology* 2010; 150: 360-365.e2.
27. Han S, Sarunic M V, Wu J, et al. Handheld forward-imaging needle endoscope for ophthalmic optical coherence tomography inspection. *Journal of biomedical optics* 2008; 13: 1–3.
28. Joos KM, Shen J-H. Miniature real-time intraoperative forward-imaging optical coherence tomography probe. *Biomedical Optics Express* 2013; 4: 1342.
29. Leisser C, Hirnschall N, Hackl C, et al. Diagnostic precision of a microscope-integrated intraoperative OCT device in patients with epiretinal membranes. *European journal of ophthalmology* 2018; 28: 329–332.
30. Ehlers JP, Griffith JF, Srivastava SK, et al. Intraoperative OCT during Vitreoretinal Surgery for Dense Vitreous Hemorrhage in the PIONEER Study. *Retina* 2015; 35: 2537–2542.
31. Tao J, Wu H, Chen Y, et al. Use of iOCT in Vitreoretinal Surgery for Dense Vitreous Hemorrhage in a Chinese Population. *Current eye research* 2019; 44: 219–224.
32. Jusufbegovic D, Ozkok A, Schaal S. Intraoperative Optical Coherence Tomography Validates the Immediate Efficacy of External Diathermy in Sealing 25-Gauge Sclerotomy Wounds. *Retina* 2017; 37: 402–404.
33. Bruyère E, Philippakis E, Dupas B, et al. Benefit of intraoperative optical coherence tomography for vitreomacular surgery in highly myopic eyes. *Retina (Philadelphia, Pa)* 2018; 38: 2035–2044.
34. Ehlers JP, Tam T, Kaiser PK, et al. Utility of intraoperative optical coherence tomography during vitrectomy surgery for vitreomacular traction syndrome. *Retina (Philadelphia, Pa)* 2014; 34: 1341–1346.
35. Rachitskaya A V, Yuan A, Marino MJ, et al. Intraoperative OCT Imaging of the Argus II Retinal Prosthesis System. *Ophthalmic Sur g Lasers Imaging Retina* 2015; 46: 964–966.
36. Kashani AH, Uang J, Mert M, et al. Surgical Method for Implantation of a Biosynthetic Retinal Pigment Epithelium Monolayer for Geographic Atrophy: Experience from a Phase 1/2a Study. *Ophthalmology Retina* 2020; 4: 264–273.

37. Kumar JB, Ehlers JP, Sharma S, et al. Intraoperative OCT for Uveitis-Related Vitreoretinal Surgery in the DISCOVER Study. *Ophthalmology Retina* 2018; 2: 1041–1049.

38. Asahina Y, Tachi N, Asahina Y, et al. Six-month postoperative outcomes of intraoperative OCT-guided surgical cystotomy for refractory cystoid macular edema in diabetic eyes. *Clinical Ophthalmology* 2017; 11: 2099–2105.

39. Vasconcelos HM, Lujan BJ, Pennesi ME, et al. Intraoperative optical coherence tomographic findings in patients undergoing subretinal gene therapy surgery. *International Journal of Retina and Vitreous* 2020; 6: 1–10.

40. Dayani PN, Maldonado R, Farsiu S, et al. Intraoperative use of handheld spectral domain optical coherence tomography imaging in macular surgery. *Retina (Philadelphia, Pa)* 2009; 29: 1457–1468.

41. Falkner-Radler CI, Glittenberg C, Gabriel M, et al. Integrated Spectral Domain Optical Coherence Tomography – Assisted Membrane Peeling. *retina* 2015; 35: 2100–2106.

42. Kumar A, Ravani R, Mehta A, et al. Outcomes of microscope-integrated intraoperative optical coherence tomography-guided center-sparing internal limiting membrane peeling for myopic traction maculopathy: a novel technique. *International ophthalmology* 2018; 38: 1689–1696.

43. Leisser C, Hirnschall N, Palkovits S, et al. Intraoperative Optical Coherence Tomography-Guided Membrane Peeling for Surgery of Macular Pucker: Advantages and Limitations. *Ophthalmologica* 2019; 241: 234–240.

44. Leisser C, Hackl C, Hirnschall N, et al. Visualizing Macular Structures During Membrane Peeling Surgery With an Intraoperative Spectral-Domain Optical Coherence Tomography Device. *Ophthalmic surgery, lasers & imaging retina* 2016; 47: 328–332.

45. hlers JP, McNutt S, Dar S, et al. Visualisation of contrast-enhanced intraoperative optical coherence tomography with indocyanine green. *British Journal of Ophthalmology* 2014; 98: 1588–1591.

46. Ehlers JP, Xu D, Kaiser PK, et al. Intrasurgical dynamics of macular hole surgery: an assessment of surgery-induced ultrastructural alterations with intraoperative optical coherence tomography. *Retina (Philadelphia, Pa)* 2014; 34: 213–221.

47. Ehlers JP, Han J, Petkovsek D, et al. Membrane Peeling-Induced Retinal Alterations on Intraoperative OCT in Vitreomacular Interface Disorders From the PIONEER Study. *Investigative ophthalmology & visual science* 2015; 56: 7324–7330.

48. Uchida A, Srivastava SK, Ehlers JP. Analysis of Retinal Architectural Changes Using Intraoperative OCT Following Surgical Manipulations With Membrane Flex Loop in the DISCOVER Study. *Investigative ophthalmology & visual science* 2017; 58: 3440–3444.

49. Itoh Y, Inoue M, Kato Y, et al. Alterations of Foveal Architecture during Vitrectomy for Myopic Retinoschisis Identified by Intraoperative Optical Coherence Tomography. *Ophthalmologica* 2019; 242: 87–97.

50. Ray R, Barañano DE, Fortun JA, et al. Intraoperative microscope-mounted spectral domain optical coherence tomography for evaluation of retinal anatomy during macular surgery. *Ophthalmology* 2011; 118: 2212–2217.

51. Ehlers JP, Itoh Y, Xu LT, et al. Factors associated with persistent subfoveal fluid and complete macular hole closure in the PIONEER study. *Investigative Ophthalmology and Visual Science* 2014; 56: 1141–1146.

52. Ehlers JP, Khan M, Petkovsek D, et al. Outcomes of Intraoperative OCT-Assisted Epiretinal Membrane Surgery from the PIONEER Study. *Ophthalmology Retina* 2018; 2: 263–267.

53. Leisser C, Hackl C, Hirnschall N, et al. Effect of Subfoveal and Extrafoveal Hyporeflective Zones due to Iatrogenic Traction during Membrane Peeling for Epiretinal Membranes on Postoperative Outcomes. *Ophthalmologica* 2020; 243: 297–302.

54. Leisser C, Hirnschall N, Hackl C, et al. Risk factors for postoperative intraretinal cystoid changes after peeling of idiopathic epiretinal membranes among patients randomized for balanced salt solution and air-tamponade. *Acta Ophthalmologica* 2018; 96: e439–e444.
55. Leisser C, Hirnschall N, Döller B, et al. Effect of Air Tamponade on Postoperative Visual Acuity and Intraretinal Cystoid Changes after Peeling of Idiopathic Epiretinal Membranes in Pseudophakic Patients. *Ophthalmologica* 2020; 243: 37–42.
56. Leisser C, Palkovits S, Hienert J, et al. Effect of iatrogenic traction during macular peeling surgery on postoperative microperimetry. *Ophthalmic Research*. Epub ahead of print 2020. DOI: 10.1159/000507633.
57. Runkle AP, Srivastava SK, Yuan A, et al. Factors Associated with Development of Dissociated Optic Nerve Fiber Layer (DONFL) Appearance in the PIONEER Intraoperative OCT Study. *Retina* 2018; 38: 103–109.
58. Hayashi A, Yagou T, Nakamura T, et al. Intraoperative changes in idiopathic macular holes by spectral-domain optical coherence tomography. *Case reports in ophthalmology* 2011; 2: 149–154.
59. Lytvynchuk LM, Falkner-Radler CI, Krepler K, et al. Dynamic intraoperative optical coherence tomography for inverted internal limiting membrane flap technique in large macular hole surgery. *Graefe's archive for clinical and experimental ophthalmology = Albrecht von Graefes Archiv fur klinische und experimentelle Ophthalmologie* 2019; 257: 1649–1659.
60. Lorusso M, Micelli Ferrari L, Cicinelli MV, et al. Feasibility and Safety of Intraoperative Optical Coherence Tomography-Guided Short-Term Posturing Prescription after Macular Hole Surgery. *Ophthalmic research* 2020; 63: 18–24.
61. Kumar V, Yadav B. A novel intraoperative optical coherence tomography feature predicting macular hole closure. *Retina* 2018; 38: 2045–2050.
62. Inoue M, Itoh Y, Koto T, et al. Intraoperative OCT Findings May Predict Postoperative Visual Outcome in Eyes with Idiopathic Macular Hole. *Ophthalmology Retina* 2019; 3: 962–970.
63. Tao J, Chen H, Zhu L, et al. Macular hole edge morphology predicts restoration of postoperative retinal microstructure and functional outcome. *BMC ophthalmology* 2020; 20: 280.
64. Riazi-Esfahani M, Khademi MR, Mazloumi M, et al. Macular surgery using intraoperative spectral domain optical coherence tomography. *Journal of Ophthalmic and Vision Research* 2015; 10: 309–315.
65. Ehlers JP, Uchida A, Srivastava SK, et al. Predictive Model for Macular Hole Closure Speed: Insights From Intraoperative Optical Coherence Tomography. *Translational vision science & technology* 2019; 8: 18.
66. Nam DH, Desouza PJ, Hahn P, et al. Intraoperative Spectral Domain Optical Coherence Tomography Imaging after Internal Limiting Membrane Peeling in Idiopathic Epiretinal Membrane with Connecting Strands. *Retina* 2015; 35: 1622–1630.
67. Gabr H, Chen X, Zevallos-Carrasco OM, et al. Visualization from intraoperative swept-source microscope-integrated optical coherence tomography in vitrectomy for complications of proliferative diabetic retinopathy. *Retina (Philadelphia, Pa)* 2018; 38: S110–S120.
68. Toygar O, Riemann CD. Intraoperative optical coherence tomography in macula involving rhegmatogenous retinal detachment repair with pars plana vitrectomy and perfluoron. *Eye (London, England)* 2016; 30: 23–30.
69. Leisser C, Varsits R, Findl O. Does perfluoro-n-octane use in 23G vitrectomy for retinal detachment surgery affect the integrity of the ellipsoid zone? *European journal of ophthalmology* 2016; 26: 639–642.
70. Abraham JR, Srivastava SK, Reese JL, et al. Intraoperative OCT Features and Postoperative Ellipsoid Mapping in Primary Macula-Involving Retinal Detachments from the PIONEER Study. *Ophthalmology Retina* 2019; 3: 252–257.

71. Ehlers JP, Ohr MP, Kaiser PK, et al. Novel microarchitectural dynamics in rhegmatogenous retinal detachments identified with intraoperative optical coherence tomography. *Retina (Philadelphia, Pa)* 2013; 33: 1428–1434.

72. Scorcia V, Busin M, Lucisano A, et al. Anterior segment optical coherence tomography-guided big-bubble technique. *Ophthalmology* 2013; 120: 471–476.

73. Au J, Goshe JG, Dupps Jr WJ, et al. Intraoperative Optical Coherence Tomography for Enhanced Depth Visuaization in DALK from PIONEER Study. *Cornea* 2016; 34: 1039–1043.

74. Steven P, Le Blanc C, Lankenau E, et al. Optimising deep anterior lamellar keratoplasty (DALK) using intraoperative online optical coherence tomography (iOCT). *The British journal of ophthalmology* 2014; 98: 900–904.

75. De Benito-Llopis L, Mehta JS, Angunawela RI, et al. Intraoperative anterior segment optical coherence tomography: a novel assessment tool during deep anterior lamellar keratoplasty. *American journal of ophthalmology* 2014; 157: 334-341.e3.

76. Guindolet D, Nguyen DT, Bergin C, et al. Double-Docking Technique for Femtosecond Laser-Assisted Deep Anterior Lamellar Keratoplasty. *Cornea* 2018; 37: 123–126.

77. Zakaria N, Ní Dhubhghaill S, Taal M, et al. Optical Coherence Tomography in Cultivated Limbal Epithelial Stem Cell Transplantation Surgery. *Asia-Pacific journal of ophthalmology (Philadelphia, Pa)* 2015; 4: 339–345.

78. Melles GRJ. Posterior Lamellar Keratoplasty. *Cornea* 2006; 25: 879–881.

79. Muijzer MB, Soeters N, Godefrooij DA, et al. Intraoperative Optical Coherence Tomography-Assisted Descemet Membrane Endothelial Keratoplasty: Toward More Efficient, Safer Surgery. *Cornea* 2020; 39: 674–679.

80. Juthani V V, Goshe JM, Srivastava SK, et al. The Association Between Transient Interface Fluid on Intraoperative OCT and Textural Interface Opacity Following DSAEK Surgery in the PIONEER Study. *Cornea* 2014; 33: 887–892.

81. Miyakoshi A, Ozaki H, Otsuka M, et al. Efficacy of Intraoperative Anterior Segment Optical Coherence Tomography during Descemet's Stripping Automated Endothelial Keratoplasty. *ISRN ophthalmology* 2014; 2014: 562062.

82. Sng C, Gimeno FL, Mehta JS, et al. Intraoperative use of spectral-domain optical coherence tomography during Descemet ' s stripping automated endothelial keratoplasty. *Clinical Ophthalmology* 2012; 6: 479–486.

83. Steverink JG, Wisse RPL. Intraoperative optical coherence tomography in descemet stripping automated endothelial keratoplasty: pilot experiences. *International Ophthalmology*. Epub ahead of print 2016. DOI: 10.1007/s10792-016-0338-9.

84. Cost B, Goshe JM, Srivastava S, et al. Intraoperative optical coherence tomography-assisted descemet membrane endothelial keratoplasty in the DISCOVER study. *American journal of ophthalmology* 2015; 160: 430–437.

85. Xu D, Dupps WJJ, Srivastava SK, et al. Automated volumetric analysis of interface fluid in descemet stripping automated endothelial keratoplasty using intraoperative optical coherence tomography. *Investigative ophthalmology & visual science* 2014; 55: 5610–5615.

86. Hallahan KM, Cost B, Goshe JM, et al. Intraoperative Interface Fluid Dynamics and Clinical Outcomes for Intraoperative Optical Coherence Tomography–Assisted Descemet Stripping Automated Endothelial Keratoplasty From the PIONEER Study. *American Journal of Ophthalmology* 2017; 173: 16–22.

87. Titiyal JS, Kaur M, Falera R, et al. Evaluation of Time to Donor Lenticule Apposition Using Intraoperative Optical Coherence Tomography in Descemet Stripping Automated Endothelial Keratoplasty. *Cornea* 2016; 35: 477–481.

88. Patel AS, Goshe JM, Srivastava SK, et al. Intraoperative Optical Coherence Tomography–Assisted Descemet Membrane Endothelial Keratoplasty in the DISCOVER Study: First 100 Cases. *American Journal of Ophthalmology* 2020; 210: 167–173.

89. Sharma N, Sahay P, Maharana PK, et al. Microscope Integrated Intraoperative Optical Coherence Tomography-Guided DMEK in Corneas with Poor Visualization. *Clinical ophthalmology (Auckland, NZ)* 2020; 14: 643–651.

90. Steven P, Le Blanc C, Velten K, et al. Optimizing Descemet membrane endothelial keratoplasty using intraoperative optical coherence tomography. *JAMA Ophthalmology* 2013; 131: 1135–1142.

91. Saad A, Guilbert E, Grise-Dulac A, et al. Intraoperative OCT-Assisted DMEK: 14 Consecutive Cases. *Cornea* 2015; 34: 802–807.

92. Godefrooij DA, Gans R, Imhof SM, et al. Nationwide reduction in the number of corneal transplantations for keratoconus following the implementation of cross-linking. *Acta Ophthalmologica* 2016; 94: 675–678.

93. Pahuja N, Shetty R, Jayadev C, et al. Intraoperative optical coherence tomography using the RESCAN 700: Preliminary results in collagen crosslinking. *BioMed Research International*; 2015. Epub ahead of print 2015. DOI: 10.1155/2015/572698.

94. Chow VWS, Biswas S, Yu M, et al. Intraoperative pachymetry using spectral-domain optical coherence tomography during accelerated corneal collagen crosslinking. *BioMed research international* 2013; 2013: 848363.

95. Ghaffari R, Mortazavi M, Anvari P, et al. Intraoperative optical coherence tomography to evaluate the effect of the eyelid speculum on corneal pachymetry during accelerated corneal cross-linking (9 mW/cm(2)). *Eye (London, England)* 2018; 32: 579–585.

96. Rechichi M, Mazzotta C, Daya S, et al. Intraoperative OCT Pachymetry in Patients Undergoing Dextran-Free Riboflavin UVA Accelerated Corneal Collagen Crosslinking. *Current Eye Research* 2016; 41: 1310–1315.

97. Ye C, Yu M, Jhanji V. Stromal bed thickness measurement during laser in situ keratomileusis using intraoperative optical coherence tomography. *Cornea* 2015; 34: 387–391.

98. Siebelmann S, Horstmann J, Scholz P, et al. Intraoperative changes in corneal structure during excimer laser phototherapeutic keratectomy (PTK) assessed by intraoperative optical coherence tomography. *Graefe's archive for clinical and experimental ophthalmology* 2018; 256: 575–581.

99. Titiyal JS, Kaur M, Sahu S, et al. Real-time assessment of intraoperative vaulting in implantable collamer lens and correlation with postoperative vaulting. *European journal of ophthalmology* 2017; 27: 21–25.

100. Torbey J, Mehanna C-J, Abdul Fattah M, et al. Comparison of intraoperative vs postoperative optical coherence tomography measurement of implantable collamer lens vaulting. *Journal of cataract and refractive surgery* 2020; 46: 737–741.

101. Bell CM, Hatch W V., Cernat G, et al. Surgeon Volumes and Selected Patient Outcomes in Cataract Surgery. A Population-Based Analysis. *Ophthalmology* 2007; 114: 405–410.

102. Ramachandran, S, Ghanem, A M, Myers SR. Assesment of microsurgery competency - where are we now? *Microsurgery* 2013; 33: 406–415.

103. Das S, Kummelil MK, Kharbanda V, et al. Microscope Integrated Intraoperative Spectral Domain Optical Coherence Tomography for Cataract Surgery: Uses and Applications. *Current Eye Research* 2016; 41: 643–652.

104. Titiyal JS, Kaur M, Ramesh P, et al. Impact of Clear Corneal Incision Morphology on Incision-Site Descemet Membrane Detachment in Conventional and Femtosecond Laser-Assisted Phacoemulsification. *Current eye research* 2018; 43: 293–299.

105. Cendelin J, Rusnak S, Hecova L. Intraoperative Optical Coherence Tomography Analysis of Clear Corneal Incision: Effect of the Lateral Stromal Hydration. *Journal of ophthalmology* 2020; 2020: 8490181.

106. Lytvynchuk LM, Glittenberg CG, Falkner-Radler CI, et al. Evaluation of intraocular lens position during phacoemulsification using intraoperative spectral-domain optical coherence tomography. *Journal of cataract and refractive surgery* 2016; 42: 694–702.

107. Sachdev MS, Malik R, Gupta H, et al. Femtosecond laser-integrated anterior segment optical coherence tomography to detect preexisting posterior capsular dehiscence and increase safety in posterior polar cataracts Mahipal. *Journal of Cataract and Refractive Surgery* 2020; 235–240.

108. Haddad JS, Rocha KM, Yeh K, et al. Lens anatomy parameters with intraoperative spectral-domain optical coherence tomography in cataractous eyes. *Clinical ophthalmology (Auckland, NZ)* 2019; 13: 253–260.

109. Hirnschall N, Norrby S, Weber M, et al. Using continuous intraoperative optical coherence measurements of the aphakic eye for intraocular lens power calculation. *The British journal of ophthalmology* 2015; 99: 7–10.

110. Hirnschall N, Amir-Asgari S, Maedel S, et al. Predicting the postoperative intraocular lens position using continuous intraoperative optical coherence tomography measurements. *Investigative ophthalmology & visual science* 2013; 54: 5196–5203.

111. Hirnschall N, Farrokhi S, Amir-Asgari S, et al. Intraoperative optical coherence tomography measurements of aphakic eyes to predict postoperative position of 2 intraocular lens designs. *Journal of cataract and refractive surgery* 2018; 44: 1310–1316.

112. Amir-Asgari S, Hirnschall N, Findl O. Using continuous intraoperative optical coherence tomography to classify swirling lens fragments during cataract surgery and to predict their impact on corneal endothelial cell damage. *Journal of Cataract and Refractive Surgery* 2016; 42: 1029–1036.

113. Titiyal JS, Kaur M, Shaikh F, et al. Elucidating intraoperative dynamics and safety in posterior polar cataract with intraoperative OCT-guided phacoemulsification. *Journal of cataract and refractive surgery* 2020; 46: 1266–1272.

114. Titiyal JS, Kaur M, Shaikh F, et al. Real-time intraoperative dynamics of white cataract-intraoperative optical coherence tomography-guided classification and management. *Journal of cataract and refractive surgery* 2020; 46: 598–605.

115. Jonas JB, Aung T, Bourne RR, et al. Glaucoma. *The Lancet* 2017; 390: 2183–2193.

116. Dada T, Angmo D, Midha N, et al. Intraoperative Optical Coherence Tomography Guided Bleb Needling. *Journal of ophthalmic & vision research* 2016; 11: 452–454.

117. Kumar RS, Jariwala MU, V SA, et al. A Pilot Study on Feasibility and Effectiveness of Intraoperative Spectral-Domain Optical Coherence Tomography in Glaucoma Procedures. *Translational vision science & technology* 2015; 4: 2.

118. Siebelmann S, Cursiefen C, Lappas A, et al. Intraoperative Optical Coherence Tomography Enables Noncontact Imaging During Canaloplasty. *Journal of glaucoma* 2016; 25: 236–238.

119. Swaminathan SS, Chang TC. Use of intraoperative optical coherence tomography for tube positioning in glaucoma surgery. *JAMA Ophthalmology* 2017; 135: 1438–1439.

120. Junker B, Jordan JF, Framme C, et al. Intraoperative optical coherence tomography and ab interno trabecular meshwork surgery with the Trabectome. *Clinical ophthalmology (Auckland, NZ)* 2017; 11: 1755–1760.

121. Tanito M. Optical Coherence Tomography Observation of Gonio Structures during Microhook Ab Interno Trabeculotomy. *Journal of ophthalmology* 2017; 2017: 6310835.

122. Ishida A, Sugihara K, Shirakami T, et al. Observation of Gonio Structures during Microhook Ab Interno Trabeculotomy Using a Novel Digital Microscope with Integrated Intraoperative Optical Coherence Tomography. *Journal of ophthalmology* 2020; 2020: 9024241.

123. Heindl LM, Siebelmann S, Dietlein T, et al. Future prospects: assessment of intraoperative optical coherence tomography in ab interno glaucoma surgery. *Current eye research* 2015; 40: 1288–1291.

124. J KA, Eleni N, Kuang H, et al. Subconjunctival draining minimally-invasive glaucoma devices for medically uncontrolled glaucoma. *Cochrane Database of Systematic Reviews*. Epub ahead of print 2018. DOI: 10.1002/14651858.CD012742.pub2.www.cochranelibrary.com.

125. Maldonado RS, Izatt JA, Sarin N, et al. Optimizing hand-held spectral domain optical coherence tomography imaging for neonates, infants, and children. *Investigative Ophthalmology and Visual Science* 2010; 51: 2678–2685.

126. Hong J, Yang Y, Cursiefen C, et al. Optimising keratoplasty for Peters' anomaly in infants using spectral-domain optical coherence tomography. *British Journal of Ophthalmology* 2017; 101: 820–827.

127. Bradfield Y, Barbosa T, Blodi B, et al. Comparative Intraoperative Anterior Segment OCT Findings in Pediatric Patients with and without Glaucoma. *Ophthalmology Glaucoma* 2019; 2: 232–239.

128. Sharma N, Priyadarshini K, Agarwal R, et al. Role of Microscope-Intraoperative Optical Coherence Tomography in paediatric keratoplasty: A comparative Study. *American journal of ophthalmology*. Epub ahead of print August 2020. DOI: 10.1016/j.ajo.2020.07.048.

129. Siebelmann S, Hermann M, Dietlein T, et al. Intraoperative optical coherence tomography in children with anterior segment anomalies. *Ophthalmology* 2015; 122: 2582–2584.

130. Pihlblad MS, Troia A, Tibrewal S, et al. Pre-, Intra-, and Post-Operative Evaluation of Extraocular Muscle Insertions Using Optical Coherence Tomography: A Comparison of Four Devices. *Journal of clinical medicine*; 8. Epub ahead of print October 2019. DOI: 10.3390/jcm8101732.

131. Mascagni P, Longo F, Barberio M, et al. New intraoperative imaging technologies: Innovating the surgeon's eye toward surgical precision. *Journal of surgical oncology* 2018; 118: 265–282.

132. Valdés PA, Roberts DW, Lu F-K, et al. Optical technologies for intraoperative neurosurgical guidance. *Neurosurgical focus* 2016; 40: E8.

133. Carrasco-Zevallos OM, Keller B, Viehland C, et al. Live volumetric (4D) visualization and guidance of in vivo human ophthalmic surgery with intraoperative optical coherence tomography. *Scientific Reports* 2016; 6: 1–16.

134. Draelos M, Keller B, Viehland C, et al. Real-time visualization and interaction with static and live optical coherence tomography volumes in immersive virtual reality. *Biomedical optics express* 2018; 9: 2825–2843.

135. hlers JP, Tao Y. Visualization of Real-Time Intraoperative Maneuvers with a Microscope-Mounted Spectrual Domain Optical Coherence Tomography System. *Retina* 2013; 33: 232–236.

136. Kishi S. Impact of swept source optical coherence tomography on ophthalmology. *Taiwan Journal of Ophthalmology* 2016; 6: 58–68.

137. Edwards TL, Xue K, Meenink HCM, et al. First-in-human study of the safety and viability of intraocular robotic surgery. *Nature Biomedical Engineering* 2018; 2: 649–656.

138. Roizenblatt M, Edwards TL, Gehlbach PL. Robot-assisted vitreoretinal surgery: current perspectives. *Robotic surgery (Auckland)* 2018; 5: 1–11.

SUPPLEMENTARY DATA:

Supplementary tables

The supplementary tables 1-8 can be accessed via: https://doi.org/10.5281/zenodo.6375052

- Supplementary table 1: Overview of studies reporting on clinical decision making
- Supplementary table 2: Overview of studies reporting on retinal membrane peeling and macula hole surgery
- Supplementary table 3: Overview of studies reporting on vitreoretinal surgery
- Supplementary table 4: Overview of studies reporting on corneal surgery
- Supplementary table 5: Overview of studies reporting on refractive surgery and corneal crosslinking
- Supplementary table 6: Overview of studies reporting on cataract surgery
- Supplementary table 7: Overview of studies reporting on glaucoma surgery
- Supplementary table 8: Overview of studies reporting on paediatric ophthalmic surgery

PART 2

APPLICATIONS OF INTRAOPERATIVE OPTICAL COHERENCE TOMOGRAPHY IN ENDOTHELIAL KERATOPLASTY

CHAPTER 3

INTRAOPERATIVE OPTICAL COHERENCE TOMOGRAPHY-ASSISTED DESCEMET MEMBRANE ENDOTHELIAL KERATOPLASTY TOWARDS MORE EFFICIENT, SAFER SURGERY

Marc B Muijzer; Nienke Soeters; Daniel A Godefrooij;
Chantal M van Luijk; Robert PL Wisse

Cornea. 2020;39(6)

ABSTRACT

Aim: To evaluate the clinical value of intraoperative optical coherence tomography (iOCT) and prolonged overpressure in Descemet membrane endothelial keratoplasty (DMEK) in terms of surgical safety, efficiency, and outcome.

Methods: All DMEK surgeries performed by the same surgeon from November 2016 through April 2018 at the University Medical Center Utrecht were included, including 6 months of follow-up. The primary outcome was the prevalence of adverse events, and the secondary outcomes included critical decision-making and surgery time. Surgeries that included prolonged (ca.12 minutes) overpressurisation of the globe were classified as group 1, and surgeries without prolonged overpressurisation of the globe were classified as group 2. In all cases, iOCT was used to determine the graft orientation, apposition, and assessment of interface fluid.

Results: A total of 38 cases were included in for analysis. In group 1 seven (43.6%) and in group 2 four (18.1%) adverse events were recorded (P=0.29). Specifically in group 1 and group 2, four and three of cases, respectively, required re-bubbling due to graft dislocation (*P*=0.15). In 43% of surgeries, iOCT proved to be of value for surgical decision-making. Surgery time differed significantly between group 1 and group 2 (*P*<0.001) and was the result of a shortened pressurization time in group 2.

Conclusion: iOCT provides a direct assessment of graft orientation and apposition, allowing the surgeon to refrain from prolonged pressurisation of the globe after graft insertion. Optimising the surgical protocol using iOCT can lead to a significant reduction in surgery time without compromising surgical safety or outcome.

INTRODUCTION

Descemet membrane endothelial keratoplasty (DMEK) is currently the preferred posterior lamellar keratoplasty (PLK) procedure for treating uncomplicated cases of Fuchs endothelial corneal dystrophy (FECD),[1] a progressive and irreversible corneal disease.[2] DMEK is considered superior to Descemet stripping endothelial keratoplasty (DSEK) in terms of visual recovery.[3] However, the thinner graft used for DMEK is more vulnerable to damage due to intraocular graft manipulation. In addition, visualising the graft with DMEK is problematic due to the graft's naturally high transparency, making it difficult to assess complete apposition of the graft. Moreover, poor graft adherence is believed to contribute to postoperative graft detachment.[4] Graft detachment is a relatively frequent and burdensome adverse event associated with all forms of PLK, [5] and several techniques can be used to achieve complete graft apposition to optimize graft adherence, including venting incisions, overpressurising the ocular globe, prolonged air tamponade, and/or corneal swiping.[6–10] However, neither the putative effects of these techniques nor their contribution to a successful outcome can be determined adequately during surgery.

In the past decades, optical coherence tomography (OCT) has become a widely used ophthalmic diagnostic tool.[11] OCT uses infrared light interferometry to generate an in-depth image of the corneal and/or retinal tissue. Importantly, because OCT is non-invasive and does not emit harmful radiation, it is considered safe even when used repeatedly.[11] Positive experiences using a portable OCT devices during ophthalmic surgery led to the integration of OCT into the ophthalmic microscope,[12–14] and several intraoperative optical coherence tomography (iOCT) platforms are now commercially available.[15]

The use of iOCT in ophthalmic surgery is increasing, and evidence suggests that iOCT can aid in the surgical decision-making process. In the DISCOVER (Determination of Feasibility and Utility of Microscope-Integrated Optical Coherence Tomography During Ophthalmic Surgery) study, Ehlers et al. found that in 38% of corneal transplant surgeries, the surgeon ultimately made a different - yet critical - surgical decision based on the OCT image.[16] The value of using iOCT during PLK is that it can be used to objectively determine the interface between the graft and host tissue, as shown in **Figure 1**.[17,18] Moreover, iOCT can be used to determine whether complete graft apposition has been achieved using the aforementioned techniques. In particular, iOCT can be used to determine the need to apply prolonged overpressurisation to the globe, a time-consuming and potentially harmful technique in which intraocular pressure is increased to approximately two or three times the normal pressure for a predetermined period of time.[19,20] Indeed, several relatively small studies reported that iOCT may be used to shorten the overpressurisation time in both DMEK and DSEK surgery.[21,22] Finally, the ability to assess the graft during surgery can help the surgeon determine the graft's orientation and avoid unnecessary manipulation.[23,24] New insights about the use of prolonged overpressure emerged after the introduction of the iOCT. Subsequently our surgical protocol was altered and the surgeon refrained from prolonged overpressure during surgery. Here, we report our experiences with iOCT-assisted DMEK surgery and our experiences with the subsequent optimisation of our surgical protocol. Specifically, we retrospectively analysed clinical outcomes in two historical cohorts, one using standard prolonged overpressurisation of the globe during surgery and the other using only brief overpressurisation.

METHODS

The patients included in our analysis underwent iOCT-assisted DMEK surgery between November 24, 2016 and April 23, 2018; November 24, 2016 was chosen as the starting date because this was the date on which iOCT became generally available at our centre, though the surgeon had previous experience with the technology. Patients who underwent combined DMEK-cataract extraction were excluded. The study was approved by the Ethics Review Board of University Medical Center Utrecht (Medical Ethics Committee file no. 18-370) and was performed in accordance with the Declaration of Helsinki and Dutch law regarding research involving human subjects.

The surgeries were retrospectively divided into two groups: group 1 consisted of grafts in which a standard period of prolonged overpressure (defined as ≥12 min of overpressure) was applied to the globe during DMEK surgery, and group 2 consisted of grafts in which only brief overpressure (defined as ≤2 minutes of overpressure, i.e. the optimised surgical protocol) was applied to the globe during surgery. In both groups, graft apposition was evaluated using iOCT. Chronologically, there was considerable overlap between the surgeries of both groups. Donor grafts were allocated by the Dutch Transplant Foundation (*Nederlandse Transplantatie Stichting*) in Leiden, the Netherlands. The grafts for DMEK were cultured and provided pre-cut by the Euro Cornea Bank (Beverwijk, the Netherlands), with a minimum endothelial cell density of 2300 cells/mm^2.

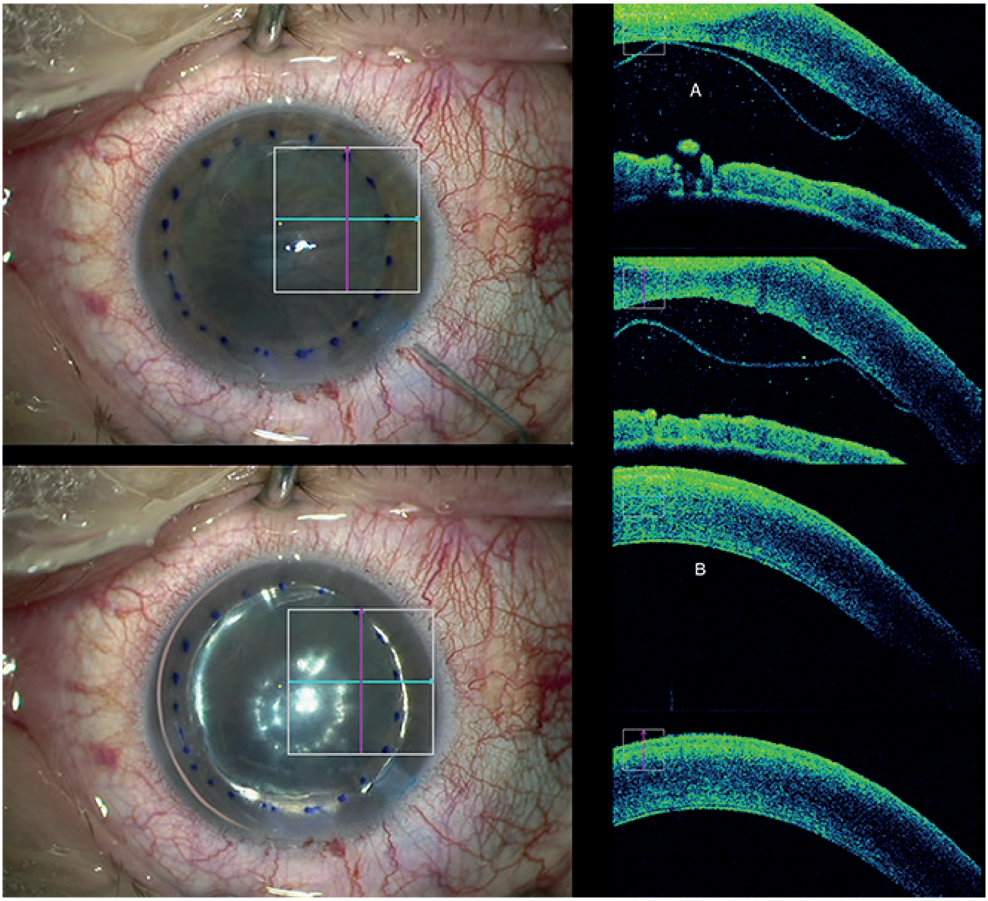

Figure 1. Intraocular DMEK lamella visualised using iOCT before and after pressurising the anterior chamber. Shown are the en face surgical view (left) and iOCT images (right) of a typical DMEK case. The orientation of the free-floating lamella can be judged easily using iOCT. Live iOCT images are reported in two perpendicular planes (the purple and turquoise crosshair). Just after graft insertion, the vertical plane (A) shows an upwards curling of the lamella, indicating proper graft orientation. After the insertion of air, the graft apposition and interface are evident (B).

Preoperative and postoperative examinations

Each patient underwent an ophthalmic examination preoperatively (i.e. at baseline) and 1 day, 1 week, 1 month, 3 months, and 6 months after surgery. Here, we report only the baseline, 3-month, and 6-month assessments and all postoperative adverse events in detail. The ophthalmic examinations included a full slit-lamp examination, fundus examination, intraocular pressure measurement, Scheimpflug tomography (Pentacam HR type 70900, Oculus GmbH, Wetzlar, Germany), automated refraction (KR8800, Topcon, Tokyo, Japan), and manifest refraction

(CV3000, Topcon). Corrected distance visual acuity (CDVA) was measured using a visual acuity chart (CC100P, Topcon) at a distance of 6 metres. At the 6-month follow-up visit, endothelial cell density was also measured (EM-4000, Tomey, Nürnberg, Germany).

Surgical procedure

All DMEK surgeries were performed by the same corneal surgeon (RW). First, a 2.8-mm self-sealing sclerocorneal incision was made at the 12 o'clock position. Next, a descemetorhexis was performed using a Price hook (Ambler Surgical, Exton, PA), followed by a surgical peripheral iridectomy at the 6 o'clock position. The pre-cut DMEK graft was stained with VisionBlue (DORC International, Zuidland, the Netherlands) and inserted into the anterior chamber using a glass injector (Geuder AG, Heidelberg, Germany). After the graft was inserted, fluid and air were used to unfold the graft and adhere the graft to the recipient stroma. A microscope-integrated OCT (Lumera 700 OPMI Rescan, Zeiss GmbH, Oberkochen, Germany) was then used to assess the graft's orientation and apposition, paying special attention to minor detachments, interface fluid, and any peripheral folds as described by Steven et al. and Xu et al.[25,26] Specifically, the orientation of the graft was based on the natural inward curling of the Descemet-endothelium complex.

In group 1, the surgeon filled the complete anterior chamber with sulphur hexafluoride (SF6) gas at approximately 30-50 mmHg in order to overpressurise the globe; this pressure was maintained for 12-15 minutes in accordance with our local PLK protocol.[23] In group 2, the anterior chamber was briefly pressurised, defined as ≤2 minutes in order to adhere the graft to the recipient stroma, and graft apposition was assessed using the iOCT image. Interface fluid, folds, and/or detachments were treated if deemed necessary by the surgeon. Once proper apposition was verified, the pressure was returned to normal. In both groups, the pressure was normalised by partially replacing SF6 gas with balanced salt solution (Alcon Ltd., Fort Worth, TX), leaving gas bubble approximately 8.5 mm in diameter (the same size as the transplant diameter). No venting incisions were made. After surgery, the patient was instructed to remain in the supine position for 2-4 hours. All patients received a peribulbar injection of 4 mg/ml dexamethasone. Surgery time (defined as the time from the first incision to the end of surgery) was documented in the surgical report. Standard postoperative medication included 0.3% ofloxacin EDO eye drops (Bausch & Lomb, Schiphol-Rijk, the Netherlands) QID for 10 days, 0.5% prednisolone ointment (Ursapharm, Luik, Belgium) daily at bedtime for 1 month, and 0.1% conservative-free dexamethasone eye drops (Thea Pharma Benelux, Wetteren, Belgium) QID for 3 months. In the event of graft detachment, re-bubbling was performed using the same procedure that was used to adhere the graft during the initial surgery.

Statistical analysis

Data were analysed using SPSS 25.0 (IBM Corp., Armonk, NY). The measured visual acuity was recalculated to a LogMAR (logarithm of the minimum angle of resolution) value for analysis. Preoperative and postoperative measurements and complications were analysed using the Student's *t*-test or Fischer's exact test. Binary logistic regression was used to perform a multivariable analysis in order to identify factors associated with graft dislocation. Differences with a *p*-value of <0.05 were considered statistically significant. Graphs were generated using GraphPad Prism (GraphPad Software Inc., La Jolla, CA).

3

RESULTS

A total of 46 DMEK surgeries were performed from November 24, 2017 through April 23, 2018. Eight of these surgeries were excluded from our analysis because they were combined with cataract extraction; thus, 38 surgeries were included in our analysis (with 16 and 22 surgeries in group 1 and group 2, respectively). The indication for surgery was FECD (32 cases), previous graft failure (5 cases), and bullous keratopathy (1 case). Six patients had pre-existing glaucoma, three patients had pre-existing retinal pathology, and two patients were amblyopic. The distribution of indications and pre-existing ophthalmic conditions was similar between the two groups, and the two groups had similar baseline measurements and donor characteristics. The baseline measurements and donor characteristics are summarised in **Table 1**.

Table 1. Summary of baseline measurements and graft characteristics of the study cohort (n=38 subjects)

		Group 1 (n=16)	Group 2 (n=22)	*p*-value
Recipient characteristics				
Age, years		70±9.74	70±10.08	0.94
Male gender, n (%)		13 (61.9%)	10 (47.6%)	0.35
CDVA	Decimal	0.51±0.26	0.43±0.25	0.34
	LogMAR	0.36±0.27	0.55±0.53	0.20
Pachymetry, µm		656±83	654±144	0.97
Graft characteristics				
Donor age, years		70±6.73	74±4.52	0.06
Graft ECD, cells/mm^2		2644±103	2677±147	0.44

CDVA, corrected distance visual acuity; ECD, endothelial cell density; LogMAR, logarithm of the minimum angle of resolution.

Except where indicated otherwise, data are presented as the mean ± standard deviation.

Surgical outcome

The use of brief overpressurisation instead of prolonged overpressurisation during surgery significantly reduced surgery time between the groups (**Table 2**). Specifically, mean surgery time was reduced from 59.88±12.03 minutes in group 1 to 44.41±11.61 minutes in group 2 (P<0.001).

The iOCT image also provided the surgeon with additional information, including unclear graft orientation, incorrect graft orientation, interface fluid, and minor graft detachments. In 16 surgeries (42% of cases, **Table 2**), this altered the surgical decision-making process. In 8 surgeries (21% of cases), OCT revealed an interface fluid or minor detachment of the graft, findings that were not noted using the en face surgical microscope view; in 4 cases, these findings led to additional intraoperative manipulation and were resolved before end of surgery. In 12 surgeries the iOCT image provided crucial information regarding the graft's orientation. In 6 cases, the iOCT image revealed an incorrect graft orientation, and these grafts were subsequently re-orientated. In another 6 cases, the iOCT image provided crucial information in determining graft orientation not noticeable using the en face surgical microscope view. The orientation of the graft was correctly determined using iOCT in all 38 surgeries.

Table 2. surgical and postoperative events for group 1 and group 2

	Group 1 (n=16)	**Group 2 (n=22)**	**Total (n=38)**	***p*-value**
Graft-related adverse events	*7 (44%)*	*4 (18%)*	*11 (29%)*	0.29
Graft dislocation, requiring re-bubbling, n (%)	*4 (25.0%)*	*3 (13.6%)*	7	0.15
Graft failure, n (%)	3 (18.8%)	1 (4.5%)	4	0.29
Altered surgical decision making based on iOCT image, n (%)	*7 (44%)*	*9 (41%)*	*16 (42%)*	*0.77*
Interface irregularities on IOCT image, n (%)	4 (25%)	4 (18%)	8	NA
Additional manipulation based on iOCT image, n (%)	2 (12,5%)	2 (9%)	4	NA
Incorrect graft orientation, n (%)	3 (19%)	3 (14%)	6	NA
Crucial information regarding graft's orientation, n (%)	2 (12,5%)	4 (18%)	6	NA
Postoperative rise in IOP, n (%)	*2 (12,5%)*	*6 (27%)*	*8 (21%)*	*0.43*
Iatrogenic, n	1	1	2	NA
Steroid induced, n	1	4	5	NA
Unknown cause, n	0	1	1	NA
Surgery duration				
Surgical skin-to-skin time (minutes)	59.88±12.03	44.41±11.61	NA	<0.001
Overpressure duration (minutes)	12.19±0.75	1.05	NA	<0.001

iOCT, intraoperative optical coherence tomography; NA, not assessed: *p*-values only determined for primary outcome parameters

Clinical outcomes

The prevalence of adverse events did not differ significantly between the two groups (**Table 2**). Four graft failures occurred and required a new graft; three of these events were in group 1, and one event was in group 2. No known risk-factors associated with the occurrence of graft detachments were identified (**Table 3**).

Table 3. Binary logistics multivariable predictor analysis for graft dislocation Descemet membrane endothelial keratoplasty

Predictors	B coefficient	95% CI	*p*-value
Preoperative pachymetry (μm)	-0.019 (0.10)	0.962 to 1.001	0.060
Prior graft failure	-22.296 (12502.76)	0.000 to 1.000	0.999
Donor age (years)	0.161 (0.152)	0.871 to 1.583	0.291
Surgical skin-to-skin time (minutes)	0.011 (0.069)	0.883 to 1.158	0.871
Overpressure duration (minutes)	0.246 (0.149)	0.995 to 1.711	0.099
Sulphur hexafluoride gas (reference: air)	2.432 (1.548)	0.548 to 236.481	0.116
Intraoperative adverse events	-3.630 (1.941)	0.001 to 1.190	0.061
Postoperative supine duration (hours)	0.729 (1.207)	0.195 to 22.069	0.546

CI; coincidence interval, SE; standard error

A total of 8 patients developed a postoperative rise in intraocular pressure (IOP) that required treatment (**Table 4**). Two of these cases were the result of iatrogenic acute glaucoma due to gas tamponade in the anterior chamber; after venting the anterior chamber, IOP returned to normal. In five cases, IOP returned to normal after an accelerated tapering of postoperative steroid-containing eye drops and two patients required chronic IOP-lowering medication in order to maintain normal IOP. Finally, one patient in group 2 developed an idiopathic medically uncontrollable rise in IOP and received a glaucoma valve. No association was found in these patients in relation to a higher incidence of graft detachment/failure or a lower endothelial cell count (data not shown).

At the 6-month follow-up visit, corrected distance visual acuity (CDVA) improved significantly in both groups compared to baseline (P=0.001) and did not differ significantly between the two groups (**Table 2**). Interestingly, group 2 had a slightly lower mean CDVA outcome at the follow-up visits. An in-depth analysis of the patients' medical files revealed that several subjects did indeed have potentially poorer visual acuity due to the severity of ocular comorbidity such as macular pathology. Moreover, graft dislocation, which required re-bubbling, did not result in poorer CDVA measured at the 3-month (P=0.25) or 6-month (P=0.97) follow-up visit. The endothelial cell density at 6 months is not statistically different, with group 2 having a slightly higher ECD measured (**Table 4**).

Table 4. Surgical outcome for group 1 and group 2.

Clinical outcomes		Group 1 (n=16)	Group 2 (n=22)	*p*-value
CDVA at 3 months	Decimal	0.68±0.25	0.65±0.32	0.78
	LogMAR	0.20±0.18	0.30±0.43	0.39
CDVA at 6 months	Decimal	0.88±0.34	0.73±0.32	0.23
	LogMAR	0.08±0.15	0.20±0.26	0.19
ECD at 6 months, cells/mm^2		1601±347	1800±480	0.25
Pachymetry at 6 months, µm		511±42	498±40	0.38

CDVA, corrected distance visual acuity; ECD, endothelial cell density; LogMAR, logarithm of the minimum angle of resolution; NA, not applicable.
Except where indicated otherwise, data are presented as the mean ± standard deviation.

DISCUSSION

Here, we report our experiences with iOCT and the clinical outcomes of refraining from overpressure. Based on advancing insights emerged from the iOCT imagery we revised our surgical protocol and refrain from overpressurising the globe for a prolonged period during DMEK surgery. This is clinically relevant, as high IOP could damage cornea endothelial cells, the retinal nerve fiber layer and/or aggravate (existing) glaucoma.[19,20] Moreover, we found that refraining from overpressuring the globe reduced overall surgical time (-24%), without jeopardizing its safety. The reduced surgical time is especially relevant aspect when surgery is performed under local anesthesia.

Importantly, the prevalence of adverse events - in particular, graft dislocation that required re-bubbling - was comparable to previous reports.[27,28] Although the lower prevalence of primary graft failure in group 2 was not significantly different than in group 1, this difference is clinically significant and may be due to intensified the relatively brief overpressurisation of the ocular globe in group 2. The longer period of overpressure in group 1 could have resulted in increased endothelial cell damage and a less viable graft explaining the difference between the groups.[29]

In our multivariable analysis, we found no associated factors or predictors that appeared to influence postoperative graft detachment or graft failure. Importantly, we found no association between graft detachment and either re-bubbling or previous graft failure, both of which have been reported to increase the risk of graft detachment.[30] In addition, no difference between the groups was found in CDVA measured at both the 3-month and 6-month follow-up visits.

The use of iOCT changed the surgical decision-making process in 42% of cases. This finding is consistent with previous findings reported by Ehlers et al. in the PIONEER (Prospective

Intraoperative and Perioperative Ophthalmic Imaging with Optical Coherence Tomography) and DISCOVER (Determination of feasibility and utility of microscope-integrated optical coherence tomography during ophthalmic surgery) studies.[15,16,31] We found that iOCT imaging was particular advantageous for assessing graft orientation. By using the iOCT, we found that six grafts were incorrectly orientated in the anterior chamber (i.e., upside down), and allowed for the timely management of these incorrectly orientated grafts. In addition, the iOCT was of crucial importance in another six surgeries, preventing additional manipulation of the graft.

Several other studies support the notion that iOCT can be used to reduce the duration of overpressurisation. For example, Stevens et al. retrospectively analyzed twenty-six DMEK surgeries and found that air tamponade duration could be reduced from 60-90 minutes to only 4 minutes.[26] In addition, in DSEK surgery Titiyal et al. found that the graft was well apposed after 3 minutes of overpressurisation in DSEK surgery, even though the air tamponade was maintained for at least 5 minutes in their study.[32]

Our results suggest that prolonged overpressurisation of the globe may be rendered obsolete in DMEK surgery. Moreover, our results cast doubt on the putative advantages of prolonged overpressurisation during DMEK surgery in general. However, we acknowledge that the retrospective nature of our analysis nor randomization of subjects precludes an independent assessment.

Our study is not a rigorous comparison and lacked the necessary power to compare adverse events between our two groups in relation to prolonged overpressure and/or iOCT use, the similar prevalence of adverse events between groups suggests that prolonged overpressurisation does not appear to affect the risk of graft detachment following DMEK surgery. Nevertheless, these results warrant future studies and have led to the design of a clinical trial to evaluate the benefits of using iOCT and the effect of refraining from prolonged overpressurisation in DMEK surgery.[33]

It is important to note that the use of iOCT may lead to additional manipulation and/or a more aggressive surgical approach, as suggested by Hallahan et al.[24] The use of iOCT enables the surgeon to assess the graft and interface in high detail and can therefore reveal interface fluid and/or minor detachment of the graft, as we found in eight surgeries. Although the clinical significance of these findings is unclear, intervention was deemed to be necessary in four of these eight cases. Nevertheless, rigorous manipulation of the graft should be avoided at all times in order to minimize the risk of graft damage and loss of endothelial cells.[34,35] A qualitative assessment of graft manipulation was beyond the scope of our study and clearly warrants future study.

In summary, iOCT is a promising new advance in lamellar corneal surgery - particularly in posterior lamellar keratoplasty - for intrasurgical assessment. The iOCT had a considerable effect on clinical decision-making. Importantly the insights obtained from iOCT were leading in the decision to refrain from prolonged overpressure of the globe. Refraining from prolonged overpressurisation did not jeopardize patient safety and decreased our surgical time by 24%. The findings on the iOCT imagery and the clinical outcome of this study support the hypothesis overpressure can be eliminated in DMEK surgery.

REFERENCES

1. Dapena I, Ham L, Melles GRJ. Endothelial keratoplasty: DSEK/DSAEK or DMEK - the thinner the better? *Current Opinion in Ophthalmology* 2009; 20: 299–307.
2. Eghrari AO, Gottsch JD. Fuchs Corneal Dystrophy. *Expert Review Ophthalmology* 2010; 5: 147–159.
3. Parker J, Parker JS, Melles GR. Descemet Membrane Endothelial Keratoplasty—A Review. *US Ophthalmic Review* 2013; 06: 29.
4. Quilendrino R, Rodriguez-Calvo de Mora M, Baydoun L, et al. Prevention and Management of Graft Detachment in Descemet Membrane Endothelial Keratoplasty. *Archives of Ophthalmology* 2012; 130: 280–291.
5. López EF, Baydoun L, Gerber-Hollbach N, et al. Rebubbling techniques for graft detachment after descemet membrane endothelial keratoplasty. *Cornea* 2016; 35: 759–764.
6. Bhogal MS, Angunawela RI, Bilotti E, et al. Theoretical, experimental, and optical coherence tomography (OCT) studies of graft apposition and adhesion in descemets stripping automated endothelial keratoplasty (DSAEK). *Investigative Ophthalmology and Visual Science* 2012; 53: 3839–3846.
7. Dapena I, Moutsouris K, Droutsas K, et al. Standardized "No-Touch" Technique for Descemet Membrane Endothelial Keratoplasty. *Archives of Ophthalmology* 2011; 129: 88–94.
8. Price FW, Price MO. Descemet's stripping with endothelial keratoplasty in 200 eyes. Early challenges and techniques to enhance donor adherence. *Journal of Cataract and Refractive Surgery* 2006; 32: 411–418.
9. Terry MA, Straiko MD, Veldman PB, et al. Standardized DMEK Technique: Reducing Complications Using Prestripped Tissue, Novel Glass Injector, and Sulfur Hexafluoride (SF6) Gas. *Cornea* 2015; 34: 845–852.
10. Melles GRJ, Ong TS, Ververs B, et al. Preliminary Clinical Results of Descemet Membrane Endothelial Keratoplasty. *American Journal of Ophthalmology*; 145. Epub ahead of print 2008. DOI: 10.1016/j.ajo.2007.09.021.
11. Fercher AF. Optische Kohärenz-Tomographie - Entwicklung, Grundlagen, Anwendungen. *Zeitschrift fur Medizinische Physik* 2010; 20: 251–276.
12. Ehlers JP, Dupps WJ, Kaiser PK, et al. The prospective intraoperative and perioperative ophthalmic imaging with optical CoherEncE TomogRaphy (PIONEER) study: 2-year results. *American Journal of Ophthalmology* 2014; 158: 999–1007.
13. Tao YK, Ehlers JP, Toth CA, et al. Intraoperative spectral domain optical coherence tomography for vitreoretinal surgery. *Optics letters* 2010; 35: 3315–3317.
14. Ehlers JP, Tao YK, Farsiu S, et al. Integration of a spectral domain optical coherence tomography system into a surgical microscope for intraoperative imaging. *Investigative ophthalmology & visual science* 2011; 52: 3153–3159.
15. Ehlers JP, Modi YS, Pecen PE, et al. The DISCOVER Study 3-Year Results. Feasibility and Usefulness of Microscope-Integrated Intraoperative OCT during Ophthalmic Surgery. *Ophthalmology* 2018; 1–14.
16. Ehlers JP, Goshe J, Dupps WJ, et al. Determination of feasibility and utility of microscope-integrated optical coherence tomography during ophthalmic surgery: The DISCOVER study RESCAN results. *JAMA Ophthalmology* 2015; 133: 1124–1132.
17. Xu D, Dupps WJ, Srivastava SK, et al. Automated Volumetric Analysis of Interface Fluid in Descemet Stripping Automated Endothelial Keratoplasty Using Intraoperative Optical Coherence Tomography. *Investigative Opthalmology & Visual Science* 2014; 55: 5610–5615.

18. Hallahan KM, Cost B, Goshe JM, et al. Intraoperative Interface Fluid Dynamics and Clinical Outcomes for Intraoperative Optical Coherence Tomography–Assisted Descemet Stripping Automated Endothelial Keratoplasty From the PIONEER Study. *American Journal of Ophthalmology* 2017; 173: 16–22.
19. Janson BJ, Alward WL, Kwon YH, et al. Glaucoma-associated corneal endothelial cell damage: A review. *Survey of Ophthalmology* 2018; 63: 500–506.
20. Fortune B, Yang H, Strouthidis NG, et al. The effect of acute intraocular pressure elevation on peripapillary retinal thickness, retinal nerve fiber layer thickness, and retardance. *Investigative Ophthalmology and Visual Science* 2009; 50: 4719–4726.
21. Titiyal JS, Kaur M, Falera R, et al. Evaluation of Time to Donor Lenticule Apposition Using Intraoperative Optical Coherence Tomography in Descemet Stripping Automated Endothelial Keratoplasty. *Cornea* 2016; 35: 477–481.
22. Steven P, Le Blanc C, Velten K, et al. Optimizing Descemet membrane endothelial keratoplasty using intraoperative optical coherence tomography. *JAMA Ophthalmology* 2013; 131: 1135–1142.
23. Steverink JG, Wisse RPL. Intraoperative optical coherence tomography in descemet stripping automated endothelial keratoplasty: pilot experiences. *International Ophthalmology*. Epub ahead of print 2016. DOI: 10.1007/s10792-016-0338-9.
24. Hallahan KM, Cost B, Goshe JM, et al. Intraoperative Interface Fluid Dynamics and Clinical Outcomes for Intraoperative Optical Coherence Tomography–Assisted Descemet Stripping Automated Endothelial Keratoplasty From the PIONEER Study. *American Journal of Ophthalmology* 2017; 173: 16–22.
25. Xu D, Dupps WJ, Srivastava SK, et al. Automated Volumetric Analysis of Interface Fluid in Descemet Stripping Automated Endothelial Keratoplasty Using Intraoperative Optical Coherence Tomography. *Investigative Opthalmology & Visual Science* 2014; 55: 5610.
26. Steven P, Le Blanc C, Velten K, et al. Optimizing Descemet membrane endothelial keratoplasty using intraoperative optical coherence tomography. *JAMA Ophthalmology* 2013; 131: 1135–1142.
27. Droutsas K, Giallouros E, Melles GRJ, et al. Descemet Membrane Endothelial Keratoplasty : Learning Curve of a Single Surgeon. *cornea* 2013; 32: 1075–1079.
28. Guerra FP, Anshu A, Price MO, et al. Descemet's membrane endothelial keratoplasty: Prospective study of 1-year visual outcomes, graft survival, and endothelial cell loss. *Ophthalmology* 2011; 118: 2368–2373.
29. Janson BJ, Alward WL, Kwon YH, et al. Glaucoma-associated corneal endothelial cell damage: A review. *Survey of Ophthalmology* 2018; 63: 500–506.
30. Nahum Y, Leon P, Mimouni M, et al. Factors Associated with Graft Detachment after Primary Descemet Stripping Automated Endothelial Keratoplasty. *Cornea* 2017; 36: 265–268.
31. Ehlers JP, Dupps WJ, Kaiser PK, et al. The prospective intraoperative and perioperative ophthalmic imaging with optical CoherEncE TomogRaphy (PIONEER) study: 2-year results. *American Journal of Ophthalmology* 2014; 158: 999–1007.
32. Titiyal J, Kaur M, Falera R, et al. Evaluation of Time to Donor Lenticule Apposition Using Intraoperative Optical Coherence Tomography in Descemet Stripping Automated Endothelial Keratoplasty. *Cornea* 2016; 35: 477–481.
33. Wisse RPL, Muijzer MB. The ADVISE Study: Advanced Visualization In Corneal Surgery Evaluation (ADVISE). *clinicalTrials.gov*, https://clinicaltrials.gov/ct2/show/NCT03763721 (2018).
34. Ishii N, Yamaguchi T, Yazu H, et al. Factors associated with graft survival and endothelial cell density after Descemet's stripping automated endothelial keratoplasty. *Scientific reports* 2016; 6: 25276.

35. Maier AKB, Gundlach E, Schroeter J, et al. Influence of the difficulty of graft unfolding and attachment on the outcome in descemet membrane endothelial keratoplasty. *Graefe's Archive for Clinical and Experimental Ophthalmology* 2015; 253: 895–900.

CHAPTER 4

OUTCOMES OF THE ADVANCED VISUALIZATION IN CORNEAL SURGERY EVALUATION (ADVISE) TRIAL; A NON-INFERIORITY RANDOMIZED CONTROL TRIAL TO EVALUATE THE USE OF INTRAOPERATIVE OCT DURING DESCEMET MEMBRANE ENDOTHELIAL KERATOPLASTY

Marc B Muijzer; Heleen Delbeke; Mor M Dickman;
Rudy MMA Nuijts; Herke Jan Noordmans;
Saskia M Imhof; Robert PL Wisse

Submitted for publication

ABSTRACT

Aim: To evaluate if an intraoperative-OCT (iOCT) optimized surgical protocol without prolonged overpressure is non-inferior to a standard protocol during Descemet membrane endothelial keratoplasty (DMEK).

Methods: A multicenter international prospective non-inferiority study, powered to include 63 patients scheduled for routine DMEK. Subjects were randomized to the control arm without iOCT-use and raising the intraocular pressure above normal physiological limits for 8 minutes (i.e., overpressure) or the intervention arm with OCT-guidance to assess graft orientation and adherence while refraining from prolonged raising the intraocular pressure. The primary outcome was the incidence of postoperative surgery-related adverse events, defined as rebubbling, graft failure, and iatrogenic acute glaucoma. The non-inferiority margin was set at a risk difference (RD) of 10%. The RD and 95% confidence intervals (95% CI) were calculated from a logistic regression model using 1,000 bootstrap samples. Secondary outcomes included the incidence of graft detachment, surgeon-reported iOCT-aided surgical decision making, surgical time, endothelial cell density (ECD), and corrected distance visual acuity (CDVA).

Results: 65 eyes of 65 subjects were included for analysis. In the control group, 13 adverse events were recorded in 10 subjects compared to 13 adverse events in 12 subjects in the intervention group. The mean unadjusted RD measured 0.38% (95%CI: -9.64–10.64) and the RD adjusted for study site measured -0.32% (95%CI: -10.29–9.84). No significant differences in ECD and CDVA were found between the two groups 3 and 6 months postoperatively. Surgeons reported that iOCT aided surgical decision-making in 40% of cases. Surgical- and graft unfolding time were, respectively, 13% and 27% shorter in the iOCT-group.

Conclusions: iOCT-guided DMEK surgery with refraining from prolonged over-pressuring was non-inferior compared to conventional treatment. Surgery times were reduced considerably, and surgeons reported the iOCT aided surgical decision-making in 40% of cases. Refraining from prolonged overpressure did not affect postoperative ECD or CDVA.

INTRODUCTION

Intraoperative-OCT (iOCT) provides surgeons with real-time feedback to assess surgical events, anatomical changes, and surgical manipulations, otherwise not possible using the *en face* view of the surgical microscope.[1] Numerous studies described the value of this emergent technology in ophthalmic surgery.[1,2] In particular, the iOCT aids clinical-decision making, enables surgeons to in-vivo study their surgical practice patterns, and achieving a greater understanding of pathophysiology and surgical tissue alterations. Nevertheless, most previous studies were observational, had small sample sizes and lacked a control group making it difficult to quantify the putative benefits of iOCT.

One promising surgery to reap the benefits of iOCT is Descemet membrane endothelial keratoplasty (DMEK).[3–6] DMEK is a recent iteration of endothelial keratoplasty and reported advantages include faster visual recovery, superior visual acuity, and reduced rates of endothelial rejection compared to Descemet stripping endothelial keratoplasty.[7–9] Despite these advantages the rate of postoperative adverse events (e.g., graft detachment requiring rebubbling) for DMEK is relatively high with a reported prevalence of ranging between 2% and 82% for rebubbling and 3% and 11% for primary graft failure.[9–12] These adverse events necessitate secondary surgical interventions and are associated with a lower graft viability and survival.[10]

The causes of graft detachment and primary graft failure are considered multifactorial and can be divided into donor, patient, and surgical factors.[10,13] The primary focus of current research considers modifications of surgical techniques to prevent these complications.[14–16] Among other factors, graft adherence issues due to fluids between the donor and recipient, insufficient anterior chamber (AC) tamponade pressure, and graft trauma have been proposed to cause postoperative complications. Several techniques have been described to promote graft adherence, such as corneal swiping and prolonged intraoperative over-pressurising of the eye.[15,17] There is no consensus about the best approach and prolonged overpressurizing the globe has been widely discussed.[16,18–21] It has been theorized that prolonged overpressure may push residual interface fluid into the stroma and improve graft adherence resulting in lower rebubbling rates.[15,16,21] Other research shows a limited effect on DMEK graft adherence.[19,20] On the other hand, overpressure may lead to potential adverse side effects, including endothelial cell loss[16], exacerbation of glaucoma[22], and a compromised retinal perfusion.[23]

iOCT enables surgeons to directly assess graft adherence, the need for additional surgical manoeuvres, and facilitates DMEK orientation without the need for external markings that may damage the graft and increase the risk of complications.[5,6] In the PIONEER and

DISCOVER study Ehlers et al. reported that iOCT aided and altered clinical decision making in, respectively, 48 and 43% of corneal surgeries.[24,25] The iOCT provided valuable feedback in evaluating graft-host apposition, graft positioning, and verifying graft orientation in DMEK. In addition, several studies show promising evidence iOCT enables faster positioning of the graft with fewer manipulations.[3–5]

These insights led to the conceptualization of an iOCT-optimized DMEK surgical protocol by our group, consisting of iOCT-guidance during unfolding and refraining from prolonged over-pressuring of the globe. In a pilot study, the incidence of postoperative adverse events was lower and operation time was shorter using this protocol.[6] Notwithstanding, in this pilot protocol changes were gradually introduced and a control without iOCT guidance was missing. The promising results warranted follow-up in a head-to-head comparison with a conventional surgical protocol. In this study we investigate whether iOCT-guidance can obviate the need for prolonged overpressure in DMEK surgery and can be considered non-inferior to a standard protocol in terms of postoperative adverse events. Here, we present the results of our prospective *Advanced Visualization In Corneal Surgery Evaluation* (ADVISE), a non-inferiority randomized clinical trial designed to answer these questions.

METHODS

Study protocol

All subjects provided written informed consent and were included in the prospective *Advanced Visualization In Corneal Surgery Evaluation* (ADVISE) trial, an international non-inferiority single-blinded RCT to investigate the utility of intraoperative optical coherence tomography (OCT) in DMEK surgery. Subjects underwent surgery between December 2018 and April 2021 in the University Medical Center Utrecht (n = 39), University Hospital Leuven (n = 14), or Maastricht University Medical Center (n= 14).

Inclusion criteria were pseudophakic adult patients with irreversible corneal endothelial dysfunction resulting from Fuchs endothelial corneal dystrophy eligible for DMEK surgery. Exclusion criteria were human-leukocyte antigen matched keratoplasty, any ocular comorbidity other than ocular surface disease, open angle glaucoma, and mild age-related macular degeneration. No combined phaco-emulsification procedures were performed and only one eye per subject was enrolled. Subjects were randomized to either the iOCT-group or control group using minimization randomization stratified for center using an embedded function of the Electronic Data Capture platform (Research Online, Julius Center, Utrecht, The Netherlands). Patients were blinded throughout the study period. The surgeons and researchers could not be blinded, as the surgeons performed the surgery and researchers were present during surgery to facilitate imaging.

All procedures were performed in accordance with the Declaration of Helsinki, local and national laws regarding research (i.e., the Act on Scientific Research Involving Humans), European directives with respect to privacy (General Data Protection Regulation 2016/679), and 2010 CONSORT standards for reporting RCT's.[26] The study was approved by the Ethics Review Boards in The Netherlands and Belgium (Medical Ethics Committee Utrecht file no. 18-487, Ethical committee Leuven file no. S61527) and registered at clinicaltrials.gov (number: NCT03763721) and CCMO.nl (number: NL64392.041.17).

Study measurements

Each patient underwent an ophthalmic examination preoperatively and 1 day, 1 week, 1 month, 3 months, and 6 months after surgery. Here, we report the baseline, 3 months, 6 months, and all adverse events in detail. The ophthalmic examinations included a full slit-lamp examination, fundus examination, intraocular pressure (IOP) measurement, Scheimpflug tomography (Pentacam HR type 70900, Oculus GmbH, Wetzlar, Germany), anterior segment OCT (Utrecht and Leuven: Zeiss Cirrus 5000, Zeiss Meditec, Oberkochen, Germany; Maastricht: Casia SS-1000, Tomey, Nagoya, Japan), and posterior segment OCT (Utrecht and Leuven: Zeiss Cirrus 5000, Zeiss Meditec, Oberkochen, Germany; Maastricht: Spectralis, Heidelberg Engineering GmbH, Heidelberg, Germany), and an endothelial cell count (EM4000, Tomey, Nagoya, Japan; SP-3000; Topcon, Nagoya, Japan). An optometrist measured the manifest refraction and the corrected distance visual acuity (CDVA) using an Early Treatment Diabetic Retinopathy Study (ETDRS) letter chart at 4 meters.

Surgical procedure

Donor grafts were allocated by the Dutch Transplant Foundation (Nederlandse Transplantatie Stichting, Leiden, the Netherlands). The grafts were organ cultured and provided pre-stripped by the ETB-Bislife (Beverwijk, the Netherlands), with a minimum endothelial cell density (ECD) of 2300 cells/mm2 and with a diameter of 8.5 mm. All surgical procedures were performed by experienced corneal surgeons (H.D., R.M.M.A.N, M.M.D., R.P.L.W.), following a largely standardized procedure. Prior to surgery, 27 subjects underwent a Nd:YAG laser iridotomy at 6 o'clock according to the preference of the surgeon. In the other 38 subjects, a surgical iridectomy was performed using a 27-gauge needle and Price hook at 6 o'clock following the Descemetorhexis. In all cases a 2.8 mm corneal incision was made, followed by a

9 mm Descemetorhexis under air in 51 subjects and a viscoelastic device in 14 subjects (Healon; Abbott Medical, Uppsala, Sweden). The graft was stained using trypan blue dye (Membrane blue n = 52, Vision Blue, n = 13, both from DORC, Zuidland, the Netherlands) and inserted into the anterior chamber using a glass injector (Geuder AG, Heidelberg, Germany, n= 52, DORC, Zuidland, the Netherlands, n = 13). No touch technique used to unfold and position the graft.[27] In 33 surgeries the randomization dictated that iOCT was not available to the surgeons. Here, a full AC fill was performed, raising the IOP above normal physiological limits for 8 minutes using air (*overpressure)*. In the other 32 surgeries the graft was positioned as described above, the iOCT (Lumera 700 OPMI Rescan, Zeiss Meditec, Oberkochen, Germany) was available for utilization at the surgeon's discretion during unfolding and used to check for complete adherence of the graft without overpressurizing the eye. At the end of surgery, the air was replaced by 20% Sulphur Hexafluoride gas and the size of the gas bubble was reduced to cover the graft (i.e., same size as the graft). Next, a validation scan of proper apposition by iOCT was performed in both the control and intervention arm, as proposed by the ethical review board. Any irregularities were treated at the discretion of the surgeon. After surgery, patients remained strictly supine for two hours at the hospital and were instructed to remain in the same position for the following 24 hours. All surgeons reported on the quality of the iOCT image and whether the iOCT aided surgical decision-making, such as unfolding the graft and determining orientation of the graft.

All surgical videos were qualitatively analyzed by two graders (M.B.M. and an independent grader blinded for the surgical outcome) to record graft unfolding grade and surgical times. Graft unfolding difficulty was classified in 4 grades depending on the required manipulation and time to unfold/position the graft as earlier described by Maier et al.[28]

Outcome measures

The primary outcome was the incidence of postoperative adverse events, defined as graft detachments requiring surgical intervention (i.e., rebubbling), primary graft failures, or iatrogenic acute glaucoma. Rebubbling was performed at the discretion of the surgeon, though principally when the graft was >30% detached or the detachment involved the visual axis. Secondary outcomes consisted of surgeon reported iOCT-aided surgical decision-making, surgical time, postoperative ECD loss, and CDVA at follow-up.

Directly after the surgery the surgeons was asked on whether the iOCT-aided surgical decision making and if applicable how the iOCT-aided surgical decision making. The surgical time was recorded, and the time of various surgical steps was determined after surgery by manual review of the surgical video. Postoperative ECD loss was determined by calculating the difference between the donor graft ECD and the post-operative specular light microscopy assessments. The ETDRS letter score of the CDVA was converted to logarithm of the minimum angle of resolution (logMAR) units by multiplying the number of letters read by -0.02 log units and adding 1.7 log units.[29] All graft detachments, defined as any non-adherence of the graft noticeable on slit lamp examination and cornea OCT imaging at any time point within 3 months after surgery, were recorded.

Sample size

Power calculation was based on the incidence of postoperative adverse events. The non-inferiority limit was set at 10% and was set as a clinically relevant risk difference (RD), based on clinical judgment and available data at the time of trial design. Thus, non-inferiority would be demonstrated if the upper boundary of the 95% confidence interval (CI) of the RD between both treatment arms is lower than 10%. Assuming an α of 0.05 (1-sided) and a power of 80%, and a non-inferiority limit of 10%, a sample size of at least 60 subjects would be required (30 per treatment arm). Considering a loss to follow up of 5%, the final computed sample size was 63 subjects. The power calculation did not provide for COVID-19 related loss to follow-up (n=4).

Statistical analysis

The primary dependent variable consisted of the total counted adverse events developed by each patient and converted to a proportion for analysis. For the analysis of the primary outcome measure a crude and adjusted marginal risk difference (RD) between the two treatment arms was estimated from a logistic regression model using 1,000 bootstrap samples.[30] The primary analysis was adjusted treatment site to correct for differences in number of inclusions, unacknowledged differences in practice patterns, and surgeon experience. *P*-values cannot be calculated from the described method and only can be estimated using the 95% CI. A stratified analysis was performed to calculate the unadjusted RD for graft detachment, rebubbling, primary graft failure, and iatrogenic acute glaucoma. For a stratified adjusted analysis, it appeared not possible to calculate reliable estimates. A secondary regression analysis was performed to estimate the effect of overpressure duration in minutes on the incidence of graft detachment and area of detachment.

Missing observation of the secondary outcomes; CDVA, central cornea thickness, ECD, retinal nerve fiber layer thickness, and IOP, were imputed using multiple imputation. Missing measurements of subjects that developed a graft failure were considered missing not at random and not imputed. The other missing observations were considered missing at random. The variables concerned and baseline variables concerned were used as predictors for imputing. The number of imputations was equal to the maximum percentage of missing data plus one.

Data are described as mean ±standard deviation (SD) for continuous variables and as individual counts and percentages for dichotomous and categorical variables. All secondary outcomes were analyzed for differences between treatment arms using the student t-test or Fisher-exact test as appropriate. Correction for multiple comparisons was performed using the Bonferroni correction. A 2-sided *p*-value < 0.05 was considered statistically significant. An intention-to-treat analysis was performed for all outcomes measures. All statistical analysis were performed using R statistical software version 4.0.3 (Comprehensive R Archive Network, Vienna, Austria). All statistical analysis were supervised by an independent statistician from the Julius Center for health sciences. In February 2020 an interim analysis and data and safety monitoring board evaluation was performed, recommending to proceed with the study without changes.

RESULTS

A total of 66 eyes of 66 patients were randomized to either the conventional protocol (control group, n = 33) or the iOCT-optimized protocol (intervention group, n = 33). One subject discontinued the study after randomization before undergoing surgery and was replaced by a new subject. In the control group 2 cross-over cases were recorded, in which the iOCT was used to salvage the graft in a complicated procedure. In both cases 8 minutes of overpressure was applied at the end of surgery. All remaining patients in both treatment arms received the allocated treatment. Four serious adverse events were recorded over the course of the study, 3 subjects underwent re-transplantation for primary graft failure and one subject included in the study died of multi-organ failure unrelated to the study before randomization. The deceased subject was subsequently excluded without replacement. In total, 7 subjects were lost to follow-up; 3 subjects dropped out after re-transplantation and 4 subjects were lost to follow-up because of reduction in care delivery caused by the COVID-19 pandemic. For all subjects who underwent surgery (n=65) the primary outcome was obtained and included for analysis (**Figure 1**).

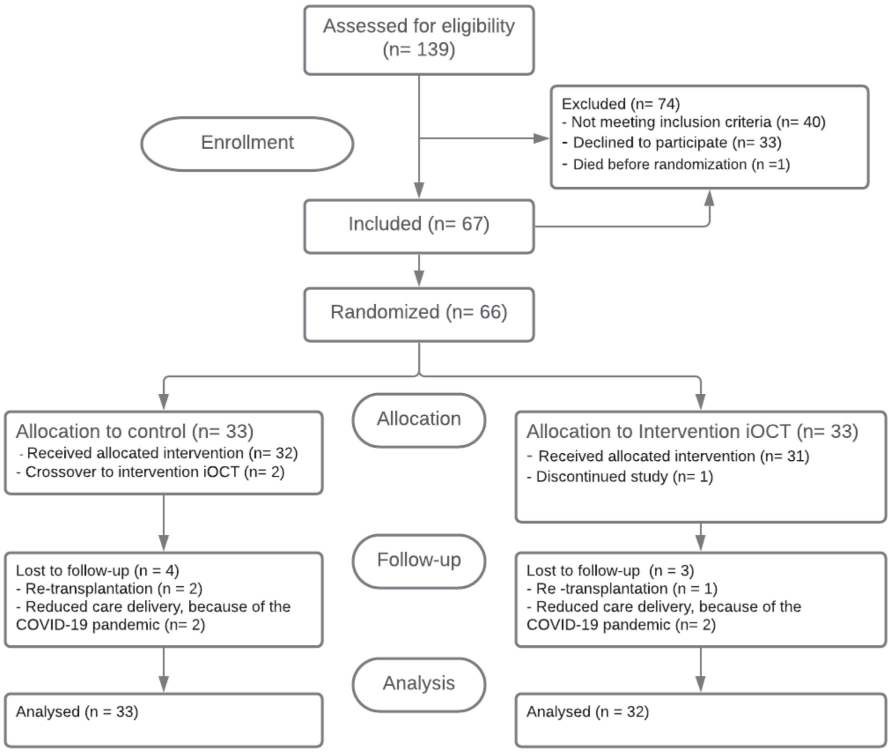

Figure 1. Consolidated standards of reporting trials flowchart. Baseline patient and donor characteristics are displayed in **Table 1**. Commensurate with the 2012 CONSORT guidelines, baseline characteristics were not tested for statistical differences.[26] During the study 5 surgical complications were recorded: 2 cases with endothelial damage due to graft manipulation and 3 cases with an anterior chamber hemorrhage.

Table 1. Baseline Patient and Donor Characteristics

	Conventional protocol (n=33)	iOCT-optimized protocol (n= 32)
Recipient characteristics		
Sex (female), n (%)	17 (52)	17 (53)
Age (years), mean (SD)	72.4 (6.6)	73.3 (6.4)
CDVA (logMAR), mean (SD)	0.42 (0.25)	0.41 (0.26)
Pachymetry (µm), mean (SD)	625 (86)	595 (62)
RFNL thickness (µm), mean (SD)	89 (13)	87 (13)
IOP (mmHg), mean (SD)	12.9 (3.3)	12.6 (3.0)
Corneal edema present, n (%)	15 (45.5)	13 (40.6)
Descemet folds present, n (%)	2 (6.1)	6 (18.8)
Bullae present, n (%)	5 (15.2)	4 (12.5)
Laser iridotomy, n (%)	15 (45.5)	12 (37.5)

	Conventional protocol (n=33)	iOCT-optimized protocol (n= 32)
Donor characteristics		
Age (years), mean (SD)	74.3 (5.0)	73.3 (5.8)
ECD (cells/mm^2), mean (SD)	2706 (174)	2719 (180)

CDVA: corrected distance visual acuity; ECD: endothelial cell density; logMAR: logarithm of the minimum angle of resolution; IOP: intra-ocular pressure; SD: standard deviation; RFNL: retinal nerve fiber layer

Incidence of postoperative adverse events and clinical outcomes

A total of 26 postoperative adverse events were recorded in 22 subjects (control group: 13 adverse events in 10 subjects, intervention group: 13 adverse events in 12 subjects). In the intervention group 17 graft detachments were recorded resulting in 11 rebubbling procedures, compared to 16 detachments resulting in 6 rebubbling procedures in the control group. The area of detachment in cases requiring rebubbling measured 44% (SD ±25%) of the cornea surface in the intervention group compared to 39% (SD ±10%) in the control group (P=0.655, 95%CI: 0.18 – 0.28). Three primary graft failures were recorded (control group n = 2, intervention group n = 1), all cases were preceded by a graft detachment and subsequent rebubbling of the graft. In the control group, 5 cases developed an iatrogenic pupillary block glaucoma in the first 24 hours after surgery compared to 1 case in the intervention group. No statistically significant differences in the incidence of adverse events were found between the intervention group and the control group (**Table 2**).

Table 2. Primary and secondary outcomes after Conventional treatment and iOCT-optimized treatment

Outcomes		Conventional treatment (n=33)	iOCT-optimized treatment (n=32)	p-value [1] (adj[2])
CDVA (LogMAR) mean (SD)				
	3 months	0.14 (0.13)	0.18 (0.19)	0.342(0.684)
	6 months	0.13 (0.14)	0.22 (0.29)	0.138 (0.276)
Pachymetry (µm) mean (SD)				
	3 months	478.33 (40.69)	470.88 (51.54)	0.519 (1.000)
	6 months	486.79 (52.13)	487.16 (55.57)	0.978 (1.000)

Outcomes		Conventional treatment (n=33)	iOCT-optimized treatment (n=32)	p-value [1] (adj[2])
ECD (cells/mm^2) mean (SD)				
	3 months	1852.81 (375.06)	1756.35 (414.97)	0.341 (0.682)
	6 months	1838.06 (359.84)	1708.81 (479.70)	0.235 (0.470)
ECD loss (cells/mm^2) mean (SD)				
	3 months	838.50 (377.48)	963.00 (393.50)	0.213 (0.426)
	6 months	857.37 (334.89)	1010.55 (450.25)	0.138 (0.276)
RFNL thickness (µm) mean (SD)				
	3 months	91.15 (13.31)	90.78 (12.93)	0.910 (1.000)
	6 months	89.85 (12.42)	90.38 (14.51)	0.876 (1.000)
IOP (mmHg) mean (SD)				
	3 months	15.03 (2.98)	15.09 (4.29)	0.945 (1.000)
	6 months	14.36 (3.85)	15.19 (5.15)	0.467 (0.934)
Total adverse events, n (%)[3]		13 (39.4)	13 (40.6)	0.644 (1.00)
Detachments		16 (48.5)	17 (53.1)	0.900 (1.00)
Rebubbling		6 (18.2)	11 (34.4)	0.229 (1.00)
Graft failure		2 (6.1)	1 (3.1)	1.000 (1.00)
Iatrogenic acute glaucoma		5 (15.2)	1 (3.1)	0.213 (1.00)

CDVA: corrected distance visual acuity; ECD: endothelial cell density; logMAR: logarithm of the minimum angle of resolution; IOP: intra-ocular pressure; iOCT: intraoperative optical coherence tomography; SD: standard deviation; RFNL: retinal nerve fiber layer

[1] Independent samples Student´s t-test

[2] Adjusted for multiple comparisons using Bonferroni method

[3] Summation of the primary outcomes, defined as rebubbling, graft failure and iatrogenic glaucoma.

We explored unadjusted and adjusted estimates of the iOCT-optimized surgical protocol on the postoperative adverse event rate. The mean unadjusted risk difference (RD) measured 0.38% (95%CI: -9.64 – 10.64) and the RD adjusted for study site measured -0.32% (95%CI: -10.29 – 9.84), meaning in short that both protocols are comparable with regards to overall surgical safety measured as total postoperative adverse event rate. After controlling for a priori planned adjustment for study site, the iOCT-optimized protocol was found non-inferior to the conventional protocol (**Figure 2**). In addition, the independent effect of overpressure duration measured in minutes was not significantly associated with the incidence of detachment (β: 0.02, 95%CI: -0.10 – 0.15, P= 0.730) or area of detachment (β: -0.012, 95%CI: -0.027 – -0.002, P= 0.121). The unadjusted and adjusted regression models of the primary outcome can be found in **Supplementary table 1**.

When reporting individual adverse events, the results show varying results regarding the RDs. Consistent with the observed adverse events the risk of graft detachment (+4.6%) and rebubbling (+16.1%) are increased compared to a lower risk of graft failure (-2.9%) and iatrogenic acute glaucoma (-12.0%) in the iOCT-optimized protocol. However, the analysis shows a high uncertainty regarding effect sizes for all adverse events and non-inferiority cannot be assessed for these stratified outcomes, because the study was not powered on these separate adverse events.

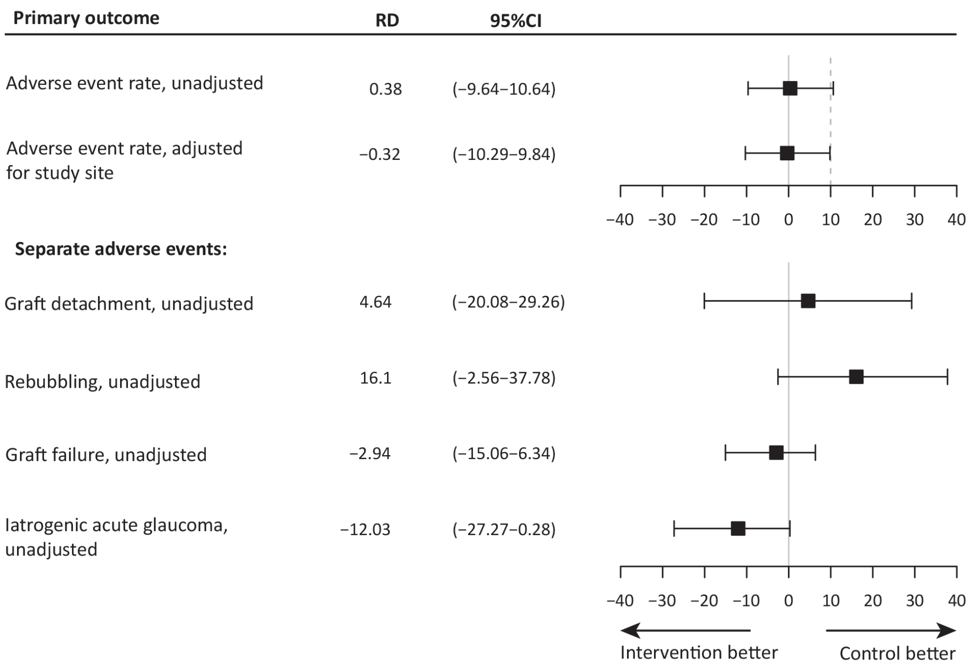

Figure 2. The risk difference between the intervention and control group. The mean risk difference (RD) and 95% confidence interval (CI) of the outcome measures are shown in respect to the non-inferiority limit (dashed line). The top panel shows the unadjusted and adjusted estimates for the primary outcome measure. The bottom panel shows the unadjusted estimates for all separate postoperative events. For these outcomes, a non-inferiority margin is not shown.

No significant differences were found between the control group and the iOCT group regarding secondary clinical outcomes at 3 and 6 months postoperative (**Table 2**). In particular, the ECD loss, RFNL, and postoperative IOP did not differ between both groups and harmful long-term effects of prolonged overpressure thus appear unlikely in patients without prior retinal nerve damage.

Usefulness of intra-operative OCT for surgical decision-making and surgical time

In 35 surgeries the iOCT was utilized, including 2 cross-over cases in an attempt to save the grafts. The graft orientation in these cases was particularly difficult to assess. The use of iOCT salvaged the graft in one case. The other graft was correctly positioned though eventually developed a graft failure, presumably because of repeated manipulation. None of the iOCT-group cases exhibited interface irregularities or graft detachment at the end of surgery. The obligatory verification scan in the control group revealed peripheral detachment of the graft in one case, resulting in repositioning of the graft and subsequent overpressure for another 4 minutes. Notwithstanding, this case developed a detachment for which a rebubbling was performed.

Surgeons reported that the iOCT benefited decision-making in 14 of 35 cases (40%); in all cases (14/14) iOCT aided determining graft orientation (incl. 8 grafts inserted upside-down) and in 21% (3/14) iOCT aided unfolding and positioning of the graft. The median time the iOCT was used measured 2 minutes and 52 seconds (IQR: 03:43, range: 00:19 – 23:40). In 28 cases the image quality was considered good (85%), in four cases acceptable (12%), and in one case poor (3%). Graft unfolding difficulty was significantly associated with surgeon reported iOCT-aided surgical decision-making (**Table 3**, P=0.011); in cases with a complicated graft unfolding the iOCT proved to benefit surgical decision-making. Notwithstanding, graft unfolding difficulty did not differ between both treatment arm (**Table 3**, P=0.474).

Table 3. Overview of graft unfolding grade in both treatment arms

Treatment arm / Graft unfolding grade[1]	**I**	**II**	**III**	**IV**	***p-value***[2]
Conventional protocol, **n**	4	14	4	11	0.474
iOCT-optimized protocol, **n**	7	14	1	9	
iOCT aided surgical decision-making	1	4	1	7	0.011
iOCT did not aid surgical decision-making	6	10	0	2	

[1] Graft unfolding grade is classified in 4 grades depending on the required manipulation and time to unfold/position the graft. Grade I: graft lamella primarily oriented correctly in the anterior chamber, straight and direct unfolding and centering; Grade II: slightly complicated, indirect unfolding and centering (duration less than five min); Grade III: difficult indirect unfolding and centering (duration longer than five min), repeated air injection with BSS exchange necessary; Grade IV: direct manipulation of the graft lamella for unfolding and centering by cannula or forceps.
[2] Fisher exact test

As expected, refraining from prolonged overpressure resulted in a shorter mean surgical skin-to-skin time in the iOCT group compared to the control group (mean difference: 4.90 minutes, SD±*2.51*, -13%). In addition, the mean graft unfolding time in the iOCT group was 1.68 minutes shorter (SD±0.85, -26.8%). An overview of the duration of the main surgical steps is shown in **Table 4**.

Table 4. Overview of surgical times Manually scored and video-graded by two independent observers

Surgical times	Conventional treatment	iOCT-optimized treatment	Relative difference (%)	95% CI
Surgical skin-to-skin time (minutes), mean (SD)	37.62 (10.09)	32.72 (10.99)	-13.0	-0.36 – 10.18
Overpressure time(minutes), mean (SD)	9.73 (1.94)	2.73 (1.29)	-71.9	6.19 – 7.82
unfolding time, minutes, (minutes), mean (SD)	6.26 (8.13)	4.58 (5.35)	-26.8	-1.75 – 5.10
Graft preparation time[1], (minutes), mean (SD)	6.83 (1.95)	6.97 (2.01)	2.0	-1.25 – 0.98
Descemetorhexis time, (minutes), mean (SD)	4.35 (4.41)	5.90 (4.84)	35.6	-3.88 – 0.78

SD: standard deviation, iOCT: intraoperative optical coherence tomography
[1] Graft preparation time for surgeries in Leuven was not available

DISCUSSION

In this study we found that an iOCT-optimized DMEK surgical protocol with iOCT-guidance and refraining from over pressurizing was non-inferior compared to a conventional protocol, with no iOCT-guidance and standard 8 minutes of over pressure. Our results do not support the perceived benefit of overpressure to promote graft adherence. Though the independent effect of iOCT use on surgical safety could not be reliably estimated, the benefits of our iOCT-optimized protocol are a shorter surgical skin-to-skin time (-13%) and assisted surgical decision making (40% of cases). Furthermore, the access to iOCT and its improved visualization proved crucial during surgery in 9% of cases in the control group (2 crossovers and 1 validation scan with observed intra-operative graft detachment).

The causes of graft detachments are considered multifactorial and a large body of research reported on risk factors, such as donor and recipient characteristics, and intraoperative factors such as overpressure of the globe.[31–34] Over-pressuring during surgery is considered by some as a protective factor against graft detachments[15,21], whereas two cohort studies did not support this.[19,20] Our study is the first head-to-head comparison of over-pressuring in DMEK surgery, and whilst graft detachments were prevalent in both treatment arms, our data do not support the notion that over-pressure prevents graft detachments nor rebubbling procedures. Apparently, the incidence of detachments is driven by other factors than assessed in this clinical trial, such as patient compliance with given instructions on immobilization, or different anterior chamber tamponade strategies (e.g. long-term complete air-fill).[35,36] Both could be interesting entry points for follow-up clinical studies.

Overall, the prevalence of adverse events did not differ significantly or materially between both treatment arms (iOCT-group, n=13; control group, n=13). However, the nature of the separate adverse events differed. For instance, the incidence of iatrogenic glaucoma was higher in the prolonged pressurization group. Potentially, a prolonged high pressure in the AC during surgery forces small amounts of gas behind the iris, subsequently leading to an episode of post-operative acute glaucoma, though the exact physiologic process remains unclear. Refraining from overpressure may help to reduce the incidence of postoperative iatrogenic acute glaucoma and benefit patients with pre-existing glaucoma. A harmful effect of prolonged overpressure in our population was not identified, though this is an interesting question for follow-up clinical studies. Interestingly, graft detachments occurred at an equal rate (n=17 vs. n=16) and the areas of detachment were of comparable size, though rebubbling procedures were performed more often in the iOCT group. The cause of this difference remain unclear as our study was not designed to assess nor explore predictors for clinical decision making regarding rebubbling procedures. However, the decision to re-adhere a graft is made by the surgeon which may be related to contextual factors not assessed in this clinical trial, such as location of detachment, tissue- or patient characteristics.

The use of iOCT benefitted the surgical decision-making process in 40% of cases. This finding is consistent with results from comparable studies, including our pilot study and the landmark PIONEER and DISCOVER studies.[3–6,24,25] Similar to these studies our surgeons reported that the iOCT imaging was particularly advantageous for assessing graft orientation and in lesser degree during the unfolding of the graft. Interestingly, we found a significant association between reported iOCT-aided surgical decision-making and the graded unfolding difficulty. This makes sense, as the circumstances and causes which make graft orientation difficult to assess (e.g., poor visualization, graft geometry and tissue properties) may also increase the difficulty of unfolding the graft[28] Hallahan et al. proposed that the iOCT-image may influence the aggressiveness of manipulations.[37] Our data indicate that the iOCT is more utilized and perceived more useful in difficult cases, though not directly related to graft unfolding difficulty nor aggressiveness of manipulations, since these occurred equally in both treatment arms.

The surgical skin-to-skin time was 13% shorter in the iOCT group, which was expected due to refraining from overpressure in the iOCT-optimized protocol. In addition, in line with similar reports we found that the iOCT enables the surgeon in a 26% faster unfolding and positioning of the graft. Though not assessed in this study a shorter duration of unfolding and positioning the graft may be related to less manipulation of the graft and improved graft viability and survival.[3–5] Efficiency gains from refraining from overpressure and a faster unfolding time may be offset by the surgeon taking time to assess the iOCT images. We recorded the time iOCT was switched on (median 2:52, IQR 3:43, range 00:19 – 23:40), though the actual time spent by the surgeon assessing iOCT images is difficult to measure. Evidently, this assessment time is much shorter than the total iOCT time. Future development in automated image analysis may aid to reduce this offset.[1,38]

Long-term follow-up results appeared comparable for both groups. Endothelial cell density is a major determinant for long-term graft survival. The postoperative ECD loss was slightly lower in the iOCT-optimized protocol compared with the conventional protocol in this study, albeit not statistically significant. In addition to other reports, the combined results may suggest that ECD is not affected by prolonged pressuring of the globe and thus not related to reduced long-term graft viability.[19,21] In our study no sequelae of prolonged pressurization were found at follow-up in regard to postoperative IOP or retinal nerve fiber layer damage, which is in line with the report from Fortune et al.[39]

The relative costs of the iOCT-system warrant discussion given the non-inferiority of our iOCT-optimized protocol. We aimed to quantify the benefit of an iOCT guided surgical protocol, which shortened surgical times considerably. iOCT improved surgical decision making, proved indispensable in selected cases according to the surgeons, and enabled adeqate management of intrasurgical events. However, this is not reflected in overall post-operative adverse event rates and clinical outcomes. Although one could hypothesize that refraining from overpressure is also non-inferior regardless intraoperative imaging, this should first be confirmed by clinical studies. Applications that benefit the surgical process beyond DMEK surgery are taking shape, which could be considered a justification of investing in iOCT technology.

Several limitations should be addressed. The study design evaluated two important outcomes in DMEK surgery: the use of iOCT and the use of overpressure. The partial effect of these individual factors is difficult to estimate reliably due to the introduced multi-collinearity. In selected cases, iOCT proved indispensable for the surgeon to complete the surgery successfully, and many reports highlight this benefit of iOCT, though it is not feasible to power a trial on these rare cases and outcomes.[1] Additionally, when iOCT is available at a center, withholding this technology from complex cases (e.g. clouded corneas) is considered unethical.[40] We firmly believe that new innovations should be tested on endpoints relevant for patients, and assessing process-related outcomes (e.g. surgical time) can only be secondary to a primary outcome that relates directly to the patient (e.g. surgical safety). In addition, we attempted to assess the actual IOP during over-pressurization using a hand-held (rebound) tonometer. These measurements proved extremely variable (data not shown) and not related to other clinical signs of over-pressure (firm globe, pupil dilation). Animal studies with custom-made intra-ocular manometers exist[41], but we assume that the measurement of IOP in air/gas filled eyes with conventional certified devices is not feasible. Another consideration is in the interpretation of outcomes regarding graft detachments and rebubbling events. In our study protocol, we listed rebubbling as a primary outcome due to its relevance from a patient perspective, though advancing insights let to the conclusion that a graft detachment is a more objective and quantifiable outcome. We therefore reported both and acknowledge that the decision to re-adhere a graft is made by the surgeon. In the study protocol we did not prescribe strict guidelines on when to intervene with a graft detachment to preserve clinical discretion, which could also be considered a limitation.

In conclusion, iOCT-guided DMEK surgery refraining from prolonged over-pressurizing was proven non-inferior to a conventional approach, though it did not reduce the overall rate of post-operative adverse events. Surgery times were reduced overall by 13% and the iOCT resulted in a 27% reduction of unfolding time. Surgeons reported a benefit of iOCT in 40% of cases. Follow-up studies should elucidate the multi-factorial origin of graft detachment after lamellar corneal transplant surgery.

ACKNOWLEDGEMENTS

The authors would like to thank Suryan Dunker, MD, and Ingeborg de Vries, BSc, for their assistance with the trial measurements, Peter Zuithoff, PhD, of the Julius Center for Health Sciences, for assistance and validation of the statistical analysis, Hanad Jimale, BSc, for his assistance in grading the surgical videos, the members of the data safety monitoring board: Ton Rouwen, MD PhD, Albert Liem, MD PhD, Hind hader, MSc, for their diligent monitoring of the study and constructive feedback, and Antoon van den Bogaerdt, PhD, from ETB-Bislife for his aid in providing donor tissue to all participating centers.

REFERENCES

1. Muijzer MB, Schellekens PAWJ, Beckers HJM, et al. Clinical applications for intraoperative optical coherence tomography: a systematic review. *Eye (Basingstoke)* 2021; 1–13.
2. Posarelli C, Sartini F, Casini G, et al. What Is the Impact of Intraoperative Microscope-Integrated OCT in Ophthalmic Surgery? Relevant Applications and Outcomes. A Systematic Review. *Journal of clinical medicine*; 9. Epub ahead of print June 2020. DOI: 10.3390/jcm9061682.
3. Saad A, Guilbert E, Grise-Dulac A, et al. Intraoperative OCT-Assisted DMEK: 14 Consecutive Cases. *Cornea* 2015; 34: 802–807.
4. Patel AS, Goshe JM, Srivastava SK, et al. Intraoperative Optical Coherence Tomography–Assisted Descemet Membrane Endothelial Keratoplasty in the DISCOVER Study: First 100 Cases. *American Journal of Ophthalmology* 2020; 210: 167–173.
5. Cost B, Goshe JM, Srivastava S, et al. Intraoperative optical coherence tomography-assisted descemet membrane endothelial keratoplasty in the DISCOVER study. *American journal of ophthalmology* 2015; 160: 430–437.
6. Muijzer MB, Soeters N, Godefrooij DA, et al. Intraoperative Optical Coherence Tomography-Assisted Descemet Membrane Endothelial Keratoplasty: Toward More Efficient, Safer Surgery. *Cornea* 2020; 39: 674–679.
7. Dunker SL, Dickman MM, Wisse RPL, et al. Descemet Membrane Endothelial Keratoplasty versus Ultrathin Descemet Stripping Automated Endothelial Keratoplasty: A Multicenter Randomized Controlled Clinical Trial. *Ophthalmology* 2020; 127: 1152–1159.
8. Dunker SL, Veldman MHJ, Winkens B, et al. Real-World Outcomes of DMEK: A Prospective Dutch registry study. *American Journal of Ophthalmology* 2021; 222: 218–225.
9. Stuart AJ, Romano V, Virgili G, et al. Descemet's membrane endothelial keratoplasty (DMEK) versus Descemet's stripping automated endothelial keratoplasty (DSAEK) for corneal endothelial failure. *Cochrane Database of Systematic Reviews*; 2018. Epub ahead of print June 25, 2018. DOI: 10.1002/14651858.CD012097.pub2.
10. Dunker S, Winkens B, Van Den Biggelaar F, et al. Rebubbling and graft failure in Descemet membrane endothelial keratoplasty: a prospective Dutch registry study. *British Journal of Ophthalmology* 2021; 1–7.
11. Singh A, Zarei-Ghanavati M, Avadhanam V, et al. Systematic Review and Meta-Analysis of Clinical Outcomes of Descemet Membrane Endothelial Keratoplasty Versus Descemet Stripping Endothelial Keratoplasty/Descemet Stripping Automated Endothelial Keratoplasty. *Cornea* 2017; 36: 1437–1443.
12. Li S, Liu L, Wang W, et al. Efficacy and safety of Descemet's membrane endothelial keratoplasty versus Descemet's stripping endothelial keratoplasty: A systematic review and meta-analysis. *PLoS ONE* 2017; 12: 1–21.
13. Terry MA, Aldave AJ, Szczotka-Flynn LB, et al. Donor, Recipient, and Operative Factors Associated with Graft Success in the Cornea Preservation Time Study. *Ophthalmology* 2018; 125: 1700–1709.
14. Dirisamer M, Van Dijk K, Dapena I, et al. Prevention and management of graft detachment in descemet membrane endothelial keratoplasty. *Archives of Ophthalmology* 2012; 130: 280–291.
15. Terry MA, Straiko MD, Veldman PB, et al. Standardized DMEK Technique: Reducing Complications Using Prestripped Tissue, Novel Glass Injector, and Sulfur Hexafluoride (SF6) Gas. *Cornea* 2015; 34: 845–852.

16. Santander-García D, Peraza-Nieves J, Müller TM, et al. Influence of Intraoperative Air Tamponade Time on Graft Adherence in Descemet Membrane Endothelial Keratoplasty. *Cornea* 2019; 38: 166–172.
17. Price FW, Price MO. Descemet's stripping with endothelial keratoplasty in 200 eyes. Early challenges and techniques to enhance donor adherence. *Journal of Cataract and Refractive Surgery* 2006; 32: 411–418.
18. Heinzelmann S, Böhringer D, Haverkamp C, et al. Influence of postoperative intraocular pressure on graft detachment after descemet membrane endothelial keratoplasty. *Cornea* 2018; 37: 1347–1350.
19. Pilger D, Wilkemeyer I, Schroeter J, et al. Rebubbling in Descemet Membrane Endothelial Keratoplasty: Influence of Pressure and Duration of the Intracameral Air Tamponade. *American Journal of Ophthalmology* 2017; 178: 122–128.
20. Schmeckenbächer N, Frings A, Kruse FE, et al. Role of Initial Intraocular Pressure in Graft Adhesion After Descemet Membrane Endothelial Keratoplasty. 2016; 0: 1–4.
21. Fajgenbaum MAP, Hollick EJ. Does Same-Day Postoperative Increased Intraocular Pressure Affect Endothelial Cell Density After Descemet Membrane Endothelial Keratoplasty? *Cornea* 2018; 37: 1484–1489.
22. Janson BJ, Alward WL, Kwon YH, et al. Glaucoma-associated corneal endothelial cell damage: A review. *Survey of Ophthalmology* 2018; 63: 500–506.
23. Khng C, Packer M, Fine IH, et al. Intraocular pressure during phacoemulsification. *Journal of cataract and refractive surgery* 2006; 32: 301–308.
24. Ehlers JP, Dupps WJ, Kaiser PK, et al. The Prospective Intraoperative and Perioperative Ophthalmic ImagiNg with Optical CoherEncE TomogRaphy (PIONEER) Study: 2-year results. *American journal of ophthalmology* 2014; 158: 999–1007.
25. Ehlers JP, Modi YS, Pecen PE, et al. The DISCOVER Study 3-Year Results: Feasibility and Usefulness of Microscope-Integrated Intraoperative OCT during Ophthalmic Surgery. *Ophthalmology* 2018; 125: 1014–1027.
26. Schulz KF, Altman DG, Moher D. CONSORT 2010 Statement: updated guidelines for reporting parallel group randomised trials. *BMJ*; 340. Epub ahead of print 2010. DOI: 10.1136/bmj.c332.
27. Dapena I, Moutsouris K, Droutsas K, et al. Standardized "No-Touch" Technique for Descemet Membrane Endothelial Keratoplasty. *Archives of Ophthalmology* 2011; 129: 88–94.
28. Maier AKB, Gundlach E, Schroeter J, et al. Influence of the difficulty of graft unfolding and attachment on the outcome in descemet membrane endothelial keratoplasty. *Graefe's Archive for Clinical and Experimental Ophthalmology* 2015; 253: 895–900.
29. Beck RW, Moke PS, Turpin AH, et al. A computerized method of visual acuity testing: Adaptation of the early treatment of diabetic retinopathy study testing protocol. *American Journal of Ophthalmology* 2003; 135: 194–205.
30. Austin PC. Absolute risk reductions, relative risks, relative risk reductions, and numbers needed to treat can be obtained from a logistic regression model. *Journal of Clinical Epidemiology* 2010; 63: 2–6.
31. Parekh M, Leon P, Ruzza A, et al. Graft detachment and rebubbling rate in Descemet membrane endothelial keratoplasty. *Survey of Ophthalmology* 2018; 63: 245–250.
32. Dunker S, Winkens B, Van Den Biggelaar F, et al. Rebubbling and graft failure in Descemet membrane endothelial keratoplasty: a prospective Dutch registry study. *British Journal of Ophthalmology* 2021; 1–7.

33. Weller JM, Schlötzer-Schrehardt U, Tourtas T, et al. Influence of Ultrastructural Corneal Graft Abnormalities on the Outcome of Descemet Membrane Endothelial Keratoplasty. *American Journal of Ophthalmology* 2016; 169: 58–67.
34. Quilendrino R, Rodriguez-Calvo de Mora M, Baydoun L, et al. Prevention and Management of Graft Detachment in Descemet Membrane Endothelial Keratoplasty. *Archives of Ophthalmology* 2012; 130: 280–291.
35. Gonzalez A, Price FW, Price MO, et al. Prevention and Management of Pupil Block after Descemet Membrane Endothelial Keratoplasty. *Cornea* 2016; 35: 1391–1395.
36. Cirkovic A, Beck C, Weller JM, et al. Anterior chamber air bubble to achieve graft attachment after DMEK: Is bigger always better? *Cornea* 2016; 35: 482–485.
37. Hallahan KM, Cost B, Goshe JM, et al. Intraoperative Interface Fluid Dynamics and Clinical Outcomes for Intraoperative Optical Coherence Tomography–Assisted Descemet Stripping Automated Endothelial Keratoplasty From the PIONEER Study. *American Journal of Ophthalmology* 2017; 173: 16–22.
38. Xu D, Dupps WJJ, Srivastava SK, et al. Automated volumetric analysis of interface fluid in descemet stripping automated endothelial keratoplasty using intraoperative optical coherence tomography. *Investigative ophthalmology & visual science* 2014; 55: 5610–5615.
39. Fortune B, Yang H, Strouthidis NG, et al. The effect of acute intraocular pressure elevation on peripapillary retinal thickness, retinal nerve fiber layer thickness, and retardance. *Investigative Ophthalmology and Visual Science* 2009; 50: 4719–4726.
40. Muijzer MB, Kroes HY, Van Hasselt P, et al. Bilateral posterior lamellar corneal transplant surgery in an infant of 17 weeks old: surgical challenges and the added value of intraoperative optical coherence tomography. *Authorea*.
41. Cheng W, Liu L, Yu S, et al. Real-Time Intraocular Pressure Measurements in the Vitreous Chamber of Rabbit Eyes During Small Incision Lenticule Extraction (SMILE). *Current Eye Research* 2018; 43: 1260–1266.

SUPPLEMENTARY DATA

Supplementary table 1. Logistic regression models for incidence of total adverse event rate

Determinants	Unadjusted model		Adjusted model	
	OR (95%CI)	P	OR (95%CI)	P
iOCT-optimized protocol	1.036 (0.454 - 2.366)	0.933	0.976 (0.421 – 2.263)	0.955
Study site 2[1]	-	-	0.123 (0.016 – 0.953)	0.045
Study site 3[1]	-	-	0.634 (0.221 – 1.819)	0.396

[1] Reference: study site 1
iOCT: intraoperative optical coherence tomography

CHAPTER 5

BILATERAL POSTERIOR LAMELLAR CORNEAL TRANSPLANT SURGERY IN AN INFANT OF 17 WEEKS OLD: SURGICAL CHALLENGES AND THE ADDED VALUE OF INTRAOPERATIVE OPTICAL COHERENCE TOMOGRAPHY

Marc B Muijzer; Hester Y Kroes;
Peter M van Hasselt; Robert PL Wisse

Clinical Case Reports. 2022; 10(4)

ABSTRACT

Aim: To describe the extensive management and use of intra-operative optical coherence tomography (iOCT) in a case of a bilateral Descemet Stripping Automated Endothelial Keratoplasty (DSAEK) corneal transplantation at 17 weeks of age for the treatment of posterior polymorphous corneal dystrophy.

Case description: A 9-week-old infant boy was referred with a bilateral corneal clouding diagnosed as a posterior polymorphous corneal dystrophy type 1 resulting from a de novo mutation of the OVOL2-gene. At 17 weeks of age a bilateral DSAEK corneal transplantation was performed. Intra-operative OCT was used during pre- and postoperative examinations and proved crucial during surgery for determining the graft orientation, -position, and –adherence in the severely clouded cornea and with a virtually absent visualization of the graft inside the eye. After surgery the right cornea cleared after surgery, whereas the left cornea remained cloudy. The iOCT image showed a detached graft, which was subsequently reattached. The cornea remained cloudy and a re-transplantation was performed. At one year of age both corneas cleared and the boy exhibits normal visual function of the right eye and limited visual function of the left eye.

Conclusion: Here, we present the first bilateral iOCT-assisted DSAEK surgery in an infant boy. The availability of intra-operative OCT was pivotal in the treatment of this case as the visualization of the graft was severely limited and iOCT had a positive influence on critical decision-making during surgery and follow-up. At one-year follow-up the boy shows a remarkably normal development and visual behavior of the right eye, though visual potential of the left eye remains unclear.

INTRODUCTION

Posterior polymorphous corneal dystrophy (PPCD) is a rare autosomal dominant corneal endothelial dystrophy. The dystrophy is characterized by abnormal endothelial cell morphology, which appear as vesicular lesions, grey-white opacities, and linear bands during slit lamp examination.[1] PPCD is genetically heterogeneous and can be caused by pathogenic mutations in the OVOL2 gene (PPCD1), COL8A2 gene (PPCD2), ZEB1 gene (PPCD3), and GRHL2 gene (PPCD4).[1,2] In general, PPCD is considered a mild condition, where only a minority develops symptoms in infancy resembling a Congenital Hereditary Endothelial Dystrophy (CHED). These symptoms include: corneal edema, peripheral iridocorneal adhesions, and glaucoma. Of these symptoms, in particular corneal edema can have a huge impact on the visual development due to amblyopia.[3]

It is estimated about 20-25% of PPCD cases who develop corneal edema require corneal transplant surgery.[4] In recent years endothelial keratoplasty is increasingly preferred as a first-choice treatment for corneal endothelial transplant surgery in children.[5,6] Here, the structural integrity of the cornea is retained and a superior acuity is achieved. However, endothelial keratoplasty requires corneal clarity and as a consequence, standard endothelial keratoplasty, is not always feasible in cases with severe corneal clouding. To this end, intraoperative optical coherence tomography (iOCT) theoretically provides a solution. iOCT is a novel application of a widely used non-invasive *in vivo* imaging based on infrared light interferometry. The iOCT signal is typically not affected by corneal clouding and provides the surgeon with high resolution in-depth images of the surgical field.[7]

We present a case of a 4-month-old infant with PPCD1 and severe corneal clouding who was successfully treated with iOCT-assisted lamellar endothelial keratoplasty in both eyes. Our extensive reporting of the surgical challenges in this case and the description of the benefits of iOCT during surgery may help ophthalmologist in similar cases.

CASE DESCRIPTION

A newborn boy of 9 weeks old was referred with progressive clouding of both eyes. Handheld slit lamp examination showed diffuse corneal clouding, a symmetrical cornea diameter of 11 mm, and intact pupillary reflexes. No evident irido-corneal adhesions or correctopia were found. The pregnancy was normal (G1P1) with a spontaneous vaginal delivery at 41 weeks gestational age. Physical examination, as performed by the pediatrician and the clinical geneticist, was uneventful. Extensive metabolic screening in urine (including glycosaminoglycans, aminoacids), and plasma (including amino acids) ruled out mucopolysaccharidoses, tyrosinemia type II, and cystinosis. A tentative diagnosis of congenital hereditary endothelial dystrophy (CHED) was made. Given the genetic heterogeneity of CHED/PPCD, genetic testing was performed by high throughput DNA-analysis and subsequent in silico analysis of 424 genes associated with visual impairment (consisting of single nucleotide variant and copy number variant analysis) followed by SNP-array. This revealed a de novo chromosomal duplication of ~49 Kb in the region 20p11.23, encompassing the entire OVOL2 gene. The duplication was absent in DNA from the parents with no known family history of PPCD or consanguinity.

Additional ophthalmic examinations were performed under general anesthesia. The intraoperative optical coherence tomography (iOCT) imaging revealed thickened corneas (OD: 1199µm, OS: 1115µm) with hyper reflective stromal lesions (**Figure 1A**). No structural abnormalities of the anterior segment were found. The red reflex in mydriasis was absent in both eyes, though ultrasound echography showed no abnormalities in the posterior segment. The intraocular pressure (IOP) measured 18 mmHg ODS (Tonopen Avia, Reichert, Inc, Depew, NY) and the axial length was 18.2mm OD and 17.85mm OS (conform his age). Sodium chloride drop 5 times daily and non-steroid anti-inflammatory (Nepafenac, 0.3%; Novartis Pharma, Amsterdam, the Netherlands) ocular drops 1 time daily were prescribed with no effect and subsequently discontinued after 2 months.

Based on the identified pathogenic *OVOL2*-duplication, the corneal clouding was diagnosed as PPCD1. The aggressive course of the disease would inevitably lead to severe visual impairment. With informed consent from both parents, and after consultation with our pediatric ophthalmologists and an international board of corneal specialists, we decided to perform a bilateral lamellar endothelial keratoplasty.

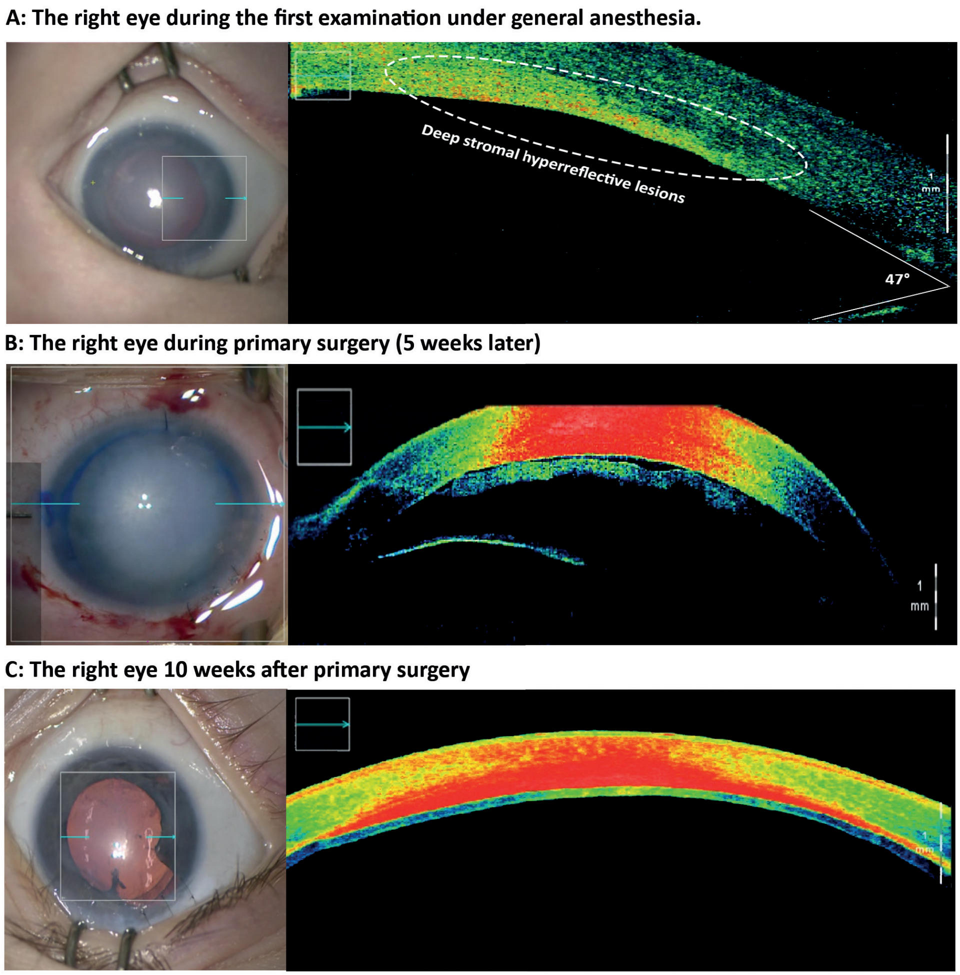

Figure 1. Intraoperative optical coherence tomography imaging. In the upper image (A) is the right eye shown during initial examination and in the lower image (B) the right eye during primary surgery. In both images the left panel shows the en face microscope view, and in the right panel the corresponding live optical coherence tomography (OCT) image. The location and direction of the live OCT image are highlighted by the turquoise arrow in the white square in the left panel. In the upper image (A) significant corneal clouding can be seen, the OCT images shows hyper reflective lesions in the stroma compared to the surrounding tissue. The anterior chamber angle measures 47 degrees and no structural abnormalities. The middle image (B) shows the right eye during primary surgery. Because of severe corneal edema the graft is poorly visible in the en face microscope view. However, using the live OCT image the surgeon was able to clearly visualize the graft during surgery. The lower image (C) shows the right eye 10 weeks after primary surgery. The en face microscope view shows a clear cornea and bright red reflex. In the OCT image an attached and de-swelled graft can be observed.

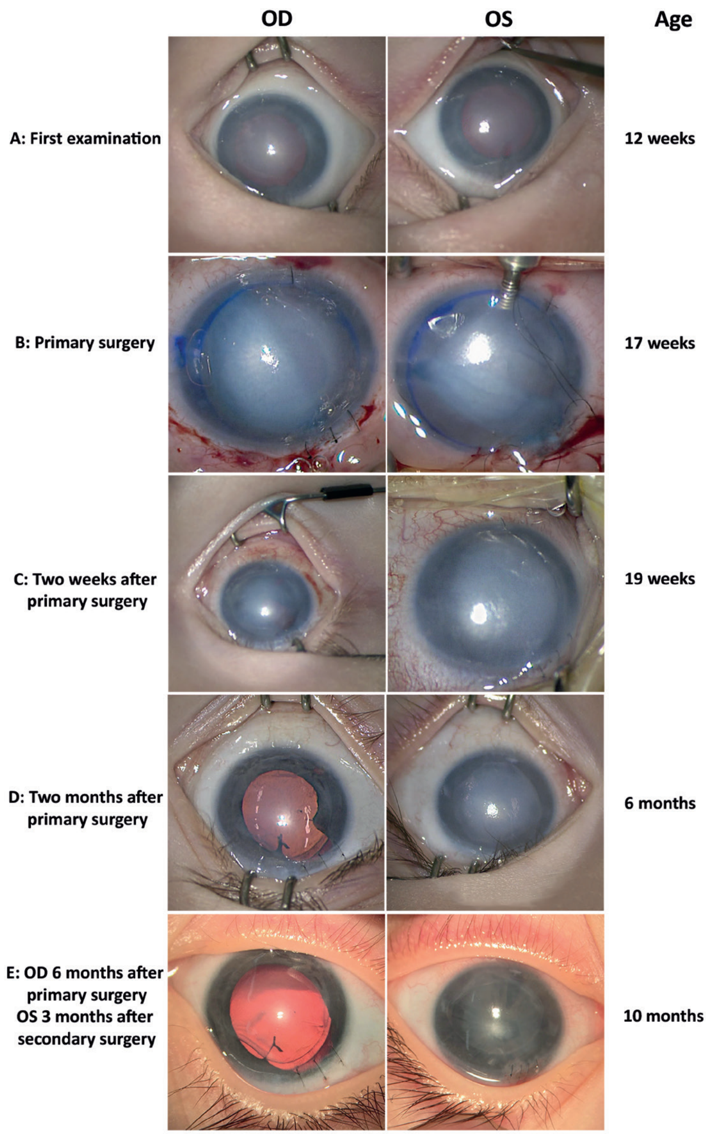

Figure 2. Timeline of major examinations. In figure 2 we constructed a timeline of important events and examinations of this case. The left image shows the right eye (OD) and the right image the left eye (OS) at the time of the intervention described left of the images (e.g., first examination, primary surgery etc.). Right of the images the age of the boy is given at the time of the intervention. At the first examination (A) there is a significant amount of corneal edema at 12 weeks of age. The images at the primary surgery (B) show the increased severity of corneal edema and the difficulty to visualize the graft. Two weeks after primary surgery (C) the graft in the left eye was found to have detached and was subsequently re-attached by injecting air in the anterior chamber. Two months after the primary surgery (D) the cornea of the right eye cleared and a red reflex is visible, the cornea of the left eye is still severely clouded and was shortly afterwards the left eye was re-grafted. At a proximally 10 months of age an examination with the use of mydriatics was performed. The right eye shows a clear cornea with a bright red reflex, whereas the left cornea is still hazy and shows no red reflex (E).

Surgical treatment:

At 17 weeks of age a bilateral Descemet Stripping Automated Endothelial Keratoplasty (DSAEK) corneal transplantation was performed in the Wilhelmina Children's hospital (**Figure 2B**). An 8.5 mm pre-cut organ cultured unmarked DSAEK tissue was provided by the eye bank (ETB-bislife, Beverwijk, the Netherlands). The graft endothelial cell density measured 2800 and 2600 cells/mm^2 and the graft thickness measured 133 μm and 106 μm for respectively the right eye and the left eye. Largely the same surgical procedure was subsequently used for both eyes. After creating two paracenteses nasally and temporally the surgeon performed a peripheral iridectomy at the 6 o'clock position. In the first procedure (OD) a Lewicky anterior chamber maintainer was used (DORC International, Zuidland, the Netherlands). In the left eye a viscoelastic device (Healon, Abbot Medical, Chicago, IL, USA) was used to maintain the anterior chamber and prevent IOP differences and rinsed carefully after graft positioning.[8] A high vitreous pressure resulted in iris prolapse in both eyes, which was subsequently repositioned. Repositioning of the iris prolapse in the right eye proved challenging because of the high vitreous pressure, which resulted in an iris defect and damage to the sphincter muscle. Repositioning of the iris in the left eye was only possible after relieving the intraocular pressure by pars plana aspiration using a 30-gauge needle. The Descemet membrane was not attempted to be removed, as the Descemet membrane cannot be identified in infants.[5] A 4mm corneal-scleral incision was made, and nylon 10-0 non-absorbable stitches (Ethicon, Sommersville, NJ, USA) were prepared. Prior to insertion and owing to the absent visualization, the graft was stained using membrane blue (DORC International, Zuidland, the Netherlands) and inserted using a Maculuso inserter (Janach Instruments, Como, Italy).

A microscope-integrated iOCT (OPMI Lumera 700; Carl Zeiss, Jena, Germany) was used during the surgery to visualize various steps during surgery, such as graft orientation, position, adherence, and interface (**Figure 1B**). Graft orientation was assessed using the acute-angled bevel sign described by Titiyal et al.; a sharp angle (<90°) between the graft' edge and recipient posterior corneal surface is indicates a correct orientation of the graft.[9] The graft was fixated using a full airfill and iOCT image revealed persistent interface fluid, which resolved after continuous corneal swiping. Afterwards, the iOCT image confirmed a fully adhered donor lenticule with no interface abnormalities and consequently no prolonged overpressure of the globe was applied. At the end of surgery, large air bubble was retained (90% of the anterior chamber volume) and left to resorb in the days after surgery monitoring the ocular pressure (and signs of acute glaucoma. The patient received a peribulbar injections of dexamethasone 4mg/ml. Postoperative medication included dexamethasone, 0.1%, and tobramycine, 0.3%, eye drops 6 times daily (TobraDex, Novartis Pharma, Amsterdam, the Netherlands) and prednisolone ointment ante noctem for 3 months (Ursapharm, Luik, Belgium). After this period the topical antibiotics was switched to 0.1% dexamethasone eyedrops QID (Thea Pharma Benelux, Wetteren, Belgium).

Outcome and follow-up

One week after surgery the right eye started to clear, whereas the cornea of the left eye remained cloudy. Because of the young age of the patients and difficulty in examining the eye repeated postoperative examinations were performed under general anesthesia. During re-examination 2 weeks post-operative iOCT showed a completely attached graft in the right eye and a >75% detached graft in in the left eye, which was re-attached directly using a complete fill of the anterior chamber with air (**Figure 2C**). Nonetheless, the cornea of the left eye remained cloudy after surgery and the boy developed an esotropia and horizontal pendular nystagmus. Another re-examination was performed 10 weeks after initial surgery (**Figure 2D**). During this examination iOCT revealed completely attached grafts in both eyes (**Figure 1C**). The graft in the left eye was markedly thicker compared to the graft of the right eye, respectively 197μm vs. 85μm, and remained cloudy indicating a graft failure. The IOP measured 24 mmHg (OD) and 28 mmHg (OS). Because the apparent dysfunction of the graft in the left eye a re-transplant was planned and IOP lowering medication was started (timolol/ brinzolamide BID).

At 29 weeks old a re-DSAEK of the left eye was performed following the same surgical procedure as described for the initial surgery for the left eye. However, during the re-transplant procedure the surgeon used a complete Sulphur hexafluoride 20% fill and 10 minutes overpressure to improve graft adherence. In the weeks after the re-transplant the cornea of the left eye started to clear and both the nystagmus and esotropia decreased. Despite the left eye lacked a proper red reflex and the pupil did not respond to mydriatics for which pediatric cataract surgery was planned. Prior to the surgery ultrasound echography was performed and no abnormalities in the posterior segment were found. During the surgery a pupillary fibrotic membrane with a clear lens was identified and the membrane could be removed without complications (**Figure 2E**). In addition, after accelerated tapering of steroids and switching 0.1% fluorometholone (Allergan Nederland BV, The Netherlands) the IOP normalized.

He exhibited a relative normal visual behavior, owing to the normal visual development in the right eye, whereas the left eye experienced a deprivation amblyopia. Despite the removal of the pupillary membrane, an intractable miosis persisted, and he did not have a proper red reflex in the left eye. Occlusive patching was commenced at 9 months of age, with mixed compliance. Importantly, orthoptic examination showed visual responses in the left eye and a decrease in the nystagmus and esotropia.

At 14 months the boy was again examined under general anesthesia. In both eyes the graft was attached and functional. In the right eye the cornea fully cleared, whereas the left cornea was relatively clear. The crystalline lens was clear in both eyes, though the left eye lacked a proper red reflex. The IOP normalized, with no apparent sequelae of the prolonged ocular hypertension. Funduscopic examination of the right eye did not reveal abnormalities in the posterior segment. To date, at 20 months of age, both corneas remained clear. The right eye showed a promising visual potential, whereas he can use left eye for spatial orientation and the recognition of coarse objects.

DISCUSSION

Here, we describe the clinical course of an infant boy with severe PPCD1 who was treated with bilateral iOCT-assisted DSAEK at 17 weeks of age. Imminent corneal blindness warranted this high-risk intervention at such a young age. After surgery corneal clarity was restored in the right eye and the boy exhibits a good visual functioning of his right eye. The left eye had a more prolonged surgical course, with eventually a functional graft was achieved after 4 surgical interventions, albeit with a suboptimal red reflex. He is currently treated for a deprivation amblyopia, with guarded hopes for the amelioration of visual function and isophoria of the left eye. In addition, the risk of secondary ocular hypertension remains present, since PPCD and steroid use are independent risk factors for the development of glaucoma. Furthermore, particularly interesting about this case is the non-hereditary mutation of the OVOL2 gene, while in the majority of the reported cases a hereditary link has been confirmed.[1,2,4]

Endothelial keratoplasty is increasingly preferred for the treatment of congenital endothelial disorders compared to penetrating keratoplasty. In children who underwent penetrating keratoplasty visual rehabilitation may be complicated because of amblyopia, suture-related complications, high astigmatism, graft rejection, and in the long-term graft failure. Nevertheless, performing endothelial keratoplasty in children is more challenging than in adults because of the smaller corneal diameter, higher scleral elasticity, shallower anterior chamber, and difficulty maintaining a supine position after surgery. Moreover, treatment is further complicated by difficulties in examination the eye. Only a few cases are reported to undergo surgery at an infant age.[4–6,10–12] The reports of endothelial keratoplasty at infant age show in general a successful procedure. Notwithstanding, most reported cases developed a graft detachment in at least one eye which required re-bubbling of the graft.

The availability of the iOCT proves a crucial asset in the treatment of this case: without endothelial keratoplasty would have been challenging. The high-resolution imagery of the iOCT provided direct and accurate 3D spatial information about the cornea, anterior segment, and graft. In line with other studies we found that the availability of iOCT had a positive influence on critical decision-making during surgery and follow-up.[7] The iOCT proved to be decisive in determining the orientation and confirming the adherence of the graft, which led to refraining from prolonged overpressure of the globe

In conclusion, we report the first bilateral iOCT-assisted DSAEK in an infant. At 20 months old he shows a remarkably normal visual behavior. We hope that reporting the extensive genetic and metabolic workup, description of the advantage of iOCT, and our judicious considerations helps other corneal surgeons in clinical decision making for these rare and high-risk cases.

PATIENT CONSENT

Consent to publish this case report has been obtained from both parents in writing.

ACKNOWLEDEMENTS

We would like to thank P.E.Q.M. Cooijmans, P.A.W.J.F. Schellekens, and E.S.M. Voskuil-Kerkhof of the department of Ophthalmology of the University Medical Center Utrecht for their involvement in the treatment of this patient and L. Haer-Wigman of the Department of Human Genetics of the Radboud University Medical Center for her assistance in making the molecular diagnosis.

REFERENCES

1. Davidson AE, Liskova P, Evans CJ, et al. Autosomal-Dominant Corneal Endothelial Dystrophies CHED1 and PPCD1 Are Allelic Disorders Caused by Non-coding Mutations in the Promoter of OVOL2. *American Journal of Human Genetics* 2016; 98: 75–89.
2. Liskova P, Dudakova L, Evans CJ, et al. Ectopic GRHL2 Expression Due to Non-coding Mutations Promotes Cell State Transition and Causes Posterior Polymorphous Corneal Dystrophy 4. *American Journal of Human Genetics* 2018; 102: 447–459.
3. Graham MA, Azar NF, Dana MR. Visual rehabilitation in children with congenital hereditary endothelial dystrophy. *International ophthalmology clinics* 2001; 41: 9–18.
4. Hermina Strungaru M, Ali A, Rootman D, et al. Endothelial keratoplasty for posterior polymorphous corneal dystrophy in a 4-month-old infant. *American Journal of Ophthalmology Case Reports* 2017; 7: 23–26.
5. Madi S, Santorum P, Busin M. Descemet stripping automated endothelial keratoplasty in pediatric age group. *Saudi Journal of Ophthalmology* 2012; 26: 309–313.
6. Busin M, Beltz J, Scorcia V. Descemet-stripping automated endothelial keratoplasty for congenital hereditary endothelial dystrophy. *Archives of Ophthalmology* 2011; 129: 1140–1146.
7. Siebelmann S, Hermann M, Dietlein T, et al. Intraoperative optical coherence tomography in children with anterior segment anomalies. *Ophthalmology* 2015; 122: 2582–2584.
8. Alqudah AA, Bauer AJ, Straiko MD, et al. Descemet stripping automated endothelial keratoplasty. *Medicine* 2020; 99: e23139.
9. Titiyal JS, Kaur M, Shaikh F, et al. “Acute-angled bevel” sign to assess donor lenticule orientation in ultra-thin descemet stripping automated endothelial keratoplasty. *BMJ case reports*; 12. Epub ahead of print February 2019. DOI: 10.1136/bcr-2018-227927.
10. Bellucci R, Chierego C, Bellucci C. Endothelial keratoplasty in a newborn baby with CHED. *Cornea* 2011; 30: 1488–1490.
11. Goshe JM, Li JY, Terry MA. Successful Descemet’s stripping automated endothelial keratoplasty for congenital hereditary endothelial dystrophy in a pediatric patient. *International Ophthalmology* 2012; 32: 61–66.
12. Sella R, Rootman D, Bahar I. Descemet’s stripping automated endothelial keratoplasty for posterior polymorphous corneal dystrophy in an 8-month-old boy. *Journal of AAPOS* 2013; 17: 94–96.

CHAPTER 6

AUTOMATIC EVALUATION OF GRAFT ORIENTATION DURING DESCEMET MEMBRANE ENDOTHELIAL KERATOPLASTY USING INTRAOPERATIVE OCT

Marc B Muijzer*; Friso G Heslinga*; Floor Couwenberg;
Herke Jan Noordmans; Abdelkarim Oahalou; Josien PW Pluim;
Mitko Veta; Robert PL Wisse

Biomedical Optics Express. 2022; 13(5)

*These authors contributed equally

ABSTRACT

Aim: To develop an image analysis method for automatic evaluation of the Descemet Membrane Endothelial Keratoplasty (DMEK) graft orientation in intraoperative optical coherence tomography (iOCT), exploiting the natural rolling behavior of the graft

Methods: A deep learning-based segmentation model was developed using 235 iOCT-frames with manual annotations of the DMEK graft locations. After post-processing of the predicted segmentation, a smooth line representation of the graft was obtained and curvature of the graft was calculated. Orientation of the graft was then predicted based on the degree of curvature. Evaluation of the automatic pipeline was done for a separate test set of 100 iOCT-frames, by comparing the predicted orientation with the ground truth.

Results: The automatic method obtained an area under the receiver operating characteristic curve (AUC) of 0.84 and was able to correctly identify the graft orientation in 78% of the iOCT-frames. When we replaced the automatic segmentation with the manual masks, the AUC increased to 0.92, corresponding to an accuracy of 86%. In comparison, two corneal specialists correctly identified graft orientation in 90% and 91% of the iOCT-frames.

Conclusion: Automated image analysis can be used to accurately detect a DMEK graft in iOCT, quantify graft curvature, and determine the graft’s orientation.

INTRODUCTION

Descemet membrane endothelial keratoplasty (DMEK) is the preferred posterior lamellar keratoplasty procedure for treating cases of symptomatic irreversible corneal endothelial cell dysfunction.[1,2] Posterior lamellar surgeries constitute the majority of grafting procedures in the developed world.[3] The thin (~30µm) and vulnerable DMEK graft – consisting of the Descemet's membrane and endothelium – is inserted as a roll and unfolded in the anterior chamber of the eye before fixation on the posterior surface of the recipient cornea.[4] A correct orientation of the graft – with the endothelium facing away from the cornea – is imperative. An inadvertently incorrectly positioned graft (i.e., upside-down) will result in severe corneal edema, damage to the graft's endothelial cell layer, and the subsequent need for repeated surgery. [5,6]

The assessment of the graft's orientation can be challenging and several methods have been described to aid the surgeon in determining the orientation. Currently, the Moutsouris sign, ink-stamps, and circular cuts are used to determine intraocular graft orientation.[4,7–9] However, poor visualization of the anterior chamber and graft hinders a proper assessment.[10–12] In addition, the presence of the Moutsouris sign is not always self-evident and both stamps and cuts damage the graft resulting in endothelial cell loss. More recently, intraoperative optical coherence tomography (iOCT) has been used to determine graft orientation, as the iOCT signal is not perturbed by corneal edema.[10–14] Residual stromal fibers in the Descemet's membrane of the DMEK graft result in a distinctive inward curve of the graft's ends indicative of a correct orientation, which can be visualized and assessed using iOCT (**Figure 1**).[13–15] This natural curling behavior of DMEK grafts can be well appreciated on the iOCT image, thereby preventing the need to use manipulation, cutting, or marking to determine the graft orientation, thus preventing endothelial cell loss.

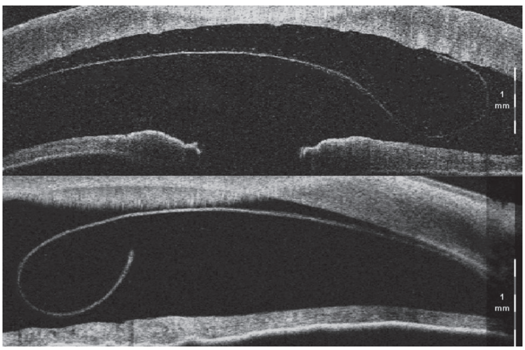

Figure 1. Two cross-sectional intraoperative OCT scans of the cornea. The natural rolling motion of the graft in Descemet membrane endothelial keratoplasty (DMEK) can be used to determine the graft's orientation. The top image depicts a correctly oriented DMEK graft, indicated by the distinctive upward curve towards the recipient's cornea. The bottom image depicts an incorrectly oriented graft (i.e., upside-down), indicated by the curling motion away from the recipient's cornea.

Several studies have reported on the use of iOCT during DMEK surgery for determining the orientation of the graft. In all studies the graft orientation could be correctly determined based on the inward rolling of the graft edges visible on the cross-sectional iOCT image.[10,12,14,16] Importantly, the surgeon was able to assess the graft orientation in cases where assessment of the Moutsouris sign or S-stamp was challenging or not possible.[10–12] However, manual assessment of graft orientation on iOCT images can be time consuming and prone to interpretation errors. In particular, when OCT image quality is suboptimal or the graft edges display little inward rolling. We believe an automated tool will aid the surgeon in fast and accurate evaluation of the orientation, thereby improving surgical workflow and reducing the risk of errors.

Several studies have reported on applications of (automated) image analysis of iOCT images showing promising potential for improving clinical decision making and clinical outcomes.[17–23] These studies used different methodologies for segmenting the area of interest from the iOCT image. For example, Weiss et al. used geometric modeling of iOCT images to track the orientation and location of a surgical needle.[20] Using a similar method, Xu et al. developed an automated algorithm to segment the fluid interface gap in Descemet stripping endothelial keratoplasty achieving a high segmentation accuracy.[18,19] In contrast, Roodaki et al. used deep learning to segment different anatomical structures in the anterior segment of the eye in iOCT images, to automatically position the OCT scan area on an anatomy of interest using voice control.[21,22] Furthermore, Keller et al. demonstrated the use of iOCT-guided robotic ophthalmic surgery using volumetric OCT scans and reinforcement learning.[23] To the best of our knowledge no automatic image analysis tool has been developed for analysis of DMEK graft orientation.

Here, we present an automated image analysis method for evaluation of the DMEK graft orientation using iOCT. The method includes a deep learning-based segmentation model to extract the DMEK graft from the iOCT scan. Then the degree of inward rolling by the graft is assessed and related to graft orientation. Our contributions include the development of a method for in-vivo DMEK graft segmentation, a pipeline of post-processing steps to obtain the graft's curvature, and a method to relate graft curvature to graft orientation.

METHODS

Data & preprocessing

All OCT-scans in this study were acquired during DMEK surgery at the ophthalmology department of the University Medical Centre Utrecht between May 2016 and October 2020 using the "No-Touch" technique for DMEK as described by Dapena et al. [4] DMEK grafts were cultured and provided pre-cut by the Euro Cornea Bank (Beverwijk, the Netherlands) and Amnitrans (Rotterdam, the Netherlands). During surgery, iOCT-scans of the anterior segment were made with a commercially available spectral domain microscope integrated OCT system (Zeiss Lumera 700 RESCAN, Carl Zeiss Meditec, Jena, Germany), using the two-line cross-sectional setting. The iOCT system has a wavelength of 850 nm and an axial resolution of 5.5 μm. The system acquires 25 two-line cross-sectional scans per second. This study was performed in accordance with the Declaration of Helsinki and Dutch law regarding research involving human subjects. Ethical approval for this study was waived by the Ethics Review Board of University Medical Center Utrecht (METC no. 18-370)

iOCT-scans of the DMEK procedures are embedded in the surgical video feed. The video feed was qualitatively reviewed for scan quality and visibility of the graft during determination of graft orientation (i.e., before adhering the graft). Scans were excluded if the graft was not visible at all or not unfolded. Included iOCT-scans were manually extracted from the video feed using the FFmpeg tool (version 3, 2016, FFmpeg Developers). Each cropped frame contained a single cross-sectional iOCT-scan (iOCT-frame). The ground truth of the graft orientation, either correctly oriented or upside-down, in each iOCT-frame was set by an experienced grader (M.B.M.) who had access to the preceding and follow-up frames and postoperative clinical information. The orientation of each graft was subsequently graded by two corneal surgeons (experts' opinion; R.W. and A.O.) based on a single iOCT-frame and blinded for the outcome (i.e., without access to the preceding and follow-up frames or postoperative clinical information).

A total of 335 iOCT-frames from 89 DMEK surgeries were obtained; 127 iOCT-frames measuring 550 × 275 (width × height) pixels acquired before 1-1-2019 and 208 iOCT-frames measuring 610 × 275 pixels acquired from 1-1-2019 onwards. The more recently acquired scans were of better image quality due to an improved scan protocol and we selected 100 recent iOCT-frames from 21 patients as a test set for final evaluation of our models. All other iOCT-frames (n = 235) were used for development and optimization of the image analysis methods and will be referred to as the development set. This development set was again divided into a training set (n = 202) and a validation set (n = 33) to determine the optimal model. The data split was done on a patient level to ensure no overlap exists between the train, validation, and test sets. The graft locations were manually annotated in the iOCT frames with marking points (image coordinates) along the graft and converting the resulting contour to a binary mask of an area containing the graft. Zero-padding was used to ensure all iOCT-frames were of width 610 for training the AI segmentation model. As a final preprocessing step, all frames were resized to 576 × 256 pixels for compatibility with the U-Net architecture.

Our image analysis tool consists of three steps (**Figure 2**). First, the area containing the DMEK graft was segmented from the iOCT-frame using a deep learning-based segmentation model. In the subsequent post-processing step, the resulting mask was converted into a one-pixel thick line representation of the graft. Artifacts and gaps in the line were removed and the graft's endings located. Finally, we build upon the work by Steven et al. to assess the curling behavior of the graft [13] and we relate curvature of the line segment to graft orientation. The predicted graft orientation was then compared to the ground truth and classification by the corneal surgeons.

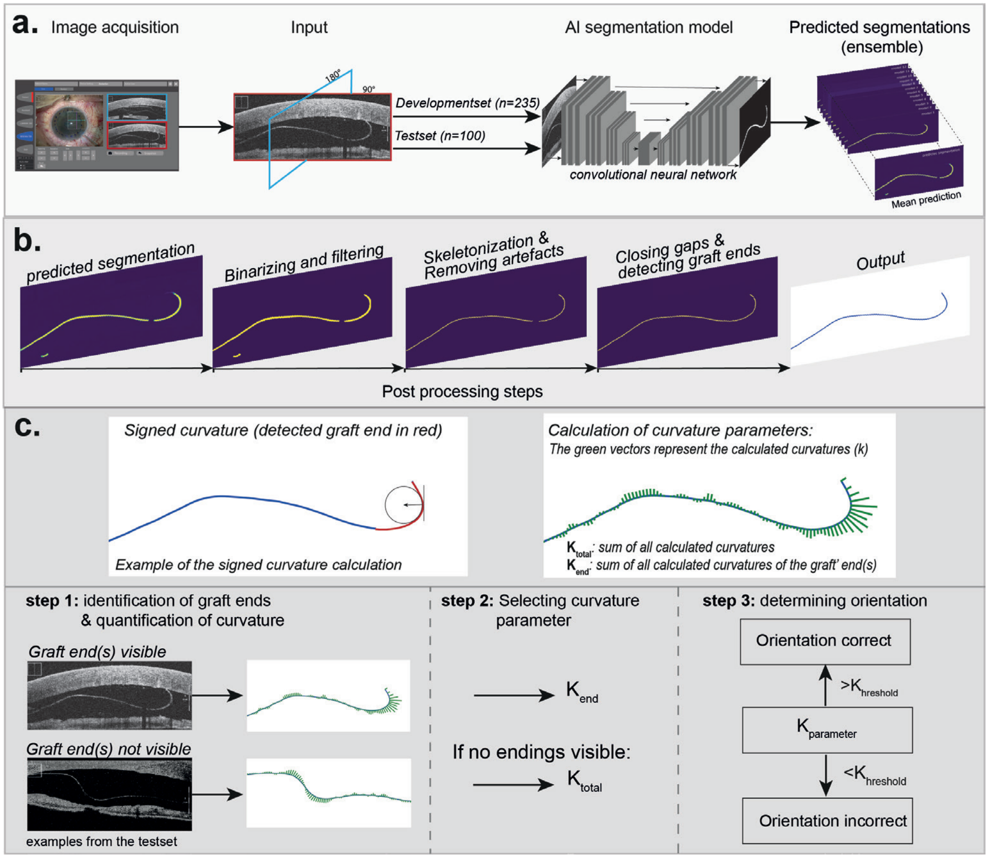

Figure 2. A schematic representation of the pipeline of the intraoperative OCT DMEK graft orientation model. Shown in section A are the image acquisition process and the automatic segmentation model. The predicted segmentation is the mean of an ensemble of 12 deep learning models. Section B shows the key post-processing steps to obtain a one-pixel line representing the graft. In section C the left top image is a schematic representation of the signed curvature. The top right image shows the polygons fitted to the line representing the graft and the defined curvature parameters. The bottom images of section C show the decision tree for selecting the curvature parameter and determining the orientation.

Segmentation

For segmentation of the DMEK graft from the iOCT frame, we used a deep learning approach.[24] Our model consists of an ensemble of 2D U-Nets.[25] The U-Net architecture incorporates a large contextual region and has resulted in state-of-the-art performance for many biomedical image segmentation tasks.[24,25] Training was done using iOCT-frames and the corresponding manually annotated masks of the trainset (n = 202). Data-augmentation was used to expand the variability in appearance of the training data set. Augmentations included random affine transformations that were applied to the iOCT frames and corresponding mask annotations: translation (< 10 pixels), rotation (< 3°), scaling (< 10%) and vertical reflection. In addition, we applied intensity shift (< 10/256), contrast shift (< 0.1) and addition of white noise (< 10/256) to the iOCT frames. Experiments with different learning rates and loss functions indicated that different models lead to different types of segmentation errors for the validation set (n = 33). We therefore constructed an ensemble of 12 U-Nets: Five models were trained using Dice loss and initial learning rates of 0.0001, 0.0002, 0.0003, 0.004, and 0.0005. Another seven models were trained based on a weighted binary cross-entropy (WBCE) loss, with a weight determining the relative penalty for misclassified foreground pixels (= DMEK graft) in comparison to background pixels. Beta values of 0.5, 1, 2, 4, 8, 12, and 16 were used, and the WBCE models were trained with an initial learning rate of 0.0003. All models were optimized with Adam for 3500 iterations where the initial learning rate was multiplied by 0.3 every 1400 iterations.[26] Each U-Net in the ensemble provides a segmentation prediction and the final segmentation was obtained by taking the mean across the 12 segmentation maps (**Figure 2A**).

6

Post-processing

To ensure the graft is represented as a single smooth line, a post-processing algorithm was developed (**Figure 2B**) consisting of the following steps: (1) Median filtering (filter size = 2 × 2) to reduce noise; (2) Binarization to assign pixels to either background or graft class; (3) Skeletonization to obtain the topological skeleton (one-pixel thick) of the segmented areas [27]; (4) Removal of small islands (<100 pixels) to get rid of small areas falsely identified as graft; (5) Morphological pruning to remove side-branches from the remaining skeletonized line segments. We implemented the pruning by finding the longest pathway for each segment and removing any pixels not belonging to these paths. The longest pathway was determined by determining the largest number of pixels needed to travel along the skeleton from any branch end to any other branch end; (6) Closing of gaps between endings of line segments with a Euclidian distance less than 100 pixels, by in painting with a one-pixel thick straight line. For the post-processing steps, all design choices and parameter selections were based empirically on results for the validation set. Next, the largest line segment was identified and the coordinates of every 15th pixel along the line were used to compute a parametric cubic smoothing spline curve. The parametrization was then used to resample 100 points along a smooth line representing the graft.

Graft orientation

To determine the orientation of the graft, we first assessed the rolling behavior of the graft. The rolling behavior can be measured as the signed curvature κ, similar to the previously described method by Steven et al. [13] A Python implementation of the Matlab LineCurvature2D package [28] was used to calculate the local curvature at each of the 100 graft points obtained with the post-processing step (**Figure 2C**). Summing all local curvatures for the length of the graft (L), the total curvature ($\kappa_{\mathbf{total}}$) can be calculated, taking into account the distance arc length steps (ds):

$$\boldsymbol{\kappa_{total}} = ds \sum_{i=1}^{L} \kappa_i$$

We are however mostly interested in the graft curvature at the endings ($\kappa_{\mathbf{end}}$), since this is typically used by our corneal specialists to determine graft orientation. The graft ending is here defined as the first and last 20% of the graft points:

$$\boldsymbol{\kappa_{end}} = ds \sum_{i=1}^{20} \kappa_i + ds \sum_{i=81}^{100} \kappa_i$$

The curvature of a graft ending was only calculated if it was visible in the iOCT-frame. A graft end is classified as invisible (out of iOCT-frame bounds) when the first or last point of the calculated curve is within 10 pixels of the original iOCT-frame boundary. Prediction of the graft's orientation is primarily based on the curvature of the graft's endings $\kappa_{\mathbf{end}}$. Alternatively, the overall curvature $\kappa_{\mathbf{total}}$ is used to determine the orientation only when: (1) both the graft's endings are not visible in the iOCT-frame or (2) the graft's endings show no curvature. To determine the orientation of the graft, the curvature of the graft ($\kappa_{\mathbf{parameter}}$) was compared with a threshold value ($\boldsymbol{\kappa}_{\mathbf{threshold}}$). A graft with a curvature smaller than this threshold was considered incorrectly oriented.

Evaluation and statistical analysis

Performance of the automatic DMEK orientation model was evaluated for the test set iOCT frames (n = 100). The predicted orientation was compared to the ground truth orientation and a receiver operating characteristic (ROC) curve was determined by varying the $\kappa_{\mathbf{threshold}}$ threshold. Sensitivity was defined as the accurate prediction of correctly oriented grafts while specificity represents true prediction of incorrectly oriented grafts (i.e., upside-down). For comparison of the automatic method with the corneal specialists, an operating point was chosen by setting a single value for $\kappa_{\mathbf{threshold}}$, based on an optimal F1-score. The set $\kappa_{\mathbf{threshold}}$ was used for all prediction methods. All statistical analysis were performed using R statistical software version 4.0.3 (CRAN, Vienna, Austria). The ROC plots were produced using the ROCR package (version 1.0-11).

Quality of the segmentations was evaluated using the Dice score. Additionally, we evaluated a pipeline that uses the manual annotated masks instead of deep learning-based segmentations. The post-processing of these segmentations was similar to the end-to-end pipeline, although steps (4) removal of pixel islands and (6) closing of gaps were skipped. This 'semi-automatic method' was evaluated on the test set as well as the recently acquired frames of the development set (n = 108), as these are comparable to the frames in the test set in terms of frame size and resolution.

RESULTS

Of the 335 iOCT-frames included in this study, 255 frames contained correctly oriented grafts versus 80 incorrectly oriented grafts (i.e., upside-down). In 195 iOCT-frames the graft was free floating (i.e., no contact with other ocular structures) and in 134 iOCT-frames a mirroring artefact of the cornea was present, which (partially) overlapped with the graft in 65 iOCT-frames. Mean age of the graft donors was 74 years (range: 55-88). The indications were Fuchs endothelial corneal dystrophy (n = 79), Pseudophakic bullous keratopathy (n = 9), and graft failure (n = 1). Segmentation performance on iOCT-frames of the test set was similar across the 12 deep learning models, with Dice scores ranging from 0.72 to 0.74. For the ensemble, where the mean prediction of the 12 models was used, the Dice score was 0.75.

Performance of the DMEK orientation model

In **Figure 3** the ROC curves are displayed for the DMEK orientation model using the deep learning-based segmentations (automatic method) and manually annotated grafts (semi-automatic method). Additionally, the performance of the corneal specialists is shown for both datasets. The automatic method achieves an AUC of 0.84, which is considered a good to excellent predictive power.[29] The semi-automatic method performs even better than the automatic method, with an AUC of 0.92 for both the development set and test set and is comparable to the performance of the corneal specialists using the same information (i.e., a single iOCT-frame). Causes for the gap in performance between the automatic and semi-automatic methods include segmentation and post-processing errors, which are described in detail in the *Qualitative analysis*.

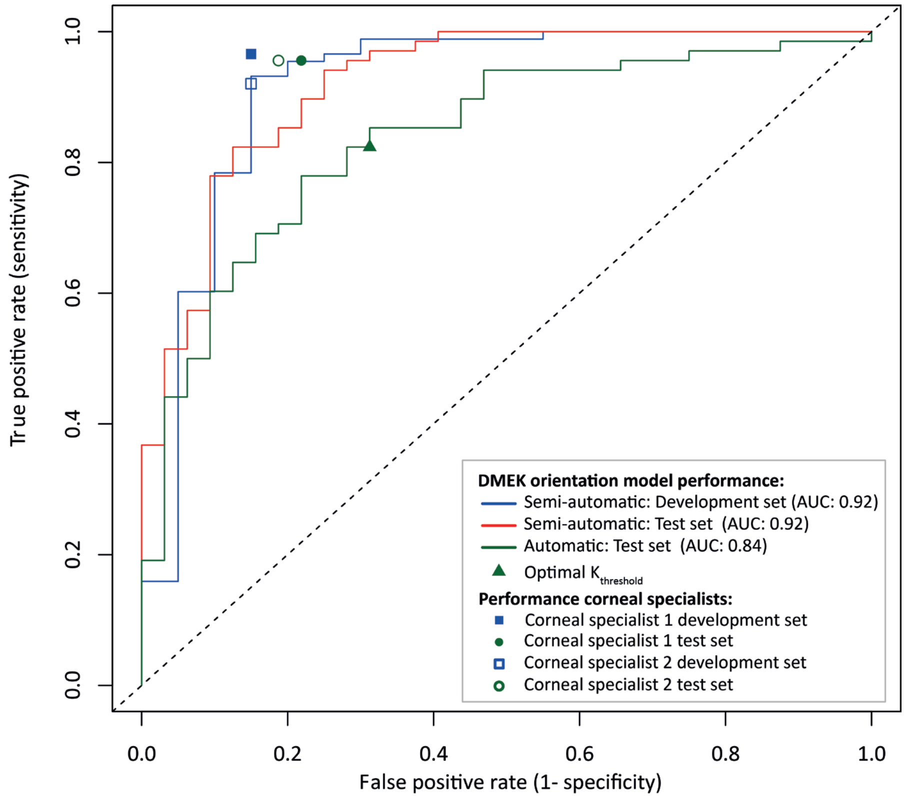

Figure 3. Performance of the prediction model using an automated and manually segmented graft. The receiver operating characteristic curves of the performance of the DMEK orientation model in the test set (n=100) and the most recent frames of the development set (n=108), obtained by varying the curvature threshold. The circles and squares represent the performance by the corneal specialists. The dashed 45-degree line constitutes a model with no discriminative power.

In line with the aim of this study – determining graft orientation using iOCT – the optimal trade-off between sensitivity and specificity was selected to determine $\kappa_{\mathbf{threshold}}$. The detailed results of the DMEK orientation model at $\kappa_{\mathbf{threshold}}$ are shown in **Table 1**. The automated method was able to correctly identify the grafts' orientation in the iOCT frames in 78% of the iOCT-frames in the test set and in 86% of the iOCT-frames for both the development and test set using manually segmented grafts. The automatic method achieved a high sensitivity (0.82) and moderate specificity (0.69). Thus, the model was able to correctly classify the majority of the correctly oriented grafts, though had only a moderate predictive power to correctly classify incorrect oriented grafts. Using the manually annotated grafts leads to slightly better sensitivity and markedly higher specificity compared to the automatic method. The outcomes of the semi-automatic methods were comparable to the performance of the corneal specialist. If only the segmentation of a single U-Net was used, the AUC varied between 0.78 and 0.86 across the 12 models in the test set (range accuracy: 0.68 – 0.80).

Table 1. Performance analysis of the orientation model and corneal specialists

Prediction	Images	Segmentation	Sensitivity	Specificity	Accuracy	AUC
DMEK orientation model	108[a]	semi-automatic	0.86	0.85	0.86	0.92
Corneal specialist 1	108[a]	-	0.97	0.85	0.94	-
Corneal specialist 2	108[a]	-	0.92	0.85	0.91	-
DMEK orientation model	100[b]	semi-automatic	0.90	0.78	0.86	0.92
DMEK orientation model	100[b]	automatic	0.82	0.69	0.78	0.84
Corneal specialist 1	100[b]	-	0.96	0.78	0.90	-
Corneal specialist 2	100[b]	-	0.96	0.81	0.91	-

AUC: area under the curve,

[a] Development set consisting of only recently acquired frames measuring 610 pixels by 275 pixels were included for comparability with the test set.
[b] Test set frames measuring 610 pixels by 275 pixels

6

Qualitative analysis of segmentation and post-processing

All deep learning-based segmentations in the test set were qualitatively evaluated for errors in the predicted segmentation or post-processing. In 54 iOCT-frames a near perfect representation of the graft was achieved after post-processing compared to the manually labeled results (**Figure 4A**) and in 46 iOCT-frames noticeable segmentation (n = 37) and/or post-processing errors (n = 13) were present after post-processing **Figure 4B-G**). A total of 22 grafts were incorrectly classified using the automatic method of the orientation model, because of segmentation errors in 8 frames, post-processing errors in 2 frames, and a limited differentiative predictive power of the model in 12 frames (i.e., in both the automated and manual method these grafts were incorrectly classified regardless of any errors; **Figure 4H**). In 29 iOCT-frames containing errors the model still correctly predicted the orientation.

The majority of the segmentation errors were considered minor, such as slightly incomplete segmentation of the graft ends or at the image boundary (**Figure 4B & Figure 4C**). Notwithstanding, despite considered minor these errors may affect the algorithms performance. Partial segmentation of the graft or large gaps between segments were considered large segmentation errors (**Figure 4D**). Causes for large segmentation errors included: corneal mirror artefacts, background noise, hypo reflectance of the graft, and contact of the graft with the cornea or iris.

All post-processing errors occurred during filtering of the frames and connecting the line segments resulting in partial or wrong segmentation. During filtering smaller segments (<100 pixels) were removed, which resulted in gaps too large to bridge in the subsequent step. Similarly, in cases with large gaps (>100 pixels) the line segments were not connected and the smaller segments were removed after identification of the largest segment (**Figure 4E**). In some frames the line segments were connected with wrong segments or an image artefact falsely identified as graft (e.g., fluid reflection, the lens capsule) resulting in an incorrect representation of the graft **Figure 4F & Figure 4G**).

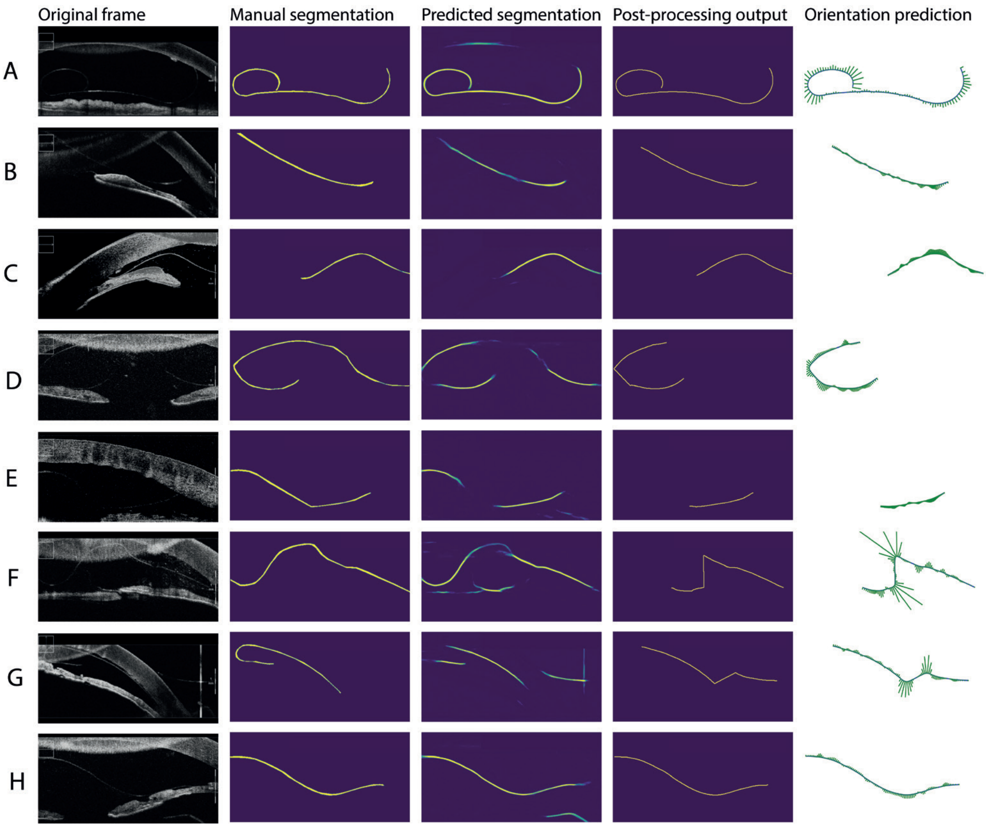

Figure 4. Examples of correct and incorrect segmentation and post-processing. A near perfect segmentation (A), a segmentation error at image boundaries (B), a segmentation error at the graft end (C), segmentation gaps resulting in partial segmentation (D), segmentation gaps too wide to connect in the post-processing (E), segments wrongly connected during post-processing (F & G), correct segmentation resulting in an incorrect prediction (H).

DISCUSSION

In this exploratory study we developed a method to *in-vivo* segment a DMEK graft using a deep-learning approach and demonstrated that an image analysis tool that can automatically identify the orientation of a DMEK graft using iOCT. Several studies have pointed out the lack of (integrated) image analysis tools and clinical decision support systems (CDSS) for iOCT that can improve the clinical value.[30–33] Computerized CDSS have the potential to improve outcomes, optimize treatments, and improve workflow efficiency.[34–36] We believe our tool might be of similar value for iOCT by improving and standardizing clinical decision making. Moreover, the tool could help ease the learning curve for starting surgeons and aid experienced surgeons in the transition towards DMEK.[13]

Determining graft orientation using iOCT is arguably more reliable and safer compared to other methods in use (i.e., the Moutsouris sign and various stamps/cuts).[10,12,14,16] However, current manual review of both live and static iOCT-scans for DMEK orientation can be time consuming and disrupt the surgical workflow hindering implementation and sustainable use of iOCT.[30,31] Our proposed automatic image analysis may alleviate these hurdles by aiding the surgeon in determining graft orientation and may reduce interpretation errors.

In recent years corneal OCT image analysis has gained interest. Several studies showed the ability of automatic tools to successful detect a DMEK graft in OCT images, quantifying graft detachment after lamellar corneal transplant surgery.[37–40] Our automatic method has a good to excellent predictive power [29] and when using manually annotated grafts the performance of our model improves considerably and is comparable to the performance of both corneal specialists. The gap in performance between the automatic and manual method is primarily the result of segmentation and post-processing errors, which in turn resulted in wrong predictions as shown with the qualitative analysis of the end-to-end outcome. Automatic segmentation of iOCT imaging is challenging because of the design and dynamic use of iOCT, which may result in higher signal noise, variable image quality, image decentration, and prevents standardized image acquisition.[19] Notwithstanding, we consider our dataset a realistic representation of images acquired in clinical practice for determining the orientation and therefor consider the performance generalizable to other datasets.

The threshold for determining the graft' orientation used in the presented results was slightly negative after optimizing the F1-score (i.e., optimal operating point), which corresponds to a slight curve downwards. This makes sense since the cornea itself also curves downward and the floating DMEK typically partly follows the shape of the cornea. In this study the optimal trade-off between sensitivity and specificity was chosen to optimize the predictive power of the model. However, it can be argued that depending on the use case or user expectations, either sensitivity or specificity may be more important.

The difference in AUC between the automatic method and the pipeline with manual annotated grafts indicates that improvements for the automatic method can be achieved by improving the automatic segmentation. In particular, correct segmentation of the graft endings could contribute to a better estimate of the graft curvature. The deep learning-based segmentation can potentially be improved by the addition of more training data, including a wider variety of anatomies and image artifacts. If a large enough training set could be obtained, an end-to-end deep learning method could be considered, where a classification model is trained only on orientation labels. However, even if enough training data would be available, such a method would come at the cost of having a CDDS without explanation for the decision-making, which could hamper acceptation by the end users. Alternatively, future research could investigate a segmentation approach that uses shape constraints [41,42], such as the fact that the graft is a continuous and smooth structure. Such an approach should take into account that not the whole graft necessarily lies in the field of view. We also experimented with the addition of extra frames to the input taken shortly before or after the investigated iOCT image, in which the location and orientation of the DMEK graft slightly differed from the center frame. For example, we added the 5th and 10th frames before and after the center frame as additional channels to the input, similar to Vu et al. [43], hypothesizing that the extra information would help the learning process. However, no benefits were found from this step and it was omitted for the final ensemble.

It should be noted that assessment of graft orientation based on a single frame does not reflect clinical practice. Instead, a corneal specialist would reduce uncertainty by assessing multiple frames or manipulate the graft until orientation is evident. Future work could incorporate such a strategy in the automatic image analysis pipeline, for example by using a recurrent neural network on follow-up frames.[44,45] For clinical implementation, the image analysis pipeline needs to be directly applied to the video-feed. In this research, iOCT frames were qualitatively reviewed for image quality and presence of characteristics on which orientation could be determined. However, the qualitative analysis indicated not every frame contains enough information for evaluation of the orientation. Future research could include an automatic frame-based quality assessment, or an uncertainty estimate and only provide a prediction if the certainty is high. A challenge for real-time image analysis is the speed at which the segmentation and post-processing can be performed. Here an ensemble of 12 U-Nets was used for the segmentation, but this might require more computational power than standardly offered with an iOCT system resulting in a longer inference time required to determine the orientation. However, the benefit of an ensemble compared to a single U-Net seemed marginal and perhaps an ensemble is not required if more annotated training data is used. Another solution could be the use of knowledge distillation techniques, which have recently been proposed to train a single segmentation model that performs similar to an ensemble.[46,47] It should be noted that we only tested our methods for a single OCT-system at a single center and additional research is needed to evaluate the feasibility for other settings. Especially the deep learning-based segmentation is known to often poorly generalize to out of distribution data. To ensure generalization to a wide variety of scanners and scanning parameters, training could be done using data from various OCT systems, or with the use of extensive data-augmentation.

In conclusion, we present an automated image analysis method for iOCT to detect a DMEK graft, quantify the curvature, and determine the graft's orientation. Our future research efforts will focus on improving automatic segmentation and predictive certainty of our algorithm.

ACKNOWLEDGEMENTS

The authors are grateful to Marijn Hiep, Suzanne de Vette, and Inge van den Berg for their assistance with the development of the DMEK orientation model and conceptualization of a user interface.

REFERENCES

1. Parker J, Parker JS, Melles GR. Descemet Membrane Endothelial Keratoplasty—A Review. *US Ophthalmic Review* 2013; 06: 29.
2. Stuart AJ, Romano V, Virgili G, et al. Descemet's membrane endothelial keratoplasty (DMEK) versus Descemet's stripping automated endothelial keratoplasty (DSAEK) for corneal endothelial failure. *Cochrane Database of Systematic Reviews*. Epub ahead of print 2018. DOI: 10.1002/14651858.CD012097.pub2.
3. Price MO, Gupta P, Lass J, et al. EK (DLEK, DSEK, DMEK): New Frontier in Cornea Surgery. *Annual Review of Vision Science* 2017; 3: 69–90.
4. Dapena I, Moutsouris K, Droutsas K, et al. Standardized "No-Touch" Technique for Descemet Membrane Endothelial Keratoplasty. *Archives of Ophthalmology* 2011; 129: 88–94.
5. Bardan AS, Goweida MB, Goweini HF El, et al. Management of upside-down descemet membrane endothelial keratoplasty: A case series. *Journal of Current Ophthalmology* 2020; 32: 428.
6. Dragnea DC, Nobacht S, Gericke A, et al. Postoperative Repositioning of Inverted Descemet Membrane Endothelial Keratoplasty Grafts. *Cornea* 2019; 38: 162–165.
7. Veldman PB, Dye PK, Holiman JD, et al. The S-stamp in Descemet Membrane Endothelial Keratoplasty Safely Eliminates Upside-down Graft Implantation. *Ophthalmology* 2016; 123: 161–164.
8. Wasielica-Poslednik J, Schuster AK, Rauch L, et al. How to Avoid an Upside-Down Orientation of the Graft during Descemet Membrane Endothelial Keratoplasty? *Journal of Ophthalmology*; 2019. Epub ahead of print 2019. DOI: 10.1155/2019/7813482.
9. Modabber M, Talajic JC, Mabon M, et al. The role of novel DMEK graft shapes in facilitating intraoperative unscrolling. *Graefe's Archive for Clinical and Experimental Ophthalmology* 2018; 256: 2385–2390.
10. Cost B, Goshe JM, Srivastava S, et al. Intraoperative optical coherence tomography-assisted descemet membrane endothelial keratoplasty in the DISCOVER study. *American Journal of Ophthalmology* 2015; 160: 430–437.
11. Sharma N, Sahay P, Maharana PK, et al. Microscope Integrated Intraoperative Optical Coherence Tomography-Guided DMEK in Corneas with Poor Visualization. *Clinical ophthalmology (Auckland, NZ)* 2020; 14: 643–651.
12. Patel AS, Goshe JM, Srivastava SK, et al. Intraoperative Optical Coherence Tomography–Assisted Descemet Membrane Endothelial Keratoplasty in the DISCOVER Study: First 100 Cases. *American Journal of Ophthalmology* 2020; 210: 167–173.
13. Steven P, Le Blanc C, Velten K, et al. Optimizing Descemet membrane endothelial keratoplasty using intraoperative optical coherence tomography. *JAMA Ophthalmology* 2013; 131: 1135–1142.
14. Saad A, Guilbert E, Grise-Dulac A, et al. Intraoperative OCT-Assisted DMEK: 14 Consecutive Cases. *Cornea* 2015; 34: 802–807.
15. Mohammed I, Ross AR, Britton JO, et al. Elastin Content and Distribution in Endothelial Keratoplasty Tissue Determines Direction of Scrolling. *American Journal of Ophthalmology* 2018; 194: 16–25.
16. Muijzer MB, Soeters N, Godefrooij DA, et al. Intraoperative Optical Coherence Tomography-Assisted Descemet Membrane Endothelial Keratoplasty: Toward More Efficient, Safer Surgery. *Cornea* 2020; 39: 674–679.
17. Ehlers JP, Uchida A, Srivastava SK, et al. Predictive Model for Macular Hole Closure Speed: Insights From Intraoperative Optical Coherence Tomography. *Translational vision science & technology* 2019; 8: 18.

18. Hallahan KM, Cost B, Goshe JM, et al. Intraoperative Interface Fluid Dynamics and Clinical Outcomes for Intraoperative Optical Coherence Tomography–Assisted Descemet Stripping Automated Endothelial Keratoplasty From the PIONEER Study. *American Journal of Ophthalmology* 2017; 173: 16–22.

19. Xu D, Dupps WJJ, Srivastava SK, et al. Automated volumetric analysis of interface fluid in descemet stripping automated endothelial keratoplasty using intraoperative optical coherence tomography. *Investigative ophthalmology & visual science* 2014; 55: 5610–5615.

20. Weiss J, Rieke N, Nasseri MA, et al. Fast 5DOF needle tracking in iOCT. *International journal of computer assisted radiology and surgery* 2018; 13: 787–796.

21. Roodaki H, Grimm M, Navab H, et al. Real-time Scene Understanding in Ophthalmic Anterior Segment OCT Images. *Investigative Ophthalmology & Visual Science*; 60.

22. Grimm M, Roodaki H, Eslami A, et al. Automatic intraoperative optical coherence tomography positioning. *International journal of computer assisted radiology and surgery* 2020; 15: 781–789.

23. Keller B, Draelos M, Zhou K, et al. Optical Coherence Tomography-Guided Robotic Ophthalmic Microsurgery via Reinforcement Learning from Demonstration. *IEEE Transactions on Robotics* 2020; 36: 1207–1218.

24. LeCun Y, Bengio Y, Hinton G. Deep learning. *Nature* 2015; 521: 436–444.

25. Ronneberger O, Fischer P, Brox T. U-Net: Convolutional Networks for Biomedical Image Segmentation. In: Navab N, Hornegger J, Wells WM, et al. (eds) *Medical Image Computing and Computer-Assisted Intervention -- MICCAI 2015*. Cham: Springer International Publishing, 2015, pp. 234–241.

26. Kingma DP, Ba JA. A method for stochastic optimization. *arXiv*; 1412.

27. Lee TC, Kashyap RL. Building skeleton models via 3-D medial surface/axis thinning algorithms. *Computer Vision, Graphics, and Image Processing* 1994; 56: 462–478.

28. Kroon DJ. 2D Line Curvature and Normals. *MATLAB Central File Exchange*, https://www.mathworks.com/matlabcentral/fileexchange/32696-2d-line-curvature-and-normals.

29. Mandrekar JN. Receiver operating characteristic curve in diagnostic test assessment. *Journal of Thoracic Oncology* 2010; 5: 1315–1316.

30. Muijzer MB, Schellekens PAWJ, Beckers HJM, et al. Clinical applications for intraoperative optical coherence tomography: a systematic review. *Eye (Basingstoke)* 2021; 1–13.

31. Ehlers JP, Modi YS, Pecen PE, et al. The DISCOVER Study 3-Year Results: Feasibility and Usefulness of Microscope-Integrated Intraoperative OCT during Ophthalmic Surgery. *Ophthalmology* 2018; 125: 1014–1027.

32. Ehlers JP, Uchida A, Srivastava SK. The Integrative Surgical Theater: Combining Intraoperative OCT and 3D Digital Visualization for Vitreoretinal Surgery in the DISCOVER Study. 2019; 38: 1–17.

33. Ehlers JP. Intraoperative optical coherence tomography: Past, present, and future. *Eye (Basingstoke)* 2016; 30: 193–201.

34. Bright TJ, Wong A, Dhurjati R, et al. Effect of clinical decision-support systems: a systematic review. *Annals of internal medicine* 2012; 157: 29–43.

35. Shortliffe EH, Sepúlveda MJ. Clinical Decision Support in the Era of Artificial Intelligence. *JAMA - Journal of the American Medical Association* 2018; 320: 2199–2200.

36. Noorbakhsh-sabet N, Zand R, Zhang Y, et al. Artificial Intelligence Transforms the Future of Healthcare. *Am J Med* 2020; 132: 795–801.

37. Heslinga FG, Alberti M, Pluim JPW, et al. Quantifying graft detachment after Descemet's membrane endothelial keratoplasty with deep convolutional neural networks. *Translational Vision Science and Technology* 2020; 9: 1–9.

38. Treder M, Lauermann JL, Alnawaiseh M, et al. Using Deep Learning in Automated Detection of Graft Detachment in Descemet Membrane Endothelial Keratoplasty: A Pilot Study. *Cornea* 2019; 38: 157–161.

39. Hayashi T, Tabuchi H, Masumoto H, et al. A Deep Learning Approach in Rebubbling After Descemet's Membrane Endothelial Keratoplasty. *Eye & contact lens* 2020; 46: 121–126.

40. van der Velden BM, Veta M, Pluim JosienPW, et al. Radial U-Net: Improving DMEK Graft Detachment Segmentation in Radial AS-OCT Scans. In: Fu H, Garvin MK, MacGillivray T, et al. (eds) *Ophthalmic Medical Image Analysis*. Cham: Springer International Publishing, 2021, pp. 72–81.

41. Wolterink JM, Leiner T, Išgum I. Graph Convolutional Networks for Coronary Artery Segmentation in Cardiac CT Angiography. In: Zhang D, Zhou L, Jie B, et al. (eds) *Graph Learning in Medical Imaging*. Cham: Springer International Publishing, 2019, pp. 62–69.

42. Bohlender S, Oksuz I, Mukhopadhyay A. A survey on shape-constraint deep learning for medical image segmentation. *arXiv*; 2101.

43. Vu MH, Grimbergen G, Nyholm T, et al. Evaluation of multislice inputs to convolutional neural networks for medical image segmentation. *Medical physics* 2020; 47: 6216–6231.

44. Valipour S, Siam M, Jagersand M, et al. Recurrent Fully Convolutional Networks for Video Segmentation. In: *2017 IEEE Winter Conference on Applications of Computer Vision (WACV)*. 2017, pp. 29–36.

45. Chen J, Yang L, Zhang Y, et al. Combining fully convolutional and recurrent neural networks for 3D biomedical image segmentation. *Advances in Neural Information Processing Systems* 2016; 3044–3052.

46. Liu Y, Chen K, Liu C, et al. Structured Knowledge Distillation for Semantic Segmentation. In: *2019 IEEE/CVF Conference on Computer Vision and Pattern Recognition (CVPR)*. 2019, pp. 2599–2608.

47. Tellez D, Balkenhol M, Otte-Höller I, et al. Whole-Slide Mitosis Detection in H&E Breast Histology Using PHH3 as a Reference to Train Distilled Stain-Invariant Convolutional Networks. *IEEE Transactions on Medical Imaging* 2018; 37: 2126–2136.

PART 3

DATA-DRIVEN APPROACHES TO IDENTIFY RISK FACTORS FOR GRAFT DETACHMENT IN DESCEMET MEMBRANE ENDOTHELIAL KERATOPLASTY

CHAPTER 7

A MACHINE LEARNING APPROACH TO EXPLORE PREDICTORS OF GRAFT DETACHMENT FOLLOWING POSTERIOR LAMELLAR KERATOPLASTY: A NATIONWIDE REGISTRY STUDY

Marc B Muijzer; Christian MW Hoven;
Laurence E Frank; Gerko Vink; Robert PL Wisse;
on behalf of the Netherlands Corneal Transplant Network (NCTN)

Submitted for publication

ABSTRACT

Aim: To use a machine learning approach to evaluate the effect of various practice patterns on the risk of graft detachment following posterior lamellar keratoplasty (PLK).

Methods: All PLK procedures recorded in the Dutch Cornea Transplant Registry from 2015 through 2018 were included, and center-specific practice patterns were identified using a 35-item questionnaire. All available data regarding the donor, graft, recipient, practice pattern, were coded into 91 factors that might be associated with the occurrence of a graft detachment. Given the large number of predictor variables, machine learning models were used to select the most predictive subset of variables for the outcome of a graft detachment. We used regularized logistic regression (lasso), classification tree analysis (CTA), and random forest classification (RFC).

Results: A total of 3647 transplants performed in 16 cornea centers were included in our analysis; 996 (27%) and 2651 (73%) were DMEK and DSEK procedures, respectively. The overall prevalence of rebubbling was 17.4% and 7.1%, respectively. The area under the curve for the lasso, CTA, and RFC machine learning models was 0.70, 0.65, and 0.72, respectively. All three models achieved moderate sensitivity and specificity. Several risk factors were identified, including performing DMEK, prior graft failure, and the use of sulfur hexafluoride gas during the procedure. Factors that reduced the risk of detachment included performing combined procedures, using pre-cut tissue, and laser iridotomy.

Conclusion: Graft detachment following PLK has a multifactorial origin, and our machine learning-based analysis identified several factors that can predict postsurgical graft detachment. These results can help surgeons review their practice patterns and can help generate new testable hypotheses. In the future, a prospective clinical study should be performed to determine the real-world performance of our machine learning analysis.

INTRODUCTION

Posterior lamellar keratoplasty is the current standard treatment to restore visual function in patients with irreversible corneal endothelial cell dysfunction.[1] Two principal treatment modalities are currently used, namely Descemet's stripping endothelial keratoplasty (DSEK) and Descemet's membrane endothelial keratoplasty (DMEK).[2] In recent years, DMEK has increased in popularity due to its potential for faster visual recovery and improved visual outcome compared to DSEK.[3,4] In both DSEK and DMEK, postoperative detachment of the graft is a relatively common complication.[5–7] Detachment can require a secondary surgical intervention, potentially resulting in a less viable graft. The reported prevalence of graft detachment ranges from 2% to 27% for DSEK and 6% to 82% for DMEK.[5–7]

The underlying cause of graft detachment is considered to be multifactorial[8–12], and a wide range of risk factors have been proposed and/or investigated, including the type of procedure (DSEK versus DMEK)[5–7], graft storage and preparation (e.g., pre-cut versus surgeon-cut)[13–16], the donor's characteristics (e.g., age, cause of death, and comorbidity)[8,16–18], the recipient's characteristics (e.g., the indication for surgery and prior corneal transplant surgery)[8,10,12,19,20], and surgical complications.[8,11,12] Furthermore, various "best practice patterns" have been proposed, resulting in a wide range of surgical tools and techniques that have been adopted when performing posterior lamellar keratoplasty.[9,21] These patterns include the insertion method[8,22,23], the size of the descemetorhexis compared to the graft size[24,25], performing a combination of surgical procedures[12,26–29], the use of anterior chamber (AC) tamponade (e.g., the agent, volume, pressure, and duration)[9,12,21,26–28,30–35], and the duration of time spent in the supine position (imposed or recommended) following surgery.[9,36]

In the Netherlands, all centers that perform corneal transplants report their procedures to the Netherlands Organ Transplant Registry (NOTR). These records include extensive follow-up data, including complications, thus providing a unique source of real-world data regarding graft survival, patient characteristics, and donor characteristics. We expanded this dataset using a 35-item questionnaire regarding the preoperative, perioperative, and postoperative procedures performed at each center, as rapidly changing practice patterns in the field of surgery made performing an independent assessment of these practice patterns in a clinical study unfeasible.

Machine learning models can be used to detect complex patterns in large datasets, and these patterns can help researchers identify factors that can predict the risk of postsurgical complications.[37,38] Here, we present the results of our machine learning analysis to identify factors that predict an increase or decrease in the risk of graft detachment following posterior lamellar keratoplasty.

METHODS

Data collection

The data used in this study were acquired from the NOTR, which is hosted by the Netherlands Transplant Foundation (NTS). We included all DSEK and DMEK procedures performed in the Netherlands between January 1, 2015, and December 31, 2018, including 12 months of follow-up data. Two cornea banks (Amnitrans EyeBank, Rotterdam and the ETB-bislife, Beverwijk) supplied all of the corneal grafts assessed in this study. The NOTR steering committee provided Institutional Review Board (IRB) approval for the extraction and analysis of data in this study. All patients provided informed consent to be included in the registry for research purposes. No identifying information of donors or patients was available to the researchers and all data were anonymized prior to delivery to the researchers. No donor tissue was were procured from prisoners. In accordance with IRB approval, the data were not stratified at the individual surgeon, center, donor or patient level. The study was conducted in accordance with the principles of the Declaration of Helsinki and Dutch legislation. The NOTR data were restructured and made accessible for machine learning analysis.

Registry data processing

All available data in the registry regarding the donor, graft, recipient, and practice patterns was collected. The donor's information included sex, age at the time of death, cause of death, endothelial cell count, interval between death and explantation of the eye, interval between explantation of the eye and preservation of the eye, and interval between death and the transplant procedure. The donor's cause of death was classified into the following five categories: neoplasms/cancer, diseases of the respiratory system, trauma, diseases of the cardiovascular system, and other causes of death. The recipient's information included sex, age at the time of surgery, indication for corneal transplantation surgery, and preoperative lens status. The indication for transplant surgery was classified into the following five categories: Fuchs corneal endothelial dystrophy (FECD), pseudophakic bullous keratopathy (PKB), graft failure, other corneal dystrophies, and other indications. Information regarding the surgical procedure included the surgeon's position (staff surgeon or surgical fellow), date of surgery, instruments used for donor preparation, instruments used for graft insertion, diameter of the donor graft, diameter of the descemetorhexis, whether it was a combined surgical procedure, and surgical complications. Combined surgical procedures were recoded into the following five groups: peripheral surgical iridectomy, cataract surgery, posterior intraocular lens insertion without cataract extraction, anterior vitrectomy, and other combined surgical procedures or unspecified. Postoperative events recorded in the NOTR were classified as surgery-related (e.g., rebubbling, graft failure, immunological reaction, iatrogenic glaucoma, and/or cystoid macula edema) and not surgery-related (e.g., intravitreal injections, posterior segment surgery after primary transplant, and/or extra-ocular events). The recoding of the variables resulted in a set of 91 predictor variables.

Practice pattern questionnaire

We used a questionnaire to determine the practice patterns used by the transplantation centers that contributed their data to the registry, including the center-specific practice patterns (e.g., method of iridectomy, instruments used during surgery, AC tamponade, and supine time) and any protocol changes that may have occurred within the data collection period. All practice patterns questionnaires were collected by the NTS and anonymized before delivery to the researchers.

The center-specific practice patterns were connected to the respective patients in the registry, and protocol changes that occurred in the period between January 2015 and December 2018 were taken into account. To reduce the potential effects of a surgical learning curve, the first 20 DMEK surgeries performed at each center were removed from the dataset.[4]

Machine learning analysis

The primary outcome measure of this study was postoperative graft detachment, which was defined as the occurrence of an intervention to re-adhere the graft (i.e., the incidence of rebubbling) reported in the NOTR. The dataset was divided into a training set and a test set, compromised of 70% and 30% of the dataset, respectively. The training set was used to develop a suitable model based on the predictive variables identified, and the test set was used to validate the model. The following three machine learning models were built: a L1 regularized logistic regression using least absolute shrinkage and selection operator (lasso) model, a classification tree algorithm (CTA), and random forest classification (RFC).

These three models have been chosen for the following reasons. Given the 91 predictors, a simple logistic regression analysis with outcome graft detachment is computationally difficult or even impossible. The lasso model is a special form of logistic regression in which the estimated regression coefficients are shrunken towards zero relative to the least squares estimates. As a result, some coefficients will be exactly zero, which leads to the selection of a subset of most predictive predictors for graft detachment. However, the Lasso will only be able to detect linear relations of the predictors with the outcome detachment. To detect non-linear relationships and higher-order relationships among the explanatory variables, we used CTA and RFC. The CTA partitioned the training dataset based on outcome (i.e., graft detachment/no graft detachment) using a series of successive splits (i.e., nodes).[50] For each split, the explanatory variable that best partitioned the records was chosen based on accuracy, until the set could not be split further. To reduce over-fitting, pruning was performed using 5-fold cross-validation, thus removing nodes that did not improve the accuracy of the tree. In the final tree, each leaf node was assigned the class with the highest frequency among its records, and each record reaching the node was predicted as being in that class. Although classification trees are very useful to detect higher-order relations and non-linear relations, they are not very robust, meaning that small changes in the data can result in large changes in the final estimated tree. RFC leads to a more robust classification model by building a large number of classification trees and splitting the data using a random sample of the entire set of explanatory variables to serve as split candidates. The resulting trees were combined by taking a majority vote, and the overall prediction was the most frequently occurring class among all predictions. By forcing each split to consider only a subset of variables, the RFC analysis overcomes the potential problem of one or more strong predictors dominating the solution, thus rendering the average of the trees less variable and therefore more reliable. In this study 1000 trees were used to build the RFC model.

The relatively low rate of graft detachment in the dataset resulted in a large imbalance between the two outcome categories (i.e., detachment versus no detachment) and can therefore affect the statistical model estimation and evaluation. To solve this imbalance, we performed random oversampling of examples (ROSE) for the lasso and the CTA.[51] The RFC model was trained in combination with weights to balance the outcome classes. No resampling techniques were used for the test set.

Statistical analysis

We summarized all quantitative and qualitative variables, including the donor characteristics, recipient characteristics, procedure characteristics, postoperative events, and practice patterns. The prevalence of graft detachment was determined separately for all procedures involving DSEK and all procedures involving DMEK independently. All statistical analyses were performed using the R statistical software package version 4.0.5 (Comprehensive R Archive Network, Vienna, Austria), except for the RFC which was performed using in Python version 3.8 and the scikit-learn package version 0.24.1 (Python Software Foundation. Python Language Reference, version 2.7).

The machine learning models were evaluated using the test set. The predicted outcome was compared with the observed outcome reported in the NOTR (i.e., the ground truth) by calculating the sensitivity, specificity, and the area under the curve (AUC).

RESULTS

A total of 3647 posterior lamellar keratoplasties were performed in the Netherlands and recorded in the NOTR registry between January 1, 2015 and December 31, 2018, including 2651 DSEK procedures (73%) and 996 DMEK procedures (27%). The surgeries were performed at sixteen centers throughout the Netherlands. Twelve of these centers submitted their practice patterns (**Supplementary Table 1** and **Supplementary Table 2**), while the other four centers did not respond to the survey. These four centers performed 227 DSEK procedures and 1 DMEK procedure; for these four centers, only the NOTR data were included in the analysis. None of the continuous explanatory variables had missing observations. Sixteen categorical explanatory variables had missing values (mean percentage of missing values: 2.7% SD ±4.3%; range: 5-20%); these values were recorded as “unknown” and were included for analysis as a new category in the respective variable.

Donor, recipient and procedure characteristics

The mean (±SD) donor age was 70±9 years, and 61.4% of donors were male. The most common cause of death was diseases of the circulatory system (53.3%), followed by diseases of the respiratory system (16%), other/unknown (20.3%), cancer (8.8%), and trauma (1.5%). The mean interval between death and the transplant procedure was 19±5 days. A complete summary of the donor characteristics is provided in **Supplementary Table 3**.

The most common indication for surgery was FECD (76.7% of cases). Interestingly, FECD was the indication for performing DMEK in 91.1% of cases, compared to 71.2% in DSEK. The majority of recipients were pseudophakic prior to surgery, with 62.3% having a posterior chamber intraocular lens. In total, 88.8% of recipients did not previously undergo a corneal transplant in the same eye. In 39.5% of cases, the graft was equal in size to the descemetorhexis; the graft was undersized in 26.1% of cases and oversized in 34.4% of cases. In 71.7% of cases, posterior lamellar keratoplasty was not combined with another surgical procedure. The most frequently performed combined surgical procedures were peripheral iridectomy and cataract surgery (12.2% and 8.6% of cases, respectively). A surgical complication was reported in the NOTR in 4.1% of all cases (3.3% of DSEK procedures and 6% of DMEK procedures) and included endothelial damage (0.8% of cases), difficulty unfolding the graft (0.7%), graft rupture or preparation problems (0.4%), iris prolapse (0.4%), and hemorrhage of the AC (0.4%). The recipient and surgery characteristics are summarized in **Supplementary Table 4** and **Supplementary Table 5**, respectively.

Table 1. Summary of graft detachments following DSEK and DMEK procedures performed in the Netherlands from 2015 through 2018.

		DSEK (n=2651)			**DMEK (n=996)**			**All procedures (n=3647)**		
		Procedures performed (n)	Detachments, n (%)	Prevalence per center, mean ± SD	Procedures performed (n)	Detachments, n (%)	Prevalence per center, mean ± SD	Procedures performed (n)	Detachments, n (%)	Prevalence per center, mean ± SD
Year	2015-2018	2651	188 (7.1)	8.4 ± 7.2%	996	173 (17.4)	13.4 ± 8.2%	3647	361 (9.9)	10 ± 6.7%
	2015	743	46 (6.2)	2.2 ± 2.8%	43	6 (14.0)	0.04 ± 0.8%	786	52 (6.6)	1.8 ± 2.6%
	2016	716	45 (6.3)	2.6 ± 3.6%	213	54 (25.4)	4.1 ± 3.2%	929	99 (10.7)	3.3 ± 3.3%
	2017	632	50 (7.9)	2.2 ± 1.6%	267	57 (21.3)	4.5 ± 2.8%	899	107 (11.9)	2.8 ± 1.6%
	2018	560	47 (8.4)	1.5 ± 1.6%	473	56 (11.8)	4.4 ± 5.2%	1033	103 (10.0)	2.2 ± 2.2%

DSEK, Descemet's stripping endothelial keratoplasty; DMEK, Descemet's membrane endothelial keratoplasty; SD, standard deviation

Postoperative complications

The incidence and prevalence of postoperative graft detachment are summarized in **Table 1**. Overall, the rate of graft detachment was 9.9% (361 out of the 3647 procedures performed over the 4-year study period). During the period from 2015 through 2018, the number of DMEK procedures performed each year increased considerably from 4 to 473, while the number of DSEK procedures performed each year decreased from 743 to 560, reflecting the growing preference for this newer surgical procedure. The prevalence of graft detachment was relatively stable among the patients who underwent DSEK, ranging from 6.2% to 8.4%; in contrast, the prevalence of graft detachment was generally higher among the patients who underwent DMEK, ranging from 11.8% to 14%.

Results of the machine learning models

After correction for the DMEK learning curve, a total of 3464 cases were included for machine learning analysis. The discriminatory power of the three machine learning models at predicting graft detachment (based on the AUC) ranged from 0.65 to 0.72 (**Table 2**). The sensitivity and specificity were similar both within and between models, indicating a similar ability to predict both detachment and non-detachments, and indicating that a considerable amount of variation was not captured by the predictive factors included in the dataset.

Table 2. The performance of the three machine learning models at predicting graft detachment in the test dataset.

Prediction model	AUC	Sensitivity*	Specificity
LASSO logistic regression	0.70	0.70	0.65
Classification tree analysis	0.65	0.65	0.62
Random forest classifier	0.72	0.68	0.62

AUC, area under the curve; LASSO, least absolute shrinkage and selection operator.
*Sensitivity measures the proportion of detachments that are correctly predicted as detachments.

An overview of each model output is presented in **Figure 1** for the RFC and in **Supplementary figure 1** and **Supplementary figure 2** for the lasso and CTA models, respectively. The three models identified different sets of predictive factors, although several factors overlapped between the three models. The results of the most predictive factors identified by the three models are shown in **Table 3**. To simplify the analysis, factors that were categorized as either “unknown” or “unspecified” were omitted from the table.

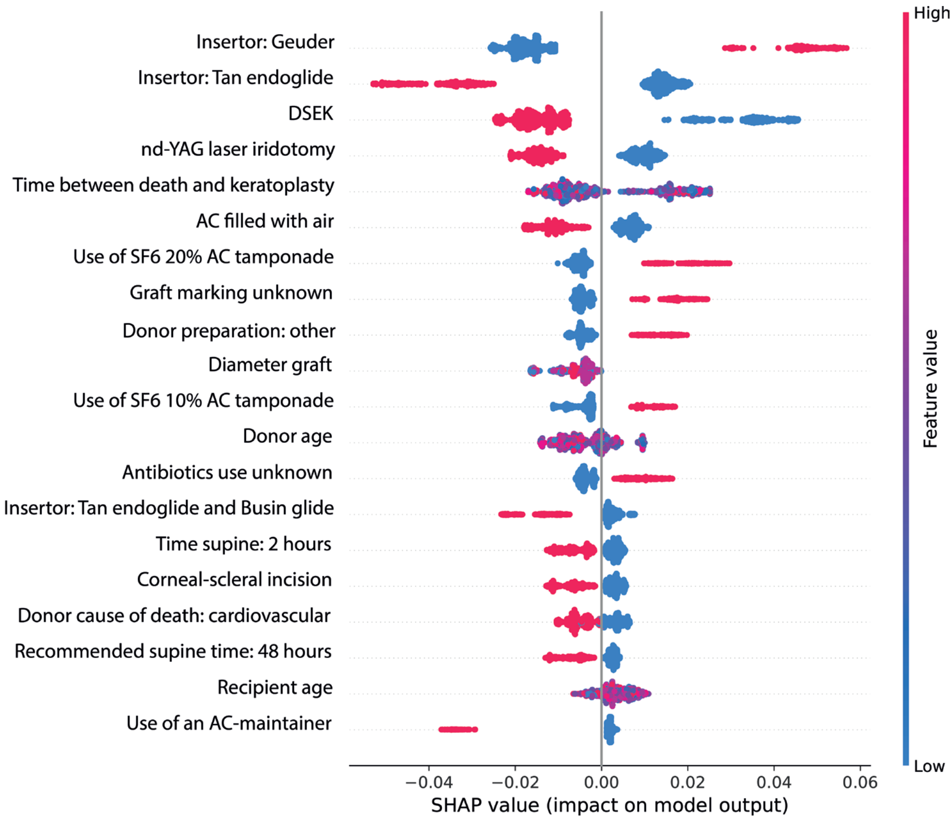

Figure 1. Summary of the SHAP values based on the random forest classifier model. The y-axis shows the most relevant features for predicting graft detachment, from highest to lowest. The x-axis displays the SHAP values, reflecting the effect of each variable on the model's outcome by indicating the predicted change in the probability of a graft detachment. A negative SHAP value represents a "protective effect" (i.e., decreased risk of detachment), while a positive SHAP value represents a "risk effect" (i.e., increased risk of detachment). Each symbol in the plot represents an individual patient in the test dataset. The color gradient ranging from blue to red represents the range of values of the variables. For binary variables, only two colors are used (red for "yes" and blue for "no"); for continuous variables, the values are depicted using the entire spectrum from red to blue.

We found that undergoing DMEK was associated with an increased risk of graft detachment in all three models. In contrast, none of the three models showed that performing a combined procedure was associated with an increased risk of postsurgical complications; however, both the LASSO and CTA models found that undergoing a combined procedure reduced the risk of graft detachment. In addition, the outcome was unclear for several factors, either because the model did not identify the factor as important or because the pattern was diffuse (**Figure 1**). Risk factors that were common to at least two of the three models included a previous graft failure, the type of insertion device, and the use of sulfur hexafluoride (SF6) gas

Table 3. Overview of the most relevant factors and their effect identified by the three machine learning models (green: reduced risk, red: increased risk, light grey: unclear).

Model effect[b] / Factor[a]	lasso	CTA	RFC
Donor characteristics			
Higher donor age	grey	red	grey
Donor cause of death: cardiovascular disease	grey	grey	green
Donor cause of death: trauma	green	grey	grey
Interval between death and transplant procedure	grey	grey	grey
Donor preparation: other	green	grey	green
Donor preparation: manual scraping of the endothelium	green	grey	grey
Graft diameter >8.4 mm	grey	green	grey
Graft marked	red	grey	grey
Recipient characteristics			
Higher recipient age	grey	grey	red
Surgical indication: FECD	grey	green	grey
Surgical indication: graft failure	red	red	grey
Surgical indication: other corneal dystrophy	red	green	grey
Practice patterns			
DSEK	grey	grey	green
Incision site: corneascleral	grey	green	green
Incision site: corneal	grey	red	grey
Use of AC maintainer for descemetorhexis	green	green	green
Descemetorhexis using OVD	grey	green	grey
Graft insertion device: Geuder cannula	red	red	red
Graft insertion device: Tan EndoGlide	green	green	green
Graft insertion device: Tan EndoGlide combined with another insertion device	red	green	green
Graft insertion device: Busin glide	grey	red	green
Graft insertion device: DORC DMEK pipette	grey	green	green
Graft insertion device: Melles glass cannula	grey	red	green
AC tamponade gas SF6 gas (10% and/or 20%)	red	grey	red
AC tamponade gas: air	grey	grey	green
Combined surgical procedure performed	green	green	grey
Laser iridotomy (preoperative)	grey	green	green
Imposed supine time: 2 hours	grey	grey	green
Recommended supine time: 48 hours	grey	grey	green
Recommended supine time: >48 hours	red	grey	grey

AC, anterior chamber; CTA; classification tree analysis; DORC, Dutch Ophthalmic Research Center; FECD, Fuchs endothelial corneal dystrophy; lasso, logistic regression using least absolute shrinkage and selection operator; OVD, ocular viscoelastic device; RFC, random forest classification; SF6, sulfur hexafluoride.

[a] *Factors with the category "unknown" or "unspecified" have been omitted.*

[b] *Green: reduced risk of detachment; red: increased risk of detachment; light grey: unclear (either diffuse pattern or not identified by the model).*

during surgery. Protective factors that were common to at least two models included “donor preparation: other”, use of an AC maintainer during descemetorhexis, and combining surgical procedures. It should be noted that by design, the type of insertion device is specific to the procedure (either DSEK or DMEK) being performed. In addition, it is important to note that “donor preparation method: other” is often entered as the method for preparing the graft for DMEK; based on a case-by-case assessment, we believe this is simply another way of saying “pre-cut tissue”. Similarly, “manual scraping of the endothelium” is likely another way of saying “pre-cut tissue” for DMEK.

DISCUSSION

Here, we report the use of three different machine learning models to explore factors that can predict the probability of graft detachment following posterior lamellar keratoplasty. The predictive power was similar between all three models and is considered to be acceptable (ranging from 0.65 to 0.72). Our identification of predictive factors can help surgeons make evidence-based changes of their practice patterns, provide insight in the marginal contribution to surgical safety of current practices, and can help generate hypotheses for empirical clinical research regarding the origins of graft detachments. Particularly, this study can function as a data-driven protocol standardization of future prospective studies regarding posterior lamellar keratoplasties.

A major strength of this study is our access to an extensive, nationwide dataset and the inclusion of practice patterns in our analysis of a national cornea transplantation registry. The real-world data of the transplantation registry are represented with practically absent inclusion bias, owing to the obligatory and incentivized data-entry in the register. The assessment of both linear and non-linear relationships between a wide range of factors is unique and revealed the complex interactions between factors.[8,11,12,20,29] Moreover, the presented approach enables the evaluation of the numerous modulations of practice patterns in use and the relative impact of proposed key factors, particularly of value in the rapidly evolving field of surgery in which assessing these practice patterns independently in a clinical study would not be feasible.

Despite these strengths several limitations warrant discussion. None of our three models explain all of the variance in our dataset, and not all factors that can affect graft detachment are registered in our dataset (e.g., patient’s behavior and compliance, unrecorded intraoperative events). Furthermore, the register lacks comprehensive contextual information and the completeness and correctness of the data in the registry could not be validated. This lack of contextual information is exemplified by our finding of unknown and/or missing observations in the model output; the interpretation of which is ambiguous and full of assumptions. We therefore chose to not report these outputs. With respect to the practice patterns, we cannot exclude response/recall bias regarding the replies to the questionnaire. Although the surgical protocols for DSEK and DMEK overlap to a large degree, they also differ in several respects. By aggregating the two procedures into a single database, procedure-specific predictive factors might not be identified. Finally, certain predictive factors, such as aphakia, were relatively rare and therefore lack the necessary power to appear in the model output, whilst experts agree on the added risk of particular condition. Therefore, the effect of certain variables cannot be estimated reliably.

The effect of donor-related factors, recipient-related factors, surgery-related factors, and practice patterns on the prevalence of graft detachment is an ongoing topic of discussion. Many surgeons in the Netherlands are transitioning from DSEK to DMEK[39], and our results indicate that DMEK is associated with an increased risk of graft detachment, consistent with previous studies.[4–6] This increased risk may be due in part to increased difficulty when handling the DMEK graft and/or the fact the DMEK graft edge is more prone to curling up, thus lifting the graft from the recipient's stromal bed.[40,41] In addition, partial detachments are more common after DMEK, possibly increasing the rate of rebubbling of the graft compared to DSEK.[42] Alternatively, the increased risk associated with DMEK may partially be related to the surgeon's learning curve. Indeed, from 2016 through 2018 the prevalence of graft detachment decreased more steeply for DMEK than for DSEK.[4] In our model, we attempted to correct for this learning curve by excluding the first 20 DMEK surgeries performed at each clinic, although the results in **Table 1** suggest a shallower learning curve; thus, our model may have overestimated the effect of the DMEK procedure and DMEK specific factors.

Our results show a diffuse pattern of donor age, recipient age, donor cause of death, and the interval between donor death and surgery. Regarding these factors, our analyses are inconclusive. Regarding preparation techniques, our results are consistent with previous studies that found no difference between pre-cut and surgeon-cut tissues.[13,15] Graft marking was associated with an increased risk of detachment in the Lasso model only. However, in the Netherlands graft marking is infrequently practiced, clouding the full assessment of the effect of this practice. Furthermore, and consistent with previous findings, our models indicate that patients who had one or more previously failed grafts had a higher risk of detachment.[20]

We also found that several types of graft insertion devices were associated with an increased risk graft detachment; however, we consider the choice of insertion device a proxy for idiosyncratic surgeon factors too subtle to be captured in our register or questionnaire. We opted not to enter to individual surgeon or center as a model factor, as this study is not designed as an exercise in benchmarking. Notwithstanding, these expected between-surgeon differences might now be attributed to proxy parameters. The insertion tools themselves are known to increase the risk of endothelial damage, although no significant differences have been found between the various commercially available insertion devices.[8,22,23] Furthermore, we found that a graft diameter >8.4 mm may be associated with a reduced risk of graft detachment. Several groups previously hypothesized that a larger graft may overlap with the retained Descemet membrane in the recipient, thus inhibiting graft attachment.[24,25] However, no effect of graft size compared to the descemetorhexis size was found. Both DMEK and DSEK are increasingly combined with other procedures such as cataract surgery and we did not find an increased risk of graft detachment with combined procedures, consistent with previous studies.[12,27,28] Finally, two of the three models in our study found that pre-operative laser peripheral iridotomy was more protective than surgical peripheral iridectomy, although none of the models found that surgical peripheral iridectomy increased the risk of detachment. This difference between laser iridotomy and surgical iridectomy may be due to the increased risk of intraoperative fibrin formation during surgical iridectomy.[43]

Interestingly, we found that using air as the tamponade agent was not associated with an increased risk of graft detachment, while using SF6 gas appeared to increase the risk of graft detachment. This finding is in contrast with previous studies suggesting that the use of SF6 gas may reduce the risk of graft detachment.[34,44,45] This discrepancy may be explained in part by the recent transition of surgeons to using SF6 gas together with the concomitant transition to performing DMEK (with a subsequent increased risk of detachment in their learning curve). Nevertheless, we believe that the previously reported putative benefits associated with using SF6 gas might have been overestimated relative to all other factors and is exemplified by continued reports of relatively high rates of graft detachment.[5,6,12,42,46,47] After posterior lamellar keratoplasties, patients are instructed to remain in the supine position in order to maximize the beneficial effects of AC tamponade, and the length of time in this position can affect the risk of graft detachment. The results of our study indicate that strictly imposing a supine duration of at least 2 hours reduced the risk of graft detachment. Similar results were also found if the patients were instructed to remain in the supine position for 48 hours following surgery, consistent with the routine practice of most surgeons.[9,36]

Lastly, several previously suggested risk and protective factors were not identified by our models. For example, we found no effect of increasing intraocular pressure above physiological limits for a certain time, consistent with previous studies suggesting that overpressuring of the eye after graft insertion has only a limited protective effect.[32,48,49] Similarly, we found no increased risk of complications either during or following surgery; however, this apparent lack of effect may have been due to the relatively low incidence of these events.

In conclusion, we applied a supervised machine learning approach to a nationwide dataset and identified the most relevant factors for predicting graft detachment following posterior lamellar keratoplasties. Our analysis revealed that performing a DMEK procedure, the use of SF6 gas, and previous graft failure increased the risk of detachment, whereas performing a DSEK procedure, preoperative laser iridotomy, larger graft size, remaining strictly supine for at least 2 hours, and a recommendation for staying in the supine position for 48 hours reduced the risk of detachment. In contrast, performing a combined procedures and the use of pre-cut tissue had no effect on the risk of graft detachment, neither did overpressuring of the eye after graft-insertion. These results can help surgeons improve their practice patterns and can help researchers formulate new, testable hypotheses. Future studies should focus on improving the performance of machine learning approaches by including more detailed, contextual information. Importantly, these models' "*in silico*" predictions should be tested in clinical practice.

ACKNOWLEDGEMENTS

The authors would like to thank the members of the Netherlands Corneal Transplantation Network (NCTN) for sharing their practice patterns and data registration, and to Mrs Cynthia Konijn of the Dutch Transplant Foundation (NTS), Leiden, the Netherlands, for processing our data application and anonymization of the questionnaires.

REFERENCES

1. Price FW, Feng MT, Price MO. Evolution of endothelial keratoplasty: Where are we headed? *Cornea* 2015; 34: S41–S47.
2. Nanavaty MA, Wang X, Shortt AJ. Endothelial keratoplasty versus penetrating keratoplasty for Fuchs endothelial dystrophy. *Cochrane Database of Systematic Reviews*. Epub ahead of print 2014. DOI: 10.1002/14651858.CD008420.pub3.
3. Parker J, Parker JS, Melles GR. Descemet Membrane Endothelial Keratoplasty—A Review. *US Ophthalmic Review* 2013; 06: 29.
4. Dunker SL, Dickman MM, Wisse RPL, et al. Descemet Membrane Endothelial Keratoplasty versus Ultrathin Descemet Stripping Automated Endothelial Keratoplasty: A Multicenter Randomized Controlled Clinical Trial. *Ophthalmology* 2020; 127: 1152–1159.
5. Stuart AJ, Romano V, Virgili G, et al. Descemet's membrane endothelial keratoplasty (DMEK) versus Descemet's stripping automated endothelial keratoplasty (DSAEK) for corneal endothelial failure. *Cochrane Database of Systematic Reviews*; 2018. Epub ahead of print 2018. DOI: 10.1002/14651858.CD012097.pub2.
6. Li S, Liu L, Wang W, et al. Efficacy and safety of Descemet's membrane endothelial keratoplasty versus Descemet's stripping endothelial keratoplasty: A systematic review and meta-analysis. *PLoS ONE* 2017; 12: 1–21.
7. Singh A, Zarei-Ghanavati M, Avadhanam V, et al. Systematic Review and Meta-Analysis of Clinical Outcomes of Descemet Membrane Endothelial Keratoplasty Versus Descemet Stripping Endothelial Keratoplasty/Descemet Stripping Automated Endothelial Keratoplasty. *Cornea* 2017; 36: 1437–1443.
8. Terry MA, Aldave AJ, Szczotka-Flynn LB, et al. Donor, Recipient, and Operative Factors Associated with Graft Success in the Cornea Preservation Time Study. *Ophthalmology* 2018; 125: 1700–1709.
9. Terry MA, Shamie N, Chen ES, et al. Endothelial Keratoplasty. A Simplified Technique to Minimize Graft Dislocation, Iatrogenic Graft Failure, and Pupillary Block. *Ophthalmology* 2008; 115: 1179–1186.
10. Baydoun L, Ham L, Borderie V, et al. Endothelial Survival After Descemet Membrane Endothelial Keratoplasty: Effect of Surgical Indication and Graft Adherence Status. *JAMA ophthalmology* 2015; 133: 1277–85.
11. Dirisamer M, van Dijk K, Dapena I, et al. Prevention and Management of Graft Detachment in Descemet Membrane Endothelial Keratoplasty. *Archives of Ophthalmology* 2012; 130: 280–291.
12. Dunker S, Winkens B, Van Den Biggelaar F, et al. Rebubbling and graft failure in Descemet membrane endothelial keratoplasty: a prospective Dutch registry study. *British Journal of Ophthalmology* 2021; 1–7.
13. Price MO, Baig KM, Brubaker JW, et al. Randomized, Prospective Comparison of Precut vs Surgeon-Dissected Grafts for Descemet Stripping Automated Endothelial Keratoplasty. *American Journal of Ophthalmology*; 146. Epub ahead of print 2008. DOI: 10.1016/j.ajo.2008.02.024.
14. Rickmann A, Wahl S, Hofmann N, et al. Precut DMEK Using Dextran-Containing Storage Medium Is Equivalent to Conventional DMEK: A Prospective Pilot Study. *Cornea* 2019; 38: 24–29.
15. Koechel D, Hofmann N, Unterlauft JD, et al. Descemet membrane endothelial keratoplasty (DMEK): clinical results of precut versus surgeon-cut grafts. *Graefe's Archive for Clinical and Experimental Ophthalmology* 2021; 259: 113–119.

16. Chen ES, Terry MA, Shamie N, et al. Precut Tissue in Descemet's Stripping Automated Endothelial Keratoplasty. Donor Characteristics and Early Postoperative Complications. *Ophthalmology* 2008; 115: 497–502.

17. Oellerich S, Ham L, Frank LE, et al. Parameters Associated With Endothelial Cell Density Variability After Descemet Membrane Endothelial Keratoplasty. *American Journal of Ophthalmology*; 211. Epub ahead of print 2020. DOI: 10.1016/j.ajo.2019.10.017.

18. Rodríguez-Calvo De Mora MR, Groeneveld-Van Beek EA, Frank LE, et al. Association between graft storage time and donor age with endothelial cell density and graft adherence after descemet membrane endothelial keratoplasty. *JAMA Ophthalmology* 2016; 134: 91–94.

19. Baydoun L, Ham L, Borderie V, et al. Endothelial Survival After Descemet Membrane Endothelial Keratoplasty: Effect of Surgical Indication and Graft Adherence Status. *JAMA ophthalmology* 2015; 133: 1277–1285.

20. Nahum Y, Leon P, Mimouni M, et al. Factors Associated with Graft Detachment after Primary Descemet Stripping Automated Endothelial Keratoplasty. *Cornea* 2017; 36: 265–268.

21. Price FW, Price MO. Descemet's stripping with endothelial keratoplasty in 200 eyes. Early challenges and techniques to enhance donor adherence. *Journal of Cataract and Refractive Surgery* 2006; 32: 411–418.

22. Droutsas K, Lazaridis A, Kymionis GD, et al. Comparison of endothelial cell loss and complications following DMEK with the use of three different graft injectors. *Eye (Basingstoke)* 2018; 32: 19–25.

23. Sati A, Moulick PS, Sharma V, et al. Sheets glide-assisted versus Busin glide-assisted insertion techniques for descemet stripping endothelial keratoplasty (DSEK): A comparative analysis. *Medical Journal Armed Forces India* 2019; 75: 370–374.

24. Tourtas T, Schlomberg J, Wessel JM, et al. Graft adhesion in Descemet membrane endothelial keratoplasty dependent on size of removal of host's Descemet membrane. *JAMA Ophthalmology* 2014; 132: 155–161.

25. Müller TM, Verdijk RM, Lavy I, et al. Histopathologic Features of Descemet Membrane Endothelial Keratoplasty Graft Remnants, Folds, and Detachments. *Ophthalmology* 2016; 123: 2489–2497.

26. Sykakis E, Lam FC, Georgoudis P, et al. Patients with fuchs endothelial dystrophy and cataract undergoing descemet stripping automated endothelial keratoplasty and phacoemulsification with intraocular lens implant: Staged versus combined procedure outcomes. *Journal of Ophthalmology*; 2015. Epub ahead of print 2015. DOI: 10.1155/2015/172075.

27. Terry MA, Shamie N, Chen ES, et al. Endothelial Keratoplasty for Fuchs' Dystrophy with Cataract. Complications and Clinical Results with the New Triple Procedure. *Ophthalmology* 2009; 116: 631–639.

28. Chaurasia S, Price FW, Gunderson L, et al. Descemet's membrane endothelial keratoplasty: Clinical results of single versus triple procedures (combined with cataract surgery). *Ophthalmology* 2014; 121: 454–458.

29. Leon P, Parekh M, Nahum Y, et al. Factors Associated With Early Graft Detachment in Primary Descemet Membrane Endothelial Keratoplasty. *American journal of ophthalmology* 2018; 187: 117–124.

30. Dapena I, Moutsouris K, Droutsas K, et al. Standardized "No-Touch" Technique for Descemet Membrane Endothelial Keratoplasty. *Archives of Ophthalmology* 2011; 129: 88–94.

31. Santander-García D, Peraza-Nieves J, Müller TM, et al. Influence of Intraoperative Air Tamponade Time on Graft Adherence in Descemet Membrane Endothelial Keratoplasty. *Cornea* 2019; 38: 166–172.

32. Schmeckenbächer N, Frings A, Kruse FE, et al. Role of Initial Intraocular Pressure in Graft Adhesion After Descemet Membrane Endothelial Keratoplasty. *Cornea* 2017; 36: 7–10.
33. Pilger D, Wilkemeyer I, Schroeter J, et al. Rebubbling in Descemet Membrane Endothelial Keratoplasty: Influence of Pressure and Duration of the Intracameral Air Tamponade. *American Journal of Ophthalmology* 2017; 178: 122–128.
34. Siebelmann S, Ramos SL, Scholz P, et al. Graft detachment pattern after descemet membrane endothelial keratoplasty comparing air versus 20% SF6 tamponade. *Cornea* 2018; 37: 834–839.
35. Srirampur A, Mansoori T. Comment on: "Influence of Lens Status on Outcomes of Descemet Membrane Endothelial Keratoplasty." *Cornea* 2019; 38: e35–e36.
36. Dapena I, Moutsouris K, Droutsas K, et al. Standardized "No-Touch" Technique for Descemet Membrane Endothelial Keratoplasty. *Archives of Ophthalmology* 2011; 129: 88–94.
37. Norgeat B, Glicksberg BS, Butte AJ. A call for deep-learning healthcare. *Nature Medicine* 2019; 25: 14–18.
38. Raghupathi W, Raghupathi V. Big data analytics in healthcare: promise and potential. *Health Information Science and Systems* 2014; 2: 1–10.
39. Dunker SL, Veldman MHJ, Winkens B, et al. Real-World Outcomes of DMEK: A Prospective Dutch registry study. *American Journal of Ophthalmology* 2021; 222: 218–225.
40. Maier AKB, Gundlach E, Schroeter J, et al. Influence of the difficulty of graft unfolding and attachment on the outcome in descemet membrane endothelial keratoplasty. *Graefe's Archive for Clinical and Experimental Ophthalmology* 2015; 253: 895–900.
41. Woo JH, Ang M, Htoon HM, et al. Descemet Membrane Endothelial Keratoplasty Versus Descemet Stripping Automated Endothelial Keratoplasty and Penetrating Keratoplasty. *American Journal of Ophthalmology* 2019; 207: 288–303.
42. Parekh M, Leon P, Ruzza A, et al. Graft detachment and rebubbling rate in Descemet membrane endothelial keratoplasty. *Survey of Ophthalmology* 2018; 63: 245–250.
43. Benage M, Korchak M, Boyce M, et al. Intraoperative fibrin formation during Descemet membrane endothelial keratoplasty. *American journal of ophthalmology case reports* 2020; 18: 100686.
44. Terry MA, Straiko MD, Veldman PB, et al. Standardized DMEK Technique: Reducing Complications Using Prestripped Tissue, Novel Glass Injector, and Sulfur Hexafluoride (SF6) Gas. *Cornea* 2015; 34: 845–852.
45. Marques RE, Guerra PS, Sousa DC, et al. Sulfur Hexafluoride 20% Versus Air 100% for Anterior Chamber Tamponade in DMEK: A Meta-Analysis. *Cornea* 2018; 37: 691–697.
46. Siebelmann S, Kolb K, Scholz P, et al. The Cologne rebubbling study: a reappraisal of 624 rebubblings after Descemet membrane endothelial keratoplasty. *British Journal of Ophthalmology* 2020; bjophthalmol-2020-316478.
47. Deng SX, Lee WB, Hammersmith KM, et al. Descemet Membrane Endothelial Keratoplasty: Safety and Outcomes: A Report by the American Academy of Ophthalmology. *Ophthalmology* 2018; 125: 295–310.
48. Muijzer MB, Soeters N, Godefrooij DA, et al. Intraoperative Optical Coherence Tomography–Assisted Descemet Membrane Endothelial Keratoplasty. *Cornea* 2020; 00: 1.
49. Titiyal JS, Kaur M, Falera R, et al. Evaluation of Time to Donor Lenticule Apposition Using Intraoperative Optical Coherence Tomography in Descemet Stripping Automated Endothelial Keratoplasty. *Cornea* 2016; 35: 477–481.

50. James, G., Witten, D., Hastie, T., Tibshirani R. *An Introduction to Statistical Learning: with Applications in R*. New Yrok: Springer, 2013.
51. Menardi R, Torelli N. Training and assessing classification rules with imbalanced data. *Data Mining and Knowledge Discovery* 2014; 28: 92–122.

SUPPLEMENTARY DATA:

Supplementary tables

Supplementary Table 1. Practice patterns for the 11 cornea centers that performed DSEK in the study period.

		Cornea center										
		1	**2**	**3**	**4**	**5**	**6**	**8**	**9**	**11**	**14**	**15**
Iridectomy method	YAG	●	●	●	●			●	●	●	●	●
	Mantoux needle					●	●	●			●	
	Segment								●	●		
Descemetorhexis												
General radius	≤8.0 mm	●		●								●
	8.5 mm					●			●			
	9.0 mm				●		●	●		●	●	
	≥9.5 mm		●									
Use of dye		No	No	No	No	No	Yes	No	Yes	No	No	No
Anterior chamber filling	Air	●		●	●		●	●		●		
	BSS								●			
	Active AC infusion with air		●			●						●
	Viscoelastic device										●	
Additional interventions	None			●		●			●			
	Exchange air with fluid	●	●									
	Fill AC with air				●			●		●		●
	Recolor with a dye						●					
	Polish with I/A							●			●	
Graft insertor	Tan EndoGlide	●	●	●	●		●	●			●	●
	Busin glide			●		●		●	●	●	●	
	Maculoso injector						●					
Incision site	Sclera	●	●						●	●		●
	Cornea-sclera				●	●	●	●				
	Cornea			●				●			●	
Incision size (mm)				3.5	5.0		4.5		4.0	4.5	4.5	4.5
Overpressure time (minutes)	0	●	●				●		●			
	<10										●	
	≥10			●	●	●		●		●		●

		Cornea center										
		1	**2**	**3**	**4**	**5**	**6**	**8**	**9**	**11**	**14**	**15**
Intracameral antibiotics		No	No	Yes	No	missing	No	No	missing	Yes	Yes	No
Postoperative AC tamponade												
Filling	Air	•	•	•		•		•	•	•		
	SF6 10%				•							•
	SF6 20%						•				•	
Time	Until resorption	•	•	•	•	•	•	•	•	•	•	•
Strict time supine after surgery	1 hour					•						
	2 hours			•	•		•				•	
	3 hours							•				•
	4 hours								•			
	24 hours	•										
	48 hours									•		
	Until resorption		•									
Recommended time supine after discharge	<24 hours			•		•						
	24 hours								•		•	
	48 hours				•		•			•		
	>48 hours		•									•

NA, not applicable.

Supplementary Table 2. Practice patterns for the 10 cornea centers that performed DMEK in the study period.

		Cornea center									
		1	**2**	**3**	**4**	**5**	**6**	**8**	**11**	**14**	**15**
Iridectomy method	YAG	●	●	●	●	●		●	●	●	●
	Mantoux needle						●	●		●	
	Segment								●		
Descemetorhexis											
General radius	≤8.0 mm	●		●							●
	8.5 mm					●					
	9.0 mm				●		●		●	●	
	≥9.5 mm		●					●			
Use of dye		No	No	No	No	No	Yes	No	No	No	No
Anterior chamber filling	Air	●		●	●	●	●	●	●		
	Active AC infusion with air		●								●
	Viscoelastic device									●	
Additional interventions	None			●		●					
	Exchange air with fluid	●	●								
	Fill AC with air				●			●	●		●
	Recolor with a dye						●				
	Polish with I/A							●		●	
DMEK procedure											
Graft marking		Yes	Yes	Yes	No	missing	No	No	No	No	Yes
Graft insertor	Geuder injector				●	●	●	●		●	
	DORC DMEK pipette	●	●						●		
	Melles glass cannula										●
Incision site	Sclera	●	●						●		
	Cornea-sclera					●	●				●
	Cornea				●			●		●	
Incision size (mm)					3.0		2.8		3.5	2.8	2.8
Overpressure time (minutes)	0	●	●				●				
	<10									●	
	≥10			●	●	●		●	●		●
Intracameral antibiotics		No	No	Yes	No	missing	No	No	Yes	Yes	No
Postoperative AC tamponade											
Filling	Air	●	●	●		●		●	●		
	SF6 10%				●						●
	SF6 20%						●			●	
Time	Until resorption	●	●	●	●	●	●	●	●	●	●

		Cornea center									
		1	**2**	**3**	**4**	**5**	**6**	**8**	**11**	**14**	**15**
Strict time supine after surgery	2 hours			●	●		●			●	
	3 hours					●		●			●
	24 hours	●									
	48 hours								●		
	Until resorption		●								
Recommended time supine after discharge	<24 hours			●		●					
	24 hours									●	
	48 hours				●		●		●		
	>48 hours		●								●

Supplementary Table 3. Donor characteristics.

	All (n=3647)	DSEK (n=2651)	DMEK (n=996)
	N (%)	N (%)	N (%)
Demographics			
Gender male	2238 (61.4)	1607 (60.6)	631 (63.4)
Age in years, mean ± SD	70 ± 9	69 ± 9	72 ± 8
Donor cause of death			
Neoplasms/cancer	320 (8.8)	246 (9.3)	74 (7.4)
Diseases of the circulatory system	1945 (53.3)	1476 (55.7)	469 (47.1)
Diseases of the respiratory system	742 (20.3)	478 (18)	264 (26.5)
Trauma	584 (16)	410 (15.5)	174 (17.5)
Other	56 (1.5)	41 (1.5)	15 (1.5)
Donor preparation			
Manual scraping of the endothelium	792 (21.7)	732 (27.6)	60 (6)
Manual lamellar dissection	1131 (31)	1101 (41.5)	30 (3)
Pre-cut	1496 (41)	814 (30.7)	682 (68.5)
Other	228 (6.3)	4 (0.2)	224 (22.5)
Graft preservation medium			
CorneaMax	1185 (32.5)	810 (30.6)	375 (37.7)
Culture medium	2462 (67.5)	1841 (69.4)	621 (62.3)
Graft preservation time			
Interval between death and explantation of the donor tissue in minutes, mean ± SD	645 ± 344	652 ± 344	627 ± 342
Interval between explantation and preservation of the donor tissue in minutes, mean ± SD	807 ± 447	794 ± 454	843 ± 424
Interval between death of the donor and corneal transplantation in days, mean ± SD	19 ± 5	19 ± 5	20 ± 5

Supplementary Table 4. Recipient characteristics.

	All (n=3647)	DSEK (n=2651)	DMEK (n=996)
	N (%)	N (%)	N (%)
Recipient age in years, mean ± SD	73 ± 11	74 ± 11	73 ± 9
Surgery indication			
Fuchs endothelial dystrophy	2772 (76)	1866 (70.4)	906 (91)
Pseudophakic bullous keratopathy	362 (9.9)	330 (12.4)	32 (3.2)
Graft failure	250 (6.9)	231 (8.7)	19 (1.9)
Other corneal dystrophies	82 (2.2)	66 (2.5)	16 (1.6)
Other	148 (4.1)	126 (4.8)	22 (2.2)
Lens status (pre-surgery)			
Phakic	539 (14.8)	437 (16.5)	102 (10.2)
Anterior chamber IOL	136 (3.7)	115 (4.3)	21 (2.1)
Posterior chamber IOL	2273 (62.3)	1574 (59.4)	669 (70.2)
IOL not specified	18 (0.5)	12 (0.5)	6 (0.6)
Aphakic	24 (0.7)	23 (0.9)	1 (0.1)
Unknown	657 (18)	490 (18.5)	167 (16.8)
Previous corneal transplant in the same eye			
No previous transplant	3240 (88.8)	2285 (86.2)	995 (95.9)
One previous transplant	354 (9.7)	317 (12)	37 (3.7)
Two previous transplants	48 (1.3)	45 (1.7)	3 (0.3)
Three previous transplants	5 (0.1)	4 (0.2)	1 (0.1)

IOL, intraocular lens.

Supplementary Table 5. Surgical details

	All (n=3647)	DSEK (n=2651)	DMEK (n=996)
	N (%)	N (%)	N (%)
Operating surgeon			
Fellow	172 (4.7)	162 (6.1)	10 (1)
Staff	3475 (95.3)	2489 (93.9)	986 (99)
Graft size compared to descemetorhexis size			
Undersized	953 (26.1)	548 (20.7)	405 (40.7)
Same size	1439 (39.5)	1006 (37.9)	433 (43.5)
Oversized	1255 (34.4)	1097 (41.4)	158 (15.9)
Combined surgical procedure			
None	2615 (71.7)	1843 (69.5)	772 (77.5)
Peripheral iridectomy	444 (12.2)	302 (11.4)	142 (14.3)
Cataract surgery	313 (8.6)	273 (10.3)	40 (4)
Peripheral iridectomy and cataract surgery	132 (3.6)	100 (3.8)	32 (3.2)
Lens implant without cataract extraction	71 (1.9)	64 (2.4)	7 (0.7)
Anterior vitrectomy	7 (0.2)	6 (0.2)	1 (0.1)
Other	65 (1.8)	63 (2.4)	2 (0.2)
Surgical complications			
Incidence of complications	148 (4.1)	88 (3.3)	60 (6)
Endothelial damage	28 (0.8)	13 (0.5)	15 (1.5)
Graft unfolding problems	24 (0.7)	5 (0.2)	19 (1.9)
Rupture of graft tissue and other preparation problems	16 (0.4)	8 (0.3)	8 (0.8)
Iris prolapse	16 (0.4)	16 (0.6)	NA
Anterior chamber hemorrhage	11 (0.3)	6 (0.2)	5 (0.5)
Graft prolapse or expulsion	10 (0.3)	4 (0.2)	6 (0.6)
Vitreous loss	8 (0.2)	6 (0.2)	2 (0.2)
Graft dislocation or adherence problems	5 (0.1)	5 (0.2)	NA
Failed/aborted procedure	5 (0.1)	4 (0.2)	1 (0.1)
Decentered trephination	4 (0.1)	3 (0.1)	1 (0.1)
Rupture of the posterior lens capsule	3 (0.1)	3 (0.1)	NA
Lens touch (unintended)	1 (0.03)	NA	1 (0.1)
Zonulolysis	1 (>.03)	1 (0.04)	NA
Other	16 (0.4)	14 (0.5)	2 (0.2)

Supplementary figures

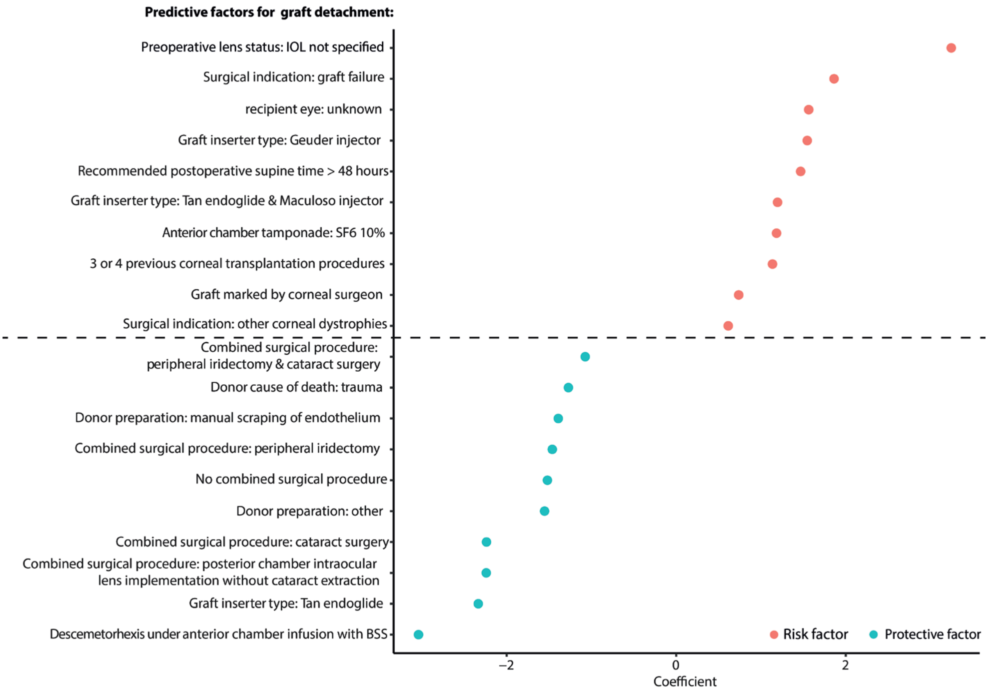

Supplementary figure 1. Overview of the strongest predictive factors for a graft detachment identified using the lasso model. Red symbols indicate factors that increase the risk of graft detachment, and the blue symbols indicate factors that reduce the risk of graft detachment. Higher absolute coefficient values (x-axis) indicate higher predictive strength of the associated factors.

7

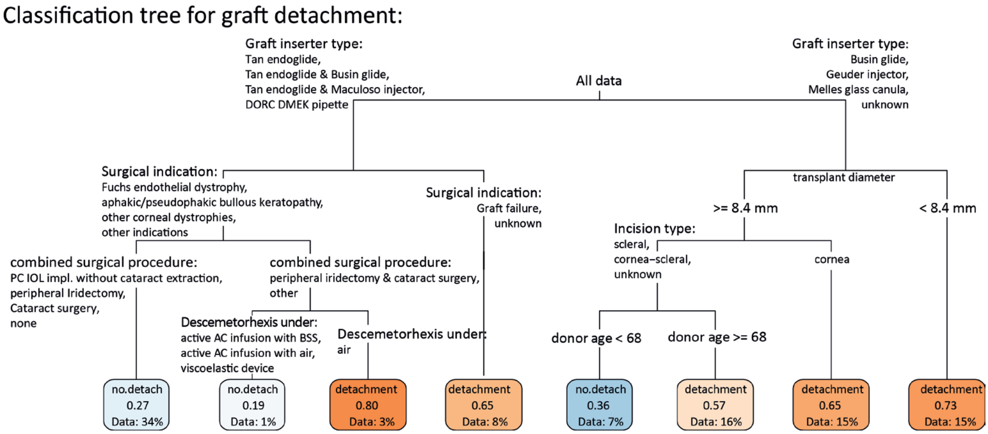

Supplementary figure 2. Classification tree analysis of graft detachment. The algorithm partitions the data into clusters of patients (leaf nodes at the bottom row of the figure) who have a comparable probability to be classified as a graft detachment, based on a shared combination of factors. The tree starts with a first split based on the best initial distinction between graft detachment versus no graft detachment. With each subsequent step down the tree, the sample is further split into subsamples based on specific combinations of factors. Within each split, factors on the left side are associated with a reduced risk of graft detachment and factors on the right side with an increased risk of graft detachment. he bottom row shows the percentage of subjects that were classified within that particular final branch and the average predicted probability of a detachment. Clusters in blue tones represent subjects who are classified as "no detachment" due to the lower predicted probabilities for a detachment (< 0.5), whereas clusters in orange tones represent subjects who are classified as "detachment" due to the higher predicted probabilities for a detachment (>0.5). For example, the cluster on the far left of the tree (bottom row) can be interpreted as follows: The patients in this cluster (which represents 34% of the total sample) share the combination of graft inserter type (one of the following: Tan endoglide, Tan endoglide + Busin glide, Tan endoglide + Maculoso injector, DORC DMEK pipette) with surgical indication (one of the following: Fuchs endothelial dystrophy, aphakic/pseudophakic bullous keratopathy, other corneal distrophies, other indications) with combined surgical procedure (one of the following: PC IOL impl. without cataract extraction, peripheral iridectomy, cataract surgery, none). This particular combination of factors is associated with an average predicted probability of 0.27 for the subjects in this cluster who are all classified as "no detachment".

CHAPTER 8

VIDEO-GRADING OF DESCEMET MEMBRANE ENDOTHELIAL KERATOPLASTY SURGERY TO IDENTIFY RISK FACTORS FOR GRAFT DETACHMENT AND REBUBBLING: A POST-HOC ANALYSIS OF THE ADVANCED VISUALIZATION IN CORNEAL SURGERY EVALUATION (ADVISE) TRIAL

Marc B Muijzer; Heleen Delbeke; Mor M Dickman;
Rudy MMA Nuijts; Hanad Jimale; Chantal M. van Luijk;
Saskia M Imhof; Robert PL Wisse

Submitted for publication

ABSTRACT

Aim: To explore video-graded intraoperative risk factors for graft detachment and rebubbling in Descemet Membrane Endothelial Keratoplasty (DMEK) surgery.

Methods: A post-hoc analysis of 65 eyes of 65 pseudophakic subjects with Fuchs Endothelial dystrophy that underwent DMEK surgery as part of the ADVISE-trial. All surgical recordings were assessed by two graders using a structured assessment form including: Descemetorhexis difficulty, graft shape after insertion, graft unfolding difficulty, graft manipulation, graft centering, and gas-bubble size. A multinominal regression was performed to estimate the independent effect of video-graded intraoperative factors on the incidence of graft detachment and rebubbling. Secondary outcomes are corrected distance visual acuity (CDVA) and endothelial cell density (ECD).

Results: In total 33 graft detachments were recorded, of which 17 required rebubbling. No significant predictors for graft detachment or rebubbling were identified in the regression analysis. However, the results revealed two clinically relevant patterns. An unfavorable graft configuration (i.e., wrinkled, tight scroll, or taco-shaped) and a gas-bubble size smaller than the graft diameter was associated with an increased risk of graft detachment (OR: 2.5 95%CI: 0.50–12.5 and OR: 2.26, 95%CI: 0.24–21.4, respectively) and rebubbling (OR: 2 95%CI: 0.44–8.98 and OR: 2.60, 95%CI:, respectively). Inversely, a larger gas-bubble size was associated with a reduced risk of graft detachment (OR: 0.37, 95%CI: 0.05–2.66) and rebubbling (0.36, 95%CI: 0.05–2.4). At 3 and 6 months postoperatively CDVA was poorer in subjects requiring a rebubbling and ECD loss was higher in subjects with a partial graft detachment.

Conclusion: Our analysis revealed that the gas-bubble size and graft shape/geometry appear to be relevant clinical factors for graft detachment and rebubbling, whereas Descemetorhexis difficulty, degree of graft manipulation, graft overlap, and a surgical iridectomy were not a associated with an increased risk.

INTRODUCTION

Descemet membrane endothelial keratoplasty (DMEK) is the preferred surgical procedure for symptomatic irreversible corneal endothelial dysfunction.[1,2] Postoperative graft detachment is the most common complication, affecting about one in five patients.[2–6] Detachments often require secondary surgical intervention (i.e. rebubbling) that is burdensome for patients, may jeopardize graft survival, and strains healthcare resources.[7,8]

The underlying cause of graft detachment is multifactorial. A wide range of risk factors have been proposed related to donor and patient characteristics and surgery.[8–13] Reported intraoperative risk factors for graft detachment and rebubbling include direct manipulation of the graft,[10,14–16] use of viscoelastic, use of sulfur-hexafluoride gas or gas, insufficient graft support by the gas-bubble in the anterior chamber,[17–22] Descemet remnant or overlap between the donor and recipient Descemet membrane.[23,24] Unfortunately, most studies have focused on a single or a few intraoperative events in their analysis. Only a handful of studies investigated the effect of surgical manipulation during graft unfolding, or the effect of variations in intraoperative tissue handling on outcomes, although both are deemed important by surgeons.

In this study, we qualitatively and quantitatively analyzed surgical videos from the prospective *Advanced Visualization In Corneal Surgery Evaluation* (ADVISE) trial to identify risk factors for graft detachment and rebubbling. The aim of this explorative study is to obtain a better understanding of the impact of surgical factors on the incidence of graft detachment and rebubbling, and subsequently offer insights to improve the safety of our surgeries.

METHODS

This manuscript a post-hoc observational analysis of surgical recordings to identify risk factors for graft detachments and rebubbling procedures of the prospective ADVISE trial, an international non-inferiority single-blinded RCT to investigate the utility of intraoperative optical coherence tomography (iOCT) in DMEK surgery. All procedures were performed in accordance with the Declaration of Helsinki, local and national laws regarding research (i.e., the Act on Scientific Research Involving Humans), European directives with respect to privacy (General Data Protection Regulation 2016/679), and 2010 CONSORT standards for reporting RCT's.[25] The study was approved by the Ethics Review Boards in the Netherlands (Medical Ethics Committee Utrecht file no. 18-487), and Belgium (Ethical committee Leuven file no. S61527). The details of this trial are previously reported in detail and registered at clinicaltrials.gov (no° NCT03763721).[26]

Subjects underwent surgery between December 2018 and April 2021 at the University Medical Center Utrecht (n = 39), University Hospital Leuven (n = 14), or Maastricht University Medical Center (n= 14). Inclusion criteria were pseudophakic adult patients with irreversible corneal endothelial dysfunction resulting from Fuchs endothelial corneal dystrophy, eligible for DMEK surgery. Exclusion criteria were human-leukocyte antigen matched keratoplasty, combined phaco-emulsification procedures, any ocular comorbidity other than ocular surface disease, open angle glaucoma, and mild age-related macular degeneration. Only one eye per subject was enrolled.

Each patient underwent a comprehensive ophthalmic examination preoperatively and 1 day, 1 week, 1 month, 3 months, and 6 months after surgery. Here, we report the baseline, 3-, and 6-months measurements in detail. The ophthalmic examination was previously reported.[26] An optometrist measured the corrected distance visual acuity (CDVA) using an Early Treatment Diabetic Retinopathy Study (ETDRS) letter chart at a distance of 4 meters and endothelial cell counts were assessed with specular microscopy (EM4000, Tomey, Nagoya, Japan; SP-3000; Topcon, Nagoya, Japan)

Surgical procedure

Donor grafts were allocated by the Dutch Transplant Foundation (Nederlandse Transplantatie Stichting, Leiden, the Netherlands). The grafts were cultured and provided pre-peeled by the ETB-Bislife (Beverwijk, the Netherlands), with a minimum endothelial cell density (ECD) of 2300 cells/mm^2 and with a diameter of 8.5 mm. Prior to surgery, 27 subjects underwent a Nd:YAG laser iridotomy at 6 o'clock. In the other 38 subjects, a surgical iridectomy was performed using a 27-gauge needle and Price hook at 6 o'clock following the Descemetorhexis during surgery.

All surgical procedures were performed by experienced corneal surgeons (H.D., R.M.M.A.N, M.M.D., R.P.L.W.), following a largely standardized procedure. The surgical procedure is previously reported in more detail.[26] In short, the procedure consisted of a 9 mm Descemetorhexis, subsequently the graft was stained and inserted in the anterior chamber using a glass injector via a 2.8 mm incision. A no-touch technique was used to unfold and position the graft. In the control group (n=33) iOCT was not available and the intra-ocular pressure was raised above physiological limits (i.e., overpressure) for 8 minutes at the end of surgery. In the intervention group (n=32), a brief AC fill was performed to adhere the graft and the iOCT was used to check for complete adherence of the graft without over pressurizing the eye. At the end of surgery, air was replaced by Sulphur Hexafluoride (SF6) 20% gas and the size of the gas-bubble was reduced to cover the graft (i.e., same size as the graft). After surgery, patients remained strictly supine for two hours at the hospital and were instructed to remain in the same position for the following 24 hours.

Video-analysis

All surgical videos recordings were analyzed by two graders (M.B.M., H.J.) using a standardized assessment form. One grader was blinded regarding the clinical outcomes of the surgery. The overall skin-to-skin surgical time and duration of surgical steps (e.g., Descemetorhexis, graft unfolding, etc.) were meticulously recorded. The difficulty of the Descemetorhexis was coded in 3 groups based on time (i.e., fast: ≤5 minutes; average: >5 - ≤10 minutes; slow: >10 minutes). Directly after insertion of the graft into the AC, graft configuration was determined based on geometry and number of folds. As such, 6 distinct shapes were distinguished: the double scroll, tight roll, loose roll, taco, pancake, and wrinkled (**Figure 1**). Based on the incidence of graft detachment/rebubbling and expert opinion the shapes were considered favorable and unfavorable to unfold and position during surgery. The shapes *double scroll, loose roll,* and *pancake* were coded favorable graft shapes to unfold, whereas the shapes *tight roll, taco,* and *wrinkled* were coded unfavorable. Ease of graft unfolding was classified in 4 mutually exclusive ordinal groups depending on the required manipulation and time to unfold/position the graft, as described by Maier et al.[14] All manual manipulations of the graft (e.g., bubble-bumping, positioning with forceps, pushing in place with a cannula) were recorded and coded in 3 nominal groups: the category *external manipulation* indicates only corneal swiping/tapping was used to unfold the graft, regardless of the time spent. *Indirect internal manipulation* refers to bubble-bumping or fluid/air exchange to unfold the graft in addition to external manipulation. *Direct internal manipulation* was scored if the graft was manually unfolded or positioned using surgical instruments in addition to external and *indirect internal manipulation*. After fixation of the graft with gas, the size of the gas-bubble was assessed, compared to the graft size, and coded in 3 nominal groups: a gas-bubble size *equal* to the graft diameter , *larger* than the graft diameter, and *smaller* than the graft diameter. Centering of the graft was determined in relationship to the Descemetorhexis area and coded dichotomously; a graft was considered centered if it was completely within the Descemetorhexis and decentered if the graft overlapped with the Descemetorhexis edge.

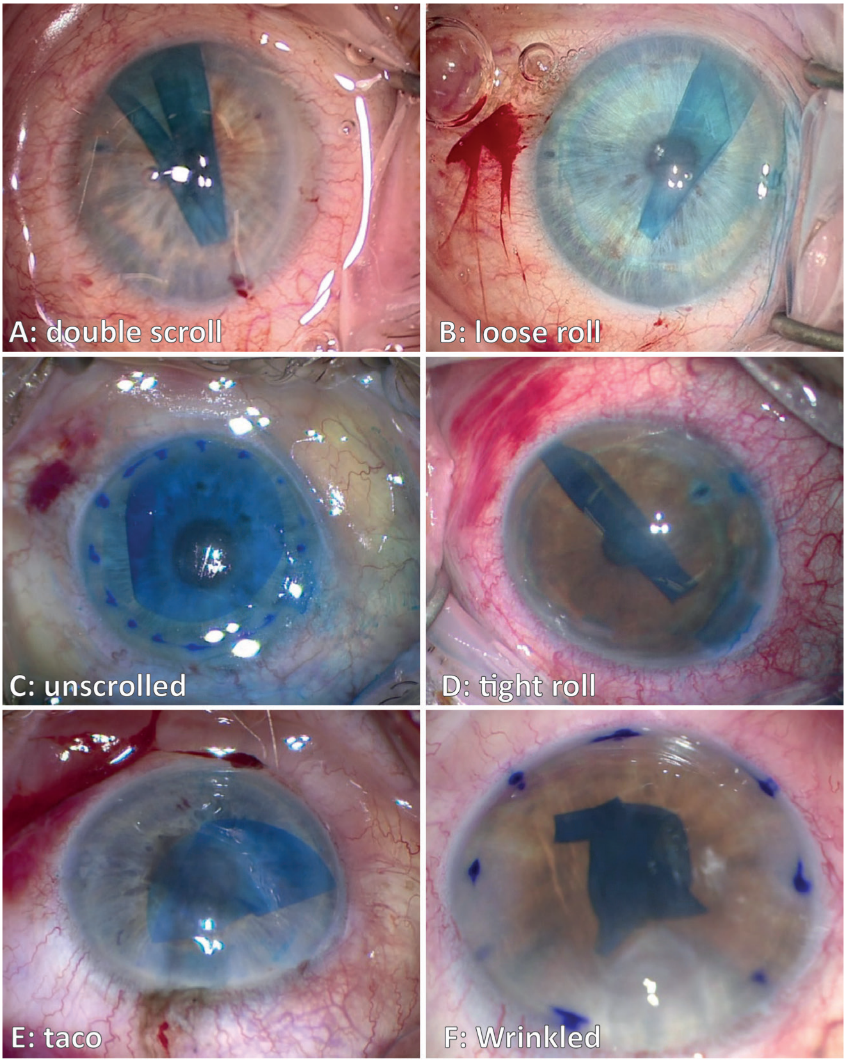

Figure 1.Various graft configurations identified. The graft shapes were coded directly after insertion in the AC, based on graft geometry and number of folds. The distinctive graft shapes were grouped as either favorable (A, B, C) or unfavorable (D, E, F).

Statistical analysis

The outcome variable of this study is the incidence of graft detachments and rebubbling procedures. A graft detachment was defined as any non-adherence of the graft noticeable on slit lamp examination and AS-OCT imaging at any time point within 3 months after surgery. Using a cornea grid consisting of 25 cornea zones, the presence and size of the graft detachments were quantified.[27] A rebubbling was defined as the re-injection of gas under the graft after a graft detachment. A rebubbling was performed if the graft was >30% detached or involved the visual axis, though no strict guidelines were set in the study protocol. Secondary outcomes are postoperative ECD and CDVA. The ETDRS letter score of the CDVA was converted to logarithm of the minimum angle of resolution (logMAR) units by multiplying the number of letters read by -0.02 log units and adding 1.7 log units.[28]

Missing observations of the CDVA and ECD, were considered missing at random and imputed using multiple imputation. Missing measurements of subject that developed a graft failure were considered missing not at random and not imputed. The variables concerned and baseline variables concerned were used as predictors for imputing. The number of imputations was equal to the maximum percentage of missing data plus one. Two surgical recordings were missing and not imputed.

Here, all cases were video analyzed irrespective of their randomization and randomization consequences (i.e., use of iOCT or prolonged overpressure of the eye) were entered as factors in the multivariable model. Subjects were post-hoc assigned in three groups: completely attached graft, graft detachment that did not require rebubbling, and graft detachment that required rebubbling. Data are described as mean ± standard deviation (SD) for continuous variables and as individual counts and percentages for dichotomous and categorical variables. Group differences were analyzed using a one-way ANOVA or Kruskal-Wallis test, as appropriate. Correction for multiple comparisons was performed using the Bonferroni correction. A 2-sided p-value < 0.05 was considered statistically significant. Internal consistency of the video-grading between the two graders was assessed using Cohen's Kappa.[29]

A multivariate multinomial regression analysis was performed to analyze the independent effect of intraoperative factors on the incidence of graft detachment and rebubbling. Predictors included: graft manipulation, graft shape, graft centering, gas-bubble size, method of peripheral iridectomy (laser vs. surgical), and overpressure duration. The analysis was adjusted for hospital (to account differences between centers, surgeons, and surgical volume), and donor age (as donor age may influence graft curvature and by extent graft shape).[30] The analysis was not adjusted for randomization group, because difference between the treatment arms regarding graft unfolding and manipulation were observed in the primary analysis of the trial. To account for treatment arm subjects were randomized to overpressure duration was included. Including both variables appeared not possible. All statistical analyses were performed using R statistical software version 4.0.3 (Comprehensive R Archive Network, Vienna, Austria).

RESULTS

A total of 65 eyes of 65 patients were included for analysis. In total 33 (51%) graft detachments were recorded over de study period, of which 17 (26%) required rebubbling. Of these 33 detachments underwent re-transplantation for primary graft failure, and all three cases were preceded by a rebubbling. Seven subjects were lost to follow-up because of graft failure (n = 3) and reduction of care following the COVID-19 pandemic (n = 4). During the study 5 intra-operative complications were recorded: 2 cases with endothelial damage due to extensive graft manipulation and 3 cases with an anterior chamber hemorrhage. No significant differences regarding the incidence of adverse events were found between the treatment arms.[26] The internal consistency between the two graders (M.M., H.J.) with regard to video grading was considered strong (Cohen's kappa: 0.84 ±0.17; agreement: 90%).[29] Baseline patient and donor characteristics are displayed in **Table 1**. At baseline, statistically significant differences were found between the groups for patient age, CDVA, and donor ECD.

Table 1. Baseline Patient and Donor Characteristics stratified in three post-hoc groups based on post-operative treatment success.

	Graft attached (n= 32)	Graft detached (n= 33)		
Recipient characteristics		No rebubbling (n= 16)	Rebubbling (n= 17)	*p*-value
Sex (female), n (%)	16 (50.0)	8 (50.0)	10 (58.8)	0.822[1]
Age (years), mean (SD)	72 (6.97)	72 (5.48)	76 (5.27)	0.040[2]
CDVA (logMAR), mean (SD)	0.37 (0.23)	0.57 (0.32)	0.37 (0.15)	0.021[2]
Pachymetry (μm), mean (SD)	608 (61.47)	669 (71.36)	600 (151.17)	0.080[2]
Corneal edema present, n (%)	11 (34.4)	9 (56.2)	8 (47.1)	0.328[1]
Descemet folds present, n (%)	2 (6.2)	2 (12.5)	4 (23.5)	0.215[1]
Bullae present, n (%)	4 (12.5)	4 (25.0)	1 (5.9)	0.270[1]
Laser iridotomy, n (%)	11 (34.4)	10 (62.5)	6 (35.3)	0.146[1]
Donor characteristics				
Age (years), mean (SD)	72 (4.97)	76 (5.72)	75 (5.45)	0.101[2]
ECD (cells/mm^2), mean (SD)	2763 (193)	2633 (150)	2688 (136)	0.049[2]

CDVA: corrected distance visual acuity; ECD: endothelial cell density; logMAR: logarithm of the minimum angle of resolution; SD: standard deviation

[1] Kruskal-Wallis test
[2] One-way ANOVA
* *p*-value significant at $\alpha \leq 0.05$ after correction for multiple comparison using the Bonferroni method.

Video-grading outcomes

The various categories of tissue handling and surgical manipulation did not show significant differences between the three post-hoc groups. In other words, intraoperative factors of detached graft and detached graft requiring rebubbling on average did not differ from uneventful post-operative course (**Table 2**). It should be noted that this study was not powered on video-graded surgical manipulations, and *p*-value s contribute little additional value. Although at first glance, analysis of the videos revealed, considerable relative differences between the groups were observed regarding the gas-bubble size at the end of surgery and post-operative adverse events: a smaller bubble was more prevalent in cases which subsequently developed a detachment (attached: 10%; all detachments: 21%). Inversely, an gas-bubble size greater than the graft diameter was more prevalent in completely attached grafts (attached: 32%; all detachments: 15%). The prevalence of an unfavorable graft shape (i.e., *wrinkled, tight scroll, or taco-shaped)* was higher in cases that developed a graft detachment (attached: 23%; all detachments: 44%).

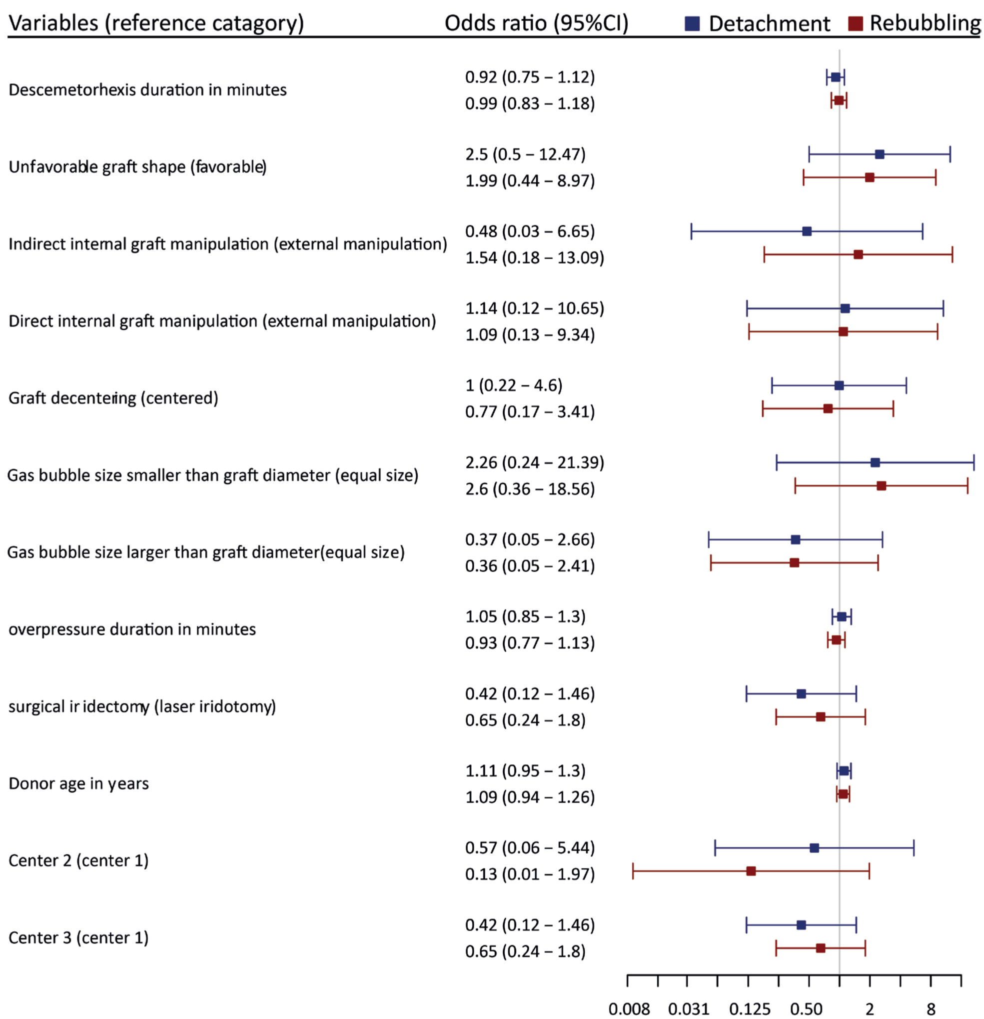

Figure 2. The odds ratio (OR) and 95% confidence interval (CI) of video-graded intraoperative factors on the incidence of a graft detachment and rebubbling compared to cases with a fully attached graft. Per parameter the reference category is noted between paracenteses. The analysis was adjusted for donor age and center.

Table 2. Overview video analysis assessment

	Graft attached (n= 32)	Graft detachment (n=33)		*p*-value
		No rebubbling (n=16)	Rebubbling (n=17)	
Descemetorhexis difficulty grade[3], n (%)				0.946[1]
Fast (≤5 minutes)	20 (64.5)	10 (71.4)	10 (58.8)	
Average (>5 - ≤10 minutes)	7 (22.6)	3 (21.4)	5 (29.4)	
Slow (>10 minutes)	4 (12.9)	1 (7.1)	2 (11.8)	
Descemet remnants present[4], n (%)	1 (3.2)	0 (0.0)	0 (0.0)	0.602[1]
Graft shape[3], n (%)				0.130[1]
Unfavorable shapes:	7 (22)	7 (43.8)	8 (47)	
Tight roll	1 (3.1)	3 (18.8)	0 (0.0)	
Taco	4 (12.5)	1 (6.2)	4 (23.5)	
Wrinkled	2 (6.2)	3 (18.8)	4 (23.5)	
Favorable shapes:	24 (75.4)	9 (56.2)	9 (53)	
Double scroll	11 (34.4)	7 (43.8)	3 (17.6)	
Loose roll	9 (28.1)	2 (12.5)	4 (23.5)	
pancake	4 (12.9)	0 (0.0)	2 (11.8)	
Graft unfolding grade[5,6], n (%)				0.736[1]
Grade 1	6 (19.4)	2 (12.5)	3 (17.6)	
Grade 2	11 (35.5)	8 (50.0)	9 (52.9)	
Grade 3	3 (9.7)	2 (12.5)	0 (0.0)	
Grade 4	11 (35.5)	4 (25.0)	5 (29.4)	
Graft manipulations[4], n (%)				0.443[1]
External manipulation only	7 (22.6)	1 (6.2)	4 (23.5)	
Indirect internal manipulation	13 (41.9)	11 (68.8)	8 (47.1)	
Direct internal manipulation	11 (35.5)	4 (25.0)	5 (29.4)	
Graft centering[7], n (%)				0.577[1]
Decentered	14 (46.7)	8 (53.3)	6 (35.3)	
Gasbubble size[4], n (%)				0.452[1]
Equal to graft diameter	18 (58.1)	9 (60.0)	11 (64.7)	
Smaller than graft diameter	3 (9.7)	3 (20.0)	4 (23.5)	
Larger than graft diameter	10 (32.3)	3 (20.0)	2 (11.8)	
Surgical duration (minutes)[4], mean (SD)				
Surgical skin-to-skin time	34.16 (10.23)	34.53 (8.59)	37.65 (13.38)	0.454[2]
Descemetorhexis duration	5.39 (4.92)	4.37 (3.10)	5.21 (5.35)	0.637[2]
Graft unfolding duration	4.44 (4.01)	6.10 (7.66)	6.67 (10.02)	0.257[2]

[1] Kruskal-Wallis test between attached grafts, detached graft not requiring rebubbling, and detached graft requiring rebubbling.
[2] One-way ANOVA between attached grafts, detached graft not requiring rebubbling, and detached graft requiring rebubbling.
[3] Three missing values
[4] Two missing values

[5] Grade I: graft lamella primarily oriented correctly in the anterior chamber, straight and direct unfolding and centering; Grade II: slightly complicated, indirect unfolding and centering (duration less than five min); Grade III: difficult indirect unfolding and centering (duration longer than five min), repeated air injection with BSS exchange necessary; Grade IV: direct manipulation of the graft lamella for unfolding and centering by cannula or forceps.
[6] One missing value
[7] Decentered was defined as the graft overlapping with the recipient Descemet's membrane.
* *p*-value significant at $\alpha \leq 0.05$ after correction for multiple comparison using the Bonferroni method

To investigate independent effects and identify potential patterns that predict treatment outcomes, we conceptualized a multinomial regression model including surgical risk factors and confounding factors. No statistically significant predictors were identified in the analysis, although again the same two clinically relevant patterns were identified; AC tamponade volume at the end of surgery and graft shape after insertion (**Figure 2** and **Supplementary table 1**). A larger gas-bubble at the end of surgery had a lower risk of graft detachment and rebubbling (OR: 0.37 and 0.36, respectively). Inversely, a smaller gas-bubble had an increased risk of graft detachment and rebubbling (OR: 2.26 and 2.60, respectively). Second, an unfavorable graft shape was associated with an increased risk of graft detachment and rebubbling (OR: 2.50 and 1.99, respectively), independent of donor age. Other interesting outcomes are that a surgical iridectomy was not related to an increased risk of graft detachment and rebubbling (OR 0.42 and 0.65, respectively). In decentered grafts, there is an apparent overlap between graft and host Descemet-endothelium, by some considered a risk factor for graft detachments.[24] Our analysis did not show a consistent effect of graft decentering on the graft detachment and rebubbling (OR: 1 and 0.77). Direct internal graft manipulation indicated a marginal increased risk of graft detachment and rebubbling (OR 1.14 and 1.09). Direct internal manipulation can be considered an iatrogenic trauma to the graft, which by some is considered related to unfavorable surgical outcomes.[31–33]

Clinical outcomes

At 3 and 6 months postoperatively, a significant difference was observed regarding the ECD in cases with a graft detachment (3 months: $p = 0.007$; 6 months: $p = 0.001$) compared to cases with a completely attached graft and the detached grafts requiring a rebubbling. After adjustment for multiple comparisons and correction for baseline donor ECD the difference between the groups were not significant. Furthermore, at 3 and 6 months postoperatively subjects that underwent a rebubbling achieved a poorer CDVA compared to the other two groups, though this difference was not statistically significant after adjustment for multiple comparisons. A complete overview of postoperative clinical outcomes is shown in **Table 3**.

Table 3. Clinical outcomes 3 and 6 months after surgery stratified in three post-hoc groups based on post-operative treatment success.

Postoperative outcomes	Graft attached (n= 32)	Graft detached (n=33)		
		No rebubbling (n=16)	Rebubbling (n=17)	*p*-value[1]
CDVA (LogMAR), mean (SD)				
3 months	0.13 (0.17)	0.13 (0.10)	0.25 (0.17)	0.033
6 months	0.13 (0.21)	0.12 (0.15)	0.31 (0.27)	0.015
Pachymetry (μm), mean (SD)				
3 months	473 (40.14)	492 (50.08)	461 (50.53)	0.160
6 months	481 (49.27)	488 (60.31)	496 (56.06)	0.642
ECD (cells/mm^2), mean (SD)				
3 months	1948 (351)	1594 (379)	1717 (399)	0.007
6 months	1920 (379)	1454 (414)	1804 (360)	0.001*
ECD loss[2] (cells/mm^2), mean (SD)				
3 months	814 (357)	1033 (364)	962 (451)	0.160
6 months	842 (372)	1190 (419)	875 (356)	0.016

CDVA: corrected distance visual acuity; ECD: endothelial cell density; logMAR: logarithm of the minimum angle of resolution; SD: standard deviation

[1] One-way ANOVA between attached grafts, detached graft not requiring rebubbling, and detached graft requiring rebubbling.

[2] calculated as the difference between the specular microscopy measurement and the graft ECD.

* *p*-value significant at $\alpha \leq 0.05$ after correction for multiple comparison using the Bonferroni method

DISCUSSION

We report an analysis of surgical video recordings to explore risk factors for graft detachment and rebubbling following DMEK. This study provides a rare opportunity to analyze surgical DMEK videos in-depth, in a well-controlled cohort of corneal transplant procedures performed by various surgeons in three clinics, with well-defined procedural trial parameters. We focused on the contribution of surgical manipulations, tissue handling, and (unnoticed) practice pattern variations to identify risk factors for graft detachment and rebubbling. Graft detachments have a notorious multifactorial origin, and several strategies to investigate this are reported: e.g., case-control,[10] case series,[9,13,23,34] cohort studies,[11,14] and registry studies.[8,35] The added value of this study is the focus on the surgical course including clinical variations and surgeon behavior, which enables further hypothesizing of the causality of these dreaded events.

The main findings of this study are that direct manipulation of the graft (i.e., judicious grabbing with a forceps) is not associated with poor surgical outcome, nor was overlap of the graft with host Descemet membrane. The gas-bubble size at the end of surgery did appear clinically relevant: bigger is better in maintaining an attached graft. Commensurate to the primary outcomes of the ADVISE trial[26], the length of over-pressuring did not relate to the incidence of graft detachments or rebubbling procedures. Another relevant factor in our model was graft configuration, a tissue characteristic that cannot be influenced by the surgeon; an unfavorable graft shape was associated with an increased risk of graft detachment and rebubbling. One could hypothesize that graft shape is a proxy for overall graft unfolding difficulty, including the associated intraoperative challenges. Still, we found no correlation between the coding of graft shape and the metrices graft unfolding difficulty ($Chi^2 = 4.87$, $P = 0.18$) and duration ($Chi^2 = 62$, $P = 0.44$) as suggested by Quilendrino et al. and Maier et al.[14,34] Apparently, there is still unexplained variation in our statistical model that predicts post-operative adverse events.

There is limited evidence regarding the causality of surgical decision making and detachment/rebubbling rates. Our results underlines that it is very difficult to predict graft detachment or rebubbling, based on how the surgery faired. Several recommended practices were not supported by our results, such as not directly manipulate the graft and preventing overlap with the host Descemet membrane. One of those recommended practices is avoidance of direct manual manipulation of the graft, which may lead to endothelial damage and graft detachment.[13,15,16,34,36–38] However, the causality between direct manual manipulation and detachment of the graft is unclear and evidence limited. Maier et al. and Leon et al. reported that manual manipulation was associated with higher incidence of graft detachment, though no significant associations were found.[10,14] In our study we did not find a higher incidence of adverse events in cases with direct graft manipulation, rather it appeared to have a reduced risk. The direct tissue effects of direct manual manipulation on endothelial cell density were not investigated in this study, only the effects on clinically relevant endpoints of graft adherence.

In our study we did not find an association between graft overlap with the recipient Descemet membrane and graft detachment or rebubbling contradicting the findings of Rock et al.[12] and Tourtas et al.[23] Furthermore, Muller et al. reported that incomplete removal of the Descemet membrane (i.e., overlap with the recipient anterior banded layer) and ultrastructural changes were related to graft detachment. However, they reported that overlap with the full thickness Descemet membrane did not result in graft detachment on histological images.[24] In our study we did not account for the extent of overlap, and actual complete removal of the Descemet membrane layers or other ultrastructural changes were not investigated.

On the other hand, our results support that a larger gas-bubble size may be protective for a graft detachment as previously reported by Leon et al. and Cirkovic et al.[10,18] Leon et al. found that an air fill <75% of the anterior chamber height was associated with an increased risk of graft detachment (OR: 2.66; P=0.027).[10] Similarly, Cirkovic et al. reported that an 80% fill of the anterior chamber was significantly associated with a decreased incidence of rebubbling (P=0.032).[18] Pralits et al. showed that graft support is dependent on the gas-bubble coverage of the graft.[19] They demonstrated that a 63% fill already leads to incomplete coverage of the graft in different gaze directions independent of type of gas filling. A larger gas-bubble may mitigate the decrease of air-bubble size by leakage and half-life time of the tamponade agent.[39]

Endothelial decay at 3- and 6-months was higher in eyes with a partial graft detachment compared to eyes with an attached graft and eyes that required a rebubbling. A similar association between partial detachments and endothelial cell loss was found by Baydoun et al. (mean difference: 330 cells/mm2; 95%CI: 208-452; P<0.001).[40] This may indicate that a partial graft detachment compromises long term graft viability, and could form an argument for early rebubbling. Mechanical loss of endothelial cells as result of tissue manipulation during surgery appear unlikely as this did not differ from the other groups in our analysis. As a result, we can only speculate on the cause of this endothelial cell loss, which may be the result of a larger area to be repopulated or unrecorded mechanical causes or trauma inhibiting cellular processes.

Furthermore, several limitations should be addressed. This study was a post hoc analysis of a trial that was not powered to determine associations between intraoperative factors and graft detachment/rebubbling. Notwithstanding, the data were derived from a well-controlled sample of corneal transplant procedures and the video-analysis enables an objective in-depth observation of the surgical course. In this study we focused on intraoperative factors affecting graft disadherence. However, an analysis including recipient and additional donor factors may reveal additional insights. Several factors were assessed in the video-analysis (e.g., presence of Descemet remnants) though not included in the analysis either because the incidence of these factors was low or could not reliably estimated in the video-analysis. Information on non-compliance of the patient and resorption time of the gas-bubble were not collected and could not retrospectively retrieved.

In conclusion, using a structured video-analysis we explored intraoperative determinants for graft detachment and rebubbling following DMEK. Our analysis revealed that the gas-bubble size and graft shape/geometry appear to be relevant clinical factors. Graft detachment and rebubbling were not associated with the degree of graft manipulation, graft positioning, a surgical iridectomy, or over pressuring the eye.

ACKNOWLEDGEMENTS

The authors would like to thank Suryan Dunker, MD, and Ingeborg de Vriens, BSc, for their assistance with the trial measurements, Peter Zuithoff, PhD, of the Julius Center for Health Sciences, for assistance and validation of the statistical analysis, and Antoon van den Bogaerdt, PhD, from ETB-Bislife for his aid in providing donor tissue to all participating centers.

REFERENCES

1. Parker J, Parker JS, Melles GR. Descemet Membrane Endothelial Keratoplasty—A Review. *US Ophthalmic Review* 2013; 06: 29.
2. Stuart AJ, Romano V, Virgili G, et al. Descemet's membrane endothelial keratoplasty (DMEK) versus Descemet's stripping automated endothelial keratoplasty (DSAEK) for corneal endothelial failure. *Cochrane Database of Systematic Reviews*; 2018. Epub ahead of print 2018. DOI: 10.1002/14651858.CD012097.pub2.
3. Dunker SL, Dickman MM, Wisse RPL, et al. Descemet Membrane Endothelial Keratoplasty versus Ultrathin Descemet Stripping Automated Endothelial Keratoplasty: A Multicenter Randomized Controlled Clinical Trial. *Ophthalmology* 2020; 127: 1152–1159.
4. Dunker SL, Veldman MHJ, Winkens B, et al. Real-World Outcomes of DMEK: A Prospective Dutch registry study. *American Journal of Ophthalmology* 2021; 222: 218–225.
5. Singh A, Zarei-Ghanavati M, Avadhanam V, et al. Systematic Review and Meta-Analysis of Clinical Outcomes of Descemet Membrane Endothelial Keratoplasty Versus Descemet Stripping Endothelial Keratoplasty/Descemet Stripping Automated Endothelial Keratoplasty. *Cornea* 2017; 36: 1437–1443.
6. Li S, Liu L, Wang W, et al. Efficacy and safety of Descemet's membrane endothelial keratoplasty versus Descemet's stripping endothelial keratoplasty: A systematic review and meta-analysis. *PLoS ONE* 2017; 12: 1–21.
7. Gibbons A, Leung E, Yoo S. Cost-Effectiveness Analysis of Descemet's Membrane Endothelial Keratoplasty Versus Descemet's Stripping Endothelial Keratoplasty in the United States. *Ophthalmology* 2019; 126: 207–213.
8. Dunker S, Winkens B, Van Den Biggelaar F, et al. Rebubbling and graft failure in Descemet membrane endothelial keratoplasty: a prospective Dutch registry study. *British Journal of Ophthalmology* 2021; 1–7.
9. Dirisamer M, Van Dijk K, Dapena I, et al. Prevention and management of graft detachment in descemet membrane endothelial keratoplasty. *Archives of Ophthalmology* 2012; 130: 280–291.
10. Leon P, Parekh M, Nahum Y, et al. Factors Associated With Early Graft Detachment in Primary Descemet Membrane Endothelial Keratoplasty. *American Journal of Ophthalmology* 2018; 187: 117–124.
11. Nahum Y, Leon P, Mimouni M, et al. Factors Associated with Graft Detachment after Primary Descemet Stripping Automated Endothelial Keratoplasty. *Cornea* 2017; 36: 265–268.
12. Röck T, Bramkamp M, Bartz-Schmidt KU, et al. Causes that influence the detachment rate after Descemet membrane endothelial keratoplasty. *Graefe's Archive for Clinical and Experimental Ophthalmology* 2015; 253: 2217–2222.
13. Terry MA, Straiko MD, Veldman PB, et al. Standardized DMEK Technique: Reducing Complications Using Prestripped Tissue, Novel Glass Injector, and Sulfur Hexafluoride (SF6) Gas. *Cornea* 2015; 34: 845–852.
14. Maier AKB, Gundlach E, Schroeter J, et al. Influence of the difficulty of graft unfolding and attachment on the outcome in descemet membrane endothelial keratoplasty. *Graefe's Archive for Clinical and Experimental Ophthalmology* 2015; 253: 895–900.
15. Liarakos VS, Dapena I, Ham L, et al. Intraocular graft unfolding techniques in Descemet membrane endothelial keratoplasty. *Archives of Ophthalmology* 2013; 131: 29–35.

16. Kruse FE, Laaser K, Cursiefen C, et al. A stepwise approach to donor preparation and insertion increases safety and outcome of descemet membrane endothelial keratoplasty. *Cornea* 2011; 30: 580–587.
17. Siebelmann S, Ramos SL, Scholz P, et al. Graft detachment pattern after descemet membrane endothelial keratoplasty comparing air versus 20% SF6 tamponade. *Cornea* 2018; 37: 834–839.
18. Cirkovic A, Beck C, Weller JM, et al. Anterior chamber air bubble to achieve graft attachment after DMEK: Is bigger always better? *Cornea* 2016; 35: 482–485.
19. Pralits JO, Alberti M, Cabreizo J. Gas-graft coverage after DMEK: A clinically validated numeric study. *Translational Vision Science and Technology*; 8. Epub ahead of print 2019. DOI: 10.1167/tvst.8.6.9.
20. Schmeckenbächer N, Frings A, Kruse FE, et al. Role of Initial Intraocular Pressure in Graft Adhesion After Descemet Membrane Endothelial Keratoplasty. 2016; 0: 1–4.
21. Santander-García D, Peraza-Nieves J, Müller TM, et al. Influence of Intraoperative Air Tamponade Time on Graft Adherence in Descemet Membrane Endothelial Keratoplasty. *Cornea* 2019; 38: 166–172.
22. Pilger D, Wilkemeyer I, Schroeter J, et al. Rebubbling in Descemet Membrane Endothelial Keratoplasty: Influence of Pressure and Duration of the Intracameral Air Tamponade. *American Journal of Ophthalmology* 2017; 178: 122–128.
23. Tourtas T, Schlomberg J, Wessel JM, et al. Graft adhesion in Descemet membrane endothelial keratoplasty dependent on size of removal of host’s Descemet membrane. *JAMA Ophthalmology* 2014; 132: 155–161.
24. Müller TM, Verdijk RM, Lavy I, et al. Histopathologic Features of Descemet Membrane Endothelial Keratoplasty Graft Remnants, Folds, and Detachments. *Ophthalmology* 2016; 123: 2489–2497.
25. Schulz KF, Altman DG, Moher D. CONSORT 2010 Statement: updated guidelines for reporting parallel group randomised trials. *BMJ*; 340. Epub ahead of print 2010. DOI: 10.1136/bmj.c332.
26. Muijzer M, Delbeke H, Dickman M, et al. Outcomes of the Advanced Visualization In Corneal Surgery Evaluation trial; a non-inferiority randomized control trial to evaluate the use of intraoperative OCT during Descemet membrane endothelial keratoplasty (preprint). *medRvix*.
27. Muijzer M, Noordmans H-J, Delbeke H, et al. Establishing a biomarker for the prediction of short-term graft detachment after Descemet membrane endothelial keratoplasty. *Cornea*; accepted.
28. Beck RW, Moke PS, Turpin AH, et al. A computerized method of visual acuity testing: Adaptation of the early treatment of diabetic retinopathy study testing protocol. *American Journal of Ophthalmology* 2003; 135: 194–205.
29. McHugh ML. Interrater reliability: the kappa statistic. *Biochemia medica* 2012; 22: 276–282.
30. Steven P, Le Blanc C, Velten K, et al. Optimizing Descemet membrane endothelial keratoplasty using intraoperative optical coherence tomography. *JAMA Ophthalmology* 2013; 131: 1135–1142.
31. Kruse FE, Laaser K, Cursiefen C, et al. A stepwise approach to donor preparation and insertion increases safety and outcome of descemet membrane endothelial keratoplasty. *Cornea* 2011; 30: 580–587.
32. Leon P, Parekh M, Nahum Y, et al. Factors Associated With Early Graft Detachment in Primary Descemet Membrane Endothelial Keratoplasty. *American Journal of Ophthalmology* 2018; 187: 117–124.
33. Maier AKB, Gundlach E, Schroeter J, et al. Influence of the difficulty of graft unfolding and attachment on the outcome in descemet membrane endothelial keratoplasty. *Graefe’s Archive for Clinical and Experimental Ophthalmology* 2015; 253: 895–900.

34. Quilendrino R, Rodriguez-Calvo de Mora M, Baydoun L, et al. Prevention and Management of Graft Detachment in Descemet Membrane Endothelial Keratoplasty. *Archives of Ophthalmology* 2012; 130: 280–291.

35. Wisse RPL, Muijzer MB, Hoven CMW, et al. A machine learning approach to identify predictors of adverse events in posterior lamellar keratoplasty; a nationwide registry study. *Acta Ophthalmologica* 2021; 99: 6.

36. Dapena I, Moutsouris K, Droutsas K, et al. Standardized “No-Touch” Technique for Descemet Membrane Endothelial Keratoplasty. *Archives of Ophthalmology* 2011; 129: 88–94.

37. Parekh M, Leon P, Ruzza A, et al. Graft detachment and rebubbling rate in Descemet membrane endothelial keratoplasty. *Survey of Ophthalmology* 2018; 63: 245–250.

38. Gerber-Hollbach N, Baydoun L, López EF, et al. Clinical outcome of rebubbling for graft detachment after descemet membrane endothelial keratoplasty. *Cornea* 2017; 36: 771–776.

39. Thompson JT. Kinetics of Intraocular Gases: Disappearance of Air, Sulfur Hexafluoride, and Perfluoropropane After Pars Plana Vitrectomy. *Archives of Ophthalmology* 1989; 107: 687–691.

40. Baydoun L, Ham L, Borderie V, et al. Endothelial Survival After Descemet Membrane Endothelial Keratoplasty: Effect of Surgical Indication and Graft Adherence Status. *JAMA ophthalmology* 2015; 133: 1277–85.

SUPPLEMENTARY DATA

Supplementary table 1. Multinomial regression analysis between surgical factors and graft detachment.

Variables	Detachment, no rebubbling		Detachment, rebubbling	
	OR (95%CI)	*p*-value	OR (95%CI)	*p*-value
Descemetorhexis duration (minutes)	0.915 (0.749-1.119)	0.388	0.988 (0.831-1.176)	0.895
Graft shape: unfavorable (reference: favorable)	2.501 (0.502-12.467)	0.263	1.99 (0.441-8.973)	0.371
Graft manipulations: external (reference)	-	-	-	-
Graft manipulations: indirect	0.478 (0.034-6.655)	0.583	1.536 (0.18-13.086)	0.694
Graft manipulations: direct	1.139 (0.122-10.655)	0.909	1.091 (0.127-9.335)	0.937
Graft centering: decentered (reference: centered)	0.995 (0.215-4.593)	0.995	0.771 (0.174-3.408)	0.731
AC tamponade size: equal to graft diameter (reference)	-	-	-	-
AC tamponade size: smaller than graft diameter	2.262 (0.239-21.398)	0.477	2.602 (0.365-18.564)	0.34
AC tamponade size: larger than graft diameter	0.368 (0.051-2.663)	0.322	0.359 (0.053-2.408)	0.291
Overpressure duration (minutes)	1.054 (0.851-1.305)	0.631	0.932 (0.767-1.133)	0.479
Surgical iridectomy (reference: laser iridotomy)	0.42 (0.12-1.463)	0.173	0.653 (0.236-1.801)	0.41
Donor age (years)	1.108 (0.946-1.298)	0.202	1.087 (0.94-1.256)	0.259
Center 1 (reference)	-	-	-	-
Center 2	0.566 (0.059-5.439)	0.622	0.134 (0.009-1.974)	0.143
Center 3	0.42 (0.12-1.463)	0.173	0.653 (0.236-1.801)	0.41

CHAPTER 9

ESTABLISHING A BIOMARKER FOR THE PREDICTION OF SHORT-TERM GRAFT DETACHMENT AFTER DESCEMET MEMBRANE ENDOTHELIAL KERATOPLASTY

Marc B Muijzer; Heleen Delbeke; Mor M Dickman;
Rudy MMA Nuijts; Herke Jan Noordmans;
Suryan Dunker; Saskia M Imhof; Robert PL Wisse

Cornea. 2022; accepted for publication

ABSTRACT

Aim: To investigate the predictive value of pachymetry mapping one-day after Descemet membrane endothelial keratoplasty (DMEK) as a biomarker for early graft detachment.

Methods: A post-hoc analysis of 65 pseudophakic subjects with Fuchs Endothelial dystrophy underwent DMEK surgery between December 2018 and April 2021 as part of the ADVISE international multicenter RCT. One eye per patient was included. Preoperatively and one-day post-operatively, patients underwent anterior-segment optical coherence tomography (AS-OCT) imaging. Using a grid consisting of 25 zones (i.e., pachymetry map), corneal thickness and presence of a graft detachment was mapped for each patient. Detachments of any size were considered, regardless of subsequent clinical interventions. Missing data was imputed and subsequently divided into a training and test set. Two prediction methods were evaluated: one based on absolute corneal thickness and a regression model.

Results: A total of 65 eyes were included for analysis of which 33 developed any form of graft detachment. Preoperatively no significant differences were observed between the groups ($p = 0.221$). Corneal thickness in the corneal zones with a detached graft was significantly increased compared to corneal zones with an attached graft ($p<0.001$). The regression prediction model had an area under the curve of 0.87 (sensitivity: 0.79, specificity: 0.75), whereas the absolute thickness cutoff model only reached 0.65.

Conclusion: Pachymetry mapping one-day after DMEK was predictive for early graft detachment and the prediction model had a good to excellent performance. This aids in identifying patients at risk for graft detachment and subsequent tailored postoperative care.

INTRODUCTION

Descemet membrane endothelial keratoplasty (DMEK) is currently the preferred procedure for treating patients with symptomatic Fuchs corneal endothelial dystrophy.[1] Postoperative detachment of the graft is a relatively frequent adverse event observed in the first weeks after surgery. It often requires surgical intervention (i.e., *rebubbling*).[2] As a result, patients are intensively monitored in the weeks after surgery to detect early graft detachment.

The causes of these graft detachments are considered multifactorial and the majority of research has focused on risk factors, such as donor and recipient characteristics, and intraoperative factors.[3–6] However, only a few studies have investigated postoperative biomarkers to predict graft detachment.[7,8]

During and directly after DMEK surgery the cornea swells significantly, restoring to normal ranges in the months to follow.[9,10] Corneal thickness often varies throughout different zones in the postoperative period.[10,11] Subsequently, a graft detachment is often associated with (regional) corneal edema at the detachment location.[8,12] Currently, the underlying physiological mechanism regarding the formation of corneal edema at the detachment site is unclear, which might be caused by or is the results of the detachment.[9,10,13] Notwithstanding, Moutsouris et al. already suggested that the persistence and/or presence of corneal edema may be indicative of an (impending) graft detachment.[8] Similarly, Dirisamer et al. reported that corneal thickness was increased in detached corneal quadrants compared to adjacent corneal quadrants and Yeh et al. found that OCT assessments shortly after surgery are predictive for graft adherence at six months.[9] In line with these findings, we hypothesize that a regional increase in corneal thickness directly after surgery is predictive for a (future) graft detachment and may be used as a biomarker after surgery.

METHODS

Study protocol and measurements

All subjects provided written informed consent and were included in the prospective *Advanced Visualization In Corneal Surgery Evaluation* (ADVISE) trial, a non-inferiority randomized controlled trial (RCT) to investigate the use of intraoperative optical coherence tomography (iOCT) in DMEK surgery. Sixty-five subjects underwent DMEK surgery between December 2018 and April 2021 in the University Medical Center Utrecht (n = 38), University Hospital Leuven (n = 13), and Maastricht University Medical Center (n= 14). Inclusion criteria were pseudophakic adult patients with irreversible corneal endothelial dysfunction resulting from Fuchs endothelial corneal dystrophy eligible for DMEK surgery. Exclusion criteria were human-leukocyte antigen matched keratoplasty, any ocular comorbidity other than mild ocular surface disease, open angle glaucoma, and age-related macular degeneration. No combined phaco-emulsification (triple) procedures were performed and only one eye per subject was enrolled. Subject were randomized to either the iOCT-group or non-iOCT group using minimization randomization stratified for center. All procedures were performed in accordance with the Declaration of Helsinki, local and national laws regarding research (i.e., the Act on Scientific Research Involving Humans), European directives with respect to privacy (General Data Protection Regulation 2016/679), and 2010 CONSORT standards for reporting RCT's.[14] The study was approved by the Ethics Review Board of University Medical Center Utrecht and Leuven (Medical Ethics Committee Utrecht file no. 18-487, Ethical committee Leuven file no. S61527) and registered at clinicaltrials.gov (number: NCT03763721) and CCMO.nl (number: NL64392.041.17). No power calculation for this study is available as it is a post-hoc analysis of the ADVISE-trial.

Each patient underwent an ophthalmic examination preoperatively, and one-day, one week, one month, three months, and six months after surgery. Here, we report the preoperative assessment, one-day assessment and all graft detachments within the first 3 months. The ophthalmic examinations described in detail include a full slit-lamp examination, applanation intraocular pressure (IOP) measurement, and anterior segment OCT (AS-OCT, Utrecht and Leuven: Zeiss Cirrus 5000, Zeiss Meditec, Oberkochen, Germany; Maastricht: Casia SS-1000, Tomey, Nagoya, Japan).

All surgical procedures were performed by experienced corneal surgeons (>50 DMEK surgeries; H.D., R.M.M.A.N, M.M.D., R.P.L.W.), following a largely standardized procedure. The donor grafts were cultured and provided pre-peeled by the ETB-Bislife (Euro Tissue Bank Beverwijk, the Netherlands), with a minimum endothelial cell density of 2300 cells/mm^2 and a diameter of 8.5 mm. No graft markings were used. A 9 mm descemetorhexis was performed and the graft was inserted into the anterior chamber using a glass injector (Geuder AG, Heidelberg, Germany). After the graft was inserted, fluid and air were used to unfold the graft – taking care to position the graft within the descemetorhexis area – and adhere the graft to the recipient stroma using gas. In 33 surgeries the randomization dictated that intraoperative OCT was not available to the surgeons. Here, a full anterior chamber (AC) fill was performed, with raising the IOP above normal physiological limits for 8 minutes using air (*overpressure)*. In the other 32 surgeries the intraoperative OCT was available for utilization at the surgeon's discretion and a brief AC fill was performed to adhere the graft without prolonged pressurizing the eye. At the end of surgery, the air was replaced by Sulphur Hexafluoride 20% gas and the size of the gas bubble was reduced to 80-90% of the AC. In concordance with the protocol in all cases the adherence of the graft was confirmed using the iOCT at the end of surgery. After surgery, the patient remained strictly supine the next 2 hours and were instructed to remain in the supine position for the following 24 hours. A rebubbling was indicated if >30% of the graft was detached or if the detachment involved the visual axis.

Pachymetry and detachment maps

Preoperatively and one-day after surgery corneal thickness was measured using AS-OCT and a grid was applied to divide the cornea to 25 zones (**Figure 1)**. Two AS-OCT devices were used in this trial. At two study sites (Utrecht & Leuven, n=51) the corneal thickness was determined using 24 radial scan lines, which resulted in a pachymetry map of the mean corneal thickness in each of the 25 zones. All scans used to generate the pachymetry map were manually reviewed to detect incorrect segmentation of the cornea. At the other study site (Maastricht, n=14) the corneal thickness was manually measured every 1 mm in eight meridians (20, 45, 70, 90, 110, 135, 160, 180 degrees) to build a pachymetry map (n = 14 subjects).

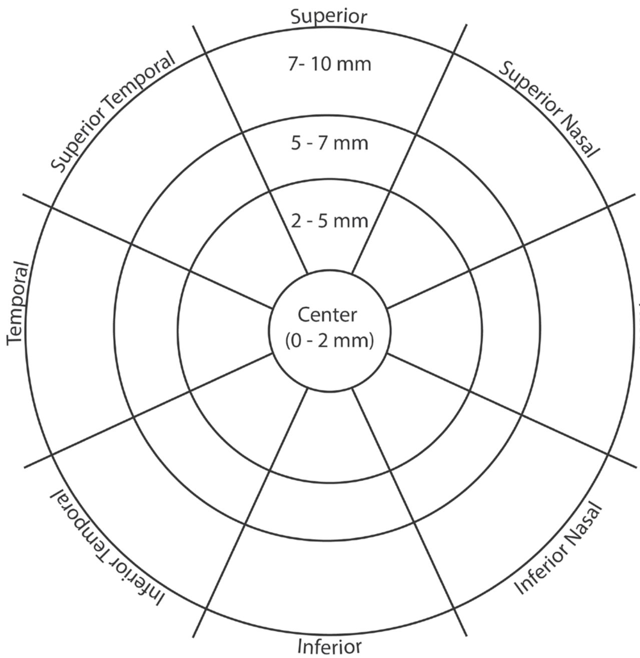

Figure 1. A corneal grid of the right eye (OD) to measure corneal thickness and presence of graft detachment. The corneal grid consists of 25 corneal zones based on the anatomical position and distance from the center. We used the grid to score if a graft detachment was present and measured the corneal thickness in each zone.

In addition, a detachment map was created for every subject, using the same grid. A graft detachment was defined as any non-adherence of the graft noticeable on slit lamp examination and AS-OCT imaging at any time point within 3 months after surgery. For cases in which AS-OCT was missing the slit lamp examination was used to determine if a detachment was present and quantify the size of the detachment. A detachment in a particular zone was classified as such based on the first recording of non-adherence within the three months after surgery, regardless of later clinical interventions or resolution.

The detachment and pachymetry maps were combined to evaluate for each subject in each zone the corneal thickness and whether a graft detachment was present. Subjects were divided in two groups based on the presence of any amount of graft detachment at any post-operative time-point: group 1: subjects with complete attachment of the graft (i.e., attached), and group 2: subjects with a noticeable graft detachment (i.e., detached).

Data processing and statistical analysis

All statistical analyses were performed using R statistical software version 4.0.3 (CRAN, Vienna, Austria). Data were described as mean ± standard deviation (SD) for continuous variables and as individual counts and percentages for dichotomous and categorical variables. All data were tested for normality. Between and within group differences were tested as appropriate using an independent, paired Student's t-test or ANOVA for continuous variables and a Fisher exact test for dichotomous and categorical variables. Correction for multiple comparisons was performed using the Bonferroni correction and a 2-sided *p*-value of less than 0.05 was considered statistically significant.

Missing observations for preoperative corneal thickness, postoperative corneal thickness, or postoperative anterior chamber (AC) volume were imputed using multiple imputation. For these three parameters the following other parameters were used as predictors when imputing: recipient sex, recipient age, corneal zone, the detachment map, rebubbling, postoperative IOP, and donor age. The number of imputations was equal to the maximum percentage of missing data plus one. No associations between the imputed variables and graft detachment were found and the missing observations are considered missing at random. Measurements in the 7-10 mm corneal zone in subjects examined using the Zeiss Cirrus 5000 were not imputed and excluded from further analysis, because the device does not calculate the corneal thickness outside a diameter of 7 mm and as a result these measurements were considered missing not at random.

The imputed dataset was divided in a training set and a test set, comprising of respectively 70% and 30% of the dataset. The training set was used to find a suitable model of predictor variables and determine the optimal thresholds for predicting graft detachment using the optimal F1-score (i.e., the optimal operating point). The test set was used to validate the prediction models. Two prediction methods were evaluated: 1) a model using corneal thickness and 2) a regression model. The corneal thickness model uses an absolute corneal thickness threshold to predict if the graft in a particular corneal zone will detach (i.e., above the optimal operating point the model will predict a detachment). In comparison, the regression model calculates the probability of a graft detachment occurring in a particular corneal zone and will predict a graft detachment above if the probability exceeds the optimal operating point. For the regression model, the association between graft detachment and predictors in the training set was analyzed using a mixed effect model with random intercepts and slopes to correct for multiple measurements in the same subject, which are assumed to be correlated. Recipient age and sex, donor age, preoperative and postoperative recipient corneal thickness, intra-ocular pressure, and the size of the postoperative AC tamponade gas bubble were included as fixed effects in the analyses. The individual patient and corneal zone were considered a random effect. In addition, two additional models were evaluated; a simpler regression model using only pre- and postoperative corneal thickness, and a subgroup analysis of subject without a graft detachment noticeable on the first day after surgery.

The performance of both prediction methods in the test set was evaluated using receiver operating characteristic (ROC) curves and the area under the curve (AUC) was calculated. Next, the predicted outcome (detachment versus no-detachment) was compared to the detachment map (i.e., the ground truth) to calculate the sensitivity and specificity. Sensitivity was defined as a graft detachment, while specificity represents an attached graft.

RESULTS

In total 65 subjects were enrolled in the ADVISE-trial and included for analysis in the current study. Of the 65 included subjects, 33 developed a graft detachment and 17 of these graft detachments underwent rebubbling. In 11 subjects a graft detachment was noticeable on the first day after surgery. The average time between surgery and detection of detachment measured 7.54 days (SD: ±9.44, range: 1 – 32 days) and the average detached area measured 31% of the surface of the grid (range: 8 – 100%). In 8 subjects the preoperative pachymetry measurements (12.3%) and in 6 cases the postoperative pachymetry measurement (9%) were missing. The incidence of graft detachment or postoperative corneal thickness across the corneal zones one day after surgery did not differ between the treatment arms of the trial intervention (data not shown).[15] The unimputed study population characteristics are shown in **Table 1**.

Table 1. The unimputed donor, recipient, pre- and postoperative characteristics.

	No graft detachment (n = 32)	Graft detachment (n = 33)	*p*-value[1]	Missing[2] (%)
Recipient age, years	72 ±7.03	74 ±5.88	0.401	0%
Recipient sex: female, n (%)	16 (50.0)	18 (54.5)	0.907	0%
Donor age, years	73 ±4.83	74 ±5.85	0.455	0%
Postoperative AC tamponade fill[3,4], %	46 ±13.17	43 ±13.15	0.426	13.3%
Postoperative IOP, mmHg[3]	13 ±3.88	13 ±4.36	0.869	0%
Mean preoperative corneal thickness across all cornea zones, µm	624.76 ±71.26	648.05 ±70.57	0.221	17.9%
Mean thickness across all corneal zones without a graft detachment within the first 3 months	624.76 ±71.26	648.05 ±65.94	0.201	NA
Mean thickness across all corneal zones with a graft detachment within the first 3 months	NA	647.28 ±78.81	NA	NA
Mean postoperative corneal thickness one day after surgery across all cornea zones, µm[3]	744.98 ±82.42	805.37 ±98.03	0.015	27.3%
Mean thickness across all corneal zones without a graft detachment within the first 3 months[3]	744.98 ±82.42	788.38 ±106.63	0.098	NA
Mean thickness across all corneal zones with a graft detachment within the first 3 months[3]	NA	845.58 ±99.64	NA	NA

AC: anterior chamber; IOP: intra-ocular pressure; NA: not applicable
Unless otherwise specified reported as mean ±standard deviation
1: independent t-test
2: Percentage of missing is defined as the total amount of datapoints (i.e., corneal zones) missing, not subjects missing.
3: measured one day after surgery
4: measured as % of total anterior chamber volume

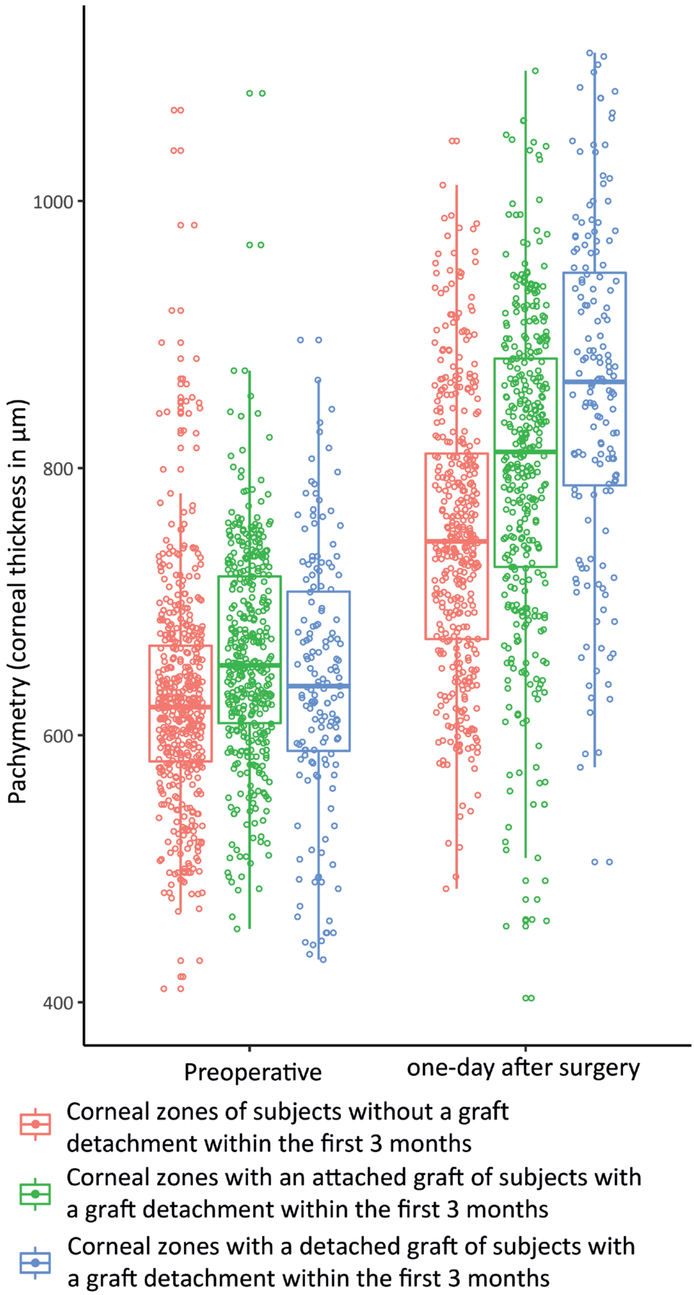

Figure 2. The corneal thickness across the corneal zones preoperatively and one-day postoperatively of subject with and without a graft detachment. The graft detachment group is stratified for corneal zones in which the graft detached following the surgery and corneal zones in which the graft remained attached.

The distribution of the pachymetry measurements for the corneal zones between assessments and within groups is shown in **Figure 2**. Preoperatively, no significant differences were found between the groups with and without graft detachment (*p* = 0.221, **Table 1**). One-day after surgery the overall mean corneal thickness was higher in subjects that developed a graft detachment compared to subject without a graft detachment (744.98 ±82.42, 805.37 ±98.03, *p* = 0.015, **Table 1**). Importantly, within subjects that developed a graft detachment the corneal zones in which the graft detached following the surgery were statistically significant thicker compared to zones in which the graft remained attached (mean of detached zones: 845.58 ±99.64 µm versus mean of attached zones: 788.38 ±106.63 µm, [95% CI: 40.73 – 76.99 µm], $p < 0.001$, adjusted *p* = 0.004). The thickness of corneal zones in which the graft remained attached in the detachment group did not differ compared to the corneal thickness in subjects without a graft detachment (*p* = 0.098).

Performance of the prediction methods

A mixed effect logistics regression was used to analyze the association between graft detachment and predictors in the training set (**Supplementary table 1**). Postoperative corneal thickness of the corneal zone was found to be the only variable associated with an increased risk for graft detachment (odds ratio: 1.004, [95% CI: 1.002 – 1.006, $p<0.001$]); indicating that for every increase of 1 µm in corneal thickness the odds for graft detachment increased by 4‰.

In **Figure 3** the ROC curves are displayed for the corneal thickness model and the regression model for predicting graft detachment in the test set. The regression model achieved an AUC of 0.87 (sensitivity: 0.79, specificity: 0.75) compared to an AUC of 0.65 for the corneal thickness model (sensitivity: 0.63, specificity: 0.63). In the subgroup analysis of cases without a graft detachment noticeable the first day after surgery both models performed comparably, the regression model achieved an AUC of 0.90 (sensitivity: 0.82, specificity: 0.73) and the corneal thickness model an AUC of 0.73 (sensitivity: 0.58, specificity: 0.79). The regression models were superior compared to the corneal thickness model in both sensitivity and specificity compared to the corneal thickness model. Moreover, the comparable sensitivity and specificity of the regression models indicates that the models are equally able to correctly predict a detached or attached graft in the respective corneal zones. A simpler model regression model using only pre- and postoperative corneal thickness of the corneal zones achieved the same performance as the primary model (AUC: 0.87, sensitivity: 0.79, specificity: 0.75). In particular, the simpler model may be more feasible for clinical practice.

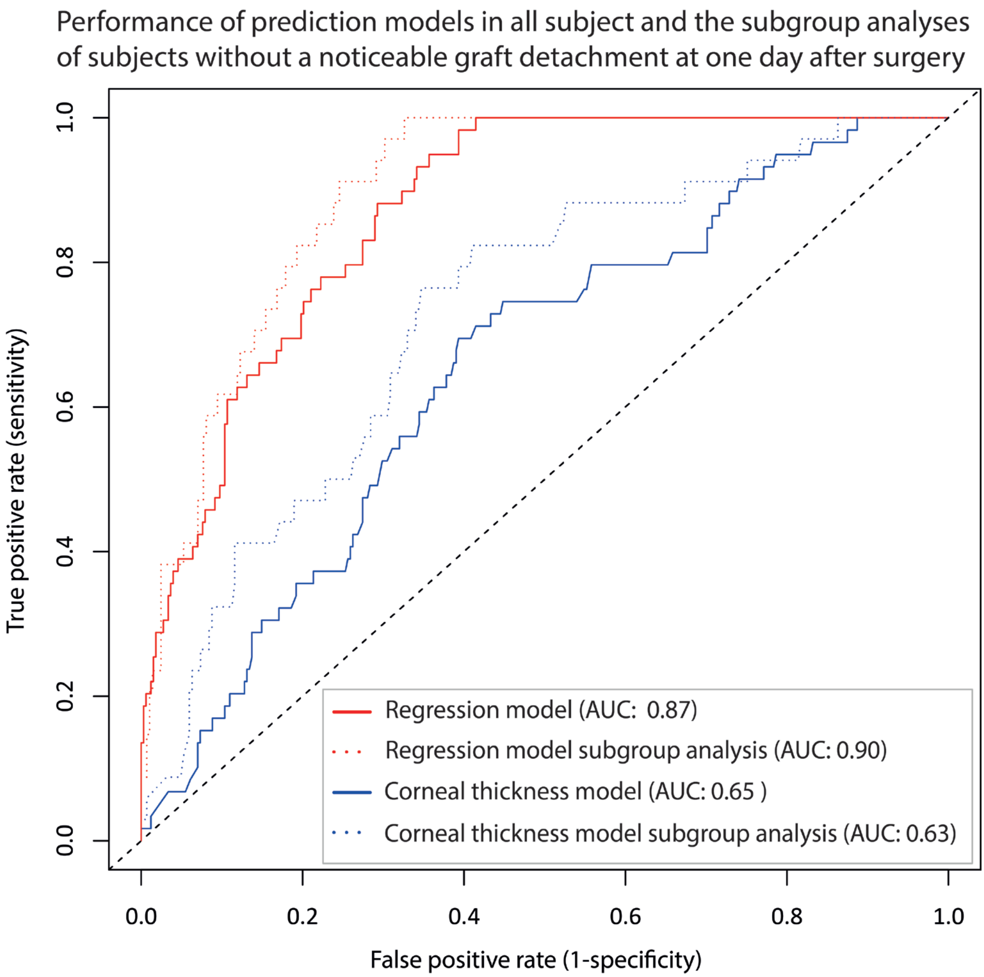

Figure 3. The performance of the prediction models for graft detachment. The receiver operating characteristic (ROC) curves of the corneal thickness model and regression model for predicting graft detachment, obtained by, respectively, varying the threshold for corneal thickness and the regression coefficient. The dashed ROC curve represents the subgroup analysis of subject without a noticeable graft detachment one day after surgery. The dashed 45-degree line constitutes a model with no discriminative power. AUC: area under the curve.

DISCUSSION

In this study we demonstrated that a locally increased corneal thickness one-day after surgery is associated with an increased risk of graft detachment. Additionally, we demonstrated the predictive power of corneal thickness mapping as a biomarker for (future) graft detachment. These findings translate to a reliable clinical risk assessment for graft detachment and enable tailored postoperative care (i.e., reduced amount of post-op visits for individuals with a low risk and vice versa).

Of the two evaluated prediction models, the mixed methods regression model was superior to the corneal thickness model. The regression models achieved a good to excellent predictive power (AUC 0.87)[16,17] and was comparably accurate at predicting corneal zones with a detached and attached graft. Both models achieved a slightly higher AUC in the subgroup analysis, although sensitivity and specificity remained comparable during evaluation of the test set. The performance gap between the regression model and corneal thickness model can be explained by the differences in prediction method between the models. The regression model predicts the outcome based on the probability of a detachment compared to an absolute cutoff used in the corneal thickness model. Evidently, the regression model accounts for differences between subjects (e.g., baseline corneal thickness per zone) and is less susceptible to outliers.

These results support our hypothesis that local corneal thickness one-day after DMEK can be predictive for graft detachment following surgery and are in line with the current body of evidence. Moutsouris et al. suggested that persistent corneal edema visually assessed on cross-sectional OCT scans may be indicative of (partial) graft detachment and Dirisamer et al. found that corneal thickness was increased in detached corneal quadrants to adjacent corneal quadrants.[89] Furthermore, in a descriptive study Yeh et al. found that long-term graft adherence can be assessed shortly after surgery by qualitative grading of corneal quadrants using AS-OCT, though no predictive modelling was reported.[7] In this study we combined the insights of these studies to construct a predictive model using the fine granularity of corneal pachymetry maps. Assessing the outcome for each corneal zone separately benefits clinical decision-making compared to a binary outcome, because graft detachments are often limited to 1 or 2 corneal quadrants.[2] Likewise, the outcome measure in this study was broadly defined as any graft detachment as opposed to surgical rebubbling. The decision to re-adhere a graft is made by the surgeon which may not necessarily be related to the severity of tissue characteristics of the cornea zones.[1] This is exemplified by the recommended practice to not rebubble partial detachments and/or detachments outside the visual axis.[6,7]

This modelling approach in our study underlines the potential of OCT based biomarkers for postoperative management after corneal surgery. Biomarkers may have the potential to advance personalized medicine, thereby improving efficiency and patient outcomes.[18–20] The prediction model described in this paper may be used to differentiate which patients are at risk of graft detachment and how large this detachment will be (**Figure 4**). Inversely, selected cases could be exempted from intensive monitoring after surgery.

This study did not assess the underlying physiological mechanism between corneal thickness and graft detachment. In all cases a properly attached graft was confirmed at the end of surgery and as such we hypothesize that a local endothelial dysfunction is likely to have caused the increase in corneal thickness. However, we can only speculate whether this local endothelial dysfunction is the cause or the result of a detachment. A graft detachment may cause an endothelial dysfunction resulting in an increase in corneal thickness as a result of a lack of physical contact between the endothelial cells and stroma[9] and by disruption of the graft barrier function.[10] On the other hand, the formation of (localized) corneal edema caused by endothelial dysfunction may impair graft attachment, wound healing or leads to ultrastructural changes, which results in graft detachment.[13]

Furthermore, several limitations of this exploratory study should be addressed. This study was a post hoc analysis of a trial that was not powered on corneal thickness as an outcome measure. In addition, a considerable proportion of the corneal thickness measurements were missing, because of missing measurement and anatomical features of patients (e.g., lid aperture) that complicated image acquisition of the whole cornea. This proved particularly challenging with swollen eyelids the day after surgery and could be an obstacle for implementation of our concept in clinical practice. The data of the training and test set were not split on a patient level, which may affect generalizability of results. The mixed-effect regression corrects for this non-independence in the data and no significant differences were observed between the training and test set. Notwithstanding, the results of this study should be validated in a new and unrelated study population. In this study two different OCT devices were used to measure corneal thickness and which have a very strong comparability.[21] However, for one of these devices measurements had to be collected manually, which may have affected measurement accuracy. Nevertheless, the measurements of the two devices were equally distributed across the training and test set and we consider it unlikely differences between the devices or measurement methods affected the study conclusions.

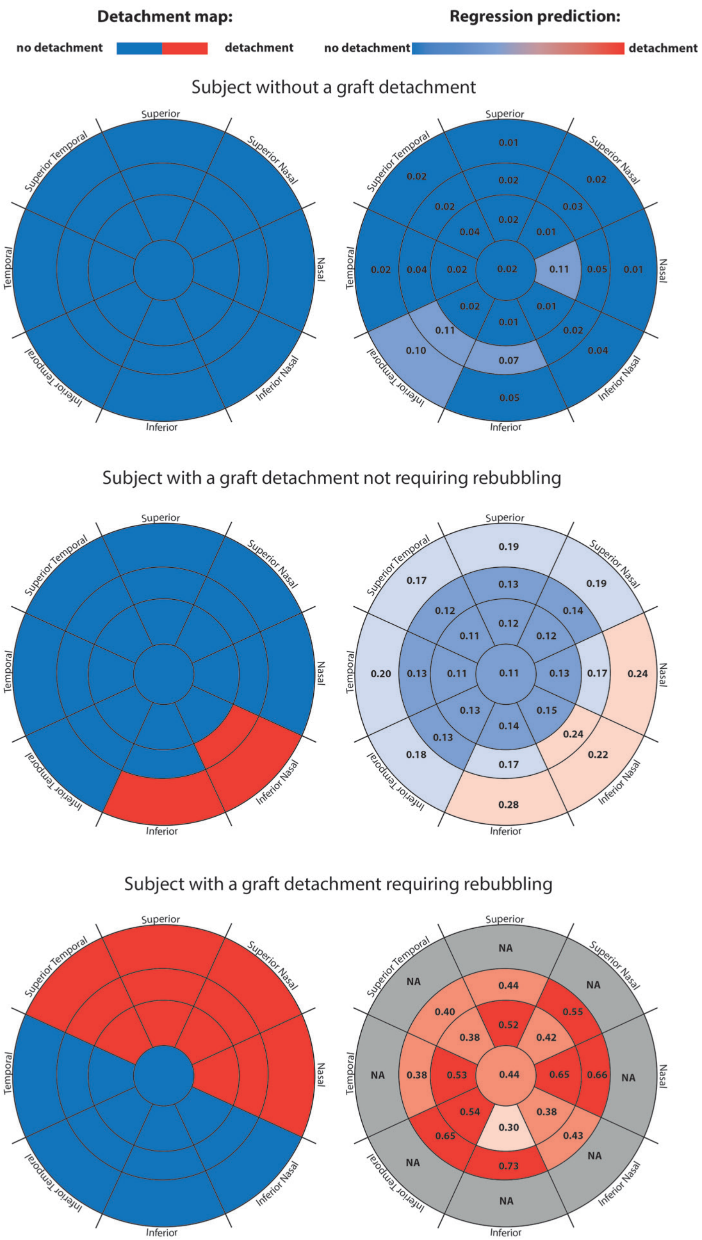

Figure 4. A conceptualization of the regression model prediction based on three subjects included in the study. The left corneal grids show the detachment maps; blue indicates an attached graft in the respective corneal zone and red a graft detached in the respective corneal zone. The right corneal grids show the regression model prediction expressed as the probability for graft to detach in each corneal zone. The shades of blue indicate a predicted attached graft in the corneal zone and the shades of red a predicted detached graft in the corneal zone. The grey corneal zones were not assessed (NA) and no prediction is available.

In conclusion, we demonstrated that increased local corneal thickness one-day after surgery is associated with graft detachment and we developed a prediction model to detect early graft detachment. Future research should focus on identification of other postoperative clinical parameters predictive for graft detachment, in addition to pre- and postoperative parameters in the prediction models, and integrating tools that likewise support postoperative decision-making.[22]

ACKNOWLEDGEMENTS

The authors would like to thank Roos Wennink, MD, and Laurence Frank, PhD for their support with and critical feedback on the statistical analysis.

REFERENCES

1. Parker J, Parker JS, Melles GR. Descemet Membrane Endothelial Keratoplasty—A Review. *US Ophthalmic Review* 2013; 06: 29.
2. Siebelmann S, Kolb K, Scholz P, et al. The Cologne rebubbling study: a reappraisal of 624 rebubblings after Descemet membrane endothelial keratoplasty. *British Journal of Ophthalmology* 2020; bjophthalmol-2020-316478.
3. Parekh M, Leon P, Ruzza A, et al. Graft detachment and rebubbling rate in Descemet membrane endothelial keratoplasty. *Survey of Ophthalmology* 2018; 63: 245–250.
4. Dunker S, Winkens B, Van Den Biggelaar F, et al. Rebubbling and graft failure in Descemet membrane endothelial keratoplasty: a prospective Dutch registry study. *British Journal of Ophthalmology* 2021; 1–7.
5. Weller JM, Schlötzer-Schrehardt U, Tourtas T, et al. Influence of Ultrastructural Corneal Graft Abnormalities on the Outcome of Descemet Membrane Endothelial Keratoplasty. *American Journal of Ophthalmology* 2016; 169: 58–67.
6. Quilendrino R, Rodriguez-Calvo de Mora M, Baydoun L, et al. Prevention and Management of Graft Detachment in Descemet Membrane Endothelial Keratoplasty. *Archives of Ophthalmology* 2012; 130: 280–291.
7. Yeh RY, Quilendrino R, Musa FU, et al. Predictive value of optical coherence tomography in graft attachment after descemet's membrane endothelial keratoplasty. *Ophthalmology* 2013; 120: 240–245.
8. Moutsouris K, Dapena I, Ham L, et al. Optical coherence tomography, scheimpflug imaging, and slit-lamp biomicroscopy in the early detection of graft detachment after descemet membrane endothelial keratoplasty. *Cornea* 2011; 30: 1369–1375.
9. Dirisamer M, Dapena I, Ham L, et al. Patterns of corneal endothelialization and corneal clearance after Descemet membrane endothelial keratoplasty for fuchs endothelial dystrophy. *American Journal of Ophthalmology* 2011; 152: 543-555.e1.
10. Zander D, Grewing V, Glatz A, et al. Predicting Edema Resolution after Descemet Membrane Endothelial Keratoplasty for Fuchs Dystrophy Using Scheimpflug Tomography. *JAMA Ophthalmology* 2021; 139: 423–430.
11. Heslinga FG, Lucassen RT, Berg MA van den, et al. Corneal Pachymetry by AS-OCT after Descemet's Membrane Endothelial Keratoplasty. *Scientific Reports* 2021; 1–9.
12. López EF, Baydoun L, Gerber-Hollbach N, et al. Rebubbling techniques for graft detachment after descemet membrane endothelial keratoplasty. *Cornea* 2016; 35: 759–764.
13. Brockmann T, Brockmann C, Maier AK, et al. Clinicopathology of graft detachment after Descemet's membrane endothelial keratoplasty. *Acta Ophthalmologica* 2014; 92: e556–e561.
14. Schulz KF, Altman DG, Moher D. CONSORT 2010 Statement: updated guidelines for reporting parallel group randomised trials. *BMJ*; 340. Epub ahead of print 2010. DOI: 10.1136/bmj.c332.
15. Muijzer MB, Nuijts RMMA, Delbeke HMS, et al. Preliminary outcomes of the advanced visualization in corneal surgery evaluation trial; a non-inferiority randomized control trial to evaluate intraoperative OCT and prolonged overpressure during Descemet membrane endothelial keratoplasty. *Acta Ophthalmologica* 2021; 99: 5.
16. Mandrekar JN. Receiver operating characteristic curve in diagnostic test assessment. *Journal of Thoracic Oncology* 2010; 5: 1315–1316.

17. DW H, Lemeshow S. Chapter 5. In: *Applied Logistic Regression 2nd Ed*. 2000, pp. 160–164.
18. Aronson JK, Ferner RE. Biomarkers—a general review. *Current Protocols in Pharmacology* 2017; 2017: 9.23.1-9.23.17.
19. Califf RM. Biomarker definitions and their applications. *Experimental Biology and Medicine* 2018; 243: 213–221.
20. Love-Koh J, Peel A, Rejon-Parrilla JC, et al. The Future of Precision Medicine: Potential Impacts for Health Technology Assessment. *PharmacoEconomics* 2018; 36: 1439–1451.
21. Pierro L, Iuliano L, Gagliardi M, et al. Central Corneal Thickness Reproducibility among Ten Different Instruments. *Optometry and Vision Science* 2016; 93: 1371–1379.
22. Heslinga FG, Alberti M, Pluim JPW, et al. Quantifying graft detachment after Descemet's membrane endothelial keratoplasty with deep convolutional neural networks. *Translational Vision Science and Technology* 2020; 9: 1–9.

SUPPLEMENTARY DATA

Supplementary table 1. Factors Associated with an increased risk of graft detachment using a mixed effect logistic regression analysis in the training set

Fixed variables	Odds ratio	95% confidence interval odds ratio	p–value
Recipient age, years	1.041	0.940 – 1.153	0.44
Sex (reference: male)	0.644	0.205 – 2.021	0.45
Donor age, years	1.073	0.953 – 1.208	0.24
Intra–ocular pressure, mmHg	1.052	0.912 – 1.213	0.49
AC tamponade fill, %[1]	0.976	0.949 – 1.004	0.09
Preoperative corneal thickness, µm	1.001	0.998 – 1.004	0.38
Postoperative corneal thickness, µm	1.004	1.002 – 1.006	<0.001

AC: anterior chamber
[1] measured as % of total anterior chamber volume
Random variables: subject and corneal zone

CHAPTER 10

GENERAL DISCUSSION AND SUMMARY

Marc B Muijzer

The aim of this research was to study the utility of intraoperative OCT and investigate predictive factors of graft detachment in DMEK surgery. This chapter summarizes and discusses the main findings of this thesis, clinical implications, and methodological considerations. The summary and discussion are organized in sections following the aims of this research: the applications and value of intraoperative OCT, specifically in posterior lamellar corneal surgery, and the identification of predictive factors for graft detachment in Descemet membrane endothelial keratoplasty. Finally, the last section will briefly point out future research perspectives.

Intraoperative optical coherence tomography

Chapter 2 summarizes the current research and practical applications of intraoperative OCT. Intraoperative OCT is increasingly utilized in ophthalmic surgery, ranging from vitreoretinal surgery to pediatric surgery. The information and direct real-time feedback of the intraoperative OCT image enables the surgeon to adequately manage intraoperative events, observe tissue alterations, and in-vivo study practice patterns. A frequently reported outcome measure to capture the benefits is the influence of intraoperative OCT on surgical-decision making. The results of chapter 2 show that the use of intraoperative OCT can significantly affect surgical decision making. In other words, the OCT images provide valuable information leading to subsequent altering of the surgical strategy accordingly. The considerable proportion of surgeries in which intraoperative OCT aided the surgical decision-making (reported rates range between 30 to 60%) suggests that intraoperative OCT fills important gaps in information relevant for surgical outcomes and safety. [1,2]

Notwithstanding, the current body of evidence mainly consists of observational or retrospective studies that focus on the benefit from a surgeon's perspective and studies frequently lacked a control group. As a consequence, the putative benefits of intraoperative OCT on surgical outcomes seen from a patient perspective is difficult to establish. This has resulted in a debate regarding the utility of intraoperative OCT and whether the considerable investment is justified. In other words, is intraoperative OCT "a nice to have" or "a need to have". The next section of this summary and discussion is dedicated to this question.

Applications of intraoperative optical coherence tomography in endothelial keratoplasty

Chapter 3 reports on our initial clinical experiences with intraoperative OCT during DMEK surgery and how this impacted the surgical protocol. Using intraoperative OCT, it was possible to objectively determine the graft' orientation inside the eye and observe its adherence to the stroma. Interestingly, the OCT image revealed that directly after injecting gas in the anterior chamber most grafts were fully adhered to the recipient stroma. In clinical practice, the gas is used to support graft adherence and normally left in the eye for a prolonged time (8-15 minutes) under an artificially high pressure (i.e., overpressure). Now, surgeons started to refrain from this precautionary and time-consuming practice and fared on the intraoperative OCT image rather than the clock.[3–5] In addition, according to surgeons less graft manipulation was required during surgery. This was attributed to the enhanced three-dimensional visualization of graft-geometry aiding graft unfolding.[6,7] The result of the study showed promising evidence that the optimized protocol had a lower endothelial cell loss (-11%) and incidence of postoperative complications (18% versus 44%). This led to the hypothesis that using intraoperative OCT prolonged overpressure may be obviated and might improve surgical outcomes in terms of complications and endothelial cell loss. An intraoperative OCT optimized surgical protocol was conceptualized consisting of OCT guidance for determining orientation, unfolding of the graft, and confirming adherence, while refraining from prolonged pressuring the eye. However, gradual implementation of the surgical protocol, retrospective analysis, and uncertainty regarding clinical outcomes warranted validation of these findings, which followed in the ADVISE-trial.

In **chapter 4** the results of the ADVISE-trial are presented: a non-inferiority randomized control trial in which we compare the intraoperative OCT-optimized surgical DMEK protocol with the conventional practice; with prolonged overpressure of the eye and without support of intraoperative OCT. The aims of the trial were to evaluate the utility of intraoperative OCT and to determine whether intraoperative OCT-guidance can obviate the need for prolonged overpressure in DMEK surgery as hypothesized in chapter 3. The study demonstrated that the intraoperative OCT-optimized protocol was non-inferior compared to a conventional protocol, although the prevalence of adverse events did not differ materially between both treatment protocols. The outcome showed that overpressure can be obviated as it does not improve graft adherence in DMEK. On the other hand, no clear harmful consequences of overpressure were observed in the study as clinical outcomes did not differ between the treatment arms and it is plausible that refraining from overpressure is non-inferior regardless of intraoperative OCT imaging. Notwithstanding, an important benefit for refraining from overpressure is the efficiency gains from omitting the time waiting while the eye is pressurized. On average this saves 6 to 7 minutes per procedure, the cumulative effect of these time saving may have considerable impact on the surgical capacity as hospital resources can be used more efficiently. In our clinical already more DMEK procedures are scheduled on a given day, which is relevant due to the increasing demand for eye care.[8,9]

To date, the ADVISE-trial is the first randomized comparison of intraoperative OCT support during an ophthalmic surgical procedure. Surgeons reported that the use of intraoperative

OCT benefitted the surgical decision-making process in 40% of surgeries in which the intraoperative OCT was used and proved indispensable in several complex surgeries, salvaging the graft in one of those cases. This indicates that intraoperative OCT may be an important asset to the surgeon to enhance the care for individual patients. The most reported use of intraoperative OCT was during determination of the grafts orientation and in lesser degree aiding the unfolding of the graft. The latter was supported by a shorter duration of unfolding and positioning of the graft in the intraoperative OCT group. However, intraoperative OCT aided surgical decision-making was not related to an easier graft unfolding nor patient outcomes. This illustrates that the perceived benefits from a surgeon's perspective and quantitative outcomes are not always coherent.

In complex cases the value of intraoperative OCT from a patient's perspective is most apparent as highlighted in **chapter 5**. Here, we describe how intraoperative OCT proved crucial for the diagnosis and treatment of an infant that underwent a bilateral corneal transplantation for severe progressive corneal edema. In cases with severe cornea edema endothelial keratoplasty may not always be feasible and thus reverted to penetrating keratoplasty.[10] However, in very young patients penetrating keratoplasty has additional disadvantages, including: poor visual outcomes increasing the risk of developing amblyopia and compromised integrity of the cornea which makes it more vulnerable to trauma during the patient' lifetime.[10,11] Intraoperative OCT enabled to visualize the graft and various surgical steps inside the eye during the procedure otherwise obscured by the clouded cornea, which allowed endothelial keratoplasty to be possible.

Several studies have demonstrated the potential of image analysis of intraoperative OCT images to improve the usability and value of intraoperative OCT. Examples include: image-based biomarkers related to treatment success[5,12–15], image analysis techniques to guide surgical instrument maneuvering to improve safety[16–20], or intraoperative OCT measurements for precise placement of intraocular lenses optimizing refractive outcomes.[21,22] Integration of automated image analysis tools and development of computerized clinical decision support systems improve the processing and transmission of information contained in the OCT images.[23] This provides in the moment the most relevant information to support clinical decision-making, whichcan improve patient outcomes, surgical safety and workflow efficiency. In **chapter 6** we demonstrate the feasibility of such a system in DMEK surgery and present a tool for automated evaluation of the graft orientation using intraoperative OCT images. The proposed tool provides a segmented representation of the graft with a predicted outcome making the current disrupting and time-consuming practice of manual targeting, focusing, and reviewing the intraoperative OCT by surgeons unnecessary. This improves the surgical workflow and may reduce the risk of interpretation errors. Challenges that affected the accuracy of the tool were the variable quality of the OCT images resulting in segmentation errors and the fact that not every OCT image contained sufficient information regarding the graft's orientation. These challenges can be overcome using technical fixes, such as a frame-based quality assessment and advanced segmentation techniques. Importantly, explicit attention should be given to explain the systems decision-making process and certainty regarding the outcome, which will contribute to surgeon's acceptance and subsequent implementation in clinical practice.

Predictive factors of graft detachment in DMEK

The causes of graft detachment are considered multifactorial relating to patient, donor, and surgical factors.[24–30] The second part of this thesis focuses on unraveling the causes of graft detachment and identifying the independent effect of predictive factors. **Chapter 7** reports on the use of a nationwide registry supplemented with the treatment protocols of Dutch corneal clinics to explore risk and protective factors for graft detachment. Three different machine learning methods (i.e., a lasso-regression, classification tree analysis, and random forest) were used to assess the marginal contribution of practice pattern variations, donor and patient characteristics on the incidence of graft detachment requiring rebubbling. In particular, three factors identified in our analysis warrant further discussion, namely: a DMEK procedure, the use of SF6 gas, and performing combined procedures.

All three models identified that a DMEK procedure and/or DMEK-specific variables were associated with an increased risk of rebubbling procedure. This finding is consistent with previous studies[31–33], however, as DMEK is a relatively new procedure these studies frequently attribute the higher prevalence of graft detachment to the surgeon's learning curve.[32,34,35] In contrast, our analysis indicated an increased risk for DMEK procedures after adjusting for the learning effect. Moreover, our descriptive results show a consistent higher annual prevalence of graft detachment in DMEK (both total prevalence as adjusted for center) compared to DSEK. It appears unlikely that the increased risk of DMEK can be fully attributed to the surgeon's learning curve. Other possible explanations for the higher prevalence of graft detachments may be related to DMEK graft tissue characteristics and that partial detachment are more common after DMEK increasing the rate of rebubbling.[28,36–38] Nonetheless, this finding warrants discussion on balancing the higher risk of complications versus the benefits in visual acuity in DMEK compared to DSEK.

We found that using SF6 as the tamponade agent was associated with an increased risk of graft detachment. This finding is in contrast with previous studies suggesting that the use

10

of SF6 gas may reduce the risk of graft detachment[39–42], whereas our results suggest that the protective effect of SF6 gas is absent relative to all other factors. A possible cause for the discrepancy might be the simultaneous adoption of SF6 and introduction of DMEK, which makes it difficult to distinguish effects between these factors from each other. Alternatively, the protective effect of SF6 found in other studies may be attributed or mediated by other related intraoperative factors that were not assessed in this study, such as gas bubble size.[43] To date only retrospective studies have provided evidence for the protective effect of SF6 gas and a comparative trial is needed to provide conclusive evidence.

Another relevant finding is that combining endothelial keratoplasty with other procedures - most commonly cataract surgery or a peripheral iridectomy - does not increase the risk of a graft detachment, but rather appears to have a protective effect. In our study only 5 of the 16 corneal centers regularly combine procedures (>15% of their procedures), whereas there is no indication that patient populations differ between centers that regularly combine procedures and those who do not regularly combine procedures. The reasons for the preference of sequential procedures were not investigated, but may relate to surgeon's beliefs. Our finding is supported by several recent studies that similarly did not find an increased risk of detachment in combined procedures.[33,44,45] Combining these findings and our results, we have to conclude that performing combined procedures has no impact on surgical safety, while combining procedures has evident advantages. These include an increased surgical capacity, reduced infection risk, lower societal costs associated with multiple procedures, and most importantly a decreased burden on patients.

The use of a nationwide quality registry with thousands of DMEK and DSEK procedure supplemented with practice patterns provides a valuable insight in real-world outcomes of practice pattern variations in endothelial keratoplasty and enabled the evaluation of numerous modulations of practice patterns in use and the relative impact of proposed key factors, which would not be feasible in a clinical study. Our initial aim to conceptualize an optimal surgical protocol using artificial intelligence proved to be challenging. Notwithstanding, the use of machine learning allowed us to explore patterns related to graft detachment, without being limited by a causal hypothesis. These insights complement clinical research by confirming outcomes in the real-world and generating new hypotheses to be tested in clinical studies. Overall, the models performed quite well (area under the curve ranging between 0.65 and 0.72), though the outcome of a substantial number of cases was incorrect predicted. This makes sense as not all factors affecting graft detachment are registered in the registry (e.g., patient's behavior and compliance with positioning advise), the questionnaires did not capture differences between reported practice pattern and actual clinical practice, and correct registration of adverse events could not be confirmed. Furthermore, the study underscored the importance of expert knowledge in machine learning research to put the results into perspective and draw meaningful conclusions that may benefit practice, as exemplified by the identification of proxy variables that represent differences between surgeons and/or centers.

Chapter 8 focusses on the underlying predictive factors for graft detachment during the surgery that could not be assessed in the analysis described in chapter 7. In this study we analyzed all surgical videos of the ADVISE-trial to assess the contribution of surgical manipulations, tissue handling, and variations in practice patterns during surgery on the incidence of graft detachment and detachments requiring a surgical rebubbling. The analysis revealed several clinically relevant insights between subjects with a fully attached graft and those with a detachment/rebubbling. A larger gas bubble covering the whole graft at the end of surgery had a lower risk of graft detachment, inversely, a smaller gas bubble had an increased risk. Recommended practices, such as minimal manipulation of the graft to prevent trauma[28,46,47] and avoiding overlap of the graft with the host Descemet membrane to improve attachment[48,49] were not associated with an evident increased or decreased risk of a detachment. These findings suggest that that providing sufficient support across the whole graft is more relevant to prevent postoperative detachment than iatrogenic trauma or impaired adhesion of the graft.

In addition, the graft configuration after insertion into the eye appeared related to the risk of a detachment. The graft configuration describes the tissue characteristics of the graft, such as the geometry and folding of the graft. Unfavorable graft shapes (i.e., tightly rolled grafts or with a lot of folds) were related to a higher risk for graft detachment compared to more favorable shapes. We hypothesize that graft configuration describes the overall graft unfolding difficulty, because unfavorable shapes are more challenging to unfold and position inside the eye. However, the association remains unclear as unfavorable graft shapes were not associated with proposed metrics that describe graft unfolding difficulty[28,50] or a higher degree of manipulation. Alternatively, this finding may suggest that a detachment cannot be fully controlled, because surgeons cannot influence tissue characteristics. Identifying the most suitable donors to select only grafts with a favorable configuration could be an option, although to date no studies have identified donor characteristics related to the incidence of graft detachment.[25,29,51–53]

In **chapter 9** we present another method to investigate the predictors of early graft detachment using corneal thickness mapping. We found that a locally increased corneal thickness assessed with a table-top anterior-segment OCT one-day after surgery was associated with an increased risk of graft detachment. The prediction model showed an excellent performance (area under the curve: 0.87) and the fine granularity of corneal pachymetry mapping allowed to estimate how large the detachment will be. This can aid in identifying patients at risk of a graft detachment requiring a rebubbling and enable tailored postoperative care (i.e., reduced amount of follow-up visits for individuals with a low risk and vice versa). We hypothesize that the variations in corneal thickness are caused by a local endothelial dysfunction as all grafts were attached at the end of surgery. However, it is unclear whether this local endothelial dysfunction is caused by or the result of the graft detachment. Investigating the underlying physiological mechanism between corneal thickness and graft detachment would be of considerable interest as it may provide insights in the origins of graft detachment.

In this study we defined graft detachment as any graft disadherence as opposed to a graft detachment requiring surgical rebubbling in most other studies. Admittedly, a rebubbling is clinically more relevant, though this is a treatment decision made by the surgeon taking into account other factors that may not necessarily relate to corneal thickness variations across the cornea. As a rebubbling is mediated by a graft detachment our model was still predictive for rebubbling, though the performance was as expected lower (area under the curve: 0.78, results not reported).

Concluding remarks and future perspectives

In addition, to the remarks made in the previous sections several conclusions can be drawn and directions for future research identified. This thesis demonstrates that intraoperative OCT is a promising new advancement in ophthalmic surgery considerably impacting surgical decision-making, improving care in complex cases, and enables surgeons to evaluate and optimize their practice patterns. However, the effect of intraoperative OCT on parameters of surgical performance and patient outcomes is not unequivocal. A challenge for future clinical research is how to define the utility of intraoperative OCT to assess the benefit on the surgical course. The broad definition of intraoperative OCT aided surgical decision-making may not be sensitive enough to assess differences in surgical outcomes.

The considerable investment in intraoperative OCT technology is frequently debated given that evidence of the benefits remains indirect. Our research shows that optimizing surgical practice patterns using intraoperative OCT reduced surgical time by at least 13% without affecting surgical safety or patient outcomes. If this increase in surgical efficiency will justify the investment remains unclear and evaluating the costs effectiveness of our optimized surgical protocol should answer this question.

As mentioned before the scientific interest for image analysis of intraoperative OCT images is gaining momentum and this is a promising direction for future research. We are beginning to obtain a better understanding of the useful information contained in intraoperative OCT images and its potential to improve patient outcomes and the delivery of care. Integrating tools for automatic information processing and clinical decision support systems are crucial to improve efficacy and usability of intraoperative OCT systems, possibly rendering manual reviewing obsolete. Another interesting development is the application of intraoperative OCT technology and image analysis in ophthalmic robotic surgery. The three-dimensional information of intraoperative OCT increases the positional accuracy and motion of instruments improving the safety and outcomes during (semi-) autonomous surgical maneuvers.[54–57]

The predictive model for graft detachments described in chapter 9 underlines the potential of OCT based biomarkers for personalized medicine after corneal surgery. We found that a local increase in corneal thickness was predictive for disadherence of the graft, which allows for customized postoperative care and aids in clinical decision-making regarding rebubbling procedures. Future research perspectives include taking into account the detachment size and location. This might improve selection of patients that require a rebubbling, while preventing unnecessary treatment. However, validation of the results is essential before application in clinical practice. Furthermore, investigating other postoperative clinical parameters or tissue characteristics predictive for graft detachment would be of interest as well.

The relative high incidence of graft detachment shows the importance of improving the safety of DMEK. This thesis demonstrated that graft detachment is caused by a complex interaction between patient-, donor-, and surgical factors. We found that previously unnoticed variations between practice patterns of surgical centers and surgical handling affected surgical safety. However, not all variation can be registered nor can all relevant factors be controlled, because patient or donor tissue characteristics cannot be changed. In addition, the rather high unexplained variation in our current studies points out that important factors were not assessed in our studies. These factors could be related to patient adherence to postoperative instructions, immunological factors on graft acceptance, endothelial cell related factors on graft adherence, or stressors in the surgical theatre that unwittingly affect surgical performance. Combining these insights, it might be hypothesized that the risk of a graft detachment is case-specific and conceptualizing an optimal practice pattern to prevent detachment will be challenging or may not even be feasible. A future approach is to use advanced analytical methods to predict the risk of graft detachment for each individual case. An individual risk projection enables tailored postoperative care, rather than focusing on (surgical) strategies to prevent graft detachment. This case-specific risk assessment allows for a multidimensional approach taking into account the relative risk of the practice pattern, patient characteristics, graft tissue properties, clinical variations, immunological factors, surgeon-reported experiences, and corneal biomarkers. We explored the potential of these novel individualized risk profiles and are involved in a prospective nationwide clinical study in Belgium where a detailed longitudinal data collection includes factors that were not assessed in our studies creating an opportunity to validate our findings.

Lastly, there are promising treatment modalities emerging that can make the struggle with graft detachment something of the past. Already, several reports have described non-keratoplasty treatment of endothelial dysfunction including Descemet stripping only [58,59], pharmaceutical treatment using Rho-kinase inhibitors (ROCK-inhibitors)[60,61], and injectable endothelial cells.[62,63] However, until these treatment modalities become commonplace endothelial keratoplasty will remain the standard of care for the management of corneal endothelial dysfunction.

REFERENCES

1. Ehlers JP, Dupps WJ, Kaiser PK, et al. The prospective intraoperative and perioperative ophthalmic imaging with optical CoherEncE TomogRaphy (PIONEER) study: 2-year results. *American Journal of Ophthalmology* 2014; 158: 999-1007.e1.
2. Ehlers JP, Modi YS, Pecen PE, et al. The DISCOVER Study 3-Year Results: Feasibility and Usefulness of Microscope-Integrated Intraoperative OCT during Ophthalmic Surgery. *Ophthalmology* 2018; 125: 1014–1027.
3. Titiyal JS, Kaur M, Falera R, et al. Evaluation of Time to Donor Lenticule Apposition Using Intraoperative Optical Coherence Tomography in Descemet Stripping Automated Endothelial Keratoplasty. *Cornea* 2016; 35: 477–481.
4. Steven P, le Blanc C, Velten K, et al. Optimizing Descemet membrane endothelial keratoplasty using intraoperative optical coherence tomography. *JAMA Ophthalmology* 2013; 131: 1135–1142.
5. Xu D, Dupps WJ, Srivastava SK, et al. Automated volumetric analysis of interface fluid in descemet stripping automated endothelial keratoplasty using intraoperative optical coherence tomography. *Investigative Ophthalmology and Visual Science* 2014; 55: 5610–5615.
6. Saad A, Guilbert E, Grise-Dulac A, et al. Intraoperative OCT-Assisted DMEK: 14 Consecutive Cases. *Cornea* 2015; 34: 802–807.
7. Patel AS, Goshe JM, Srivastava SK, et al. Intraoperative Optical Coherence Tomography–Assisted Descemet Membrane Endothelial Keratoplasty in the DISCOVER Study: First 100 Cases. *American Journal of Ophthalmology* 2020; 210: 167–173.
8. World Health Organization. *World report on vision*. 2019.
9. *2019 eye banking statistical report: Analysis of Surgical Use and Indications for Corneal Transplant*, www.restoresight.org (2019).
10. Bellucci R, Chierego C, Bellucci C. Endothelial Keratoplasty in a Newborn Baby With CHED. *Cornea* 2011; 30: 1488–1490.
11. Graham MAR, Nathalie F, Azar MR, et al. Visual Rehabilitation in Children with Congenital Hereditary Endothelial Dystrophy. *International Ophthalmology Clinics* 2001; 41: 9–18.
12. Tao J, Chen H, Zhu L, et al. Macular hole edge morphology predicts restoration of postoperative retinal microstructure and functional outcome. *BMC Ophthalmology*; 20. Epub ahead of print July 11, 2020. DOI: 10.1186/s12886-020-01541-7.
13. Kumar V, Yadav B. Hole-Door Sign: A Novel Intraoperative Optical Coherence Tomography Feature Predicting Macular Hole Closure. *Retina* 2018; 38: 2045–2050.
14. Ehlers JP, Uchida A, Srivastava SK, et al. Predictive model for macular hole closure speed: Insights from intraoperative optical coherence tomography. *Translational Vision Science and Technology*; 8. Epub ahead of print January 1, 2019. DOI: 10.1167/tvst.8.1.18.
15. Pahuja N, Shetty R, Jayadev C, et al. Intraoperative optical coherence tomography using the RESCAN 700: Preliminary results in collagen crosslinking. *BioMed Research International*; 2015. Epub ahead of print 2015. DOI: 10.1155/2015/572698.
16. Weiss J, Rieke N, Nasseri MA, et al. Fast 5DOF needle tracking in iOCT. *International Journal of Computer Assisted Radiology and Surgery* 2018; 13: 787–796.
17. El-Haddad MT, Tao YK. Automated stereo vision instrument tracking for intraoperative OCT guided anterior segment ophthalmic surgical maneuvers. *Biomedical Optics Express* 2015; 6: 3014.
18. Pasricha ND, Shieh C, Carrasco-Zevallos OM, et al. Needle Depth and Big-Bubble Success in Deep Anterior Lamellar Keratoplasty. *Cornea* 2016; 35: 1471–1477.

19. Keller B, Draelos M, Tang G, et al. Real-time corneal segmentation and 3D needle tracking in intrasurgical OCT. *Biomedical Optics Express* 2018; 9: 2716.
20. Draelos M, Tang G, Keller B, et al. Optical Coherence Tomography Guided Robotic Needle Insertion for Deep Anterior Lamellar Keratoplasty. *IEEE Transactions on Biomedical Engineering* 2020; 1–1.
21. Hirnschall N, Farrokhi S, Amir-Asgari S, et al. Intraoperative optical coherence tomography measurements of aphakic eyes to predict postoperative position of 2 intraocular lens designs. *Journal of Cataract and Refractive Surgery* 2018; 44: 1310–1316.
22. Hirnschall N, Norrby S, Weber M, et al. Using continuous intraoperative optical coherence tomography measurements of the aphakic eye for intraocular lens power calculation. *British Journal of Ophthalmology* 2015; 99: 7–10.
23. Shaikh F, Dehmeshki J, Bisdas S, et al. Artificial Intelligence-Based Clinical Decision Support Systems Using Advanced Medical Imaging and Radiomics. *Current Problems in Diagnostic Radiology* 2021; 50: 262–267.
24. Nahum Y, Leon P, Mimouni M, et al. *Factors Associated With Graft Detachment After Primary Descemet Stripping Automated Endothelial Keratoplasty*, www.corneajrnl.com (2017).
25. Leon P, Parekh M, Nahum Y, et al. Factors Associated With Early Graft Detachment in Primary Descemet Membrane Endothelial Keratoplasty. *American Journal of Ophthalmology* 2018; 187: 117–124.
26. Dirisamer M, van Dijk K, Dapena I, et al. Prevention and management of graft detachment in descemet membrane endothelial keratoplasty. *Archives of Ophthalmology* 2012; 130: 280–291.
27. Röck T, Bramkamp M, Bartz-Schmidt KU, et al. Causes that influence the detachment rate after Descemet membrane endothelial keratoplasty. *Graefe's Archive for Clinical and Experimental Ophthalmology* 2015; 253: 2217–2222.
28. Maier AKB, Gundlach E, Schroeter J, et al. Influence of the difficulty of graft unfolding and attachment on the outcome in descemet membrane endothelial keratoplasty. *Graefe's Archive for Clinical and Experimental Ophthalmology* 2015; 253: 895–900.
29. Dunker S, Winkens B, van den Biggelaar F, et al. Rebubbling and graft failure in Descemet membrane endothelial keratoplasty: a prospective Dutch registry study. *British Journal of Ophthalmology* 2021; bjophthalmol-2020-317041.
30. Terry MA, Straiko MD, Veldman PB, et al. *Standardized DMEK Technique: Reducing Complications Using Prestripped Tissue, Novel Glass Injector, and Sulfur Hexafluoride (SF 6) Gas*, https://www.youtube.com/watch?v=NuC7ZjHGICc (2015).
31. Singh A, Zarei-Ghanavati M, Avadhanam V, et al. Systematic Review and Meta-Analysis of Clinical Outcomes of Descemet Membrane Endothelial Keratoplasty Versus Descemet Stripping Endothelial Keratoplasty/Descemet Stripping Automated Endothelial Keratoplasty. *Cornea* 2017; 36: 1437–1443.
32. Li S, Liu L, Wang W, et al. Efficacy and safety of Descemet's membrane endothelial keratoplasty versus Descemet's stripping endothelial keratoplasty: A systematic review and meta-analysis. *PLOS ONE* 2017; 12: e0182275.
33. Dunker SL, Dickman MM, Wisse RPL, et al. Descemet Membrane Endothelial Keratoplasty versus Ultrathin Descemet Stripping Automated Endothelial Keratoplasty. *Ophthalmology* 2020; 127: 1152–1159.
34. Dapena I, Ham L, Droutsas K, et al. Learning Curve in Descemet's Membrane Endothelial Keratoplasty. *Ophthalmology* 2011; 118: 2147–2154.

35. Deng SX, Lee WB, Hammersmith KM, et al. Descemet Membrane Endothelial Keratoplasty: Safety and Outcomes. *Ophthalmology* 2018; 125: 295–310.

36. Parekh M, Leon P, Ruzza A, et al. Graft detachment and rebubbling rate in Descemet membrane endothelial keratoplasty. *Survey of Ophthalmology* 2018; 63: 245–250.

37. Woo J-H, Ang M, Htoon HM, et al. Descemet Membrane Endothelial Keratoplasty Versus Descemet Stripping Automated Endothelial Keratoplasty and Penetrating Keratoplasty. *American Journal of Ophthalmology* 2019; 207: 288–303.

38. Price MO, Gupta P, Lass J, et al. EK (DLEK, DSEK, DMEK): New Frontier in Cornea Surgery. *Annual Review of Vision Science* 2017; 3: 69–90.

39. Siebelmann S, Lopez Ramos S, Scholz P, et al. Graft Detachment Pattern After Descemet Membrane Endothelial Keratoplasty Comparing Air Versus 20% SF6 Tamponade. *Cornea* 2018; 37: 834–839.

40. Marques RE, Guerra PS, Sousa DC, et al. Sulfur Hexafluoride 20% Versus Air 100% for Anterior Chamber Tamponade in DMEK: A Meta-Analysis. *Cornea* 2018; 37: 691–697.

41. Terry MA, Shamie N, Chen ES, et al. Endothelial Keratoplasty. A Simplified Technique to Minimize Graft Dislocation, Iatrogenic Graft Failure, and Pupillary Block. *Ophthalmology* 2008; 115: 1179–1186.

42. Güell JL, Morral M, Gris O, et al. Comparison of Sulfur Hexafluoride 20% versus Air Tamponade in Descemet Membrane Endothelial Keratoplasty. *Ophthalmology* 2015; 122: 1757–1764.

43. Pralits JO, Alberti M, Cabreizo J. Gas-Graft Coverage After DMEK: A Clinically Validated Numeric Study. *Translational vision science & technology* 2019; 8: 9.

44. Shahnazaryan D, Hajjar Sese A, Hollick EJ. Endothelial Cell Loss After Descemet's Membrane Endothelial Keratoplasty for Fuchs' Endothelial Dystrophy: DMEK Compared to Triple DMEK. *American Journal of Ophthalmology* 2020; 218: 1–6.

45. Chaurasia S, Price FW, Gunderson L, et al. Descemet's membrane endothelial keratoplasty: clinical results of single versus triple procedures (combined with cataract surgery). *Ophthalmology* 2014; 121: 454–458.

46. Liarakos VS, Dapena I, Ham L, et al. Intraocular Graft Unfolding Techniques in Descemet Membrane Endothelial Keratoplasty. *JAMA Ophthalmology* 2013; 131: 29.

47. Kruse FE, Laaser K, Cursiefen C, et al. A Stepwise Approach to Donor Preparation and Insertion Increases Safety and Outcome of Descemet Membrane Endothelial Keratoplasty. *Cornea* 2011; 30: 580–587.

48. Tourtas T, Schlomberg J, Wessel JM, et al. Graft Adhesion in Descemet Membrane Endothelial Keratoplasty Dependent on Size of Removal of Host's Descemet Membrane. *JAMA Ophthalmology* 2014; 132: 155.

49. Röck T, Bramkamp M, Bartz-Schmidt KU, et al. Causes that influence the detachment rate after Descemet membrane endothelial keratoplasty. *Graefe's Archive for Clinical and Experimental Ophthalmology* 2015; 253: 2217–2222.

50. Quilendrino R, Rodriguez-Calvo de Mora M, Baydoun L, et al. Prevention and Management of Descemet Membrane Endothelial Keratoplasty Complications. *Cornea* 2017; 36: 1089–1095.

51. Oellerich S, Ham L, Frank LE, et al. Parameters Associated With Endothelial Cell Density Variability After Descemet Membrane Endothelial Keratoplasty. *American Journal of Ophthalmology* 2020; 211: 22–30.

52. Schaub F, Enders P, Zachewicz J, et al. Impact of Donor Age on Descemet Membrane Endothelial Keratoplasty Outcome: Evaluation of Donors Aged 17–55 Years. *American Journal of Ophthalmology* 2016; 170: 119–127.

53. Terry MA, Aldave AJ, Szczotka-Flynn LB, et al. Donor, Recipient, and Operative Factors Associated with Graft Success in the Cornea Preservation Time Study. *Ophthalmology* 2018; 125: 1700–1709.
54. Sommersperger M, Weiss J, Ali Nasseri M, et al. Real-time tool to layer distance estimation for robotic subretinal injection using intraoperative 4D OCT. *Biomedical Optics Express* 2021; 12: 1085.
55. Channa R, Iordachita I, Handa JT. Robotic Vitreoretinal Surgery. *Retina* 2017; 37: 1220–1228.
56. Chen C-W, Francone AA, Gerber MJ, et al. Semiautomated optical coherence tomography-guided robotic surgery for porcine lens removal. *Journal of Cataract and Refractive Surgery* 2019; 45: 1665–1669.
57. Keller B, Draelos M, Zhou K, et al. Optical Coherence Tomography-Guided Robotic Ophthalmic Microsurgery via Reinforcement Learning from Demonstration. *IEEE Transactions on Robotics* 2020; 36: 1207–1218.
58. Franceschino A, Dutheil F, Pereira B, et al. Descemetorhexis Without Endothelial Keratoplasty in Fuchs Endothelial Corneal Dystrophy: A Systematic Review and Meta-Analysis. *Cornea*, www.corneajrnl.com (2021).
59. Colby K. Descemet Stripping Only for Fuchs Endothelial Corneal Dystrophy: Will It Become the Gold Standard? *Cornea* 2021; 41: 269–271.
60. Okumura N, Sakamoto Y, Fujii K, et al. Rho kinase inhibitor enables cell-based therapy for corneal endothelial dysfunction. *Scientific Reports*; 6. Epub ahead of print May 18, 2016. DOI: 10.1038/srep26113.
61. Schlötzer-Schrehardt U, Zenkel M, Strunz M, et al. Potential Functional Restoration of Corneal Endothelial Cells in Fuchs Endothelial Corneal Dystrophy by ROCK Inhibitor (Ripasudil). *American Journal of Ophthalmology* 2021; 224: 185–199.
62. Kinoshita S, Koizumi N, Ueno M, et al. Injection of Cultured Cells with a ROCK Inhibitor for Bullous Keratopathy. *New England Journal of Medicine* 2018; 378: 995–1003.
63. Okumura N, Kinoshita S, Koizumi N. Cell-Based Approach for Treatment of Corneal Endothelial Dysfunction. *Cornea* 2014; 33: S37–S41.

Appendices

NEDERLANDSE SAMENVATTING

DANKWOORD

ABOUT THE AUTHOR

LIST OF PUBLICATIONS

NEDERLANDSE SAMENVATTING

Het doel van dit onderzoek was het onderzoeken van de toepassingen van intra-operatieve OCT in oogheelkundige chirurgie, specifiek tijdens lamellaire cornea transplantatie technieken, en het identificeren van prognostische factoren voor het loslaten van het transplantaat na een DMEK operatie. In de afgelopen decennia heeft corneachirurgie grote veranderingen ondergaan en één van de grootste veranderingen was de introductie van lamellaire keratoplastiek. Hierbij wordt selectief het aangedane weefsel vervangen wordt door gezond donor weefsel. Deze techniek heeft penetrerende keratoplastiek grotendeels vervangen als de chirurgische voorkeursbehandeling voor aandoeningen van het cornea endotheel.

Sinds de introductie van de endotheliale keratoplastiek is de techniek geëvolueerd naar steeds dunnere transplantaten, waarbij met grotere precisie het zieke weefsel vervangen kan worden. Hierdoor is de kwaliteit van leven en gezichtsscherpte voor veel patiënten verbeterd. Niettemin is een relatief frequente complicatie dat het transplantaat loslaat na de operatie. Vaak vereist dit een her-operatie om het transplantaat weer tegen de cornea te fixeren. De oorzaak van deze complicatie is vaak onduidelijk, maar over het algemeen wordt aangenomen dat de loslating van het transplantaat verband houdt met patiëntkenmerken, donoreigenschappen en/of chirurgische factoren.

Intra-operatieve OCT

De introductie van intra-operatieve OCT maakt het mogelijk tijdens de operatie met microscopische precisie scans te maken van het hoornvlies en het transplantaat. Dit biedt nieuwe mogelijkheden om de operatie verder te verfijnen en de oorzaken van het loslaten van het transplantaat te onderzoeken. Het is echter nog onduidelijk wat de toegevoegde waarde van OCT is voor de operatie en hoe we deze techniek (het beste) kunnen inzetten.

In hoofdstuk 2 wordt een overzicht gegeven van de ontwikkeling van intra-operatieve OCT en toepassingen in oogheelkundige chirurgie. Het onderzoek laat zien dat chirurgen in toenemende mate intra-operatieve OCT gebruiken tijdens operaties en dat dit een positieve invloed op de chirurgische besluitvorming heeft. De voordelen van OCT voor de chirurg zijn uitvoerig onderzocht, maar de toegevoegde waarde voor patiënten is nog onduidelijk.

Toepassingen van intra-operatieve OCT tijdens endotheliale keratoplastiek

In hoofdstuk 3 beschrijven we onze eerste ervaringen met de intra-operatieve OCT technologie tijdens DMEK chirurgie en hoe dit ons chirurgisch protocol heeft beïnvloed. Het gebruik van

OCT maakt het mogelijk het transplantaat in 3D te visualiseren. Hierdoor kan je chirurg objectief de boven- en onderkant van het transplantaat kan bepalen (i.e., de oriëntatie) en na injectie van gas in het oog de hechting van het transplantaat met de cornea beoordelen. In de klinische praktijk wordt het gas gebruikt om de hechting van de transplantaten te ondersteunen en wordt het gewoonlijk gedurende langere tijd (8-15 minuten) in het oog gelaten onder een kunstmatig hoge druk (i.e., overdruk). Op basis van het intra-operatieve OCT beeld kunnen de chirurgen afzien van deze voorzorgs- en tijdrovende praktijk. De resultaten van deze studie laten veelbelovende uitkomsten zien, waarbij het gebruik van OCT en afzien van overdruk tot minder loslatingen en een verbeterde vitaliteit van het transplaat leidt.

Hoofdstuk 4 beschrijft een klinische trial waarbij het geoptimaliseerde operatieprotocol zoals beschreven in hoofdstuk 3 wordt vergeleken met de standaard praktijk waarbij de chirurg geen toegang heeft tot OCT en het oog op overdruk moet brengen. In deze studie wordt aangetoond dat het geoptimaliseerde operatieprotocol niet inferieur is aan de standaard praktijk en het aantal complicaties na de operatie gelijk is tussen beide operatieprotocollen. Het op overdruk brengen van het oog lijkt geen toegevoegde waarde te hebben, maar er werden ook geen negatieve consequenties van het toepassen van deze preventieve handeling gevonden.

Volgens de chirurgen verbeterde de intra-operatieve OCT de chirurgische besluitvorming in 40% van de operaties en bleek onmisbaar in verscheidene complexe operaties. De intra-operatieve OCT werd het meest gebruikt om de oriëntatie van het transplantaat te bepalen en in mindere mate tijdens het ontvouwen en positioneren van het transplantaat. Dit laatste werd ondersteund door een kortere operatieduur in de intra-operatieve OCT-groep. Een verbeterde chirurgische besluitvorming bleek echter niet gerelateerd aan uitkomsten tijdens of na de operatie.

In hoofdstuk 5 wordt een casus beschreven waarbij de intra-operatieve OCT cruciaal bleek voor de diagnose en behandeling van een baby met ernstig cornea oedeem veroorzaakt door een zeldzame cornea aandoening. De intra-operatieve OCT maakte het mogelijk om endotheliale keratoplastiek uit te voeren. Met behulp van intra-operatieve OCT was het mogelijk het transplantaat en de chirurgische handelingen tijdens de operatie te visualiseren in de zeer troebele cornea.

In hoofdstuk 6 beschrijven wij de ontwikkeling van een beeldanalyse algoritme waarmee geautomatiseerd de oriëntatie van het transplantaat in het oog kan worden bepaald met behulp van intra-operatieve OCT. Het algoritme kan automatisch het transplantaat segmenteren en de boven- en onderkant van het transplantaat bepalen, waardoor de huidige tijdrovende manuele beoordeling van de OCT beelden door chirurgen overbodig is.

Voorspellende factoren voor de loslating van het transplantaat

Het tweede deel van dit proefschrift richt zich op het ontrafelen van de oorzaken van loslating van het transplaat na een corneatransplantatie en het identificeren van voorspellende factoren. Het gebruik van kunstmatige intelligentie biedt nieuwe mogelijkheden om complexe interacties en risicofactoren voor een loslating van het transplaat te identificeren. In hoofdstuk 7 beschrijven we hoe we met machine learning de bijdrage van patiënt kenmerken, donor eigenschappen en chirurgische factoren aan een loslating van het transplantaat kunnen bepalen, gebaseerd op de data van het Nederlands Orgaan transplantatie register en de operatieprotocollen van de deelnemende centra.

De klinische praktijk is vaak afwijkend van de vastgestelde operatieprotocollen en het effect van deze variatie hebben wij onderzocht in hoofdstuk 8. Hierbij hebben we alle video-opnames van operaties in de ADVISE trial geanalyseerd om de bijdrage weefsel manipulatie, weefsel hantering en klinische variatie op de incidentie van loslating van het transplantaat te beoordelen. Uit de resultaten bleek dat het bieden van voldoende steun d.m.v. van een gasbel na de operatie relevanter is voor het voorkomen van postoperatieve loslating dan iatrogeen weefsel trauma of het voorkomen van overlap tussen het transplantaat en het Descemet membraan van de patiënt. Daarnaast waren weefseleigenschappen van de donor die het ontvouwen van het transplantaat moeilijker maken gerelateerd aan postoperatieve loslating. Deze eigenschappen uitten zich in een karakteristieke vorm van het transplantaat in het oog.

In hoofdstuk 9 beschrijven we dat een plaatselijk verdikking van de cornea de dag na de operatie geassocieerd is met een verhoogd risico op loslating van het transplantaat. Een voorspellend model was in staat om met hoge accuraatheid een loslating te voorspellen en hoe groot het losgelaten gebied is. Dit helpt bij het identificeren van patiënten bij wie het risico op loslating van het transplantaat en waarvoor chirurgische interventie noodzakelijk is. Hiermee kan postoperatieve zorg op maat mogelijk gemaakt worden, waarbij patiënten met een hoog risico meer controles ondergaan en patiënten met een laag risico minder controles nodig hebben.

DANKWOORD

Nu de inhoud is opgeschreven, kan dit proefschrift nog niet afgerond worden zonder iedereen te bedanken die heeft bijgedragen aan de totstandkoming van dit proefschrift. Allereerst wil ik de patiënten bedanken voor hun medewerking zonder wie dit onderzoek niet mogelijk was geweest. Daarnaast wil ik graag een aantal personen in het bijzonder bedanken.

Beste Robert, allereerst wil ik jou bedanken aangezien jij aan de basis stond van mijn wetenschappelijke carrière. Na mijn wetenschapsstage bood jij mij de kans om aan te blijven als onderzoeker wat uiteindelijk resulteerde in een promotieonderzoek en ik ben je nog steeds heel dankbaar voor dit vertrouwen in mij. Jouw aanstekelijke optimisme gecombineerd met een "can-do" mentaliteit zijn inspirerend. Je hebt mij gemotiveerd om het beste uit mezelf te halen op wetenschappelijk alsmede persoonlijk vlak en hiervoor alle ruimte geboden. Daarnaast waardeer ik ook dat je deur altijd open stond en je tijd vrij wist te maken als ik wilde overleggen, ondanks dat je een duizendpoot met een overvolle agenda bent. Ik kan mij gelukkig prijzen met jou als begeleider.

Beste Herke Jan, je was vanaf het begin betrokken bij het onderzoek, maar werd pas later formeel copromotor. Door jouw ervaring met medische beeldverwerking had je een sleutelrol bij het vormgeven en ontwikkelen van het DMEK oriëntatie algoritme, maar ook de sturing bij andere projecten was van grote waarde. Jouw nuchtere blik en pragmatische aanpak zijn verhelderend en droegen bij aan het succes van dit proefschrift.

Beste Saskia, ook jou ben ik zeer dankbaar voor het vertrouwen dat je in mij hebt gesteld. Bij de start van het promotieonderzoek bleek jouw sturing van grote waarde. Ik bewonder jouw vermogen om overzicht te houden en focus aan te brengen in een promotieonderzoek. Daarnaast waardeer ik jou steun toen ik besloot een master naast mijn promotieonderzoek te doen. Dit is tekenend voor de waarde die je hecht aan persoonlijke ontwikkeling en de ruimte die je daarvoor geeft.

De leden van de beoordelingscommissie: prof. dr. Sorcha Ni Dhubhghaill, prof dr. Jelle Ruurda, prof. dr. Martine de Jager, prof. dr. Mies van Genderen, prof dr. Peter van der Heijden, graag wil ik jullie bedanken voor het lezen en beoordelen van mijn proefschrift.

Alle medeauteurs van de studies in dit proefschrift wil ik bedanken voor de samenwerking en jullie bijdrage aan dit proefschrift. In het bijzonder wil ik de PI's van Maastricht; prof. dr. Rudy Nuijts en Mor Dickman, en Leuven; Heleen Delbeke, bedanken voor het mogelijk maken van de ADVISE studie. Daarnaast wil ik Suryan en Inge bedanken voor jullie ondersteuning bij de coördinatie van de ADVISE trial in Maastricht en Leuven. Laurence en Gerko zonder jullie kennis en expertise was hoofdstuk 7 van dit proefschrift nooit tot stand gekomen. Friso, het begon met een biertje op DOPS en eindigde in een productieve en fijne samenwerking. Ik heb veel geleerd van jouw uitgebreide kennis op het gebied van kunstmatige intelligentie.

Graag wil ik iedereen bedanken die ondersteunend zijn geweest in de uitvoering van het onderzoek. Onderzoek is teamwork en jullie hulp is van onschatbare waarde. Suzan en Petra, bedankt dat ik altijd terecht kon voor alle praktische en logistieke vragen. De dames van de planning: Joke, Nanny en Joke. Jullie hulp bij het inplannen van de operaties van studiepatiënten word zeer gewaardeerd. Peter Zuithoff, dank voor de hulp met alle statistische vragen en ondanks dat ik soms met meer vragen bij je wegging heeft het me altijd verder geholpen. De medewerkers van het onderzoeksbureau, dank voor de alle hulp met juridische, financiële en praktische zaken rondom onderzoek. In bijzonder wil ik nog Tamara bedanken voor het meedenken en jouw kritische blik op mijn onderzoeksvoorstellen. Ferry en Ruud, bedankt voor het helpen met alle ICT-zaken. Antoon van den Bogaerdt bedankt voor jouw hulp met het verkrijgen van voldoende donor corneas voor de ADVISE studie. Cynthia Konijn van de Nederlandse transplantatie stichting, dank voor jouw ondersteuning op het gebied van data verstrekking en het verspreiden van vragenlijsten onder de cornea chirurgen in Nederland. Beste Ton, Albert en Hind dank voor jullie zitting in de DSMB van de ADVISE trial en jullie feedback op de studie.

De stafartsen, AIOS en medewerkers van de afdeling oogheelkunde, bedankt voor al jullie interesse en hulp tijdens mijn promotie. In het bijzonder wil ik Cindy, Sophie en Chantal bedanken. Jullie waren altijd bereid om de studiemetingen te verrichten wanneer ik verhinderd was.

Beste studenten, Marijn, Suzanne, Floor, Inge, Christian, Hanad en Gabriella. Bedankt voor jullie inzet en enthousiasme. Het was een zeer leerzaam om jullie wetenschappelijke stages te mogen begeleiden en ik heb genoten van de samenwerking. Jullie werk heeft een belangrijke bijdrage geleverd aan dit proefschrift en ik wens jullie veel succes met jullie verdere carrière.

Een bijzonder woord van dank wil ik richten tot mijn collega-onderzoekers. Fleurieke en Kamil als ervaren onderzoekers stonden jullie altijd klaar met advies en hulp wanneer nodig en dit werd zeer gewaardeerd. Nienke, als wetenschapsstudent bij jou en Robert zette ik de eerste stappen in het onderzoek en door onze gedeelde achtergrond was jij een rolmodel dat mijn ambitie om promotieonderzoek te doen heeft vormgegeven. Bedankt voor alle hulp en begeleiding in de afgelopen jaren. Anna en Sara, dank voor het warme onthaal in het A-hok. Sara bedankt voor de vele interessante discussies en niet onbelangrijk jij was degene die me stukje bij beetje het vegetarische pad op duwde. Anna, jouw baksels waren de aanleiding voor veel lange doch gezellige koffiemomenten, waarvoor veel dank. Roos, Myrthe en Evianne zonder jullie hadden de afgelopen jaren een stuk minder kleur gehad waarvoor ik jullie zeer dankbaar ben. Roos, jouw opruiende humor zorgde voor de nodige afleiding, maar ook bedankt voor alle keren dat je tijd maakte om mee te lezen en je hulp wanneer met iemand van gedachten moest wisselen. Myrthe, jouw nuchtere persoonlijkheid wist het b-hok in balans te houden, behalve als het over jouw eetgewoontes ging (een biefstuk is ten slotte een goede bodem voor elke uitdaging). Bedankt voor gezelligheid en het luisterend oor waar ik altijd mijn frustraties kon delen. Evianne, jij bent geconcentreerde gezelligheid! Jouw vrolijkheid maakt de dag leuker. Els, helaas was onze samenwerking van korte duur, maar desondanks kijk ik met plezier terug waarvoor dank. Janneau en Casper, als mede-promovendi van Robert hebben we in veel projecten samengewerkt. Bedankt voor de leuke (thuis)werksessies en cornea borrels. Wouter, Brendan, Carlyn, Lude, Cansu bedankt voor alle gezelligheid, koffiemomenten, uitjes en feestjes.

Mijn Paranimfen Robbert Jongeneel en Tim Kies. Robbert, ik ben blij dat we al zoveel jaren bevriend zijn en ik koester onze vriendschap zeer. Je bent bij alle grote momenten in mijn leven geweest en het voelt als een eer om jou naast me te hebben staan. Tim, naast de vele avonturen wordt onze vriendschap gekenmerkt door de vele diepgaande discussies. Bedankt voor alle leuke herinneringen op dat er nog vele mogen volgen

Ik ben Maurits, Maarten, Frans, Thijs, David, Tim, Bjorn, Kevin en Thom enorm dankbaar voor jullie interesse in mijn onderzoek en het bieden van de nodige afleiding de afgelopen jaren. Dear Valentina, you are familiar with all the struggles of a PhD-life and I'm thankful for our dinner parties and providing a much-needed outlet.

Ik ben mijn familie en schoonfamilie dankbaar voor jullie interesse in mijn onderzoek en de steun afgelopen jaren.

Lieve Gerard, Marianne, Eva en Flora, hoewel we soms continenten van elkaar gescheiden zijn voelt het altijd vertrouwd en fijn om samen te zijn. Bedankt voor jullie onvoorwaardelijke steun en liefde. Pap en mam, zonder jullie zou ik niet zijn waar ik nu ben. Jullie hebben ons altijd gestimuleerd om jezelf te blijven ontwikkelen en daar mogen jullie trots op zijn.

Lieve Nicole, wat ben ik blij dat ik jou in mijn leven heb. Woorden schieten tekort om aan te geven hoeveel jij voor mij betekent en de steun die je hebt gegeven. Jij haalt het beste in mij naar boven en bent de persoon waar ik altijd op kan terugvallen. In de afgelopen turbulente jaren was je er altijd voor hulp of het bieden van een luisterend oor als het moeilijk was of ik gewoon mijn gedachten moest ventileren. Kortom, je bent geweldig en ik hou van je! Nu is het tijd voor het volgende hoofdstuk in ons leven en ik kijk uit naar alle mooie momenten die we samen met Nala gaan hebben.

ABOUT THE AUTHOR

Marc Bastiaan Muijzer was born on November 25th 1992 in Schiedam, the Netherlands. He is the son of Gerard and Marianne and has two older sisters, Eva and Flora. After graduating secondary school in 2010, he began studying Biology, switching to optometry in Utrecht in 2012. In the final year of his study he pursued an research internship at the University Medical Center Utrecht and developed an interest for scientific research.

He graduated his studies in 2017 and started to work at the Ophthalmology department of the Alrijne Hospital. During this time he also worked as a junior researcher at the University Medical Center Utrecht under supervision of Robert Wisse. His work as a junior researcher formed the basis of his PhD research, which he started in May 2018 under supervision of prof. dr. Saskia Imhof, dr. Robert Wisse, and dr. ir. Herke Jan Noordmans. Parallel to conducting his PhD research, Bas completed a master in health care management at the Erasmus University. Next to the research presented in this thesis, he was involved in a clinical trial to validate a novel digital tool to measure refractive errors, which sparked his interest for digital health.

Bas lives together with his partner Nicole and their dog Nala in Utrecht. He enjoys traveling, cooking, and playing guitar. Bas started in April 2022 as vision scientist at Easee BV, where he is joining their R&D team to develop innovative digital products to aid ophthalmic care

LIST OF PUBLICATIONS

Muijzer MB, Soeters N, Godefrooij DA, van Luijk CM, Wisse RPL. Intraoperative Optical Coherence Tomography-Assisted Descemet Membrane Endothelial Keratoplasty: Toward More Efficient, Safer Surgery. Cornea. 2020 Jun;39(6):674-679.

Muijzer MB, Schellekens PAWJ, Beckers HJM, de Boer JH, Imhof SM, Wisse RPL. Clinical applications for intraoperative optical coherence tomography: a systematic review. Eye (Lond). 2022 Feb;36(2):379-391.

Muijzer MB, Noordmans HJ, Delbeke H, Dickman MM, Nuijts RMMA, Dunker S, Imhof SM, Wisse RPL. Establishing a Biomarker for the Prediction of Short-Term Graft Detachment After Descemet Membrane Endothelial Keratoplasty. Cornea. 2022 Feb 19.

Muijzer MB, Heslinga FG, Couwenberg F, Noordmans HJ, A Oahalou A, Pluim JPW, Veta M, Wisse RPL. Automatic evaluation of graft orientation during Descemet Membrane Endothelial Keratoplasty using intraoperative OCT. Biomedical Optics Express. 2022.

Muijzer MB, Kroes HY, Van Hasselt PM, Wisse RPL. Bilateral posterior lamellar corneal transplant surgery in an infant of 17 weeks old: surgical challenges and the added value of intraoperative optical coherence tomography. Clinical Case Report. 2022 March

Muijzer MB, Delbeke H, Dickman MM, Nuijts RMMA, Imhof SM, Wisse RPL. Outcomes of the Advanced Visualization In Corneal Surgery Evaluation (ADVISE) trial; a non-inferiority randomized control trial to evaluate the use of intraoperative OCT during Descemet membrane endothelial keratoplasty. Submitted.

Muijzer MB, Noordmans HJ, Delbeke H, Dickman MM, Nuijts RMMA, Imhof SM, Wisse RPL. Video-grading of Descemet Membrane Endothelial Keratoplasty surgery to identify risk factors for graft detachment and rebubbling: a post-hoc analysis of the Advanced Visualization In Corneal Surgery Evaluation (ADVISE) trial. Submitted.

Muijzer MB, Hoven CMW, Frank LE, Vink G, Wisse RPL, Netherlands Corneal Transplant Network. A machine learning approach to explore predictors of graft detachment following posterior lamellar keratoplasty: a nationwide registry study. Submitted.

NOT INCLUDED IN THIS THESIS

Soeters N, **Muijzer MB**, Molenaar J, Godefrooij DA, Wisse RPL. Autorefraction Versus Manifest Refraction in Patients With Keratoconus. J Refract Surg. 2018 Jan 1;34(1):30-34.

Muijzer MB, van Luijk CM, van den Bogaerdt AJ, Kruit PJ, Groeneveld-van Beek E, Melles GRJ, Wisse RPL. Prospective evaluation of clinical outcomes between pre-cut corneal grafts prepared using a manual or automated technique: with one-year follow-up. Acta Ophthalmol. 2019 Nov;97(7):714-720.

Wisse RPL, **Muijzer MB**, Cassano F, Godefrooij DA, Prevoo YFDM, Soeters N. Validation of an Independent Web-Based Tool for Measuring Visual Acuity and Refractive Error (the Manifest versus Online Refractive Evaluation Trial): Prospective Open-Label Noninferiority Clinical Trial. J Med Internet Res. 2019 Nov 8;21(11):e14808.

Wisse RPL, Simons RWP, van der Vossen MJB, **Muijzer MB**, Soeters N, Nuijts RMMA, Godefrooij DA. Clinical Evaluation and Validation of the Dutch Crosslinking for Keratoconus Score. JAMA Ophthalmol. 2019 Jun 1;137(6):610-616.

Muijzer MB, Claessens JLJ, Cassano F, Godefrooij DA, Prevoo YFDM, Wisse RPL. The evaluation of a web-based tool for measuring the uncorrected visual acuity and refractive error in keratoconus eyes: A method comparison study. PLoS One. 2021 Aug 18;16(8):e0256087.